NEUROPLASTICITY AND COMPLEMENTARY/ ALTERNATIVE THERAPIES: INNOVATIONS FROM NEURAL MECHANISMS TO CLINICAL PRACTICE

EDITED BY: Siyi Yu, Jian Kong, Jiao Liu and Binlong Zhang

PUBLISHED IN: Frontiers in Molecular Neuroscience

frontiers Research Topics

frontiers

ISSN 1664-8714
ISBN 978-2-83250-124-5
DOI 10.3389/978-2-83250-124-5

About Frontiers

Frontiers is more than just an open-access publisher of scholarly articles: it is a pioneering approach to the world of academia, radically improving the way scholarly research is managed. The grand vision of Frontiers is a world where all people have an equal opportunity to seek, share and generate knowledge. Frontiers provides immediate and permanent online open access to all its publications, but this alone is not enough to realize our grand goals.

Frontiers Journal Series

The Frontiers Journal Series is a multi-tier and interdisciplinary set of open-access, online journals, promising a paradigm shift from the current review, selection and dissemination processes in academic publishing. All Frontiers journals are driven by researchers for researchers; therefore, they constitute a service to the scholarly community. At the same time, the Frontiers Journal Series operates on a revolutionary invention, the tiered publishing system, initially addressing specific communities of scholars, and gradually climbing up to broader public understanding, thus serving the interests of the lay society, too.

Dedication to Quality

Each Frontiers article is a landmark of the highest quality, thanks to genuinely collaborative interactions between authors and review editors, who include some of the world's best academicians. Research must be certified by peers before entering a stream of knowledge that may eventually reach the public - and shape society; therefore, Frontiers only applies the most rigorous and unbiased reviews.
Frontiers revolutionizes research publishing by freely delivering the most outstanding research, evaluated with no bias from both the academic and social point of view. By applying the most advanced information technologies, Frontiers is catapulting scholarly publishing into a new generation.

What are Frontiers Research Topics?

Frontiers Research Topics are very popular trademarks of the Frontiers Journals Series: they are collections of at least ten articles, all centered on a particular subject. With their unique mix of varied contributions from Original Research to Review Articles, Frontiers Research Topics unify the most influential researchers, the latest key findings and historical advances in a hot research area! Find out more on how to host your own Frontiers Research Topic or contribute to one as an author by contacting the Frontiers Editorial Office: frontiersin.org/about/contact

NEUROPLASTICITY AND COMPLEMENTARY/ ALTERNATIVE THERAPIES: INNOVATIONS FROM NEURAL MECHANISMS TO CLINICAL PRACTICE

Topic Editors:
Siyi Yu, Chengdu University of Traditional Chinese Medicine, China
Jian Kong, Massachusetts General Hospital, Harvard Medical School, United States
Jiao Liu, Fujian University of Traditional Chinese Medicine, China
Binlong Zhang, Guang'anmen Hospital, China Academy of Chinese Medical Sciences, China

Citation: Yu, S., Kong, J., Liu, J., Zhang, B., eds. (2022). Neuroplasticity and Complementary/Alternative Therapies: Innovations From Neural Mechanisms to Clinical Practice. Lausanne: Frontiers Media SA. doi: 10.3389/978-2-83250-124-5

Table of Contents

frontiers in Molecular Neuroscience

ORIGINAL RESEARCH
published: 23 February 2022
doi: 10.3389/fnmol.2022.825286

Real-Time fMRI Neurofeedback Training Changes Brain Degree Centrality and Improves Sleep in Chronic Insomnia Disorder: A Resting-State fMRI Study

Xiaodong Li[1†], Zhonglin Li[1†], Zhi Zou[1†], Xiaolin Wu[2†], Hui Gao[3], Caiyun Wang[1], Jing Zhou[4], Fei Qi[1], Miao Zhang[1], Junya He[1], Xin Qi[1], Fengshan Yan[1], Shewei Dou[1], Hongju Zhang[5], Li Tong[3] and Yongli Li[4]**

[1] Department of Radiology, Henan Provincial People's Hospital, People's Hospital of Zhengzhou University, Zhengzhou, China, [2] Department of Nuclear Medicine, Henan Provincial People's Hospital, People's Hospital of Zhengzhou University, Zhengzhou, China, [3] Henan Key Laboratory of Imaging and Intelligent Processing, PLA Strategic Support Force Information Engineering University, Zhengzhou, China, [4] Health Management Center, Henan Provincial People's Hospital, People's Hospital of Zhengzhou University, Zhengzhou, China, [5] Department of Neurology, Henan Provincial People's Hospital, People's Hospital of Zhengzhou University, Zhengzhou, China

Background: Chronic insomnia disorder (CID) is considered a major public health problem worldwide. Therefore, innovative and effective technical methods for studying the pathogenesis and clinical comprehensive treatment of CID are urgently needed.

Methods: Real-time fMRI neurofeedback (rtfMRI-NF), a new intervention, was used to train 28 patients with CID to regulate their amygdala activity for three sessions in 6 weeks. Resting-state fMRI data were collected before and after training. Then, voxel-based degree centrality (DC) method was used to explore the effect of rtfMRI-NF training. For regions with altered DC, we determined the specific connections to other regions that most strongly contributed to altered functional networks based on DC. Furthermore, the relationships between the DC value of the altered regions and changes in clinical variables were determined.

Results: Patients with CID showed increased DC in the right postcentral gyrus, Rolandic operculum, insula, and superior parietal gyrus and decreased DC in the right supramarginal gyrus, inferior parietal gyrus, angular gyrus, middle occipital gyrus, and middle temporal gyrus. Seed-based functional connectivity analyses based on the altered DC regions showed more details about the altered functional networks. Clinical scores in Pittsburgh sleep quality index, insomnia severity index (ISI), Beck depression inventory, and Hamilton anxiety scale decreased. Furthermore, a remarkable positive correlation was found between the changed ISI score and DC values of the right insula.

Conclusions: This study confirmed that amygdala-based rtfMRI-NF training altered the intrinsic functional hubs, which reshaped the abnormal functional connections caused

OPEN ACCESS

Edited by:
Siyi Yu,
Chengdu University of Traditional Chinese Medicine, China

Reviewed by:
Muliang Jiang,
First Affiliated Hospital of Guangxi Medical University, China
Yang Qiang,
National Digital Switching System Engineering and Technological Research Centre, China

***Correspondence:**
Li Tong
tttocean_tl@hotmail.com
Yongli Li
shyliyongli@126.com

[†] These authors have contributed equally to this work

Specialty section:
This article was submitted to Neuroplasticity and Development, a section of the journal Frontiers in Molecular Neuroscience

Received: 30 November 2021
Accepted: 31 January 2022
Published: 23 February 2022

Citation:
Li X, Li Z, Zou Z, Wu X, Gao H, Wang C, Zhou J, Qi F, Zhang M, He J, Qi X, Yan F, Dou S, Zhang H, Tong L and Li Y (2022) Real-Time fMRI Neurofeedback Training Changes Brain Degree Centrality and Improves Sleep in Chronic Insomnia Disorder: A Resting-State fMRI Study. Front. Mol. Neurosci. 15:825286. doi: 10.3389/fnmol.2022.825286

by insomnia and improved the sleep of patients with CID. These findings contribute to our understanding of the neurobiological mechanism of rtfMRI-NF in insomnia treatment. However, additional double-blinded controlled clinical trials with larger sample sizes need to be conducted to confirm the effect of rtfMRI-NF from this initial study.

Keywords: insomnia disorder, real-time fMRI, neurofeedback, degree centrality, functional connectivity

INTRODUCTION

Chronic insomnia disorder (CID) is considered a major public health problem worldwide and is characterized by difficulty in falling asleep at bedtime, frequent awakening in the middle of the night, and waking up early in the morning (Buysse et al., 2017). These symptoms, which persist over at least 3 months, reduce the quality of daily life, affect work efficiency, and cause mental symptoms, such as depression and anxiety, which might become life threatening (Spiegelhalde et al., 2015; Buysse et al., 2017). However, the pathogenesis of insomnia is still unclear, causing challenges to its treatment (Kay and Buysse, 2017). Therefore, innovative therapies and pathogenesis of CID need to be studied.

The current treatment for CID includes drug and non-drug therapies (Buysse et al., 2017; Sateia et al., 2017). Long-term clinical drug treatment has limitations, causing a series of side effects and drug dependence (Buysse et al., 2017; Zhao et al., 2020). The "American College of Physicians Guidelines for the Clinical Diagnosis and Treatment of Insomnia in Adults" and the "Guidelines for the Diagnosis and Treatment of Insomnia in Adults in China" recommend non-pharmacological treatments as first-line treatments for CID (Qaseem et al., 2016; Buysse et al., 2017). The main clinical non-drug adjuvant treatments for insomnia are cognitive behavioral therapy (CBT) and neurofeedback (Buysse et al., 2017; Zhao et al., 2020). CBT improves sleep through interviews, psychological counseling, and changes in sleep habits. However, this method has a certain degree of blindness. Moreover, it cannot observe changes in brain activity in real time and clarify changes in brain neurobiology and its effective neurobiological mechanisms (Zhao et al., 2020). The neurofeedback method based on electroencephalogram (EEG) signals can overcome the shortcomings of CBT, but the spatial resolution is low; it cannot record EEG signals from the deep brain areas (Weiskopf, 2012; Samantha et al., 2020; Zhao et al., 2020). Hence, innovative and effective technical methods for studying the pathogenesis and clinical comprehensive treatment of CID need to be developed urgently.

Real-time fMRI neurofeedback (rtfMRI-NF) is a new intervention with great application value that trains subjects to adjust brain neural activity autonomously to improve cognition or cure diseases (Weiskopf, 2012; Watanabe et al., 2017; Samantha et al., 2020). In comparison with other neurofeedback techniques, such as EEG and non-invasive physical stimulation techniques (e.g., transcranial magnetic stimulation, TMS), rtfMRI-NF has higher spatial resolution and localization accuracy and better access to deep relevant brain structures (Weiskopf, 2012; Watanabe et al., 2017; Samantha et al., 2020). This technology enables subjects to regulate brain activity and improve the clinical symptoms of major depressive disorder (MDD), anxiety, schizophrenia, and other diseases (Morgenroth et al., 2020; Tursic et al., 2020; Tsuchiyagaito et al., 2021). rtfMRI-NF may be an efficient method for the treatment of patients with CID (Spiegelhalde et al., 2015). However, this technology has not been applied in CID treatment.

Dysfunctional emotional responses might mediate the interaction between cognitive and autonomic hyperarousal, thus maintaining insomnia (Baglioni et al., 2010). Moreover, dysfunctions in sleep–wake-regulating neural circuitries can reinforce emotional disturbances (Baglioni et al., 2010). The use of fMRI technology in exploring the deep neural functional changes in CID has revealed multiple local and overall dysfunctions in the brain, which are concentrated in the amygdala and other emotion- and cognition-related brain areas (Huang et al., 2012; Baglioni et al., 2014; Spiegelhalde et al., 2015). Baglioni et al. (2014) found that CID is associated with increased amygdala responsiveness to negative stimuli, and insomnia treatment may benefit from strategies that modulate its association with emotion. By using resting-state fMRI, Huang et al. (2012) found that the amygdala has decreased functional connectivity (FC) with the insula, striatum, and thalamus and increased FC with the premotor and sensorimotor cortex. The amygdala is located in the center of the limbic system, and it plays a key role in the generation and expression of emotions and the perception of negative emotions; thus, the amygdala may be involved in the pathogenesis of CID (Pessoa, 2010). Many researchers have successfully used rtfMRI-NF training to help patients regulate the activity of the left amygdala through positive autobiographical memory to change brain function and clinical symptoms (Watanabe et al., 2017; Samantha et al., 2020; Tursic et al., 2020). Therefore, the selection of amygdala activity as the target of rtfMRI-NF regulation may improve sleep in CID and provide a new breakthrough point for studying neural mechanism.

Recently, resting-state fMRI has been increasingly used to address changes in brain FC following effective treatments (Dichter et al., 2015). Resting-state FC is a highly effective and sensitive method for mapping complex neural circuits that may reflect the underlying neurobiological mechanism (Wang et al., 2012; Fasiello et al., 2021). Altered FC could be calculated by comparing resting-state FC during different stages (e.g., before and after training) and may indicate the effect of rtfMRI-NF training. Voxel-wise degree centrality (DC) is a data-driven method used to measure the FC number of a given voxel with all other voxels within the entire brain, thus enabling the identification of FC hubs in the human brain (Yan et al., 2018, 2020). Unlike seed-based or independent component analysis (ICA) approaches, voxel-wise DC was developed to reveal regions with consistent global connections even when the individual

connections vary across regions for different subjects or patients (Yan et al., 2018, 2020). Voxel-based DC has high sensitivity, specificity, and test–retest reliability and has been widely used to investigate diseases such as CID, MDD, Alzheimer's disease, and Parkinson's disease (Zuo and Xing, 2014; Yan et al., 2018, 2020). Thus, voxel-wise DC analysis could be used to gain insight into the neural mechanisms underlying rtfMRI-NF training.

Taken together, we hypothesized that amygdala-based rtfMRI-NF training could change DC and improve the sleep of patients with CID. rtfMRI-NF was used to train patients with CID to regulate their amygdala activity for three sessions in 3 weeks to test our hypothesis. Resting-state fMRI data were collected before and after training. Then, voxel-based DC method was used to explore the effect of training. For regions with altered DC, we determined the specific connections to other regions that most strongly contributed to altered functional hubs based on DC. We also investigated the relationships between the DC value of altered regions and changes in clinical variables.

MATERIALS AND METHODS

Participants

This study was approved by the Ethics Committee of Henan Provincial People's Hospital. All patients with CID were outpatients from the neurology department of the hospital or recruited *via* advertising. These patients were recruited from January 2018 to December 2021. All participants provided written informed consent to participate in the study and received equal financial compensation. The subjects underwent complete physical and neurological examination, standard laboratory tests, and certain psychological assessments, such as Pittsburgh sleep quality index (PSQI), insomnia severity index (ISI), Hamilton depression scale (HAMD), Beck depression inventory (BDI), and Hamilton anxiety scale (HAMA). Moreover, the participants should meet the criteria for CID in the fifth edition of Diagnostic and Statistical Manual of Mental Disorders and should not have taken medication that would influence brain function 2 weeks before the experiment. The inclusion criteria are as follows: (1) duration of insomnia symptoms, such as fatigue, testiness, or cognitive decline, of no less than 3 months, (2) PSQI score $\geq$ 8, (3) no neurological or psychiatric disorders, such as stroke, (4) no other sleep disorders such as sleep-related movement disorders, hypersomnia, or parasomnia, (5) right-hand dominance and native Chinese speaker, (6) 18–70 years old, (7) no medication or substance abuse, such as excessive intake of caffeine, nicotine, or alcohol, and (8) no abnormal signal found by T2-weighted dark-fluid and T1-weighted MR images. Furthermore, overnight polysomnography (PSG) was performed using an ambulatory recording system (Compumedics Siesta, Australia) to exclude participants with occult sleep disorders other than insomnia. PSG characteristics, including total sleep time, sleep efficiency, sleep onset latency, and the number of awakenings, were collected. Finally, 33 subjects participated and completed all the procedures of our experiment. However, four subjects were excluded because of large head motion during the resting-state scan. One subject dropped out because of a pause in training.

Procedure

The experimental procedure is shown in **Figure 1**. Participants were required to visit the hospital six times to complete the experiment. During visit 1, we collected the general demographic characteristics of the participants. The participants also completed PSQI, ISI, HAMD, BDI, and HAMA. During visit 2, all subjects underwent MRI scans and were familiar with the MRI scanning environment. Routine axial T2-weighted dark-fluid and T1-weighted MR images were acquired to exclude brain structure abnormality. High-resolution T1-weighted structural images were acquired to register the template of the amygdala from the standard space to the subject space for real-time processing data during training. Afterward, overnight PSG was performed. During visit 3, 4, and 5, the participants completed the same clinical and self-report measures as visit 1 and their three rtfMRI-NF training sessions. The following section details the rtfMRI-NF training process. During visit 6, the participants completed resting-state fMRI scan, overnight PSG, the same clinical, and self-report measures similar to visit 3. An interval of approximately 1 week from the previous visit was set. Throughout the training period, the subjects were required not to take drugs that help sleep. The subjects were informed that they can withdraw from the training at any time.

Real-Time fMRI Neurofeedback Training Paradigm

Before rtfMRI-NF training, we asked the subjects to write down three or more specific autobiographical memories about themselves and explained the specific tasks under the experimental stimulation. They received information on brain activity signals from the left amygdala region, as defined from the Talairach space with a radius of 7 mm and the coordinates (−21, −5, −16) (Young et al., 2017). Amygdala activity was displayed as temperature bars and updated once per retention time (TR, 2 s). Real-time online data-processing was performed using OpenNFT system (Koush et al., 2017). The detailed steps and parameters are provided in the paper published by Koush et al. (2017). Each training session has seven runs, including pre-rest, practice training, three NF training, transfer training, and post-rest, which lasted for approximately 50 min. Pre-rest and post-rest were carried out for 7 min. All the five other runs were carried out for 6 min and 50 s. Resting-state fMRI data were collected in the pre-rest and post-rest runs. During the resting-state fMRI data acquisition, all subjects were instructed to fix their vision on the green cross, keep awake, and think of nothing in particular. The practice and transfer training runs shared the same paradigms with NF training but without a feedback signal. The practice training run was designed to familiarize the subjects with the training procedures. The transfer training run was designed to test whether the subjects had mastered the regulation strategy. Each NF training run consisted of alternating 30 s of rest and 30 s of happy blocks with seven rest blocks and six happy blocks. During rest blocks, the subjects were asked to stare at the green cross on the screen to calm their mind. During happy blocks, the subjects were instructed to increase the

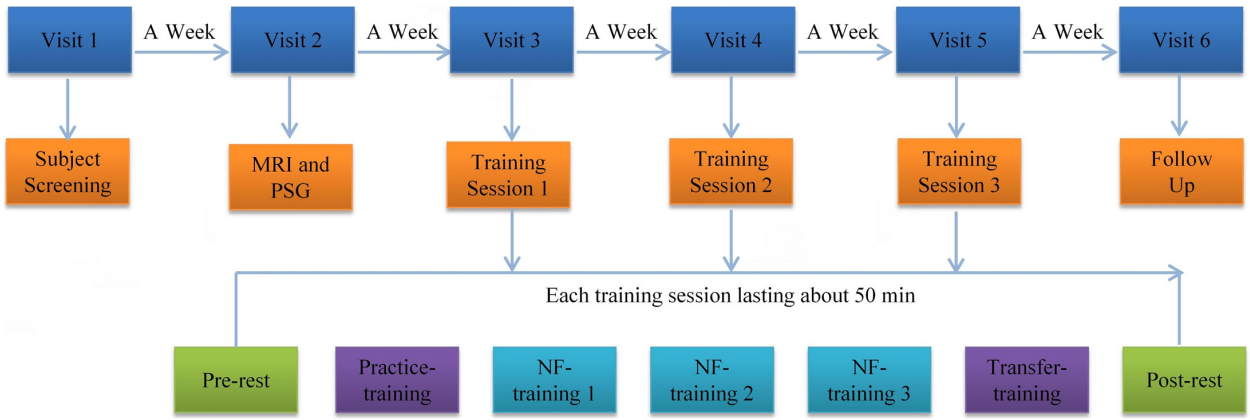

FIGURE 1 | Procedure of rtfMRI-NF training experiment. The experimental protocol consisted of six visits lasting for approximately 35 days. Each rtfMRI-NF training session included seven runs lasting for approximately 50 min. The pre- and post-rest runs were carried out for 7 min. The five remaining runs were carried out for 6 min and 50 s. rtfMRI-NF, real-time fMRI neurofeedback.

height of the thermometer on the screen by recalling a positive autobiographical memory.

Data Acquisition

All fMRI data were acquired using a MAGNETOM Prisma 3T MR scanner (Siemens Healthcare, Erlangen, Germany) with a 64-channel head–neck coil at the Medical Imaging Center of our hospital. Foam pads were used to minimize the subjects' head motions and diminish scanner noise. Medical tape was attached to their foreheads for them to feel their head movements and prevent out-of-range movements. Routine axial T2-weighted dark-fluid and T1-weighted MR images were acquired. fMRI data were acquired using an echo-planar imaging sequence with the following parameters: TR = 2,000 ms, echo time (TE) = 30 ms, field of vision (FOV) = 224 mm × 224 mm, matrix size = 112 × 112, slices = 27, slice thickness = 4 mm, flip angle = 90°. In total, 210 volumes lasting for 420 s were collected. High-resolution T1-weighted structural images were acquired with the following parameters: TR = 2,300 ms, TE = 2.27 ms, FOV = 250 mm × 250 mm, matrix size = 256 × 256, slices = 192, slice thickness = 1 mm, flip angle = 8°.

Data Processing

The resting-state fMRI data collected in visit 6 and the pre-rest run of visit 3 were used for analysis in the present study. Image pre-processing was performed using Data Processing and Analysis of Brain Imaging (DPABI, version 4.3) toolbox (Yan et al., 2016). First, the removal of the first 10 volumes, slice timing, and head motion correction were done by preprocessing functional data. Data with a maximum displacement in head rotation of larger than 2° or any directions larger than 2 mm were excluded from further analysis. For the precise spatial normalization of the fMRI data, individual high-resolution T1-anatomic images were registered to the mean fMRI data, and the resulting aligned T1-weighted images were segmented and transformed into standard Montreal Neurological Institute space by using the DARTEL toolbox. Furthermore, white matter and cerebrospinal fluid signals and 24 head realignment parameters were regressed out as covariates. Subsequently, the regressed functional images were normalized to the group template by using the transfer parameter estimated by DARTEL segmentation and resampled to 3 × 3 × 3 mm^3 voxels. Finally, linear trend and temporal band-pass filtering (0.01–0.1 Hz) was applied.

Degree Centrality Calculation

Degree centrality maps were generated *via* voxel-based whole-brain correlation analysis on the preprocessed resting-state fMRI data as previously described (Yan et al., 2018, 2020). The Pearson's correlation coefficient (r) between each pair of brain gray matter voxels was computed. A binary undirected correlation matrix was obtained by thresholding each correlation

TABLE 1 | Clinical characteristics of pre-training and post-training.

Variables	Pre-training	Post-training	T/Z value	*p* value
PSQI (score)	13.86 ± 3.35	11.25 ± 3.31	4.87	0.000
ISI (score)	17.82 ± 4.83	14.18 ± 6.14	3.463	0.002
HAMD (score)	19.11 ± 8.01	16.86 ± 7.47	1.759	0.090
BDI (score)	19.29 ± 10.70	15.89 ± 9.25	2.878	0.008
HAMA (score)	19.82 ± 9.45	16 ± 12.15	2.653	0.013
Total sleep time (min)	380.11 ± 101.70	404.27 ± 81.22	1.176	0.250
Sleep efficiency (%)	78.75 (66.25–84.78)	78.6 (71.33–89.98)	−0.615	0.539
Sleep onset latency (min)	20.5 (7.25–58.13)	12 (6.63–27.13)	−1.946	0.052
Number of awakenings	20.5 (10.25–26.75)	15 (8–26.5)	−1.488	0.137

Normal distribution data is presented as mean ± SD and p values were obtained by two-tailed paired t-test. Nor-normal distribution data is presented as median and inter-quartile range and p values were obtained by Wilcoxon signed-rank test. PSQI, Pittsburgh sleep quality index; ISI, insomnia severity index; HAMD, Hamilton Depression Rating Scale; BDI, Beck depression inventory; HAMA, Hamilton Anxiety Rating Scale.

at $r > 0.25$ to remove the weak correlations caused by noises. DC maps were also calculated for the thresholds at $r = 0.15$, 0.20, 0.30, 0.35 to assess the robustness of the chosen threshold (Zuo and Xing, 2014; Yan et al., 2018, 2020). Only positive correlations were considered in the DC calculations. Then, the DC maps of individuals were converted into z-score maps *via* Fisher-Z transformation. Finally, the DC maps were spatially smoothed with a smooth kernel of 6 mm. A group template of 90% was generated for fMRI processing and statistics. The weighted version of DC was also computed. The whole-brain DC differences between post- and pre-training conditions were compared using paired *t*-test to assess the effect of rtfMRI-NF on the brain of patients with CID. Based on previous studies that used the DC method on CID, Gaussian random field (GRF) theory correction procedure was used for multiple comparisons (Huang et al., 2017; Liu et al., 2018; Yan et al., 2018).

Seed-Based Functional Connectivity Calculation

Seed-based interregional correlation analysis was performed using the DPABI software package to explore more details about resting-state FC alterations. The seed regions were defined based on altered DC regions (post-training vs. pre-training) by drawing a 6 mm-radius sphere region of interest (ROI) around the activated center of mass coordinates (Gao et al., 2021). By using the DPABI toolbox, we calculated the FC maps by correlating the mean time series of all voxels within the ROI to the time courses of all brain voxels in the gray matter mask. Afterward, Fisher-Z transform analysis was applied to the FC maps to obtain an approximately normal distribution. Finally, a spatially smooth step was added to the z-score FC maps by using a 6 mm kernel. Paired *t*-test was used to compare the differences of FC maps between post- and pre-training conditions.

Statistical Analysis

Demographic and Clinical Data Analysis

Statistical analysis of demographic and clinical data was performed using SPSS version 22.0 (Chicago, IL, United States). The threshold for statistical significance was set at $p < 0.05$, and all hypothesis tests were two-tailed. The distribution of clinical data and DC values were tested using Kolmogorov–Smirnov method. Continuous variables with normal distribution were analyzed using independent paired *t*-test and expressed as mean ± standard deviation. Otherwise, Wilcoxon signed-rank test was used to analyze the data with non-normal distribution, and the results are expressed as median and interquartile range.

Brain–Behavior Correlation Analysis

The averaged DC values of altered brain regions in post-training were extracted to calculate the Partial (normally distributed data) or Spearman (non-normally distributed data) correlation between DC values and changes in clinical scores and PSG indexes, including PSQI, ISI, HAMD, HAMA, BDI, total sleep time, sleep efficiency, sleep onset latency, and number of awakenings, with age, gender, and education as covariates. Statistical significance was considered at $p < 0.05$.

RESULTS

Demographic and Clinical Data

Finally, the data of 28 patients with CID were analyzed in this paper (7 males; age: 45.7 ± 13.2 years; education: 13.1 ± 3.3 years). The clinical characteristics (PSQI, ISI, HAMD, HAMA, BDI, and total sleep time) and DC values of the altered regions were normally distributed. Sleep efficiency, sleep onset latency, and the number of awakenings had a non-normal distribution. In comparison with pre-training, patients with CID showed significant differences in PSQI, ISI, BDI, and HAMA in post-training ($p < 0.05$; **Table 1**). However, HAMD, total sleep time, sleep efficiency, sleep onset latency, and the number of awakenings showed no remarkable differences.

Degree Centrality Analysis

The results of altered binary DC maps are shown in **Figure 2**. Detailed information on activation centers are provided in **Table 2** and **Supplementary Table 1**. All results were set at voxel-level ($p < 0.01$), cluster-level ($p < 0.05$), and $t = 2.77$ (GRF-corrected). The results clearly showed a highly similar altered binary DC in several thresholds at $r = 0.15$, 0.20, 0.25, 0.30, 0.35. Besides, the weighted version of DC, which assures the robustness of the findings with nearly identical results, is shown in **Supplementary Figure 1**. The present study reports the results of DC at the correlation threshold of 0.25 as previously described (Yan et al., 2018, 2020). After rtfMRI-NF training, DC increased in the right postcentral gyrus (PoCG), Rolandic operculum (ROL), insula, and superior parietal gyrus (SPG) and decreased in the right supramarginal gyrus (SMG), inferior

TABLE 2 | Brain regions exhibited altered DC at $r = 0.25$ (post-training vs. pre-training).

Brain regions	Whole cluster size	Cluster size	MNI coordinates			*t* score
			x	y	z	
R Postcentral gyrus	405	76	39	−30	42	3.961
R Rolandic operculum		71	48	−21	21	5.865
R Insula		56	33	−6	12	5.388
R Superior parietal gyrus		20	24	−51	60	3.821
R Supramarginal gyrus	524	157	60	−42	36	−7.105
R Inferior parietal gyrus		99	51	−42	45	−4.831
R Angular gyrus		86	33	−54	42	−4.883
R Middle occipital gyrus		60	33	−75	30	−3.688
R Middle temporal gyrus		46	48	−69	21	−3.527

Results were set at voxel-level: $p < 0.01$, cluster-level: $p < 0.05$, $t = 2.77$ (Gaussian random field corrected). DC, degree centrality; R, right; MNI, Montreal Neurological Institute.

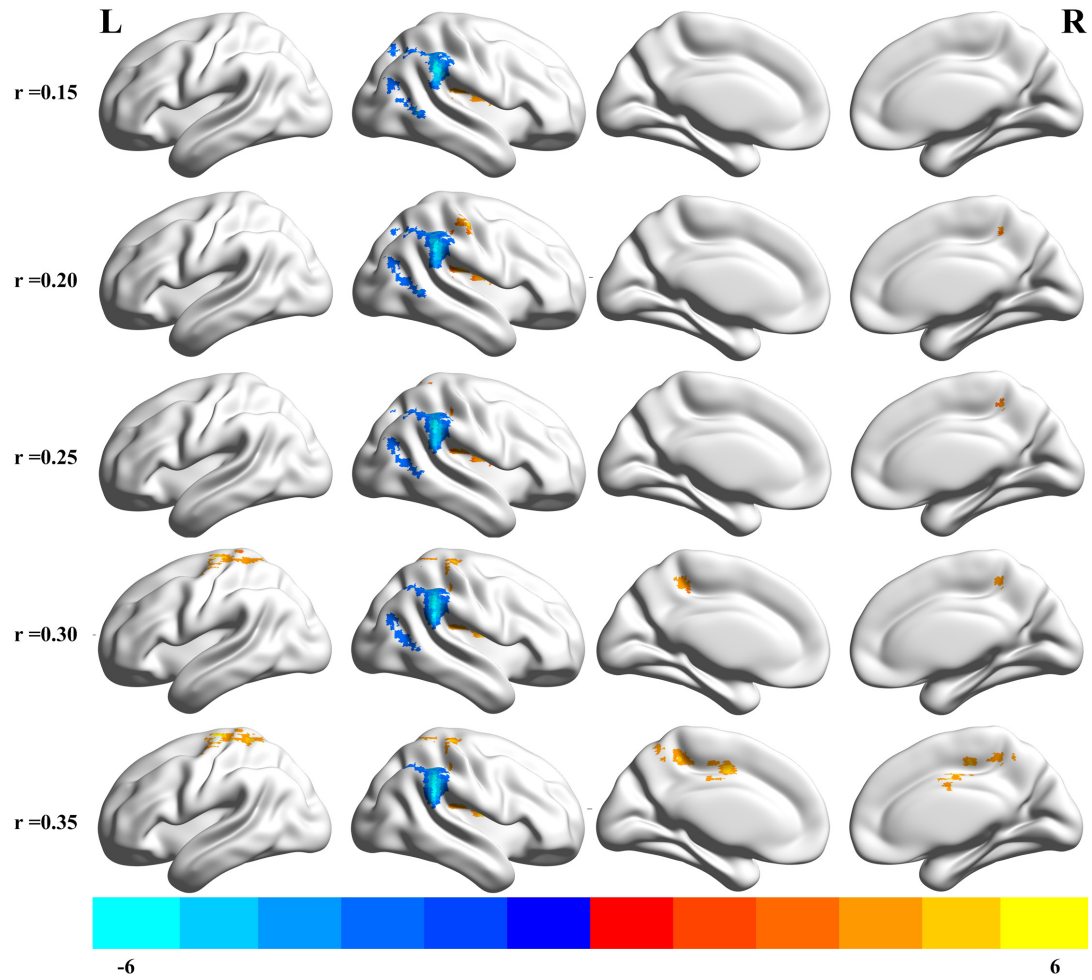

FIGURE 2 | Brain areas that exhibited altered binary DC induced by real-time fMRI neurofeedback training using different cut off thresholds (r = 0.15, 0.20, 0.25, 0.30, 0.35). Results were set at voxel-level $p < 0.01$, cluster-level $p < 0.05$, and $t = 2.77$ (Gaussian random field corrected). Warm colors indicate regions in which DC remarkably increased, whereas cool colors indicate regions in which DC remarkably decreased. The color bar indicates the t value. DC, degree centrality; L, left; R, right.

parietal gyrus (IPG), angular gyrus (ANG), middle occipital gyrus (MOG), and middle temporal gyrus (MTG).

Seed-Based Functional Connectivity Analysis

We examined the FC of altered DC regions with whole-brain regions to backtrack the connectivity patterns. Results were set at voxel-level ($p < 0.01$), cluster-level ($p < 0.05$), and $t = 2.77$ (GRF-corrected). The detailed information of the activated brain regions is specified in **Figures 3**, **4** and **Supplementary Tables 2**, **3**. Our results indicate increased or decreased FC with regions of altered DC across the whole brain. Increased FC was observed within the prefrontal cortex, frontal cortex, parietal cortex, occipital cortex, temporal cortex, and subcortex. Decreased FC was observed within the prefrontal cortex, parietal cortex, occipital cortex, temporal cortex, and subcortex. However, no cluster survived at voxel-level $p < 0.01$ in the seeds of MOG and MTG.

Brain–Behavior Correlation Analysis

As shown in **Figure 5**, significant positive correlation was found between the changed ISI score (post-training minus pre-training) and DC values of the right insula after rtfMRI-NF training ($r = 0.425$, $p = 0.034$). The other changed clinical scores and indexes of PSG had no remarkable correlations with the DC values of altered brain regions.

DISCUSSION

By using resting-state fMRI technology combined with voxel-vise DC approach, we explored whether the functional hubs in patients with CID could be regulated by rtfMRI-NF training with improved clinical symptoms. The results validated our prior hypothesis that patients with CID showed altered DC and decreased clinical scores after rtfMRI-NF training. DC increased in the right PoCG, ROL, insula, and SPG and decreased in the

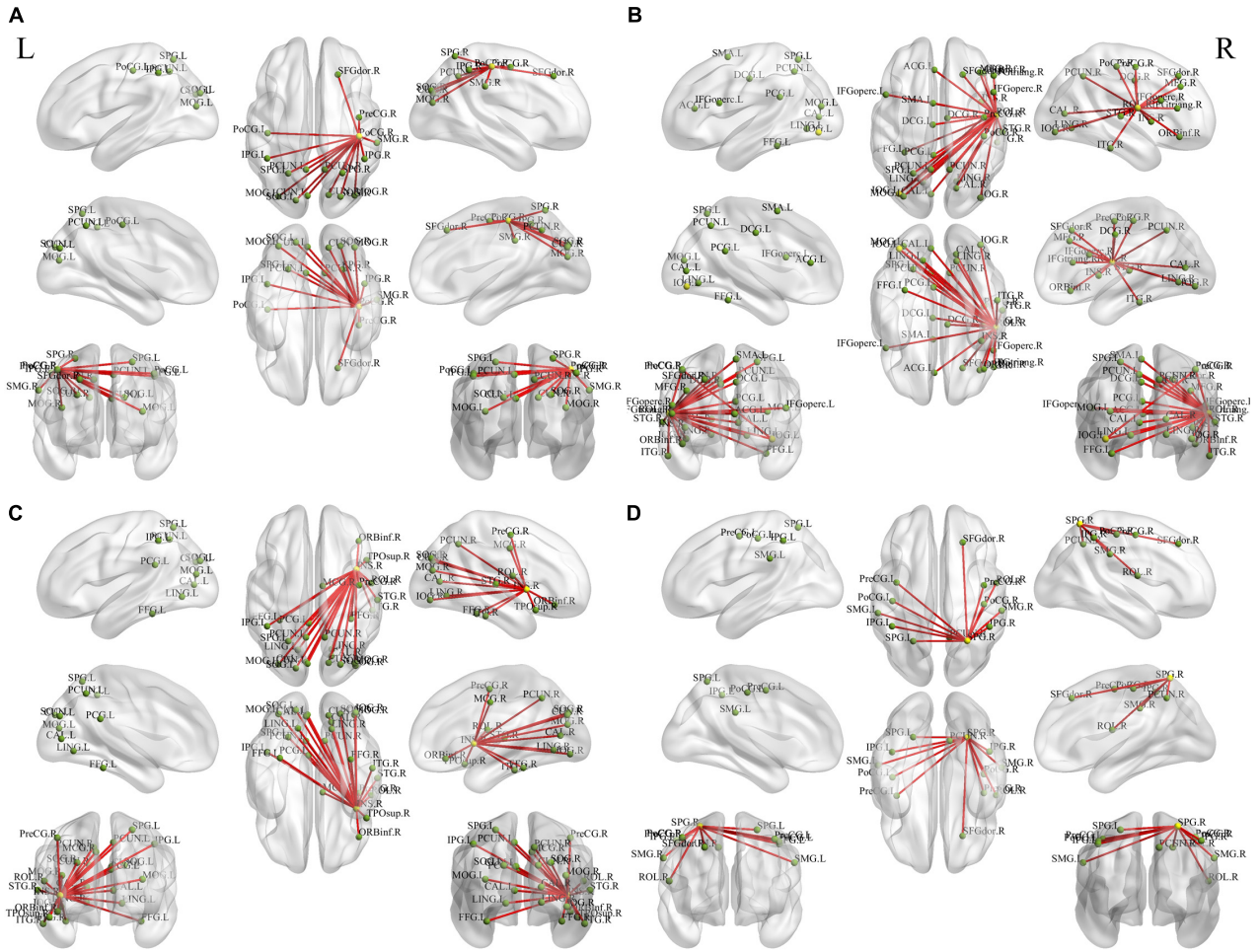

FIGURE 3 | Holistic view of the differences in seed-based (increased DC regions) FC between pre- and post-training in patients with chronic insomnia disorder. Results were set at voxel level $p < 0.01$, cluster-level $p < 0.05$, and $t = 2.77$ (Gaussian random field corrected). The seed regions are represented by yellow nodes, including the right postcentral gyrus **(A)**, Rolandic operculum **(B)**, insula **(C)**, and superior parietal gyrus **(D)**. The red lines represent increased FC strength. The abbreviations for brain regions are listed in **Supplementary Table 2**. DC, degree centrality; FC, functional connectivity; L, left; R, right.

right SMG, IPG, ANG, MOG, and MTG. The seed-based FC analyses based on the altered DC regions showed more details about the altered functional networks. Clinical scores, including PSQI, ISI, BDI, and HAMA scores, decreased. Furthermore, a remarkable positive correlation was found between the changed ISI score and DC values of the right insula after rtfMRI-NF training. These results support our hypothesis that rtfMRI-NF training could change brain DC and improve the sleep of patients with CID.

The insula of the salience network plays key roles in saliency detection, decision-making, motor/sensory processes, emotion and attention regulation, and cognition (Uddin, 2015). Patients with CID exhibit insula abnormalities in task and rest (Martin et al., 2015; Liu et al., 2016; Lu et al., 2017). During an immediate and impulsive monetary decision task, patients with CID show smaller activations in the bilateral insula than HCs (Martin et al., 2015). Liu et al. (2016) found a decreased fractional amplitude of low-frequency fluctuation (ALFF) in the left anterior insula and bilateral posterior insula. In comparison with the non-early improvement group, the early improvement group following treatment with antidepressants had stronger FC between the right anterior insula and left dorsolateral prefrontal cortex (Yuan et al., 2020). Therefore, the resting-state FC between the insula and other regions may represent an early symptom improvement in self-perceptual anxiety and insomnia. By using the insula as the target of rtfMRI-NF training, Yao et al. (2016) discovered an increase in the FC of the insula with the superior temporal gyrus, IPG, posterior cingulate cortex, insula, and cuneus after training. The enhanced FC network in our study is consistent with the above study (**Figure 3C** and **Supplementary Table 2**). By using the same method of voxel-wise DC, Huang et al. (2017) and Liu et al. (2018) both found decreased FC in the bilateral insula of patients with CID and a positive linear correlation between the strength of FC pairs between the right and left insula and the HAMA score. Notably, the DC of the right insula decreased, and a significant positive correlation ($r = 0.425$, $p = 0.034$, **Figure 5**)

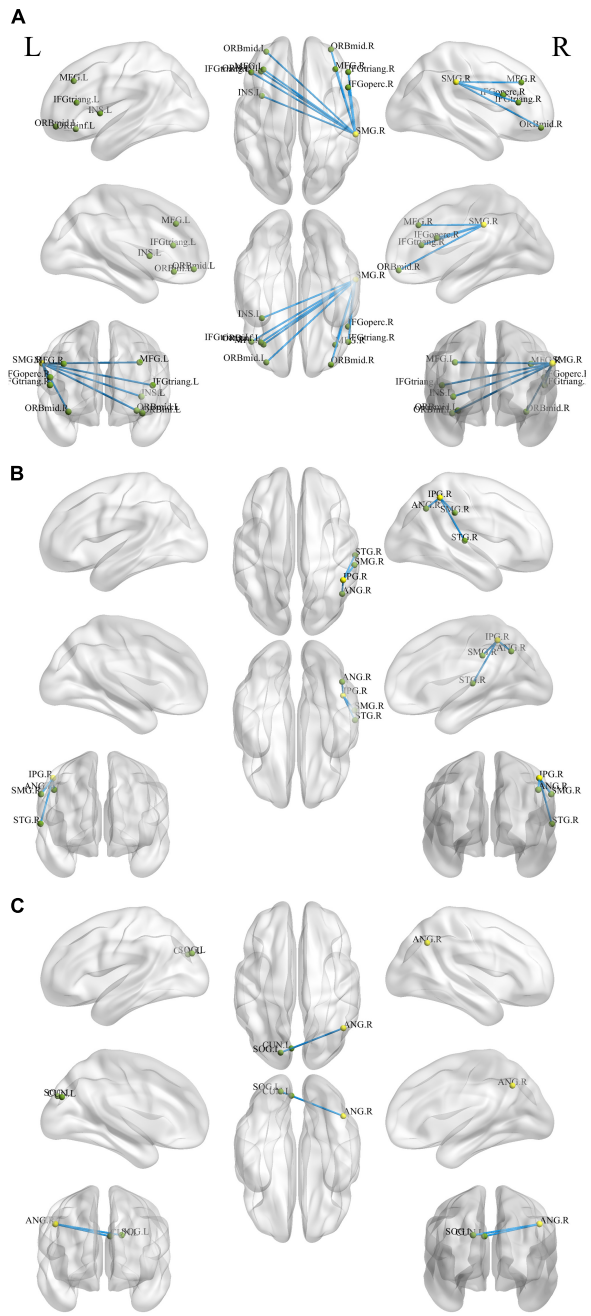

FIGURE 4 | Holistic view of the differences in seed-based (decreased DC regions) FC between pre- and post-training in patients with chronic insomnia disorder. Results were set at voxel level $p < 0.01$, cluster-level $p < 0.05$, and $t = 2.77$ (Gaussian random field corrected). The seed regions are represented by yellow nodes, including the right supramarginal gyrus **(A)**, inferior parietal gyrus **(B)**, and angular gyrus **(C)**. The blue lines represent decreased FC strength. The abbreviations for brain regions are listed in **Supplementary Table 3**. DC, degree centrality; FC, functional connectivity; L, left; R, right.

was found between the changed ISI score and DC values of the right insula after rtfMRI-NF training. In summary, rtfMRI-NF training may enhance the FC of the insula in patients with CID within these networks, and this phenomenon is associated with a broad range of emotional processing and emotion regulation ability to improve sleep. Moreover, the insula may be a target for rtfMRI-NF training. However, more studies are needed to confirm these findings.

In the present study, we discovered that patients with CID showed increased DC in the parietal cortex, including PoCG and SPG. The PoCG is the main receptive region for external stimuli as the location of the primary somatosensory cortex (Joo et al., 2013). Gray matter volume (GMV) in the right PoCG is reduced in patients with CID (Joo et al., 2013; Chou et al., 2021). Moreover, sleep latency and quality are negatively correlated with GMV in the right PoCG (Joo et al., 2013; Chou et al., 2021). Relative to HCs, regions with decreased integrity of structural covariance were observed in the bilateral PoCG (Chou et al., 2021). Therefore, the PoCG structure network of the patient with CID was disrupted. By using the bilateral PoCG as seed, Dai et al. (2020) reported decreased FC with cuneus (positively correlated with CID duration) and with superior frontal gyrus (SFG). A recent meta-analysis also found reduced frontal–parietal activation following sleep deprivation (Ma et al., 2015). Based on seed-based FC analysis, our study found that the right PoCG showed increased FC with the cuneus and dorsolateral SFG (**Figure 3A** and **Supplementary Table 2**). Therefore, rtfMRI-NF training could reshape the disrupted FC of PoCG. Thus, the increased DC of the PoCG suggests that rtfMRI-NF training may enhance the patient's ability to process external information.

The SPG is critically important for the manipulation of information in spatial working memory (Koenigs et al., 2009). The SPG of patients with CID showed lower activation during a spatial memory task (Li Y. et al., 2016). Based on seed-based FC analysis, patients with CID had weaker connectivity between the right SFG and bilateral SPG (Li et al., 2014). Li et al. (2018) reported reduced FC in the regions of the right fronto-parietal network, including SFG and SPG, in patients with CID compared with HC. Patients with CID have deficits in working memory tasks and several attentional processes (Koenigs et al., 2009; Li et al., 2014, 2018; Li Y. et al., 2016). After rtfMRI-NF training, we found that the SPG had enhanced interaction with regions in the default mode network (DMN), including the dorsolateral SFG, IPG, and precuneus (**Figure 3D** and **Supplementary Table 2**). Kay et al. (2016) found that the SPG with abnormal metabolism might be a meaningful target for cognitive training, mindfulness meditation, or repetitive TMS. Therefore, the increased DC of the SPG might enhance the working memory and attention process capacity of patients with CID.

The ROL plays a recognized role in various neurologic and psychiatric conditions (Mălîia et al., 2018; Sutoko et al., 2020). Its complex functions include sensory, motor, autonomic, cognitive, and emotion processing. These functions are implemented by highly specialized neuronal populations and their widespread connections (Mălîia et al., 2018). Sutoko et al. (2020) found that the high severity level in other psychological domains (e.g., apathy, depression, and anxiety) is associated with the high lesion degree at the right ROL. Janse et al. (2019) reported that compared with neutral images, the ROL has reduced neural response to emotional images in alcohol-dependent patients

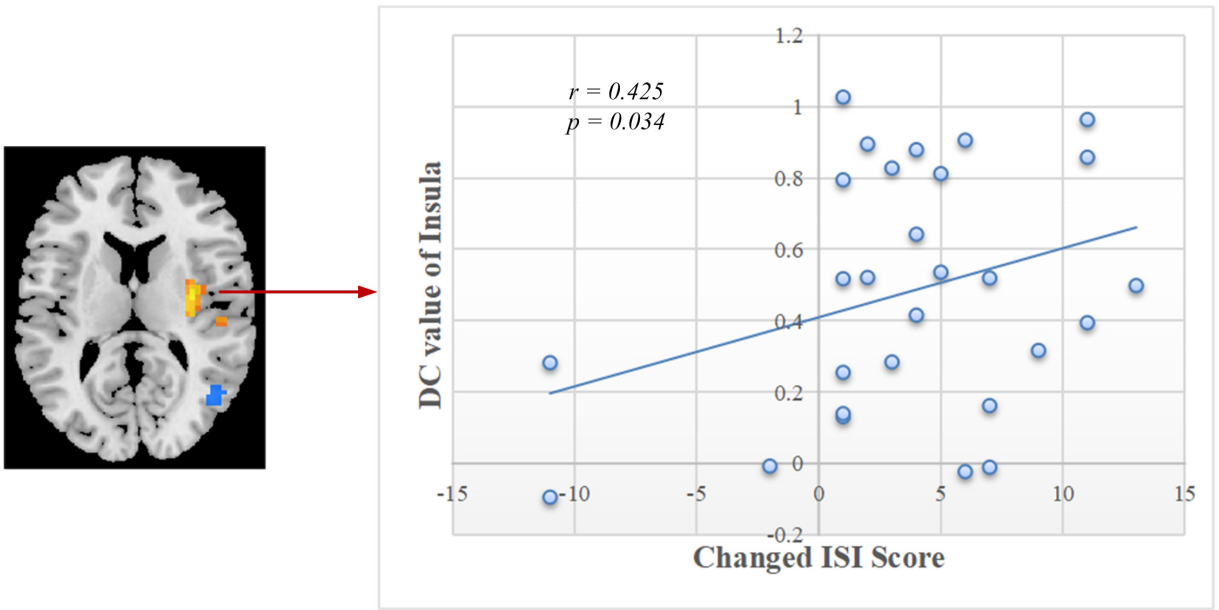

FIGURE 5 | Correlation between the changed ISI scores and DC values of the right insula in post-training. ISI, Insomnia Severity Index; DC, degree centrality.

versus HCs. In comparison with HCs, Huang et al. (2017) found decreased FC between left insula and left ROL in patients with CID. Moreover, simultaneous enhancement and reduction of connections were observed with the right ROL (Fasiello et al., 2021). In the present study, increased FC between right ROL and right insula was found after rtfMRI-NF training (**Figure 3B** and **Supplementary Table 2**). Hence, rtfMRI-NF training may enhance the CID emotion processing ability by enhancing the ROL's connections with other related brain regions.

The MTG, IPG, ANG, and SMG are important hubs of DMN (Raichle et al., 2001; Fox and Raichle, 2007; Nie et al., 2015) that showed decreased DC after rtfMRI-NF training. The DMN plays a central role in the modulation of consciousness and is associated with self-referential mental activity, emotional and episodic memory processing, or mind wandering when individuals are not focused on the external environment (Raichle et al., 2001; Nie et al., 2015). CID may be conceptualized as a disorder associated with the overactivity of certain brain areas of the DMN (Buysse et al., 2011; Marques et al., 2015). The widespread hyperarousal of several systems (e.g., cognitive, physiological, emotional) occurs during insomnia, thus preventing relaxation (Marques et al., 2015). The MTG is related to declarative memory, information retrieval, and cognitive processes (Squire et al., 2004; Wang et al., 2017). Patients with CID showed high regional homogeneity and ALFF values in the MTG (Dai et al., 2014; Li C. et al., 2016; Zhou et al., 2017). During an eye-closed resting-state condition, a high-density EEG study reported that patients with CID have higher beta activity than HCs in the right temporal lobe (Colombo et al., 2016). In comparison with HCs, patients with CID showed an increased response in the DMN (including right MTG) upon exposure to self-related words (Marques et al., 2018). Zhou et al. (2020) discovered increased short DC in the MTG compared with HCs. By using the ICA method, Marques et al. (2017) found that patients with CID exhibited increased activation in the right MTG and IPG compared with HCs. The IPG is a multimodal complex that receives somatosensory, visual, and auditory inputs and consists of the ANG and SMG (Leichnetz, 2011; Lee et al., 2018). Zhou et al. (2017) discovered that the ALFF of the right IPG increased, and this phenomenon is related to lower sleep quality and higher anxiety.

The ANG belongs to the posterior heteromodal association cortex and is involved in various cognitive functions, including attention, memory retrieval, conflict resolution, and theory of mind (Wei et al., 2019). Wei et al. (2019) reported that the right ANG is a hub of enhanced structural connectivity in CID. Hyperconnectivity within the identified subnetwork may contribute to increased reactivity to stimuli and may signify vulnerability to CID (Wei et al., 2019). The SMG and ANG share a similar role in somatosensory functions (Bjoertomt et al., 2009). Sleep diary-assessed sleep efficiency is inversely related to relative glucose metabolism in the right SMG (Kay et al., 2016). In comparison with the HCs, the CID group showed increased locus coeruleus noradrenergic FC in the left SMG and left MOG (Gong et al., 2021). The MOG is involved in visual and spatial information processing (Renier et al., 2010). These results support the hyperarousal hypothesis, in which patients with CID often show hyperperfusion in the sensory perception of tactile, visual, and auditory stimuli (Kay and Buysse, 2017; Gong et al., 2021). After rtfMRI-NF training, the FC of the SMG decreased with brain regions located in the prefrontal and subcortical regions, including the middle frontal gyrus, inferior frontal gyrus, and insula (**Figure 4C** and **Supplementary Table 3**). The FC of IPG with SMG and ANG also decreased (**Figure 4B** and **Supplementary Table 3**). The reduced DC of the right IFG,

MTG, ANG, and SMG indicate a decreased interaction with other regions across the whole brain, and this condition may inhibit the processing of sensory information to avoid excessive activation, indicating the potential neurobiological mechanism in which rtfMRI-NF training improves the sleep of patients with CID.

After the intervention by amygdala-based rtfMRI-NF, the BDI, HAMA, ISI, and PSQI decreased, suggesting the improvement of mood state and sleep. During training, the subjects tried to increase the activity of amygdala by recalling positive autobiographical memory, which may enhance the affective or attentional significance of these memories. The amygdala is a critical region of the neural circuitry for emotion and is part of the salience network (Pessoa, 2010; Young et al., 2017). After training, we discovered increased DC region (insula) in the salience network, and altered DC regions outside it. These results indicated that positive autobiographical memory may promote the activity of amygdala and emotion regulation related brain circuits. The synergy between amygdala activity and positive autobiographical memory may drive the clinical improvements of mood state and sleep. The CID has a close relationship with depression and anxiety (Alvaro et al., 2013). Therefore, in the future treatment of CID, the patient's anxiety and depression should be considered at the same time.

CONCLUSION

In summary, our findings support our hypothesis that amygdala-based rtfMRI-NF training altered the intrinsic functional hubs and improved the sleep of patients with CID. Based on voxel-wise and seed-based FC, we discovered that rtfMRI-NF training reshaped the abnormal FC caused by insomnia. These findings improved our understanding of the neurobiological mechanism of rtfMRI-NF in the treatment of insomnia. However, additional double-blinded controlled clinical trials with larger sample sizes are necessary to confirm the effect of rtfMRI-NF from this initial study.

LIMITATIONS AND STRENGTHS

Several limitations should be considered in our study. First, a sham control group was not used, thus possibly decreasing the credibility of the conclusion. Patients with CID participating in experiment hope to improve sleep, thereby reducing the suffering of insomnia. Their compliance is greatly reduced; if they find the effect as not significant, they may realize that they are in the sham feedback group. Therefore, only an amygdala-based feedback group was included to ensure the training effect of patients with CID in this initial study. Accordingly, we intend to add three sham feedback sessions before three real feedback sessions in the future study. Second, the sample size of this study was small. Larger sample sizes are necessary to confirm the credibility of our results in this initial study. Third, this paper used a relatively loose threshold. Considering the lack of HC, the threshold was set at voxel-level $p < 0.01$ for comparing our results with previous studies (Huang et al., 2017; Liu et al., 2018; Yan et al., 2018), which may result in a high risk of false positives. However, when the threshold was set at voxel-level $p < 0.001$ (cluster-level $p < 0.05$, $t = 3.29$, GRF-corrected), the main altered brain regions remained, including ROL, insula, SMG, and IPG, except for PoCG, SPG, ANG, MOG, and MTG. Detail information is listed in **Supplementary Table 4**. Hence, the results should be carefully interpreted with regard to the brain regions which did not survive at voxel-level $p < 0.001$. In addition, although the participants were carefully instructed before the experiment and asked about their states during post-experiment scans, we could not ensure the sleep–wake state of the subjects during the resting-state scan without fMRI-compatible EEG. Thus, future studies have to adopt certain measures to monitor the state of the subjects.

DATA AVAILABILITY STATEMENT

The raw data supporting the conclusions of this article will be made available by the authors, without undue reservation.

ETHICS STATEMENT

The studies involving human participants were reviewed and approved by the Ethics Committee of the Henan Provincial People's Hospital. The patients/participants provided their written informed consent to participate in this study.

AUTHOR CONTRIBUTIONS

XL, ZL, ZZ, and XW conceived the study, analyzed the data, and wrote the manuscript. HG, CW, JZ, FY, and SD designed and performed the experiments. FQ, MZ, JH, XQ, and HZ collected the clinical samples and performed the experiments. LT and YL conceived the study, designed the experiments, supervised the project, and wrote the manuscript. All authors contributed to the article and approved the submitted version.

FUNDING

This study was supported by the National Natural Science Foundation of China (82071884), Scientific and Technological Project of Henan Provincial Department of Science and Technology (212102310737 and 222102310198), Young and Middle-aged Health Science and Technology Innovative Talent Cultivation Project of Henan Provincial-Leading Talents (YXKC2020004), Medical Science and Technology Research Plan of Henan Provincial (SB201901077).

SUPPLEMENTARY MATERIAL

The Supplementary Material for this article can be found online at: https://www.frontiersin.org/articles/10.3389/fnmol.2022.825286/full#supplementary-material

REFERENCES

Alvaro, P. K., Roberts, R. M., and Harris, J. K. (2013). A systematic review assessing bidirectionality between sleep disturbances, anxiety, and depression. *Sleep* 36, 1059–1068. doi: 10.5665/sleep.2810

Baglioni, C., Spiegelhalder, K., Lombardo, C., and Riemann, D. (2010). Sleep and emotions: a focus on insomnia. *Sleep Med. Rev.* 14, 227–238. doi: 10.1016/j.smrv.2009.10.007

Baglioni, C., Spiegelhalder, K., Regen, W., Feige, B., Nissen, C., Lombardo, C., et al. (2014). Insomnia disorder is associated with increased amygdala reactivity to insomnia-related stimuli. *Sleep* 37, 1907–1917. doi: 10.5665/sleep.4240

Bjoertomt, O., Cowey, A., and Walsh, V. (2009). Near space functioning of the human angular and supramarginal gyri. *J. Neuropsychol.* 3, 31–43. doi: 10.1348/174866408X394604

Buysse, D. J., Germain, A., Hall, M., Monk, T. H., and Nofzinger, E. A. (2011). A neurobiological model of insomnia. *Drug Discov. Today Dis. Models* 8, 129–137. doi: 10.1016/j.ddmod.2011.07.002

Buysse, D. J., Rush, A. J., and Reynolds, C. F. (2017). Clinical management of insomnia disorder. *JAMA* 318, 1973–1974. doi: 10.1001/jama.2017.15683

Chou, K. H., Lee, P. L., Liang, C. S., Lee, J. T., Kao, H. W., Tsai, C. L., et al. (2021). Identifying neuroanatomical signatures in insomnia and migraine comorbidity. *Sleep* 44:zsaa202. doi: 10.1093/sleep/zsaa202

Colombo, M. A., Ramautar, J. R., Wei, Y., Gomez-Herrero, G., Stoffers, D., Wassing, R., et al. (2016). Wake high-density electroencephalographic spatiospectral signatures of insomnia. *Sleep* 39, 1015–1027. doi: 10.5665/sleep.5744

Dai, X. J., Liu, B. X., Ai, S., Nie, X., Xu, Q., Hu, J., et al. (2020). Altered inter-hemispheric communication of default-mode and visual networks underlie etiology of primary insomnia. *Brain Imag. Behav.* 14, 1430–1444. doi: 10.1007/s11682-019-00064-0

Dai, X. J., Peng, D. C., Gong, H. H., Wan, A. L., Nie, X., Li, H. J., et al. (2014). Altered intrinsic regional brain spontaneous activity and subjective sleep quality in patients with chronic primary insomnia: a resting-state fMRI study. *Neuropsychiatr. Dis. Treat.* 10:2163. doi: 10.2147/NDT.S69681

Dichter, G. S., Gibbs, D., and Smoski, M. J. (2015). A systematic review of relations between resting-state functional-MRI and treatment response in major depressive disorder. *J. Affect. Disord.* 172, 8–17. doi: 10.1016/j.jad.2014.09.028

Fasiello, E., Gorgoni, M., Scarpelli, S., Alfonsi, V., Strambi, L. F., and De Gennaro, L. (2021). Functional connectivity changes in Insomnia disorder: a systematic review. *Sleep Med. Rev.* 61:101569. doi: 10.1016/j.smrv.2021.101569

Fox, M. D., and Raichle, M. E. (2007). Spontaneous fluctuations in brain activity observed with functional magnetic resonance imaging. *Nature Rev. Neurosci.* 8, 700–711. doi: 10.1038/nrn2201

Gao, M., Feng, N., Liu, X., Sun, J., Hou, G., Zhang, L., et al. (2021). Abnormal degree centrality in lifelong premature ejaculation patients: an fMRI study. *Brain Imag. Behav.* 15, 1412–1419. doi: 10.1007/s11682-020-00340-4

Gong, L., Shi, M., Wang, J., Xu, R., Yu, S., Liu, D., et al. (2021). The abnormal functional connectivity in the locus coeruleus-norepinephrine system associated with anxiety symptom in chronic insomnia disorder. *Front. Neurosci.* 15:522. doi: 10.3389/fnins.2021.678465

Huang, S., Zhou, F., Jiang, J., Huang, M., Zeng, X., Ding, S., et al. (2017). Regional impairment of intrinsic functional connectivity strength in patients with chronic primary insomnia. *Neuropsychiatr. Dis. Treat.* 13:1449. doi: 10.2147/NDT.S137292

Huang, Z., Liang, P., Jia, X., Zhan, S., Li, N., Ding, Y., et al. (2012). Abnormal amygdala connectivity in patients with primary insomnia: evidence from resting state fMRI. *Eur. J. Radiol.* 81, 1288–1295. doi: 10.1016/j.ejrad.2011.03.029

Janse, J. M., van den Heuvel, O. A., van der Werf, Y. D., De Wit, S. J., Veltman, D. J., Van Den Brink, W., et al. (2019). Emotion processing, reappraisal, and craving in alcohol dependence: a functional magnetic resonance imaging study. *Front. Psychiatry* 10:227. doi: 10.3389/fpsyt.2019.00227

Joo, E. Y., Noh, H. J., Kim, J. S., Koo, D. L., Kim, D., Hwang, K. J., et al. (2013). Brain gray matter deficits in patients with chronic primary insomnia. *Sleep* 36, 999–1007. doi: 10.5665/sleep.2796

Kay, D. B., and Buysse, D. J. (2017). Hyperarousal and beyond: new insights to the pathophysiology of insomnia disorder through functional neuroimaging studies. *Brain Sci.* 7:23. doi: 10.3390/brainsci7030023

Kay, D. B., Karim, H. T., Soehner, A. M., Hasler, B. P., Wilckens, K. A., James, J. A., et al. (2016). Sleep-wake differences in relative regional cerebral metabolic rate for glucose among patients with insomnia compared with good sleepers. *Sleep* 39, 1779–1794. doi: 10.5665/sleep.6154

Koenigs, M., Barbey, A. K., Postle, B. R., and Grafman, J. (2009). Superior parietal cortex is critical for the manipulation of information in working memory. *J. Neurosci.* 29, 14980–14986. doi: 10.1523/JNEUROSCI.3706-09.2009

Koush, Y., Ashburner, J., Prilepin, E., Sladky, R., Zeidman, P., Bibikov, S., et al. (2017). OpenNFT: an open-source Python/Matlab framework for real-time fMRI neurofeedback training based on activity, connectivity and multivariate pattern analysis. *Neuroimage* 156, 489–503. doi: 10.1016/j.neuroimage.2017.06.039

Lee, Y. J. G., Kim, S., Kim, N., Choi, J. W., Park, J., Kim, S. J., et al. (2018). Changes in subcortical resting-state functional connectivity in patients with psychophysiological insomnia after cognitive-behavioral therapy. *Neuroimage Clin.* 17, 115–123. doi: 10.1016/j.nicl.2017.10.013

Leichnetz, G. R. (2011). *Supramarginal Gyrus. Encyclopedia of Clinical Neuropsychology*. New York, NY: Springer, 180. doi: 10.1007/978-0-387-79948-3_369

Li, C., Ma, X., Dong, M., Yin, Y. I., Hua, K., Li, M., et al. (2016). Abnormal spontaneous regional brain activity in primary insomnia: a resting-state functional magnetic resonance imaging study. *Neuropsychiatr. Dis. Treat.* 12:1371. doi: 10.2147/NDT.S109633

Li, S., Tian, J., Li, M., Wang, T., Lin, C., Yin, Y., et al. (2018). Altered resting state connectivity in right side frontoparietal network in primary insomnia patients. *Eur. Radiol.* 28, 664–672. doi: 10.1007/s00330-017-5012-8

Li, Y., Liu, L., Wang, E., Zhang, H., Dou, S., Tong, L., et al. (2016). Abnormal neural network of primary insomnia: evidence from spatial working memory task fMRI. *Eur. Neurol.* 75, 48–57. doi: 10.1159/000443372

Li, Y., Wang, E., Zhang, H., Dou, S., Liu, L., Tong, L., et al. (2014). Functional connectivity changes between parietal and prefrontal cortices in primary insomnia patients: evidence from resting-state fMRI. *Eur. J. Med. Res.* 19, 1–7. doi: 10.1186/2047-783X-19-32

Liu, C. H., Liu, C. Z., Zhang, J., Yuan, Z., Tang, L. R., Tie, C. L., et al. (2016). Reduced spontaneous neuronal activity in the insular cortex and thalamus in healthy adults with insomnia symptoms. *Brain Res.* 1648, 317–324. doi: 10.1016/j.brainres.2016.07.024

Liu, X., Zheng, J., Liu, B. X., and Dai, X. J. (2018). Altered connection properties of important network hubs may be neural risk factors for individuals with primary insomnia. *Sci. Rep.* 8, 1–13. doi: 10.1038/s41598-018-23699-3

Lu, F. M., Liu, C. H., Lu, S. L., Tang, L. R., Tie, C. L., Zhang, J., et al. (2017). Disrupted topology of frontostriatal circuits is linked to the severity of insomnia. *Front. Neurosci.* 11:214. doi: 10.3389/fnins.2017.00214

Ma, N., Dinges, D. F., Basner, M., and Rao, H. (2015). How acute total sleep loss affects the attending brain: a meta-analysis of neuroimaging studies. *Sleep* 38, 233–240. doi: 10.5665/sleep.4404

Mălîia, M. D., Donos, C., Barborica, A., Popa, I., Ciurea, J., Cinatti, S., et al. (2018). Functional mapping and effective connectivity of the human operculum. *Cortex* 109, 303–321. doi: 10.1016/j.cortex.2018.08.024

Marques, D. R., Gomes, A. A., Clemente, V., dos Santos, J. M., and Castelo-Branco, M. (2015). Default-mode network activity and its role in comprehension and management of psychophysiological insomnia: a new perspective. *New Ideas Psychol.* 36, 30–37. doi: 10.1016/j.newideapsych.2014.08.001

Marques, D. R., Gomes, A. A., Clemente, V., dos Santos, J. M., Duarte, I. C., Caetano, G., et al. (2018). Self-referential dysfunction and default-mode hyperactivation in psychophysiological insomnia patients: a case-control fMRI study. *J. Psychophysiol.* 32:140. doi: 10.1027/0269-8803/a000194

Marques, D. R., Gomes, A. A., Clemente, V., dos Santos, J. M., Duarte, I. C., Caetano, G., et al. (2017). Unbalanced resting-state networks activity in psychophysiological insomnia. *Sleep Biol. Rhythms.* 15, 167–177. doi: 10.1007/s41105-017-0096-8

Martin, L. E., Pollack, L., McCune, A., Schulte, E., Savage, C. R., and Lundgren, J. D. (2015). Comparison of obese adults with poor versus good sleep quality during a functional neuroimaging delay discounting task:

a pilot study. *Psychiatry Res.* 234, 90–95. doi: 10.1016/j.pscychresns.2015.08.011

Morgenroth, E., Saviola, F., Gilleen, J., Allen, B., Lührs, M., Eysenck, M. W., et al. (2020). Using connectivity-based real-time fMRI neurofeedback to modulate attentional and resting state networks in people with high trait anxiety. *Neuroimage* 25:102191. doi: 10.1016/j.nicl.2020.102191

Nie, X., Shao, Y., Liu, S. Y., Li, H. J., Wan, A. L., Nie, S., et al. (2015). Functional connectivity of paired default mode network subregions in primary insomnia. *Neuropsychiatr. Dis. Treat.* 11:3085. doi: 10.2147/NDT.S95224

Pessoa, L. (2010). Emotion and cognition and the amygdala: from "what is it?" to "what's to be done?". *Neuropsychologia* 48, 3416–3429. doi: 10.1016/j.neuropsychologia.2010.06.038

Qaseem, A., Kansagara, D., Forciea, M. A., Cooke, M., and Denberg, T. D. (2016). Clinical guidelines committee of the american college of physicians. Management of chronic insomnia disorder in adults: a clinical practice guideline from the american college of physicians. *Ann. Int. Med.* 165, 125–133. doi: 10.7326/M15-2175

Raichle, M. E., MacLeod, A. M., Snyder, A. Z., Powers, W. J., Gusnard, D. A., and Shulman, G. L. (2001). A default mode of brain function. *Proc. Natl. Acad. Sci. U.S.A.* 98, 676–682. doi: 10.1073/pnas.98.2.676

Renier, L. A., Anurova, I., De Volder, A. G., Carlson, S., VanMeter, J., and Rauschecker, J. P. (2010). Preserved functional specialization for spatial processing in the middle occipital gyrus of the early blind. *Neuron.* 68, 138–148. doi: 10.1016/j.neuron.2010.09.021

Samantha, J. F., Sarah, F. D., Thushini, M., and Reza, M. (2020). A guide to literature informed decisions in the design of real time fmri neurofeedback studies: a systematic review. *Front. Hum. Neurosci.* 14:60. doi: 10.3389/fnhum.2020.00060

Sateia, M. J., Buysse, D. J., Krystal, A. D., Neubauer, D. N., and Heald, J. L. (2017). Clinical practice guideline for the pharmacologic treatment of chronic insomnia in adults: an American academy of sleep medicine clinical practice guideline. *J. Clin. Sleep Med.* 13, 307–349. doi: 10.5664/jcsm.6470

Spiegelhalde, R. K., Regen, W., Baglioni, C., Nissen, C., Riemann, D., and Kyle, S. D. (2015). Neuroimaging insights into insomnia. *Curr. Neurol. Neurosci. Rep.* 15, 1–7. doi: 10.1007/s11910-015-0527-3

Squire, L. R., Stark, C. E., and Clark, R. E. (2004). The medial temporal lobe. *Annu. Rev. Neurosci.* 27, 279–306. doi: 10.1146/annurev.neuro.27.070203.144130

Sutoko, S., Atsumori, H., Obata, A., Funane, T., Kandori, A., Shimonaga, K., et al. (2020). Lesions in the right rolandic operculum are associated with self-rating affective and apathetic depressive symptoms for post-stroke patients. *Sci. Rep.* 10, 1–10. doi: 10.1038/s41598-020-77136-5

Tsuchiyagaito, A., Smith, J. L., El-Sabbagh, N., Zotev, V., Misaki, M., Al Zoubi, O., et al. (2021). Real-time fMRI neurofeedback amygdala training may influence kynurenine pathway metabolism in major depressive disorder. *Neuroimage* 29:102559. doi: 10.1016/j.nicl.2021.102559

Tursic, A., Eck, J., Lührs, M., Linden, D. E., and Goebel, R. (2020). A systematic review of fMRI neurofeedback reporting and effects in clinical populations. *Neuroimage* 28:102496. doi: 10.1016/j.nicl.2020.102496

Uddin, L. Q. (2015). Salience processing and insular cortical function and dysfunction. *Nat. Rev. Neurosci.* 16, 55–61. doi: 10.1038/nrn3857

Wang, L., Hermens, D. F., Hickie, I. B., and Lagopoulos, J. (2012). A systematic review of resting-state functional-MRI studies in major depression. *J. Affect. Disord.* 142, 6–12. doi: 10.1016/j.jad.2012.04.013

Wang, T., Yan, J., Li, S., Zhan, W., Ma, X., Xia, L., et al. (2017). Increased insular connectivity with emotional regions in primary insomnia patients: a resting-state fMRI study. *Eur. Radiol.* 27, 3703–3709. doi: 10.1007/s00330-016-4680-0

Watanabe, T., Sasaki, Y., Shibata, K., and Kawato, M. (2017). Advances in fMRI real-time neurofeedback. *Trends Cogn. Sci.* 21, 997–1010. doi: 10.1016/j.tics.2017.09.010

Wei, Y., Bresser, T., Wassing, R., Stoffers, D., Van Someren, E. J., and Foster-Dingley, J. C. (2019). Brain structural connectivity network alterations in insomnia disorder reveal a central role of the right angular gyrus. *Neuroimage Clin.* 24:102019. doi: 10.1016/j.nicl.2019.102019

Weiskopf, N. (2012). Real-time fMRI and its application to neurofeedback. *Neuroimage* 62, 682–692. doi: 10.1016/j.neuroimage.2011.10.009

Yan, C. G., Wang, X. D., Zuo, X. N., and Zang, Y. F. (2016). DPABI: data processing & analysis for (resting-state) brain imaging. *Neuroinformatics* 14, 339–351. doi: 10.1007/s12021-016-9299-4

Yan, C. Q., Huo, J. W., Wang, X., Zhou, P., Zhang, Y. N., Li, J. L., et al. (2020). Different degree centrality changes in the brain after acupuncture on contralateral or ipsilateral acupoint in patients with chronic shoulder pain: a resting-state fMRI study. *Neural plasticity* 2020:5701042. doi: 10.1155/2020/5701042

Yan, C. Q., Wang, X., Huo, J. W., Zhou, P., Li, J. L., Wang, Z. Y., et al. (2018). Abnormal global brain functional connectivity in primary insomnia patients: a resting-state functional MRI study. *Front. Neurol.* 9:856. doi: 10.3389/fneur.2018.00856

Yao, S., Becker, B., Geng, Y., Zhao, Z., Xu, X., Zhao, W., et al. (2016). Voluntary control of anterior insula and its functional connections is feedback-independent and increases pain empathy. *Neuroimage.* 130, 230–240. doi: 10.1016/j.neuroimage.2016.02.035

Young, K. D., Siegle, G. J., Zotev, V., Phillips, R., Misaki, M., Yuan, H., et al. (2017). Randomized clinical trial of real-time fMRI amygdala neurofeedback for major depressive disorder: effects on symptoms and autobiographical memory recall. *Am. J. Psychiatry* 174, 748–755. doi: 10.1176/appi.ajp.2017.16060637

Yuan, H., Zhu, X., Tang, W., Cai, Y., Shi, S., and Luo, Q. (2020). Connectivity between the anterior insula and dorsolateral prefrontal cortex links early symptom improvement to treatment response. *J. Affect. Disord.* 260, 490–497. doi: 10.1016/j.jad.2019.09.041

Zhao, W. R., Li, C. Y., Chen, J. J., and Lei, X. (2020). Insomnia disorder and hyperarousal: evidence from resting-state and sleeping EEG (in Chinese). *Sci. Sin. Vitae.* 50, 270–286. doi: 10.1360/SSV-2019-0234

Zhou, F., Huang, S., Zhuang, Y., Gao, L., and Gong, H. (2017). Frequency-dependent changes in local intrinsic oscillations in chronic primary insomnia: a study of the amplitude of low-frequency fluctuations in the resting state. *Neuroimage Clin.* 15, 458–465. doi: 10.1016/j.nicl.2016.05.011

Zhou, F., Zhu, Y., Zhu, Y., Huang, M., Jiang, J., He, L., et al. (2020). Altered long-and short-range functional connectivity density associated with poor sleep quality in patients with chronic insomnia disorder: a resting-state fMRI study. *Brain Behav.* 10:e01844. doi: 10.1002/brb3.1844

Zuo, X. N., and Xing, X. X. (2014). Test-retest reliabilities of resting-state FMRI measurements in human brain functional connectomics: a systems neuroscience perspective. *Neurosci. Biobehav. Rev.* 45, 100–118. doi: 10.1016/j.neubiorev.2014.05.009

Conflict of Interest: The authors declare that the research was conducted in the absence of any commercial or financial relationships that could be construed as a potential conflict of interest.

frontiers in Molecular Neuroscience

ORIGINAL RESEARCH
published: 24 February 2022
doi: 10.3389/fnmol.2022.778139

Early Fractional Amplitude of Low Frequency Fluctuation Can Predict the Efficacy of Transcutaneous Auricular Vagus Nerve Stimulation Treatment for Migraine Without Aura

Menghan Feng[1,2†], Yue Zhang[1†], Zeying Wen[2,3], Xiaoyan Hou[1], Yongsong Ye[1], Chengwei Fu[2], Wenting Luo[2] and Bo Liu[1]*

[1] Department of Radiology, The Second Affiliated Hospital of Guangzhou University of Chinese Medicine, Guangzhou, China, [2] The Second Clinical College, Guangzhou University of Chinese Medicine, Guangzhou, China, [3] Department of Radiology, The First Affiliated Hospital of Henan University of Chinese Medicine, Zhengzhou, China

OPEN ACCESS

Edited by:
Siyi Yu,
Chengdu University of Traditional Chinese Medicine, China

Reviewed by:
Penghong Liu,
First Hospital of Shanxi Medical University, China
Gaoxiong Duan,
Hospital of Guangxi University of Chinese Medicine, China
Jinping Liu,
Guilin Medical University, China

***Correspondence:**
Bo Liu
liubogzcm@163.com

[†] These authors share first authorship

Specialty section:
This article was submitted to Neuroplasticity and Development, a section of the journal Frontiers in Molecular Neuroscience

Received: 16 September 2021
Accepted: 25 January 2022
Published: 24 February 2022

Citation:
Feng M, Zhang Y, Wen Z, Hou X, Ye Y, Fu C, Luo W and Liu B (2022) Early Fractional Amplitude of Low Frequency Fluctuation Can Predict the Efficacy of Transcutaneous Auricular Vagus Nerve Stimulation Treatment for Migraine Without Aura. Front. Mol. Neurosci. 15:778139. doi: 10.3389/fnmol.2022.778139

Migraine is a common primary headache disorder. Transcutaneous auricular vagus nerve stimulation (taVNS) has been verified to be effective in patients with migraine without aura (MWoA). However, there are large interindividual differences in patients' responses to taVNS. This study aimed to explore whether pretreatment fractional amplitude of low frequency fluctuation (fALFF) features could predict clinical outcomes in MWoA patients after 4-week taVNS. Sixty MWoA patients and sixty well-matched healthy controls (HCs) were recruited, and migraineurs received 4-week taVNS treatment. Resting-state functional magnetic resonance imaging (rs-fMRI) data were collected, and the significant differences of fALFF were detected between MWoA patients and HCs using two-sample *t*-test. A mask of these significant regions was generated and used for subsequent analysis. The abnormal fALFF in the mask was used to predict taVNS efficacy for MWoA using a support vector regression (SVR) model combining with feature select of weight based on the LIBSVM toolbox. We found that (1) compared with HCs, MWoA patients exhibited increased fALFF in the left thalamus, left inferior parietal gyrus (IPG), bilateral precentral gyrus (PreCG), right postcentral gyrus (PoCG), and bilateral supplementary motor areas (SMAs), but decreased in the bilateral precuneus and left superior frontal gyrus (SFG)/medial prefrontal cortex (mPFC); (2) after 4-week taVNS treatment, the fALFF values significantly decreased in these brain regions based on the pretreatment comparison. Importantly, the decreased fALFF in the bilateral precuneus was positively associated with the reduction in the attack times (r = 0.357, p = 0.005, Bonferroni correction, 0.05/5), whereas the reduced fALFF in the right PoCG was negatively associated with reduced visual analog scale (VAS) scores (r = −0.267, p = 0.039, uncorrected); (3) the SVR model exhibited a good performance for prediction (r = 0.411, p < 0.001),which suggests that these extracted fALFF features could be used as reliable biomarkers to predict the treatment response of taVNS for MWoA patients. This study demonstrated that the baseline fALFF features have good potential for predicting

individualized treatment response of taVNS in MWoA patients, and those weight brain areas are mainly involved in the thalamocortical (TC) circuits, default mode network (DMN), and descending pain modulation system (DPMS). This will contribute to well understanding the mechanism of taVNS in treating MWoA patients and may help to screen ideal patients who respond well to taVNS treatment.

Keywords: migraine without aura (MWoA), transcutaneous auricular vagus nerve stimulation (taVNS), fractional amplitude of low frequency fluctuation (fALFF), functional magnetic resonance imaging (fMRI), support vector regression (SVR)

INTRODUCTION

Migraine, a common chronic neurological disorder, is characterized by recurrent headache and typically accompanied by nausea, photophobia, and sensitivities to light–sound–smell (Steiner et al., 2013). Migraine without aura (MWoA) subtype is the most prevalent type, which accounts for nearly 70% of the total (Rasmussen and Olesen, 1992). Currently, medication therapy for MWoA could provide pain control at 45 min to 48 h and easily lead to addiction and other adverse effects (Diener et al., 2012; Lanteri-Minet, 2014; Westergaard et al., 2014; Abu Bakar et al., 2016; Buse et al., 2016). Transcutaneous auricular vagus nerve stimulation (taVNS), one kind of non-invasive neuromodulation technique, has been verified to relieve headache intensity and reduce the frequency of migraine attacks for MWoA patients in several clinical trials (Luo W. et al., 2020; Zhang et al., 2021). Notably, despite the effectiveness of taVNS for MWoA, the efficacy varies considerably across different subjects. Therefore, identifying a valid and objective biomarker for treatment response will be of great importance as it could help screen ideal migraineurs to improve the clinical efficacy and avoid the waste of medical resources.

Resting-state functional magnetic resonance imaging (rs-fMRI) is an emerging non-invasive imaging technique, which could be used to identify brain areas of the aberrant functional activities through measuring the spontaneous brain activity by low-frequency fluctuations in blood oxygen level-dependent (BOLD) signals (Biswal et al., 1995; Guo et al., 2011; Liu et al., 2012). Currently, the common analysis methods of fMRI data include the fractional amplitude of low-frequency fluctuation (fALFF), regional homogeneity (ReHo), and functional connectivity (FC). However, ReHo is easily affected by some parameters such as the magnitude of spatial smoothing (Zang et al., 2004) and is insensitive to shape differences (Cole et al., 2010). As for FC, it focuses on the whole functional activity of the brain but is dependent on the user-defined region of interests (ROIs) based on the prior knowledge (Cole et al., 2010; Smitha et al., 2017). As known, fALFF is an index reflecting the intensity of spontaneous neuronal activity in local brain regions, and more neuroimaging studies applied fALFF to explore the underlying pathophysiology mechanism of different diseases, including in MWoA (Xue et al., 2013; Wang et al., 2016; Li et al., 2017; Hu et al., 2019). Researchers have demonstrated that taVNS could regulate the disrupted brain functional activities in MWoA patients (Zhang et al., 2019a; Luo W. et al., 2020), which provides a new perspective to reveal the neural mechanism of treatment. In addition, fALFF has been proved to be more objective and sensitive in prediction studies (Sui et al., 2018; Li et al., 2020). To sum up, we used the fALFF to perform the analysis of brain function in this study. However, currently, conventional fMRI studies were mainly based on univariate and group-level statistical methods, few is known about whether the altered fALFF could be used in the prediction of an individual patient with MWoA.

Under the limited translational applicability of standard mass-univariate analytical methods that are typically used in neuroimaging, a great hope is given to a data-driven multivariate machine learning technique—multivariate pattern analysis (MVPA), which is sensitive to the fine-grained spatial discriminative patterns and exploration of inherent multivariate nature from high-dimensional neuroimaging data. Previous studies have widely applied MVPA in the classification or prediction of individual treatment response (Redlich et al., 2016; Cash et al., 2019; Tu et al., 2019; Messina and Filippi, 2020; Yin et al., 2020; Yu et al., 2020). For example, one recent study applied MVPA to identify the useful biomarkers of the FC between the medial prefrontal cortex (mPFC) and specific subcortical regions, which could significantly predict the changes in symptoms in patients with chronic low back pain receiving 4-week acupuncture treatment (Tu et al., 2019). Similarly, Hou et al. (2016) employed multivariate analysis to construct a model for the prediction of Parkinson's disease (PD) severity ratings from the baseline individual fMRI data. In addition, several researchers selected meaningful categorical features between migraine patients and healthy controls (HCs) as a region of interest (ROI) to predict the efficacy of acupuncture using a support vector regression (SVR) model (Tu et al., 2020).

Even though MVPA has been proved to be a promising approach in the application of predicting neurological disorders, to date, no literature has been published on the individual prediction of taVNS treatment for MWoA. In this study, we will explore the differences in resting-state brain activities between MWoA patients and well-matched HCs and further test the predictive ability of those baseline fALFFs as the biomarkers for the clinical outcomes of taVNS treatment in MWoA patients using SVR. Therefore, we proposed three hypotheses: (1) MWoA patients would be associated with altered activities in specific brain regions compared with HCs. We compared the fALFF differences between MWoA patients and HCs, and a mask of these significant abnormal regions was generated and used for the subsequent analysis. (2) We hypothesized that taVNS could treat the MWoA through modulating the abnormal fALFF of these

regions. Then, we explored how the taVNS could modulate those abnormal fALFFs in patients with MWoA, through comparing the fALFF differences between pre- and posttreatment in the mask. (3)We further supposed that the abnormal fALFF of these regions in the mask at baseline could serve as a reliable biomarker to predict the taVNS treatment outcomes for MWoA patients using a SVR model combined with feature select of weight based on the LIBSVM toolbox. We hope that our study could provide a quantitative benchmark for selecting suitable MWoA patients for taVNS treatment.

MATERIALS AND METHODS

Participants

In our previous published article (Zhang et al., 2021), the taVNS has been confirmed as an effective treatment for MWoA relieving acute pain [especially in reducing visual analog scale (VAS) scores] in migraine patients, and This study was an advanced exploration to predict the efficacy of taVNS based on the SVR algorithm. Sixty right-handed MWoA patients who received 4-week taVNS treatment and sixty age-, gender-, and education-level-matched healthy controls were recruited. The Research Ethics Committee of the Second Affiliated Hospital of Guangzhou University of Chinese Medicine approved the study. This study protocol was registered on the Chinese Clinical Trial Registry (ChiCTR-INR-17010559). Written informed consent was obtained from all participants.

Episodic migraineurs without aura were diagnosed by licensed neurologists according to the 2nd Edition International Classification of Headache Disorders for Migraine Without Aura (Headache Classification Subcommittee of the International Headache Society, 2004). The detailed inclusion criteria for the MWoA patients are as follows: (1) aged 18–45 years old, (2) right-handed, (3) have at least 6 months of migraine duration, (4) have at least two headache attacks per month, (5) have not taken any prophylactic headache medications during the past 1 month, and (6) have not taken any psychoactive or vasoactive drugs during the past 3 months. Excluded criteria include the following: (1) headache induced by other diseases, (2) headache attack within 48 h prior to the experiment or during the experiment, (3) pregnancy or lactation, (4) any other chronic pain conditions, (5) severe head deformity or intracranial lesions, (6) score on the Self-Rating Anxiety Scale (SAS) or the Self-Rating Depression Scale (SDS) > 50.

Interventions

For the patients with MWoA, we applied auricular vagus nerve electrical stimulation at the left cymba concha (**Figure 1**). The stimulation was applied with the MRI compatible electronic acupuncture treatment instrument (SDZII, Huatuo, Suzhou, China) by trained physicians. Similar to a previous taVNS study on migraine (Straube et al., 2015), we have chosen the frequency of 1 Hz with the duration of 0.2 ms. The stimulation was continuously applied for 30 min during each treatment session. Stimulation intensity was adjusted to approximately 1.5–5 mA, the strongest sensation that patients could tolerate without pain.

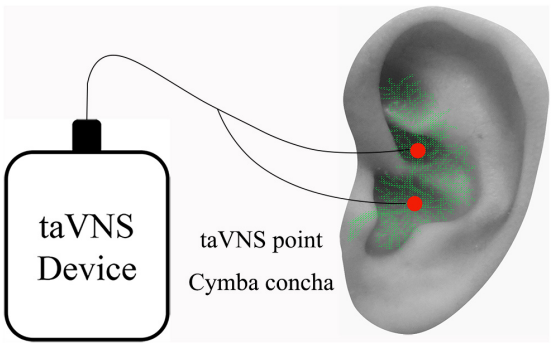

FIGURE 1 | taVNS stimulation site on the left ear. Red dots indicate regions of taVNS (ABVN, green color). *ABVN*, auricular branch of the vagus nerve; *taVNS*, transcutaneous auricular vagus nerve stimulation.

All MWoA patients who were included in the final analysis completed a total of 12 treatment sessions during the 4-week treatment period.

Clinical Outcome Measures

The treatment effect of tVNS for migraines has been confirmed in many literatures (Silberstein et al., 2016; Tassorelli et al., 2018; Diener et al., 2019). In our previous published article (Zhang et al., 2021), the taVNS also has been confirmed as an effective treatment for MWoA, and this study was an advanced exploration to predict the efficacy of taVNS based on the SVR algorithm. According to the results of Kinfe Thomas M study (Kinfe et al., 2015) and our previous study (Zhang et al., 2021), which suggest that tVNS can relieve acute pain (especially in reducing VAS scores) in migraine patients. So, we selected the improvement in VAS scores (post–pretreatment) as the primary outcome and the secondary outcome included attack times, total duration, Migraine-Specific Quality-of-Life Questionnaire (MSQ), Zung SDS, and Zung SAS in this study. In addition, according to the guidelines (Zheng, 2002), we take 25% reducing VAS scores as the judging criterion of the taVNS effective treatment.

The study lasted for 8 weeks: 4 weeks before the treatment (the baseline) and 4 weeks during the treatment. Patients were instructed to complete headache diary records after enrollment until this study finished. The diaries, MSQ, Zung SDS, and Zung SAS were collected at week four and week eight. The headache diary documented the onset time, duration, pain intensity (measured by VAS score), accompanying symptoms, and rescue medication use (ibuprofen suspension). To avoid prophylactic medication, we just selected occasional migraine patients, who tended to have a relatively low migraine attack frequency. Before the trial, ibuprofen suspension (H19991011, Shanghai Johnson and Johnson Pharmaceuticals, Ltd., 10 ml each time) was uniformly administered to MWoA patients according to the guidelines for diagnosis and treatment of migraine (Li et al., 2011). Patients were instructed not to use the medicine unless it is necessary. If the patient took the medication, the time, frequency, and dosage of each medication use would be recorded

in the headache diary. In addition, patients were advised to forbid barbiturates, opiates, and prophylactic medication.

Magnetic Resonance Imaging Data Acquisition

All rs-fMRI scanning was conducted on a 3.0T Siemens MRI scanner (Siemens MAGNETOM Verio 3.0T, Erlangen, Germany) with a 24-channel phased-array head coil. Subjects were told to stay awake, remain motionless, and keep their eyes closed during the scan. Tight, but comfortable, foam padding was used to minimize head motion, and earplugs were used to reduce scanner noise.

All patients participated in identical fMRI scanning sessions before and after 4 weeks of treatment. The scanning sessions include the 8-min resting-state fMRI scan and T1-weighted high-resolution structural images. rs-fMRI encompassing the whole brain was acquired in 8 min with a gradient-recalled echo-planar imaging pulse sequence and imaging parameters were as follows: repetition time (TR) = 2,000 ms, echo time (TE) = 30 ms, field of view (FOV) = 224 mm × 224 mm, matrix = 64 × 64, flip angle = 90°, slice thickness = 3.5 mm, interslice gap = 0.7 mm, 31 axial slices paralleled, and 240 time points. T1-weighted high-resolution structural images were applied with the following parameters: TR = 1,900 ms, TE = 2.27 ms, flip angle = 9°, FOV = 256 mm × 256 mm, matrix = 256 × 256, and slice thickness = 1.0 mm.

Resting-State Functional Magnetic Resonance Imaging Data Processing

rs-fMRI data were preprocessed and analyzed using the SPM12[1] and DPABI 3.0. The main steps included the following: (1) discarding the first 10 time points; (2) slice-timing correction, realignment, and discarding subjects with a mean framewise displacement value exceeding 0.5 mm or a maximum displacement greater than one voxel size (Power et al., 2012; Luo N. et al., 2020); (3) reorienting functional and T1 images with six rigid-body parameters; (4) coregistering T1 images to functional space, segmentation, and normalizing the functional images to Montreal Neurological Institute (MNI) space; (5) correcting head motion with Friston 24-parameter model (Friston et al., 1996; Yan et al., 2013), removing linear trend, and regressing out the white matter and cerebrospinal fluid signals; (6) resampling the functional images to 3 mm × 3 mm × 3 mm cubic voxels and smoothing functional images with a 6-mm Gaussian kernel of full width at half maximum; (7) temporally filtering (0.01–0.08 Hz) (Sun et al., 2021) to generate the ALFF value, and then, the fALFF map was obtained by dividing the total ALFF values from 0.01 to 0.025 Hz; and (8) transforming the fALFF map to the *z*-fALFF map with normal *z* transformation.

Statistical Analysis

Statistical Analysis of Clinical Outcomes

Statistical analyses were performed with SPSS v20.0, and the significance threshold was set to $p < 0.05$ (two-tailed). Baseline demographic and clinical data were compared between MWoA patients and HCs using the chi-square test for categorical variables and the Student's *t*-test for continuous ones (if normally distributed), and Mann–Whitney test (if not normally distributed). In addition, paired *t*-tests were employed to determine whether the alterations in clinical outcomes were significant after taVNS treatment for patients with MWoA, if characteristics were normally distributed and Wilcoxon signed rank test if not normally distributed.

Statistical Analysis of Functional Magnetic Resonance Imaging Data

The intergroup analysis (MWoA patients vs. HCs) of fALFF at baseline was applied using a two-sample *t*-test, with the age, sex, education level, and mean FD as covariates. A threshold of voxel-wise $p < 0.005$ uncorrected and a cluster-level $p < 0.05$ corrected by false discovery rate (FDR) were used for multiple comparison corrections between MWoA patients and HCs. The intragroup comparison of fALFF (pretreatment vs. posttreatment migraineurs) was performed using a paired *t*-test with the voxel-wise $p < 0.001$ uncorrected and cluster-level $p < 0.05$ family-wise error (FWE) corrected, and the mean FD and medication use dosage (ibuprofen suspension) were used as covariates. Moreover, to assess the association of neuroimaging findings with clinical outcomes, we performed a partial correlation analysis between pre- and posttreatment fALFF alterations and corresponding changed clinical variables (VAS score and attack times) after taVNS treatment for patients with MWoA, and Bonferroni correction was used for multiple comparisons.

Multivariate Pattern Analysis

This study applied MVPA method to explore whether the fALFF indicator was able to predict the treatment response of taVNS for patients with MWoA. We selected the abnormal regions, which indicate significant changes between migraine patients and HCs as our mask and proposed that these fALFF values at baseline would be used for predicting the taVNS treatment efficacy.

Here, MVPA based on linear SVR (implemented by LIBSVM[2]) was employed to verify our hypothesis. We set the changes in pain severity (VAS change) as the dependent variable and abnormal fALFF in the mask as independent variables (predictors) in all MWoA patients. A feature selection based on weight was used to reduce the data dimensions. The fixed 10-fold crossvalidation (CV) method was the compromising choice for bias and training sample size to avoid the risk of overfitting, with training sample and testing sample 9 and 1 part, respectively. We calculated the correlation coefficient of prediction-outcome correlation (r), which was defined as the correlation between the actual and predicted value, to evaluate the predictive ability of SVR model. To further assess the performance of the model and evaluate the significance of r, we ran permutation testing. In each test, we randomly permuted the labels of the data prior to training. Ten-fold CV was then performed on the permuted datasets, and the

[1]http://www.fil.ion.ucl.ac.uk/spm

[2]https://www.csie.ntu.edu.tw/~cjlin/libsvm/index.html

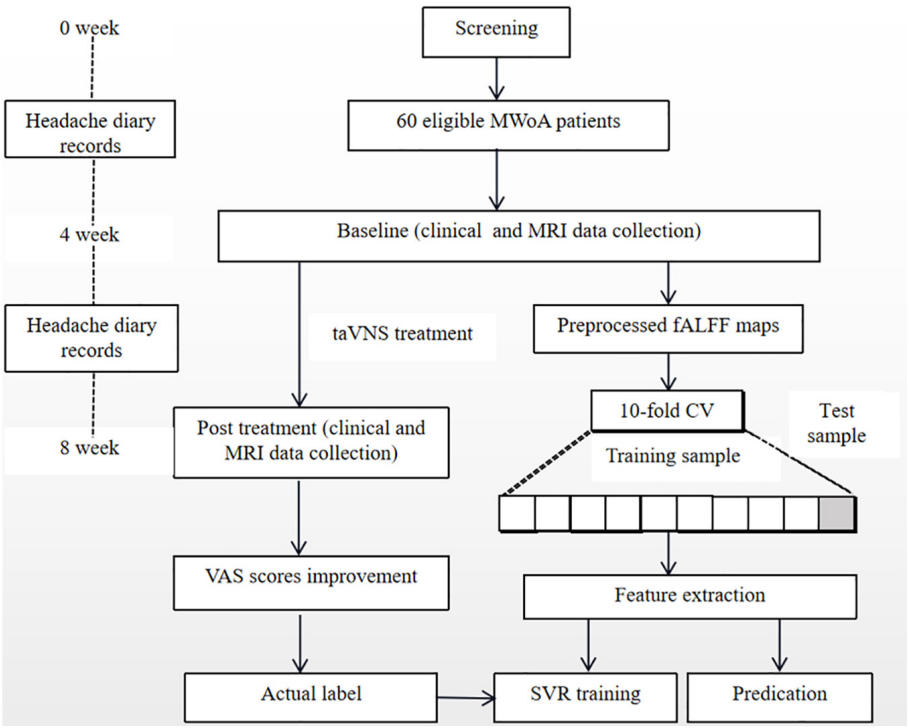

FIGURE 2 | Flowchart of prediction analysis. *MWoA*, migraine without aura; *fALFF*, fractional amplitude of low-frequency fluctuation; *VAS*, visual analog scale; *CV*, crossvalidation; *SVR*, support vector regression; *taVNS*, transcutaneous auricular vagus nerve stimulation.

procedure was repeated 1,000 times to determine whether the performance occurred by chance, and $p < 0.001$ was considered to be statistically significant.

The flowchart of the prediction analyses is shown in **Figure 2**.

RESULTS

Demographic Characteristics and Clinical Outcomes

In this study, a total of 60 right-handed MWoA patients (13 men and 47 women, age of 31.72 ± 6.65 years, 54 higher education and 6 lower than higher education) and also 60 gender-, age-, and education-level-matched HCs (15 men and 45 women, age of 29.25 ± 7.26 years, 53 higher education and 7 lower than higher education) finished this study.

Baseline demographic characteristics between MWoA patients and HCs were compared as follows. The age, as a continuous variable, was tested to be normally distributed. Additionally, the two-sample *t*-test result showed that compared with HCs, there was no significant difference ($p > 0.05$) in age in MWoA patients. We divided the education level into two subgroups, higher education and lower than higher education similar to Jasilionis's study (Jasilionis and Shkolnikov, 2016). The chi-square test was used to compare the gender and education-level difference, and results indicated that the gender and education level of MWoA patients were not significantly different ($p > 0.05$), compared with HCs. The details are presented in **Table 1**.

Clinical outcomes between pre- and posttreatment MWoA patients were compared as follows. The continuous variables (VAS scores, attack times, total duration, MSQ, SDS, and SAS) were tested to be normally distributed, and the paired *t*-test results showed significant improvement in clinical outcomes ($p < 0.05$), which include VAS scores, attack times, total duration, MSQ, SAS, and SDS after 4 weeks taVNS treatment (**Table 1**). The using dosage of the ibuprofen suspension was not normally distributed, so the Wilcoxon signed rank test was used, and the results indicated that there was no significant post- (median 0 ml, p25–p75 range 0–0 ml) and pretreatment (median 0 ml, p25–p75 range 0–10 ml) difference ($p > 0.05$) in the dosage of ibuprofen suspension for migraine patients (see **Supplementary Table 1**).

Intergroup and Intragroup Comparison of Fractional Amplitude of Low Frequency Fluctuation

To explore the underlying mechanism of pathophysiology of MWoA, we compared patients with MWoA to HCs using a two-sample *t*-test to detect significant abnormal regions which was used as a mask for subsequent analysis, with the age, sex, education level, and mean FD as covariates. A threshold of voxel-wise $p < 0.005$ uncorrected and a cluster-level $p < 0.05$ corrected by FDR was used for multiple comparison corrections. The results indicated that, compared with HCs, pretreatment MWoA

TABLE 1 | Demographic characteristics and clinical outcomes of MWoA and HCs.

Item		HCs (n = 60)	MWoA (n = 60)			P
			Pretreatment	Posttreatment	Post–pre[95% CI]	
Gender	Male	15	13	13		0.666
	Female	45	47	47		
Education level	Lower than higher education	7	6	6		0.769
	Higher education	53	54	54		
Age (Years)		29.25 ± 7.26	31.72 ± 6.65	31.72 ± 6.65		0.060
VAS scores			49.1 ± 16.6	32.1 ± 20.5	17.0 [11.40; 22.50]	< 0.001
Attack times			3.4 ± 2.2	2.5 ± 1.9	0.90 [0.30; 1.50]	0.005
Total duration			61.5 ± 69.2	29.1 ± 39.4	32.4 [14.50; 50.30]	0.001
MSQ			58.6 ± 10.6	71.6 ± 9.3	−13.0 [−16.10; −9.97]	< 0.001
SDS			46.6 ± 8.6	43.3 ± 8.8	3.30 [1.60; 5.10]	< 0.001
SAS			45.3 ± 9.56	41.6 ± 8.03	3.66 [1.69; 5.64]	< 0.001

VAS, visual analog scale; MSQ, Migraine-Specific Quality-of-Life Questionnaire; SAS, Self-Rating Anxiety Scale; SDS, Self-Rating Anxiety Scale; CI (confidence interval. The p-values were obtained by paired or two-sample t-test or chi-square test.

TABLE 2 | Brain regions showing differences in fALFF for migraineurs compared to HCs.

Condition	Brain region	MNI coordinates			Peak T-value	Cluster
		X	Y	Z		
MWoA > HC	Left thalamus	−18	−15	12	4.25	57
	Right postcentral gyrus	45	−18	33	4.17	52
	Right precentral gyrus	54	9	30	4.42	60
	Bilateral supplementary motor areas	6	−9	57	4.62	138
	Left inferior parietal gyrus	−39	−57	39	6.71	60
	Left precentral gyrus	−29	−11	58	4.93	48
MWoA < HC	Bilateral precuneus	0	−66	54	−4.19	54
	Left superior frontal gyrus/mPFC	−12	51	42	−4.54	55

A threshold of voxel-wise $p < 0.005$ uncorrected and cluster-level $p < 0.05$ FDR corrected was applied for second-level analyses. mPFC, medial prefrontal cortex.

patients exhibited increased fALFF in the left thalamus, left inferior parietal gyrus (IPG), bilateral precentral gyrus (PreCG), right postcentral gyrus (PoCG), and bilateral supplementary motor areas (SMAs), but decreased in the bilateral precuneus and left superior frontal gyrus (SFG)/medial prefrontal cortex (mPFC) (**Table 2** and **Figures 3**, **4**).

Paired t-tests were performed to compare post- and pretreatment fALFF differences for migraines with the voxel-wise $p < 0.001$ uncorrected and cluster-level $p < 0.05$ FWE corrected, and the mean FD and medication use dosage (ibuprofen suspension) were used as covariates. We observed the significant decreased fALFF in the thalamocortical (TC) circuits and default mode network after 4-week taVNS treatment. These regions were located in the left thalamus, bilateral PreCG, right PoCG, bilateral SMA, left IPG, bilateral precuneus, and left SFG/mPFC (**Table 3** and **Figures 4**, **5**).

Relationship Between Fractional Amplitude of Low Frequency Fluctuation Measures and Clinical Variables

We performed the correlation analysis between altered regions showing significant fALFF changes in the intragroup comparison and corresponding clinical outcomes, with Bonferroni correction applied for multiple comparisons. Correlation analysis indicated that the pre- and posttreatment fALFF changes in the right PoCG after taVNS treatment were negatively associated with corresponding reduction of VAS scores in MWoA patients ($r = -0.267$, $p = 0.039$, uncorrected), and the decreased fALFF in the bilateral precuneus was positively associated with the reduction in the attack times ($r = 0.357$, $p = 0.005$) across all subjects after Bonferroni correction (0.05/5). The detailed correlation analysis results are shown in **Figure 6**.

Subject-Level Prediction of Transcutaneous Auricular Vagus Nerve Stimulation Efficacy

We selected the regions indicating significant changes between pretreatment MWoA patients and HCs as our mask to predict treatment responses of taVNS (reduction of VAS scores) based on a SVR model for MWoA patients. As shown in **Figure 7A**, the prediction results showed that the baseline fALFF features could effectively predict the VAS score changes after 4-week taVNS treatment with a relatively high prediction-outcome correlation of 0.411. In addition, the permutation tests showed that the results could not be obtained by chance ($p < 0.001$) (**Figure 7B**).

Those weight brain areas with strong predictive power were located in the left thalamus, bilateral SMA, right PoCG, left IPG, bilateral precuneus, and left SFG/mPFC (see **Figure 8** and **Table 4**).

In addition, we predicted the treatment effect without using the difference which compared migraines with HCs as the

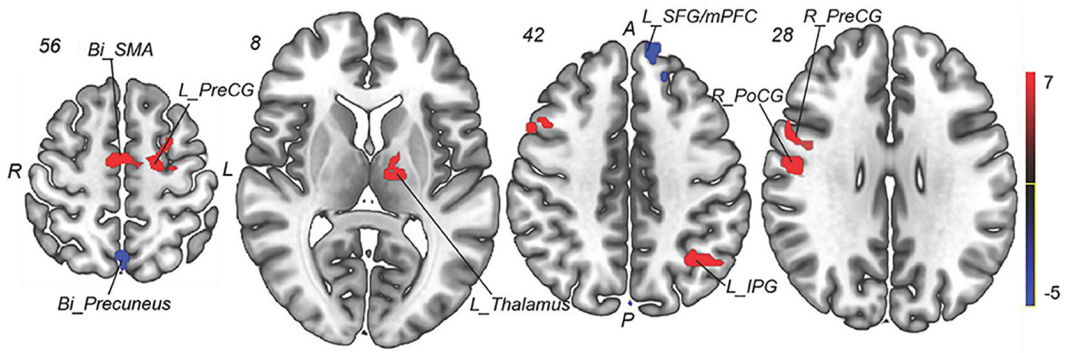

FIGURE 3 | Group comparison of fALFF between the MWoA patients and HCs. Compared with HCs, pretreatment MWoA patients exhibited increased fALFF in the left thalamus, left IPG, bilateral PreCG, right PoCG, and bilateral SMA, but decreased in the bilateral precuneus and left SFG/mPFC. Red colors indicate regions with increased fALFF; blue colors indicate regions with decreased fALFF. *Bi,* bilateral; *R,* right; *L,* left; *PoCG,* postcentral gyrus; *PreCG,* precentral gyrus; *SPG,* superior parietal gyrus; *SMAs,* supplementary motor areas; *SFG,* superior frontal gyrus; *mPFC,* medial prefrontal cortex; *IPG,* inferior parietal gyrus.

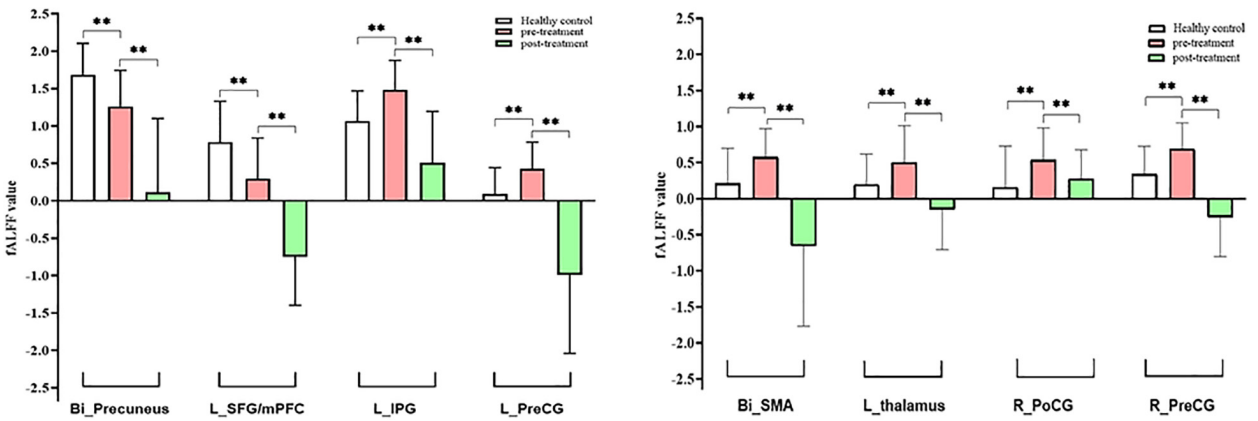

FIGURE 4 | Intergroup and intragroup comparison of fALFF differences. Compared with HCs, pretreatment MWoA patients exhibited increased fALFF in the left thalamus, left IPG, bilateral PreCG, right PoCG, and bilateral SMA, but decreased in the bilateral precuneus and left SFG/mPFC; compared with pretreatment MWoA patients, migraineurs receiving 4-week taVNS treatment showed decreased fALFF in the left thalamus, bilateral PreCG, right PoCG, bilateral SMA, left IPG, bilateral precuneus, and left SFG/mPFC, but no significantly increased brain regions. White color represents healthy control; red color represents pretreatment migraine patients; green color represents posttreatment migraine patients. *Bi,* bilateral; *R,* right; *L,* left; *PoCG,* postcentral gyrus; *PreCG,* precentral gyrus; *SMA,* supplementary motor areas; *SFG,* superior frontal gyrus; *mPFC,* medial prefrontal cortex; *IPG,* inferior parietal gyrus. The **represents that the difference is statistically significant.

preliminary feature selection and we also got similar results (see in **Supplementary Figure 1** for details).

DISCUSSION

This study was an advanced exploration based on our previously published article which taVNS has been confirmed as an effective treatment for MWoA relieving acute pain (especially in reducing VAS scores) in migraine patients (Zhang et al., 2021). The current design enlarges the taVNS sample to predict the efficacy of taVNS before treatment at a subject level based on the SVR algorithm and rs-fMRI indicators.

To the best of our knowledge, this is the first study to predict the efficacy of taVNS treatment for patients with MWoA based on the mask of significant abnormal regions between the pretreatment MWoA and HCs using a SVR model combined with feature select of weight. Our results showed that the SVR model works well at predicting the treatment response of taVNS for MWoA patients at baseline (r = 0.411), and those weight brain areas are located in the left thalamus, bilateral SMA, right PoCG, left IPG, the bilateral precuneus, and left SFG/mPFC, mainly involved in the TC circuits, default mode network (DMN), and descending pain modulation system (DPMS). These findings suggested that the baseline fALFF values could serve as the potential biomarkers to predict taVNS treatment efficacy for MWoA.

As well known, the TC circuits have been documented involving in processing spatial and intensity aspects of noxious stimuli and also mediating the perception of pain (Magon et al., 2015; Amin et al., 2018; Martucci and Mackey, 2018; Ellingson et al., 2019). Specifically, first, as one key node of TC circuits, the

TABLE 3 | Brain regions showing differences in fALFF for patients between pre- and posttreatment.

Condition	Brain region	MNI coordinates			Peak *T*-value	Cluster
		X	Y	Z		
Post < Pre	Left thalamus	−9	−15	9	−8.38	12
	Right postcentral gyrus	57	0	33	−8.27	31
	Bilateral precentral gyrus	51	9	39	−12.94	41
	Bilateral supplementary motor areas	3	−9	66	−8.13	43
	Left inferior parietal gyrus	−33	−60	51	−11.31	38
	Left precentral gyrus	−24	−11	56	−11.59	62
	Bilateral precuneus	6	−60	66	−8.16	52
	Left superior frontal gyrus/mPFC	−18	36	45	−9.68	48
Post > Pre	No regions survive the threshold					

A threshold of voxel-wise $p < 0.001$ uncorrected and cluster-level $p < 0.05$ FWE corrected was applied for second-level analyses. mPFC, medial prefrontal cortex.

thalamus holds an important position in our understanding of allodynia, central sensitization, and photophobia in migraineurs (Younis et al., 2019). Investigators have found alteration of thalamic FC in brain regions associated with pain modulating and pain encoding networks during migraine attacks (Amin et al., 2018). Second, another significant component in TC circuits, the sensorimotor network (SMN), including the PreCG, PoCG, and SMA, is thought to be activated by various sensory information from the somatosensory and motor cortices to modulate corresponding behaviors. For example, Zhang et al. (2017) have observed decreased spontaneous activity in the SMN and less FC between primary sensory areas and superior and inferior parietal lobes and also anterior cingulate cortex in MWoA patients compared with HCs. Additionally, as known, functional alterations in the TC circuits are involved in the development and maintenance of migraines (Magon et al., 2015; Amin et al., 2018; Martucci and Mackey, 2018). Increased fALFF in the TC circuit has been detected during interictal phase of migraine, and this increased fALFF in the thalamus was selectively associated with headache frequency (Hodkinson et al., 2016). In accordance with previous studies, our study showed that patients with MWoA exhibited increased fALFF in the left thalamus, bilateral PreCG, right PoCG, and bilateral SMA, compared with HCs. These findings emphasized and extended the predominant role of TC circuits in the neuropathological mechanism of MWoA.

Furthermore, this study also indicated the possibility of this circuit serving as a potential therapeutic target for patients with MWoA. In our study, we found that the aberrant fALFF in the right PoCG within TC circuits in MWoA patients was close to the normal level of HCs after 4-week treatment, and the altered fALFF in the right PoCG was negatively associated with the reduction of VAS scores ($r = -0.267$, uncorrected), which suggest that TC circuits could be identified as the useful biomarkers for taVNS response in patients with MWoA. This is in line with our previous study, in which decreased FC between the thalamic subregions and bilateral PoCG was observed with a significantly negative correlation to the reduction of the migraine days following taVNS treatment (Zhang et al., 2021).

More importantly, the predictive ability of TC circuits as candidate biomarkers for treatment response remained stable when we used a SVR model ($r = 0.411$). These findings revealed the utility of this machine learning approach for elucidating neural markers of treatment response based on TC pathways and allowed the personal differences to be rationalized. But interestingly, different from our results that the weight brain regions were mainly located in the bilateral SMA and right PoCG involving in the TC circuits, a recent study using SVR as algorithm reported that the zALFF of the bilateral middle occipital gyrus could effectively predict the relief of symptoms for migraine and hence performed a strong predictive power (Yin et al., 2020). The most possible explanation for this discrepancy might lie in the sample differences. For example, the

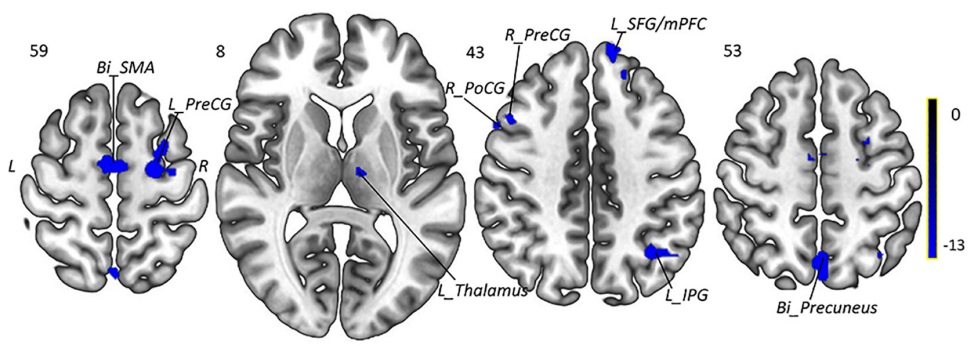

FIGURE 5 | Intragroup comparison of fALFF in patients with MWoA after 4-week treatment. Compared with pretreatment MWoA patients, migraineurs receiving 4-week taVNS treatment showed decreased fALFF in the left thalamus, bilateral PreCG, right PoCG, bilateral SMA, left IPG, bilateral precuneus, and left SFG/mPFC, but no significantly increased brain regions. Blue colors indicate regions with decreased fALFF. *Bi,* bilateral; *R,* right; *L,* left; *PoCG,* postcentral gyrus; *PreCG,* precentral gyrus; *SMA,* supplementary motor areas; *SFG,* superior frontal gyrus; *mPFC,* medial prefrontal cortex; *IPG,* inferior parietal gyrus.

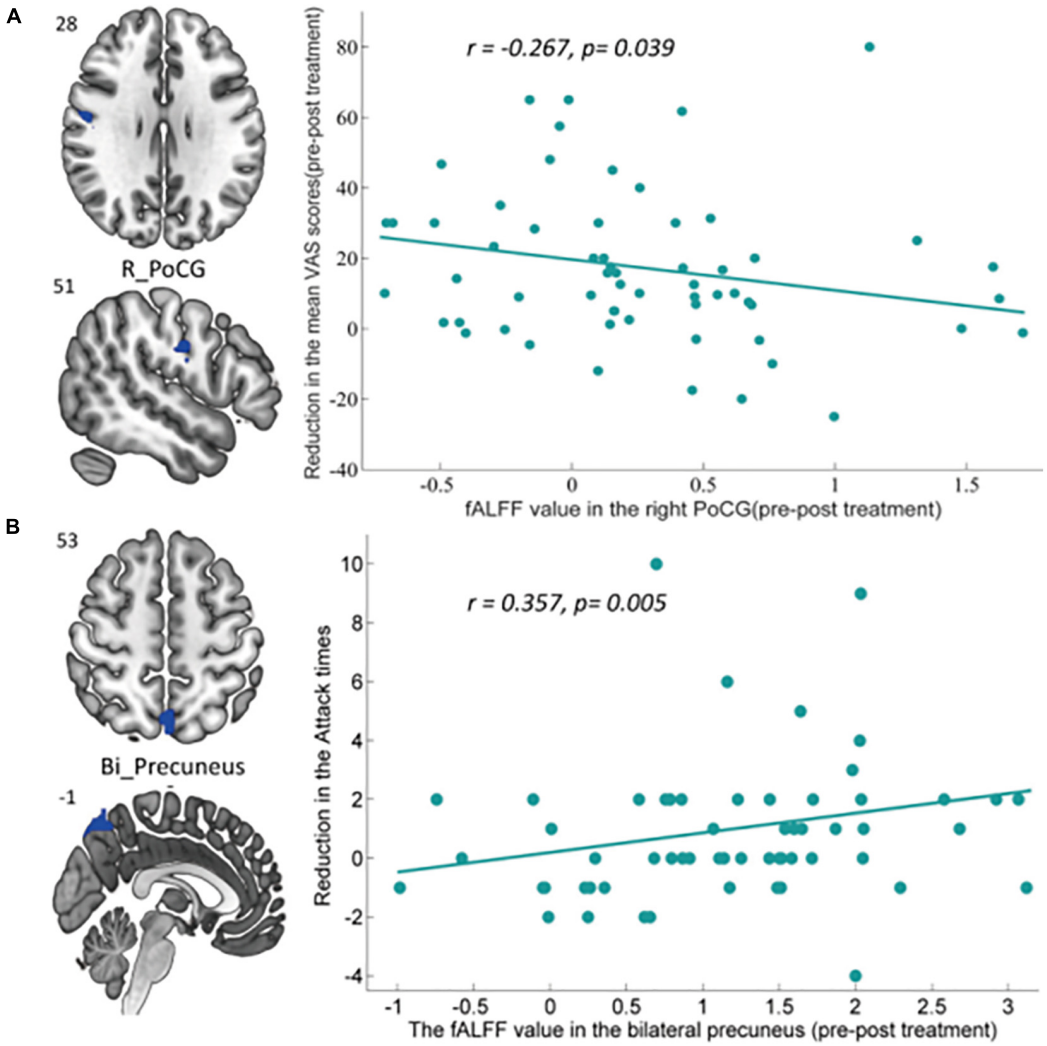

FIGURE 6 | Significant correlation between the altered intragroup fALFF and clinical outcomes. **(A)** Correlation between the altered fALFF in the right PoCG (pre–posttreatment) and the reduction of VAS scores. The decreased fALFF in the right PoCG after 4-week taVNS treatment was negatively associated with corresponding reduction of VAS scores in MWoA patients (r = –0.267, p = 0.039, uncorrected). **(B)** Correlation between the altered fALFF in the bilateral precuneus (pre–posttreatment) and the reduction of migraine attack times. The decreased fALFF in bilateral precuneus after 4-week taVNS treatment was positively associated with the reduction of attack times (r = 0.357, p = 0.005, Bonferroni correction, 0.05/5). *Bi,* bilateral; *L,* left; *PoCG,* postcentral gyrus.

participants in this study have relative lighter visual symptoms such as photophobia; another likely reason is due to the different intervention methods (acupuncture intervention vs. taVNS) which might produce diverse effect on brain activities. A large sample size and well-designed study should be implemented to investigate the more specific role of the TC circuits in MWoA patients after taVNS intervention.

In addition to the TC circuits, the DMN was also shown to be as the indicators of pathophysiology and treatment response for MWoA patients. Converging findings have suggested that DMN is involved in the core processes of brain function (such as internal mentation, attention, and monitoring of the surrounding environment) (Broyd et al., 2009). Disruption of the DMN has been detected in some neuropsychological disorders (Wang et al., 2013; Yin et al., 2016) and also migraine (Xue et al., 2012; Tessitore et al., 2013; Zhao et al., 2013). Consistently, in this study, we observed altered brain activities within DMN including decreased fALFF in the bilateral precuneus, left SFG/mPFC and increased fALFF in the left IPG in MWoA patients compared with HCs. What is more, as an important network closely associated with the pathophysiology of migraine, DMN is also proposed to be linked with the treatment responsiveness. As shown in our results, the increased fALFF in the left IPG in MWoA patients was normalized after effective taVNS treatment. Additionally, we found that the altered fALFF in the bilateral precuneus was positively correlated with the reduced attack times (r = 0.357, Bonferroni correction, 0.05/5) in MWoA patients. Coincidently, a recent acupuncture study demonstrated that the reduced FC in the left superior prefrontal cortex and precuneus in migraine patients returned to the normal level of

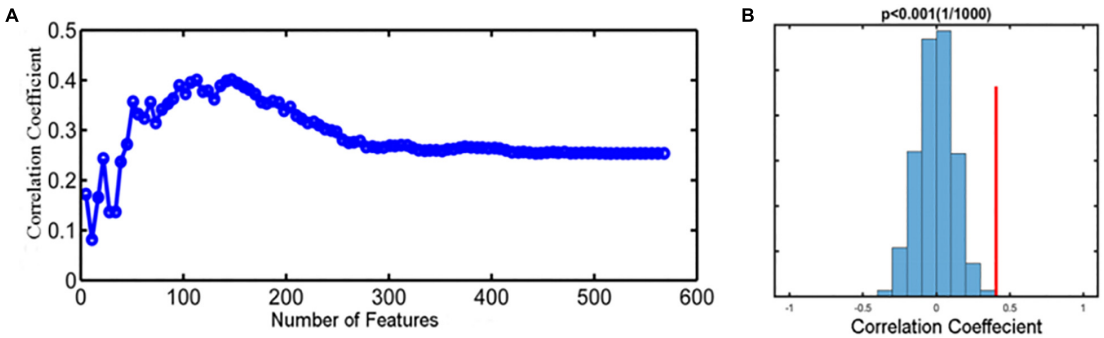

FIGURE 7 | Prediction performance for taVNS treatment. **(A)** The feature selection curve reflected the changing prediction-outcome correlation following the increased number of features, and the highest correlation coefficient is 0.411. **(B)** The histogram showed the result of permutation test with highest correlation coefficient, reflecting the stability of the SVR model ($p < 0.001$).

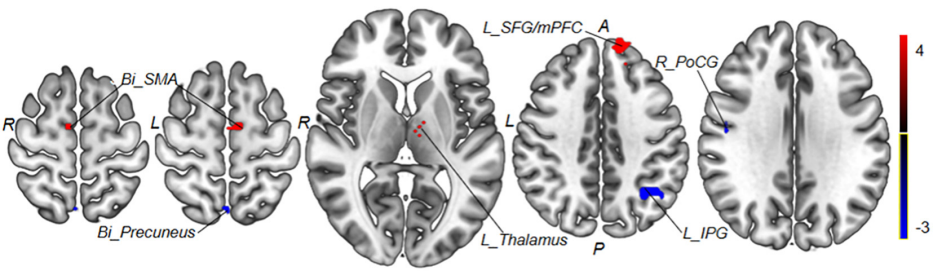

FIGURE 8 | Regions with the most predictive features. Positive weight brain areas with strong predictive power are located in the left thalamus, bilateral SMA, and left SFG/mPFC; negative weight brain areas with strong predictive power are located in the right PoCG, left IPG, and bilateral precuneus. Red colors indicate regions with positive weight; blue colors indicate regions with negative weight. *Bi,* bilateral; *R,* right; *L,* left; *PoCG,* postcentral gyrus; *SMA,* supplementary motor areas; *SFG,* superior frontal gyrus; *mPFC,* medial prefrontal cortex; *IPG,* inferior parietal gyrus.

TABLE 4 | The regions' weight in predicting the treatment effect of taVNS in patients with MWoA.

Weight	Brain region	MNI coordinates			Peak *T*-value	Cluster
		X	Y	Z		
Positive weight	Left thalamus	−12	−6	6	1.71	5
	Bilateral supplementary motor areas	9	−6	63	2.14	24
	Left superior frontal gyrus/mPFC	−12	39	51	3.37	29
Negative weight	Right postcentral gyrus	48	−9	30	−2.4	15
	Left inferior parietal gyrus	−39	−36	36	−1.42	20
	Bilateral precuneus	0	−63	60	−1.47	17

mPFC, medial prefrontal cortex.

HCs, and this alteration was associated with the alleviation of headache intensity after treatment (Zou et al., 2019). Thus, we speculated that the DMN could be used as imaging biomarkers for understanding the therapeutic mechanisms and further predicting treatment outcomes for MWoA.

Consistent with such assumption, the SVR model in this study showed that the DMN contributed much to predict the efficacy of taVNS. Interestingly, Tu et al. (2020) employed a MVPA approach together with abnormal FC within the DMN as the features to test the predictive capacity of DMN for MWoA patients, and the results demonstrated the potential role of this network for the prediction of treatment response. Similarly, another important application of machine learning showed that the FC between mPFC and subcortical regions could significantly predict therapeutic outcomes following 4-week acupuncture treatment for patients with chronic low back (Tu et al., 2019). To some extent, these findings may hint that the DMN could be used as a robust biomarker for treatment outcomes. Further investigations using different interventions are needed to validate the strong performance of DMN in patients with MWoA.

Notably, mPFC, which is not only a crucial component of DMN, but also involved in the DPMS (Ong et al., 2019), possessed high predictive weight in treatment responsiveness of taVNS in our study. As well known, the DPMS played an essential role in pain modulation and the physiopathology of chronic pain (Fields, 2004; Borsook and Burstein, 2012; Ossipov et al., 2014). Neuroimaging researches have demonstrated that chronic pain may be associated with alterations in multiple brain networks, such as the DMN, SMN, and DPMS (Kucyi and Davis, 2015, 2017). These particular networks, involved in the cognitive, sensorimotor, and affective aspects of pain, have been implicated in the core symptomatology of chronic pain and treatment response (Shi et al., 2015; Wu et al., 2016; Low et al., 2017;

Lee et al., 2019; Zhang et al., 2019b). For instance, migraine patients exhibited reduced FC between the mPFC/rACC and periaqueductal gray (PAG), another key region in the DPMS compared with HCs (Li et al., 2016). More importantly, impaired brain function within the DPMS could be normalized after effective acupuncture treatment, and these changes of FCs were associated with alleviation of headache intensity. Similarly, in our study, we found decreased fALFF in the mPFC after 4-week taVNS treatment for MWoA patients, and in the following MPVA, we also revealed mPFC as an important brain region to predict the treatment responses before clinical intervention. Our findings provide potential evidence suggesting that taVNS may relieve MWoA symptoms through the mPFC-related DMN and DPMS, further which could be taken as a promising biomarker for taVNS treatment.

Limitations

Limitations of this study should be noted. First, the sample size was relatively small. Although we did not perform the sample size estimation, we determined it according to the previously published similar article (Yin et al., 2020). Further larger scale study will be conducted to enhance the data reliability. Second, we did not take into account gender difference in our MVPA study. Considering there are less male migraines in our data, we have not further analyzed the sex difference. It is a very good idea to explore the effect of gender in migraine patients, and we will further explore it in the follow-up study. Third, patients were imaged during the interictal phase of migraine (not within 48 h before and after migraine attack or headache attack during the experiment). Larger sample size with MWoA patients at different phases such as ictal and interictal period should be designed to enhance the data integrity and reliance in the future study. Fourth, our patients were all from one single center, and the model was not externally validated. Independent and multicenter imaging datasets will be necessary to confirm our results. Finally, in the current MVPA study, only fALFF features were performed to achieve the prediction. Future studies should utilize multiple imaging modalities including structural and functional MRI analysis to validate our findings.

CONCLUSION

In summary, this study preliminarily demonstrated that fALFF features at baseline have good potential for predicting individualized treatment response of taVNS for MWoA patients, and those weight brain areas are mainly involved in the TC circuits, DMN, and DPMS. This will contribute to well understanding the mechanism of taVNS in MWoA and may help to screen ideal patients who respond well to taVNS treatment.

DATA AVAILABILITY STATEMENT

The raw data supporting the conclusions of this article will be made available by the authors, without undue reservation.

ETHICS STATEMENT

The studies involving human participants were reviewed and approved by the Ethics Committee of Guangdong Provincial Hospital of Chinese Medicine. The patients/participants provided their written informed consent to participate in this study.

AUTHOR CONTRIBUTIONS

BL, MF, and YZ designed the study. MF and YZ acquired the data. YZ, MF, BL, ZW, and XH performed the data analysis. MF, ZW, YZ, and YY interpreted the results. MF, BL, YZ, ZW, CF, and WL prepared the manuscript. All the authors contributed to manuscript revision and approved the submitted version.

FUNDING

This study was supported by the Medical Scientific Research Foundation of Guangdong Province of China (A2017234), the Administration of Traditional Chinese Medicine of Guangdong Province of China (20182047), Traditional Chinese Medicine Science and Technology Project of Guangdong Hospital of Traditional Chinese Medicine (YN2020MS09), and Science and Technology Program of Guangzhou (202102010260).

ACKNOWLEDGMENTS

We would like to acknowledge the generous support and contribution of all our trial participants.

SUPPLEMENTARY MATERIAL

The Supplementary Material for this article can be found online at: https://www.frontiersin.org/articles/10.3389/fnmol.2022.778139/full#supplementary-material

Supplementary Figure 1 | Prediction of the treatment effect without using the difference which compared migraines with HCs as the preliminary feature selection (r = 0.392, permutation p = 0.0004).

REFERENCES

Abu Bakar, N., Tanprawate, S., Lambru, G., Torkamani, M., Jahanshahi, M., and Matharu, M. (2016). Quality of life in primary headache disorders: a review. *Cephalalgia* 36, 67–91. doi: 10.1177/0333102415580099

Amin, F. M., Hougaard, A., Magon, S., Sprenger, T., Wolfram, F., and Rostrup, E. (2018). Altered thalamic connectivity during spontaneous attacks of migraine without aura: a resting-state fMRI study. *Cephalalgia* 38, 1237–1244. doi: 10.1177/0333102417729113

Biswal, B., Yetkin, F. Z., Haughton, V. M., and Hyde, J. S. (1995). Functional connectivity in the motor cortex of resting human brain using echo-planar MRI. *Magn. Reson. Med.* 34, 537–541. doi: 10.1002/mrm.1910340409

Borsook, D., and Burstein, R. (2012). The enigma of the dorsolateral pons as a migraine generator. *Cephalalgia* 32, 803–812. doi: 10.1177/0333102412453952

Broyd, S. J., Demanuele, C., Debener, S., Helps, S. K., James, C. J., and Sonuga-Barke, E. J. (2009). Default-mode brain dysfunction in mental disorders: a systematic review. *Neurosci. Biobehav. Rev.* 33, 279–296. doi: 10.1016/j.neubiorev.2008.09.002

Buse, D. C., Scher, A. I., Dodick, D. W., Reed, M. L., Fanning, K. M., Manack Adams, A., et al. (2016). Impact of migraine on the family: perspectives of people with migraine and their spouse/domestic partner in the CaMEO Study. *Mayo. Clin. Proc. S.* 002, 126–129. doi: 10.1016/j.mayocp.2016.02.013

Cash, R., Cocchi, L., Anderson, R., Rogachov, A., Kucyi, A., and Barnett, A. J. (2019). A multivariate neuroimaging biomarker of individual outcome to transcranial magnetic stimulation in depression. *Hum. Brain Mapp.* 40, 4618–4629. doi: 10.1002/hbm.24725

Cole, D. M., Smith, S. M., and Beckmann, C. F. (2010). Advances and pitfalls in the analysis and interpretion of resting-state FMRI data. *Front. Syst. Neurosci.* 4:8. doi: 10.3389/fnsys.2010.00008

Diener, H. C., Dodick, D. W., Goadsby, P. J., Lipton, R. B., Olesen, J., and Silberstein, S. D. (2012). Chronic migraine—classification, characteristics and treatment. *Nat. Rev. Neurol.* 8, 162–171. doi: 10.1038/nrneurol.2012.13

Diener, H. C., Goadsby, P. J., Ashina, M., Al-Karagholi, M. A., Sinclair, A., and Mitsikostas, D. (2019). Non-invasive vagus nerve stimulation (nVNS) for the preventive treatment of episodic migraine: the multicentre, double-blind, randomised, sham-controlled PREMIUM trial. *Cephalalgia* 39, 1475–1487. doi: 10.1177/0333102419876920

Ellingson, B. M., Hesterman, C., Johnston, M., Dudeck, N. R., Charles, A. C., and Villablanca, J. P. (2019). Advanced Imaging in the Evaluation of Migraine Headaches. *Neuroimag. Clin. N. Am.* 29, 301–324. doi: 10.1016/j.nic.2019.01.009

Fields, H. (2004). State-dependent opioid control of pain. *Nat. Rev. Neurosci.* 5, 565–575. doi: 10.1038/nrn1431

Friston, K. J., Williams, S., Howard, R., Frackowiak, R. S., and Turner, R. (1996). Movement-related effects in fMRI time-series. *Magn. Reson. Med.* 35, 346–355. doi: 10.1002/mrm.1910350312

Guo, W. B., Liu, F., Xue, Z. M., Yu, Y., Ma, C. Q., and Tan, C. L. (2011). Abnormal neural activities in first-episode, treatment-naïve, short-illness-duration, and treatment-response patients with major depressive disorder: a resting-state fMRI study. *J. Affect. Disord.* 135, 326–331. doi: 10.1016/j.jad.2011.06.048

Headache Classification Subcommittee of the International Headache Society. (2004). The International Classification of Headache Disorders: 2nd edition. *Cephalalgia* 24, 9–160. doi: 10.1111/j.1468-2982.2003.00824.x

Hodkinson, D. J., Wilcox, S. L., Veggeberg, R., Noseda, R., Burstein, R., and Borsook, D. (2016). Increased Amplitude of Thalamocortical Low-Frequency Oscillations in Patients with Migraine. *J. Neurosci.* 36, 8026–8036. doi: 10.1523/JNEUROSCI.1038-16.2016

Hou, Y., Luo, C., Yang, J., Ou, R., Song, W., and Wei, Q. (2016). Prediction of individual clinical scores in patients with Parkinson's disease using resting-state functional magnetic resonance imaging. *J. Neurol. Sci.* 366, 27–32. doi: 10.1016/j.jns.2016.04.030

Hu, B., Yu, Y., Dai, Y. J., Feng, J. H., Yan, L. F., Sun, Q., et al. (2019). Multi-modal MRI reveals the neurovascular coupling dysfunction in chronic migraine. *Neuroscience* 419, 72–82. doi: 10.1016/j.neuroscience.2019.09.022

Jasilionis, D., and Shkolnikov, V. M. (2016). Longevity and Education: a Demographic Perspective. *Gerontology* 62, 253–262. doi: 10.1159/000438901

Kinfe, T. M., Pintea, B., Muhammad, S., Zaremba, S., Roeske, S., Simon, B. J., et al. (2015). Cervical non-invasive vagus nerve stimulation (nVNS) for preventive and acute treatment of episodic and chronic migraine and migraine-associated sleep disturbance: a prospective observational cohort study. *J. Headache Pain* 16:101. doi: 10.1186/s10194-015-0582-9

Kucyi, A., and Davis, K. D. (2015). The dynamic pain connectome. *Trends Neurosci.* 38, 86–95. doi: 10.1016/j.tins.2014.11.006

Kucyi, A., and Davis, K. D. (2017). The neural code for pain: from single-cell electrophysiology to the dynamic pain connectome. *Neuroscientist* 23, 397–414. doi: 10.1177/1073858416667716

Lanteri-Minet, M. (2014). Economic burden and costs of chronic migraine. *Curr. Pain Headache Rep.* 18:385. doi: 10.1007/s11916-013-0385-0

Lee, J., Eun, S., Kim, J., Lee, J. H., and Park, K. (2019). Differential Influence of Acupuncture somatosensory and cognitive/affective components on functional brain connectivity and pain reduction during low back pain state. *Front. Neurosci.* 13:1062. doi: 10.3389/fnins.2019.01062

Li, S., Li, Y., and Liu, Z. (2011). Guidelines for diagnosis and treatment of migraine in China. *CHIN. J. Pain Med.* 17, 65–86. doi: 10.3969/jissn.1006-9852.2011.02.001

Li, Z., Liu, M., Lan, L., Zeng, F., Makris, N., Liang, Y., et al. (2016). Altered periaqueductal gray resting state functional connectivity in migraine and the modulation effect of treatment. *Sci. Rep.* 6:20298. doi: 10.1038/srep20298

Li, Z., Zeng, F., Yin, T., Lan, L., Makris, N., and Jorgenson, K. (2017). Acupuncture modulates the abnormal brainstem activity in migraine without aura patients. *Neuroimag. Clin.* 15, 367–375. doi: 10.1016/j.nicl.2017.05.013

Li, Z., Zhou, J., Cheng, S., Lan, L., Sun, R., and Liu, M. (2020). Cerebral fractional amplitude of low-frequency fluctuations may predict headache intensity improvement following acupuncture treatment in migraine patients. *J. Tradit. Chin. Med.* 40, 1041–1051. doi: 10.19852/j.cnki.jtcm.2020.06.016

Liu, F., Hu, M., Wang, S., Guo, W., Zhao, J., and Li, J. (2012). Abnormal regional spontaneous neural activity in first-episode, treatment-naive patients with late-life depression: a resting-state fMRI study. *Prog. Neuropsychopharmacol. Biol. Psychiatry* 39, 326–331. doi: 10.1016/j.pnpbp.2012.07.004

Low, I., Kuo, P. C., Liu, Y. H., Tsai, C. L., Chao, H. T., and Hsieh, J. C. (2017). Altered brain complexity in women with primary dysmenorrhea: a resting-state magneto-encephalography study using multiscale entropy analysis. *Entropy* 19:680. doi: 10.3390/e19120680

Luo, N., Sui, J., Abrol, A., Lin, D., Chen, J., Vergara, V. M., et al. (2020). Age-related structural and functional variations in 5,967 individuals across the adult lifespan. *Hum. Brain Mapp.* 41, 1725–1737. doi: 10.1002/hbm.24905

Luo, W., Zhang, Y., Yan, Z., Liu, X., Hou, X., Chen, W., et al. (2020). The instant effects of continuous transcutaneous auricular vagus nerve stimulation at acupoints on the functional connectivity of amygdala in migraine without aura: a preliminary study. *Neural Plast* 2020:8870589. doi: 10.1155/2020/8870589

Magon, S., May, A., Stankewitz, A., Goadsby, P. J., Tso, A. R., and Ashina, M. (2015). Morphological Abnormalities of Thalamic Subnuclei in Migraine: a Multicenter MRI Study at 3 Tesla. *J. Neurosci.* 35, 13800–13806. doi: 10.1523/JNEUROSCI.2154-15.2015

Martucci, K. T., and Mackey, S. C. (2018). Neuroimaging of Pain: human Evidence and Clinical Relevance of Central Nervous System Processes and Modulation. *Anesthesiology* 128, 1241–1254. doi: 10.1097/ALN.0000000000002137

Messina, R., and Filippi, M. (2020). What We Gain From Machine Learning Studies in Headache Patients. *Front. Neurol.* 11:221. doi: 10.3389/fneur.2020.00221

Ong, W. Y., Stohler, C. S., and Herr, D. R. (2019). Role of the Prefrontal cortex in pain processing. *Mol. Neurobiol.* 56, 1137–1166. doi: 10.1007/s12035-018-1130-9

Ossipov, M. H., Morimura, K., and Porreca, F. (2014). Descending pain modulation and chronification of pain. *Curr. Opin. Supp. Palliat. Care.* 8, 143–151. doi: 10.1097/SPC.0000000000000055

Power, J. D., Barnes, K. A., Snyder, A. Z., Schlaggar, B. L., and Petersen, S. E. (2012). Spurious but systematic correlations in functional connectivity MRI networks arise from subject motion. *NeuroImage* 59, 2142–2154. doi: 10.1016/j.neuroimage.2011.10.018

Rasmussen, B. K., and Olesen, J. (1992). Migraine with aura and migraine without aura: an epidemiological study. *Cephalalgia* 12, 186–221. doi: 10.1046/j.1468-2982.1992.1204221.x

Redlich, R., Opel, N., Grotegerd, D., Dohm, K., Zaremba, D., Bürger, C., et al. (2016). Prediction of Individual Response to Electroconvulsive Therapy via Machine Learning on Structural Magnetic Resonance Imaging Data. *JAMA Psychiatry* 73, 557–564. doi: 10.1001/jamapsychiatry.2016.0316

Shi, Y., Liu, Z., Zhang, S., Li, Q., Guo, S., Yang, J., et al. (2015). Brain network response to acupuncture stimuli in experimental acute low back pain: an fMRI study. *Evid. Based Compl. Alternat. Med.* 2015:210120. doi: 10.1155/2015/210120

Silberstein, S. D., Calhoun, A. H., Lipton, R. B., Grosberg, B. M., Cady, R. K., Dorlas, S., et al. (2016). Chronic migraine headache prevention with non-invasive vagus nerve stimulation: the EVENT study. *Neurology* 87, 529–538. doi: 10.1212/WNL.0000000000002918

Smitha, K. A., Akhil Raja, K., Arun, K. M., Rajesh, P. G., Thomas, B., and Kapilamoorthy, T. R. (2017). Resting state fMRI: a review on methods in resting state connectivity analysis and resting state networks. *Neuroradiol. J.* 30, 305–317. doi: 10.1177/1971400917697342

Steiner, T. J., Stovner, L. J., and Birbeck, G. L. (2013). Migraine: the seventh disabler. *Headache* 53, 227–229. doi: 10.1111/head.12034

Straube, A., Ellrich, J., Eren, O., Blum, B., and Ruscheweyh, R. (2015). Treatment of chronic migraine with transcutaneous stimulation of the auricular branch of the vagal nerve (auricular t-VNS): a randomized, monocentric clinical trial. *J. Headache Pain* 2015:543. doi: 10.1186/s10194-015-0543-3

Sui, J., Qi, S., van Erp, T., Bustillo, J., Jiang, R., and Lin, D. (2018). Multimodal neuromarkers in schizophrenia via cognition-guided MRI fusion. *Nat. Commun.* 9:3028. doi: 10.1038/s41467-018-05432-w

Sun, R., He, Z., Ma, P., Yin, S., Yin, T., Liu, X., et al. (2021). The participation of basolateral amygdala in the efficacy of acupuncture with deqi treating for functional dyspepsia. *Brain Imag. Behav.* 15, 216–230. doi: 10.1007/s11682-019-00249-7

Tassorelli, C., Grazzi, L., de Tommaso, M., Pierangeli, G., Martelletti, P., and Rainero, I. (2018). Non-invasive vagus nerve stimulation as acute therapy for migraine: the randomized PRESTO study. *Neurology* 91, e364–e373. doi: 10.1212/WNL.0000000000005857

Tessitore, A., Russo, A., Giordano, A., Conte, F., Corbo, D., De Stefano, M., et al. (2013). Disrupted default mode network connectivity in migraine without aura. *J. Headache Pain* 14:89. doi: 10.1186/1129-2377-14-89

Tu, Y., Ortiz, A., Gollub, R. L., Cao, J., Gerber, J., Lang, C., et al. (2019). Multivariate resting-state functional connectivity predicts responses to real and sham acupuncture treatment in chronic low back pain. *Neuroimag. Clin.* 23:101885. doi: 10.1016/j.nicl.2019.101885

Tu, Y., Zeng, F., Lan, L., Li, Z., Maleki, N., Liu, B., et al. (2020). An fMRI-based neural marker for migraine without aura. *Neurology* 94, e741–e751. doi: 10.1212/WNL.0000000000008962

Wang, J. J., Chen, X., Sah, S. K., Zeng, C., Li, Y. M., Li, N., et al. (2016). Amplitude of low-frequency fluctuation (ALFF) and fractional ALFF in migraine patients: a resting-state functional MRI study. *Clin. Radiol.* 71, 558–564. doi: 10.1016/j.crad.2016.03.004

Wang, L., Li, H., Liang, Y., Zhang, J., Li, X., Shu, N., et al. (2013). Amnestic mild cognitive impairment: topological reorganization of the default-mode network. *Radiology* 268, 501–514. doi: 10.1148/radiol.13121573

Westergaard, M. L., Hansen, E. H., Glümer, C., Olesen, J., and Jensen, R. H. (2014). Definitions of medication-overuse headache in population-based studies and their implications on prevalence estimates: a systematic review. *Cephalalgia* 34, 409–425. doi: 10.1177/0333102413512033

Wu, T. H., Tu, C. H., Chao, H. T., Li, W. C., Low, I., Chuang, C. Y., et al. (2016). Dynamic changes of functional pain connectome in women with primary dysmenorrhea. *Sci. Rep.* 6:24543. doi: 10.1038/srep24543

Xue, T., Yuan, K., Cheng, P., Zhao, L., Zhao, L., Yu, D., et al. (2013). Alterations of regional spontaneous neuronal activity and corresponding brain circuit changes during resting state in migraine without aura. *NMR Biomed.* 26, 1051–1058. doi: 10.1002/nbm.2917

Xue, T., Yuan, K., Zhao, L., Yu, D., Zhao, L., Dong, T., et al. (2012). Intrinsic brain network abnormalities in migraines without aura revealed in resting-state fMRI. *PLoS One* 7:e52927. doi: 10.1371/journal.pone.0052927

Yan, C. G., Cheung, B., Kelly, C., Colcombe, S., Craddock, R. C., and Di Martino, A. (2013). A comprehensive assessment of regional variation in the impact of head micromovements on functional connectomics. *NeuroImage* 76, 183–201. doi: 10.1016/j.neuroimage.2013.03.004

Yin, T., Sun, G., Tian, Z., Liu, M., Gao, Y., Dong, M., et al. (2020). The Spontaneous Activity pattern of the middle occipital gyrus predicts the clinical efficacy of acupuncture treatment for migraine without aura. *Front. Neurol.* 11:588207. doi: 10.3389/fneur.2020.588207

Yin, Y., Wang, Z., Zhang, Z., and Yuan, Y. (2016). Aberrant topographical organization of the default mode network underlying the cognitive impairment of remitted late-onset depression. *Neurosci. Lett.* 629, 26–32. doi: 10.1016/j.neulet.2016.06.048

Younis, S., Hougaard, A., Noseda, R., and Ashina, M. (2019). Current understanding of thalamic structure and function in migraine. *Cephalalgia* 39, 1675–1682. doi: 10.1177/0333102418791595

Yu, S., Xie, M., Liu, S., Guo, X., Tian, J., Wei, W., et al. (2020). Resting-state functional connectivity patterns predict acupuncture treatment response in primary dysmenorrhea. *Front. Neurosci.* 14:559191. doi: 10.3389/fnins.2020.559191

Zang, Y., Jiang, T., Lu, Y., He, Y., and Tian, L. (2004). Regional homogeneity approach to fMRI data analysis. *NeuroImage* 22, 394–400. doi: 10.1016/j.neuroimage.2003.12.030

Zhang, J., Su, J., Wang, M., Zhao, Y., Zhang, Q. T., and Yao, Q. (2017). The sensorimotor network dysfunction in migraineurs without aura: a resting-state fMRI study. *J. Neurol.* 264, 654–663. doi: 10.1007/s00415-017-8404-4

Zhang, Y., Huang, Y., Li, H., Yan, Z., Zhang, Y., Liu, X., et al. (2021). Transcutaneous auricular vagus nerve stimulation (taVNS) for migraine: an fMRI study. *Reg. Anesth. Pain Med.* 46, 145–150. doi: 10.1136/rapm-2020-102088

Zhang, Y., Liu, J., Li, H., Yan, Z., Liu, X., Cao, J., et al. (2019a). Transcutaneous auricular vagus nerve stimulation at 1 Hz modulates locus coeruleus activity and resting state functional connectivity in patients with migraine: an fMRI study. *Neuroimag. Clin.* 24:101971. doi: 10.1016/j.nicl.2019.101971

Zhang, Y., Zhang, H., Nierhaus, T., Pach, D., Witt, C. M., and Yi, M. (2019b). Default mode network as a neural substrate of acupuncture: evidence, challenges and strategy. *Front. Neurosci.* 13:100. doi: 10.3389/fnins.2019.00100

Zhao, L., Liu, J., Dong, X., Peng, Y., Yuan, K., Wu, F., et al. (2013). Alterations in regional homogeneity assessed by fMRI in patients with migraine without aura stratified by disease duration. *J. Headache Pain* 14:85. doi: 10.1186/1129-2377-14-85

Zheng, X. (2002). *The Guidelines for Clinical Research on New Chinese Medicines[M]*. Beijing: The Medicine Science and Technology Press of China.

Zou, Y., Tang, W., Li, X., Xu, M., and Li, J. (2019). Acupuncture reversible effects on altered default mode network of chronic migraine accompanied with clinical symptom relief. *Neural Plast* 2019:5047463. doi: 10.1155/2019/5047463

Conflict of Interest: The authors declare that the research was conducted in the absence of any commercial or financial relationships that could be construed as a potential conflict of interest.

Publisher's Note: All claims expressed in this article are solely those of the authors and do not necessarily represent those of their affiliated organizations, or those of the publisher, the editors and the reviewers. Any product that may be evaluated in this article, or claim that may be made by its manufacturer, is not guaranteed or endorsed by the publisher.

frontiers in Molecular Neuroscience

ORIGINAL RESEARCH
published: 01 March 2022
doi: 10.3389/fnmol.2022.812035

Lateral Hypothalamic Orexin Neurons Mediate the Reward Effects of Pain Relief Induced by Electroacupuncture

*Can Wang†, Meiyu Chen†, Chuan Qin†, Xiaoyi Qu, Xueyong Shen and Sheng Liu**

School of Acupuncture-Moxibustion and Tuina, Shanghai University of Traditional Chinese Medicine, Shanghai, China

The reward of pain relief caused by acupuncture has been found to be clinically significant. However, the molecular mechanisms underlying acupuncture-induced reward of pain relief in chronic pain remain unclear and have not been analyzed in suitable preclinical models. Here, we investigated whether acupuncture could potentially induce the reward of pain relief and orexin neuronal signaling in the lateral hypothalamus (LH) and exhibit a possible role in electroacupuncture (EA)-induced reward in spared nerve injury (SNI) rats. Therefore, by using conditioned place preference (CPP) paradigm, we noticed that EA induced the preference for cues associated with EA-induced pain relief in the early, but not late, phase of chronic pain. These observations were different from the immediate antihyperalgesic effects of EA. c-Fos/orexin double labeling revealed that EA stimulation on 14 days but not on 28 days after SNI modeling activated greater numbers of c-Fos positive orexin neurons in the LH after the CPP test. Moreover, the administration of an orexin-A antagonist in the LH significantly blocked the reward effects of pain relief induced by EA. Furthermore, by using cholera toxin b subunit combined with c-Fos detection, we found that the orexin circuit from the LH to the nucleus accumbens (NAc) shell was significantly activated after EA induced CPP. Microinjection of the orexin antagonist into the NAc shell substantially attenuated the CPP induced by EA. Intravenous injection of low-dose orexin-A together with EA resulted in significantly greater antihyperalgesia effects and CPP scores. Together, these findings clearly demonstrated that LH orexin signaling could potentially play a critical role in the reward effects of pain relief induced by acupuncture. The observations of the present study extended our understanding of orexin signaling in the LH and its role in EA-induced reward, providing new insights into the mechanisms of acupuncture analgesia.

Keywords: acupuncture, reward, pain relief, orexin, lateral hypothalamus

OPEN ACCESS

Edited by:
Siyi Yu,
Chengdu University of Traditional Chinese Medicine, China

Reviewed by:
Dietmar Benke,
University of Zurich, Switzerland
Feifei Guo,
Qingdao University, China

****Correspondence:***
Sheng Liu
liusheng@shutcm.edu.cn

† These authors have contributed equally to this work

Specialty section:
This article was submitted to Neuroplasticity and Development, a section of the journal Frontiers in Molecular Neuroscience

Received: *09 November 2021*
Accepted: *03 February 2022*
Published: *01 March 2022*

Citation:
Wang C, Chen M, Qin C, Qu X, Shen X and Liu S (2022) Lateral Hypothalamic Orexin Neurons Mediate the Reward Effects of Pain Relief Induced by Electroacupuncture. Front. Mol. Neurosci. 15:812035. doi: 10.3389/fnmol.2022.812035

INTRODUCTION

It is well established that the current conceptualizations of pain in humans are predominantly multidimensional, mainly including the perception of the noxious stimulus and the affective features of pain. Moreover, both onset of pain and pain relief have been reported to be motivationally salient events, which can lead to generating avoidance (withdrawal) and approach

behavior (Porreca and Navratilova, 2017). It is generally accepted that the relief of pain can give rise to negative reinforcement, which has been appropriately described as a reward (Navratilova and Porreca, 2014). The reward effects of pain relief could facilitate learning and memory associated with relief, and drive motivation and behavior to seek a cue (context) associated with pain relief that can significantly accelerate recovery. Mounting evidence also suggest that extensive brain areas [such as anterior cingulated cortex, hypothalamus, ventral tegmental area, and nucleus accumbens (NAc)] and neurochemicals (dopamine and opioids) can possibly overlap between pain and reward pathways (Watanabe and Narita, 2018; Serafini et al., 2020). For instance, reduced analgesic efficacy has been found to be related to maladaptation of the neural circuits involved in reward induced by pain relief (Serafini et al., 2020). In laboratory animals, the conditioned place preference (CPP) paradigm has been widely used to evaluate the reward effects of pain relief (Truini et al., 2013) and the efficacy of various analgesics, especially in alleviating the aversive aspects of pain (King et al., 2009; Navratilova and Porreca, 2014; Navratilova et al., 2015). Furthermore, investigations using the CPP paradigm in rats have been found to be consistent with psychological studies in humans that can conceptualize relief of pain as a reward (Leknes et al., 2008; King et al., 2009).

Accumulating evidence has demonstrated the effectiveness of acupuncture in the clinical treatment of both acute and chronic pain (Vickers and Linde, 2014; Vickers et al., 2018). Acupuncture or electroacupuncture (EA) can not only alleviate the sensory of the noxious stimulus, but can also markedly inhibit pain affect (Zhang et al., 2012; Duanmu et al., 2017). However, the reward effect of pain relief induced by acupuncture has not been well studied in preclinical models. In fact, various lines of evidence suggest that acupuncture-induced reward of pain relief can be clinically significant. First, many patients with different types of pain feel pleasure after receiving acupuncture treatment and an expectation of pain relief can produce markedly greater acupuncture analgesia in patients with pain (Kong et al., 2009). Second, it has been shown that the cognitive and emotional control of pain is modulated effectively by different reward/motivational circuits (Elman and Borsook, 2016). Interestingly, fMRI studies have demonstrated specific functional responses in the brain reward systems associated with acupuncture analgesia (Wang Z. et al., 2017; Yu et al., 2020b). Third, altered neuronal processing in the reward/motivational systems may also be involved in the regulation of pain sensitivity and tolerance (DosSantos et al., 2017; Yu et al., 2020a). This raises an important issue that should be addressed in preclinical models, namely, whether the pain relief produced by acupuncture can possibly induce a reward and drive pain relief-related approach behaviors that can potentially accelerate the recovery. Such findings may greatly help to extend our understanding of the mechanisms underlying acupuncture analgesia. Given that chronic pain can induce long-term plasticity in the brain, and neuroplasticity can adversely affect pain behaviors ranging from symptomology to the treatment response in different stages of pain (Latremoliere and Woolf, 2009), we aimed to assess the CPP induced by acupuncture during different durations of chronic pain by using a spared nerve injury (SNI) model.

Orexin (also known as hypocretin) specifically located in the hypothalamus is produced from a prepro orexin molecule orexin neurons. Several lines of evidence have suggested that the orexin neurons in the lateral hypothalamus (LH) may play a pivotal role in reward effects, including drug, food, and alcohol rewards (Harris et al., 2005; Harris and Aston-Jones, 2006). LH orexin neurons have been found to be related to behavioral preference with c-Fos activation during both the food and drugs reward processing (Harris et al., 2005; Marchant et al., 2009). Notably, the orexin system has also been shown to be involved in analgesia and has been implicated in the descending pain inhibition (Ossipov et al., 2010). Activation of orexin neurons can give rise to analgesic effects in both neuropathic and inflammatory pain conditions and can effectively suppress the aversive response to various noxious stimuli (Zhou et al., 2018). Interestingly, several studies have suggested that acupuncture analgesia might involve the orexin neuronal system. For instance, Feng et al. (2012) found that EA could significantly alleviate postlaparotomy pain through the spinal orexin-A receptor. Recent work has also shown that the median nerve electrical stimulation (EA at SP6) can induce the activation of hypothalamic orexin neurons *via* the activation of cannabinoid receptor 1, and can thereby mediate the disinhibition of the periaqueductal gray (PAG), which can effectively contribute to EA analgesia (Chen et al., 2018). In addition, there is extensive innervation of the NAc by LH orexin neurons, and orexin receptors have also been found to be highly expressed in these areas (Patyal et al., 2012; Burdakov, 2020; Khosrowabadi et al., 2020). The NAc can integrate the rewarding valence of the stimuli and exhibit plastic adaptations in pain processing (Massaly et al., 2019; Makary et al., 2020). We hypothesized that LH orexin neurons and their potential neural circuit to the NAc represent an important mechanism for regulating acupuncture-induced reward of pain relief.

MATERIALS AND METHODS

Animals

Adult male Sprague-Dawley rats (230–300 g; Slack) were purchased from the Laboratory Animal Center of Shanghai University of TCM. The rats were allowed to acclimatize for 7 days. The rats were housed in a clean animal environment (temperature of 24 C ± 2 C, 12/12-h light/dark schedule). The animal experiments were approved by the Shanghai University of TCM Animal Ethics Committee (SZY 201710008). The animal license was No. PZSHUTCM210709001. The experiments were conducted in accordance with NIH standard guidelines for the use and care of experimental animals.

Drugs

Orexin-A (purchased from Tocris Bioscience, Minneapolis, MN, United States) was dissolved in 0.9% sterile saline. The orexin-A receptor antagonist SB-334867 (SB; obtained from MedChem Express, Monmouth Junction, NJ, United States) was dissolved in a vehicle [50% dimethyl sulfoxide (DMSO), 50% saline]

to prepare a stock solution of 3.0 nmol/0.3 μl for use. The dose was selected according to a previous study (Narita et al., 2006). Cholera toxin b subunit [CTb; Sigma, St Louis, MO, United States, 0.5% dissolved in 0.1 M phosphate buffer (PB)] was used for retrograde neuronal tracing.

Spared Nerve Injury Animal Model

As described in the previous studies (Decosterd and Woolf, 2000; Shields et al., 2003), the rats were anesthetized with isoflurane (5%). To separate the biceps femoris and to expose the sciatic nerve and its associated branches, an incision proximal to the lateral side of the right knee was made and thereafter the biceps femoris was separated. The sciatic nerve and its branches were exposed. A silk suture was then used to ligate the common peroneal and tibial nerve branches. We removed about 1 mm of the nerve and kept the sural nerve intact. In the Sham SNI group, the operation was performed by following the same procedure, but we did not cut-off or ligate the sciatic nerve, peroneal nerve, and tibial nerve branches.

Electroacupuncture Treatment

We first restrained the rats gently. Thereafter, the rats were subjected to EA with two stainless steel needles (0.3 mm diameter) inserted bilaterally into ST36 and SP6 at a depth of 5 mm (**Figure 2A**), as previously described (Wang X. et al., 2017). Acupuncture point ST36 is located between the muscle anterior tibialis and muscle extensor digitorum longus near the knee joint. In contrast, SP6 is located at 3 mm proximal to the superior border of the medial malleolus. A constant current square wave electric stimulation produced by using a stimulator (Model G-6805-2, China) was continuously transferred *via* the needles. We set a 2-Hz stimulation frequency with increasing stimulation intensity (from 0.5, 1.5 to 2 mA, 10 min each step). In the Sham EA, the needles were inserted into acupoints, but without any electric stimulation.

Behavioral Testing

Paw Withdrawal Latency

We measured paw withdrawal latency (PWL) in the rats by using an IITC Model 390 Paw Stimulator Analgesia Meter (IITC/Life Science Instruments, United States). We placed the rats in an inverted plastic cage. After the rats were accommodated for 30 min, a radiant heat was used to warm the hind paw of rats until they lifted their paw. We adjusted the radiant heat intensity to induce the response around 12–13 s in a normal rat. Thereafter, the PWL scores were analyzed by calculating the time from onset of radiant heat application to the paw withdrawal. The test was repeated three times independently in each rat to calculate the mean values of the PWL scores.

Conditional Place Preference

The CPP paradigm is shown in **Figure 2B**. A standard two-chamber balanced design was used to test the reward effects of pain relief induced by EA. On the preconditioning day, the rats were allowed to travel the chambers freely for 15 min, and the amount of time spent in each chamber was recorded. Next, two conditioning sessions (for EA and gentle handling) were performed for three consecutive days. Rats were treated with either EA or gentle handling for 30 min each in the morning and afternoon. We immediately placed the rats into the pairing chamber and confined them to the chamber for 30 min after administration of 30 min EA or gentle handling. For every conditioned animal, EA and gentle handling were carried out alternatively in the morning and afternoon sessions. The morning and afternoon EA/gentle handling were conducted at least 4 h apart. A preference test was conducted 3 days after the conditioning. The rats were allowed to freely access the apparatus for 15 min. The preference scores were analyzed by calculating the amount of time the animals spent in the EA-reward paired chamber minus the time they spent in the gentle handling chamber. The rats in the SNI group were conditioned in each chamber without any specific treatment, while the Sham EA group was conditioned with Sham EA treatment.

Protocols for Behavioral Experiment

Chronic pain differs fundamentally from acute pain in that it can potentially induce long-term plasticity in the central nervous system during the course of the disease, leading to an association of various modulatory factors to induce distinct changes in perception and behavior. Acupuncture has shown significant analgesic effects in various animal models of chronic pain (Koo et al., 2002; Zhang et al., 2014; Li et al., 2019). However, only a few studies have previously investigated the immediate effect of EA on pain at the different phases of chronic pain. Here, we tested the immediate antihyperalgesic effects of EA on the different stages of chronic pain using an SNI animal model. We randomly divided the rats into eight different groups (eight rats per group): Sham SNI, SNI, EA + 7 days SNI, EA + 14 days SNI, EA + 21 days SNI, EA + 28 days SNI, EA + 45 days SNI, and Sham EA groups. The control group did not undergo any substantial SNI modeling. The rats received EA treatment for 30 min on day 7 (EA + 7 days SNI group), day 14 (EA + 14 days SNI group), day 21 (EA + 21 days SNI group), day 28 (EA + 28 days SNI group), and day 45 (EA + 45 days SNI) after the establishment of the SNI model. Sham EA rats were subjected to the same treatment regimen but were not given any electrical stimulation. Thermal hyperalgesia was thereafter determined for 90 min after the end of the EA treatment using the PWL test. The CPP procedure induced by 4-day EA stimulation was performed on the day following the PWL test. Five Sham SNI rats subjected to the same EA regimen were as controls.

Cannula Surgeries and Microinjections

Cannula Surgeries

We implanted cannulae in the LH and the NAc shell similar to those described in our previous publications (Hou et al., 2021). The rats were first anesthetized with pentobarbital sodium (50 mg/kg, i.p.) and were then mounted on a stereotaxic frame. During the surgery, the rats received isoflurane through a nosecone (1.5–2%). We then implanted guide cannulae (26 gauge, Plastics One) in the LH (−2.7 mm AP; ±1.7 mm ML; −8.6 mm DV) or the NAc (+1.8 mm AP; ±2.1 mm ML; −7.3 mm DV; 10° from Bregma). The cannula was then fixed to the skull with dental cement, and three steel screws and obturators were inserted into the cannula immediately following the surgery, with the tips extending into the intended site of injection. The rats

were given systemic antiseptic solution (benzylpenicillin sodium, 60,000 units) to avoid contamination and were allowed to recover 5–7 days after the surgery.

Microinfusion

The rats received a bilateral injection of SB (3.0 nmol/0.3 μl) or vehicle (DMSO) in each LH or NAc shell 5 min before the CPP test. For microinjections, the obturators were first removed from the guide cannulae and 33-gauge injector needles were inserted so that the tips extended 2 mm beyond the end of the guide cannula. The drug or DMSO solutions were then infused bilaterally and delivered over a 60-s period while the rat moved freely in a plastic housing cage. An injector cannula was kept in place for 60 s after the end of the drug infusion to facilitate the diffusion into the surrounding tissues. We verified all cannula placements by microinfusion at the injection site, removing the brains under deep anesthesia, slicing them into 40 μm sections, and staining the tissues with Nissl stain for microscopic inspection. Two rats were excluded from the CPP task because of cannula misplacements. The cannula placements are shown in the behavior-associated figures.

Anterograde Tracing

The rats were anesthetized by administering pentobarbital sodium (50 mg/kg, i.p.) and a small hole was drilled through the skull above the LH to remove the dura. A 30-gauge needle was lowered into the right LH (−2.7 mm AP; +1.7 mm ML; −8.6 mm DV). A total of 30 nl of CTb was delivered *via* the pressure injection. Thereafter, the injection was performed over 1 min. After the injection, the needle was left in place for 15 min. CTb injections that diffused outside LH were not included in this study. The rats were allowed to recover for 7 days after the surgery before CPP conditioning and testing. To confirm the potential CTb sites in the LH, tissue sections were reacted with rabbit anti-CTb antibodies (1:500, Sigma) and then incubated for 2 h in Alexa Fluor 488 anti-rabbit (1:500, Sigma).

Immunohistochemistry

The rats were anesthetized with 100 mg/kg pentobarbital sodium (i.p.) 90 min after CPP test. Next, rats were transcardially perfused with 200 ml saline and 250 ml of 4% paraformaldehyde in 0.1 mol/L PB. The brains were then removed and placed in a fresh fixative for an additional 4 h at 4°C. The brains were thereafter stored in 30% sucrose at 4°C for 3–5 days. The coronal sections (40 μm) of the different brain areas were cut using a cryostat at −25°C. All the sections were collected in 0.01 M phosphate-buffered saline (PBS).

c-Fos/Orexin Double Labeling

The sections were stained for c-Fos and orexin using procedures previously described by us (Hou et al., 2021). We incubated free-floating sections in 1% bovine serum albumin for 2 h at 4°C. Thereafter, the sections were sequentially incubated at 4°C with two different primary antibodies, including anti-mouse c-Fos primary antibody (1:500; ab208942, Abcam, Cambridge, United Kingdom) and orexin polyclonal antibody (1:1,000, produced by recombinant technology for high batch-to-batch consistency; ab255294, Abcam) for 48 h. Thereafter, the sections were incubated in the goat anti-mouse IgG (1:500; ab150115, Abcam) and the goat polyclonal secondary antibody to rabbit IgG (1:500; ab150077, Abcam) for 2 h at room temperature and washed again. Finally, the brain sections were placed on clean and antifluorescence quenching slides.

Cholera Toxin b/c-Fos Double Labeling

We performed the CTb/c-Fos double label immunohistochemistry using the same procedure as described for c-Fos/orexin double labeling. We used rabbit c-Fos primary antibody (1:500, SAB2100833, Sigma) and goat anti-CTb primary antibody (1:500, C730, Sigma) as the two primary antibodies. The donkey anti-goat Alexa Fluor 488 (1:500, SAB4600387, Sigma) and goat anti-rabbit Alexa Fluor 647 (1:500, AF647, Sigma) antibodies were used as secondary antibodies.

Neuronal Counting

We used a Leica Laser Confocal Microscope (Leica, Germany) to analyze the various stained sections. The stereotaxic plane sections of the LH and NAc shell were identified as per the instructions in Paxinos and Watson's atlas (George and Charles, 1986), with the numbers of positive cells per section being assessed (20×). An automatically generated 200 μm × 500 μm rectangle was placed in a fixed area of the NAc shell, LH, perifornical area (PFA), and DMN. The analysis software (Image Pro, China) was used to count the number of positive neurons per section. The numbers of the positive neurons per section for analysis were determined. A blinded observer counted the number of positive neurons on the saved image. The dorsal and ventral subregions of the NAc shell were analyzed separately. Given that there were no significant differences found in either c-Fos, CTb, or CTb/c-Fos counts between the dorsal and ventral NAc shells, the results were combined after analysis. For c-Fos/orexin labeling, % of orexin neurons that were c-Fos positive in the hypothalamus were calculated.

Statistical Analysis

The experimental data were presented as mean ± SEM. The preference scores and immunohistochemistry data among the groups were compared *via* one-way analysis of variance (ANOVA). We analyzed the PWL scores using repeated measures ANOVA (time as a within-subject factor and group as a between-subject factor). When significance was found using ANOVA procedures, *post hoc* analysis was carried out using Fisher's LSD test. $p < 0.05$ was the threshold of significance for these analyses.

RESULTS

The Immediate Antihyperalgesic Effect of Electroacupuncture During the Different Stages of Chronic Pain

As shown in **Figure 1A**, the PWL scores were found to be significantly reduced immediately after SNI modeling in comparison with the Sham SNI group and were maintained

for at least 45 days after SNI. The immediate antihyperalgesic effect of EA was assessed on days 7, 14, 21, 28, and 45 after SNI. It was observed that compared with the PWL scores before EA stimulation, the scores were significantly increased 0 and 30 min after EA in EA + 7 days SNI group, EA + 14 days SNI, EA + 21 days SNI, EA + 28 days SNI, and EA + 45 days SNI groups (**Figure 1B**). No significant differences were observed in the PWL scores before and after Sham EA ($p > 0.05$). This indicated that EA produced a significant immediate antihyperalgesic effect at different stages of chronic pain (**Figure 1B**). The PWL scores were observed to be increased immediately after EA stimulation, reaching maximal levels within 30 min and declining to a minimum at 90 min after EA stimulation in all groups except the Sham EA group (**Figure 1B**).

Electroacupuncture Induced Conditioned Place Preference at the Early Phase of Chronic Pain but Not During the Late Phase

In the CPP analyses, we found significant differences in the CPP scores among the seven different groups [$F(7,47) = 3.84$, $p < 0.01$]. As shown in **Figure 2**, the EA + 7 days SNI, EA + 14 days SNI, and EA + 21 days SNI rats exhibited marked preferences for the EA-paired chamber compared with the SNI group ($p < 0.05$). However, no significant differences were found in the CPP scores among the SNI, EA + 28 days SNI, EA + 45 days SNI, and Sham EA groups ($p > 0.05$). It was observed that EA did not induce CPP in the Sham-operated animals compared with the SNI group ($p > 0.05$), indicating that EA did not induce a reward in the absence of pain. These findings clearly indicated that EA induced the reward effects of pain relief at the early phase of chronic pain but not at the late phase.

Conditioned Place Preference Induced by Electroacupuncture Activated c-Fos-Positive Orexin Neurons in the Lateral Hypothalamus

For this experiment, 1.5 h after the CPP test, 4 or 5 rats per group selected randomly from the control, SNI, and EA + 14 days SNI groups as well as the EA + 28 days SNI group and were deeply anesthetized for immunohistochemistry. We thereafter measured the total number of orexin neurons in the LH, PFA, and dorsomedial hypothalamus (DMH) expressing c-Fos protein by using double immunofluorescent labeling of c-Fos protein and orexin-A. As shown in **Figure 3**, significant differences in the percentages of orexin neurons that were c-Fos positive in the LH were detected among the four groups [$F(3,32) = 4.61$; $p = 0.009$]. EA stimulation on day 14 after SNI modeling increased the numbers of c-Fos-positive orexin neurons in the LH compared with the control group, the SNI group, and the EA + 28 days SNI group ($p < 0.01$). We did not notice any significant differences in the percentages of orexin neurons that were c-Fos positive in the LH among the control group, the SNI group, and the EA + 28 days SNI group ($p > 0.05$), indicating that EA on day 28 after SNI surgery did not activate LH orexin neurons. In addition, no significant differences were observed in c-Fos-positive orexin neurons among the different groups in the PFA [$F(3,32) = 0.81$, $p > 0.05$] and the DMH [$F(3,32) = 1.14$, $p > 0.05$].

Microinjection of Orexin Antagonist SB334867 Into the Lateral Hypothalamus Can Significantly Ablate Electroacupuncture Induced Conditioned Place Preference in Spared Nerve Injury Rats

To further decipher the potential effects of LH orexin neurons on the reward of pain relief induced by EA in SNI model rats, microinjection of orexin antagonist SB334867 into the LH was carried out 18 days after the establishment of the SNI model (**Figure 4A**). We detected significant differences in the preference scores among the different groups [$F(3,18) = 13.77$; $p < 0.01$, **Figure 4**]. It was found that the SNI + EA group exhibited a preference for the EA-paired chamber compared with the SB + SNI group and SB + EA group ($p < 0.01$). Moreover, LH microinjection of SB334867 (SB + SNI + EA group) significantly reduced the preference scores relative to rats in the SNI + EA group (55.8 ± 30.4s vs. 299.3 ± 49.1 s; $p < 0.01$). These observations indicated that administration of the orexin antagonist into the LH ablated EA-induced seeking behavior in SNI rats.

The Orexinergic Neural Pathway From the Lateral Hypothalamus to the Nucleus Accumbens Could Be Activated by Electroacupuncture-Induced Reward of Pain Relief

The NAc shell is an important target of orexin neuronal projections that has been found to be involved in orexin effects involving pain and reward. It has been suggested that the NAc shell and its interactions with LH orexin neurons might be involved in drug-, food-, and alcohol-seeking behaviors (Millan et al., 2010; Marchant et al., 2012). We next tested whether EA-induced CPP activated the afferents from the LH to NAc shell using CTb/c-Fos double-label immunohistochemistry. There were significant differences found among the different groups in the preference scores [$F(3,18) = 13.77$; $p < 0.001$, **Figures 5**, **6**]. Moreover, the EA-treated rats still displayed higher preference scores for the EA-paired chamber compared with the SNI group ($p < 0.05$). The distribution of CTb neurons after microinjection into the LH was observed to be similar to the previous studies, including the NAc shell, the prefrontal cortex, the raphe, the locus ceruleus, and the ventral tegmental area (Hamlin et al., 2008; Petrovich et al., 2012). We primarily focused on NAc shell in the present study. **Figure 6B** shows a representative photomicrograph of CTb microinjection in the LH. There was significant difference found among the various groups in c-Fos expression and double-labeled CTb/Fos neurons in the NAc shell [$F(2,9) = 6.06$, $p < 0.05$; $F(2,9) = 4.87$, $p < 0.05$; respectively]. The EA groups also showed marked increases in c-Fos-positive

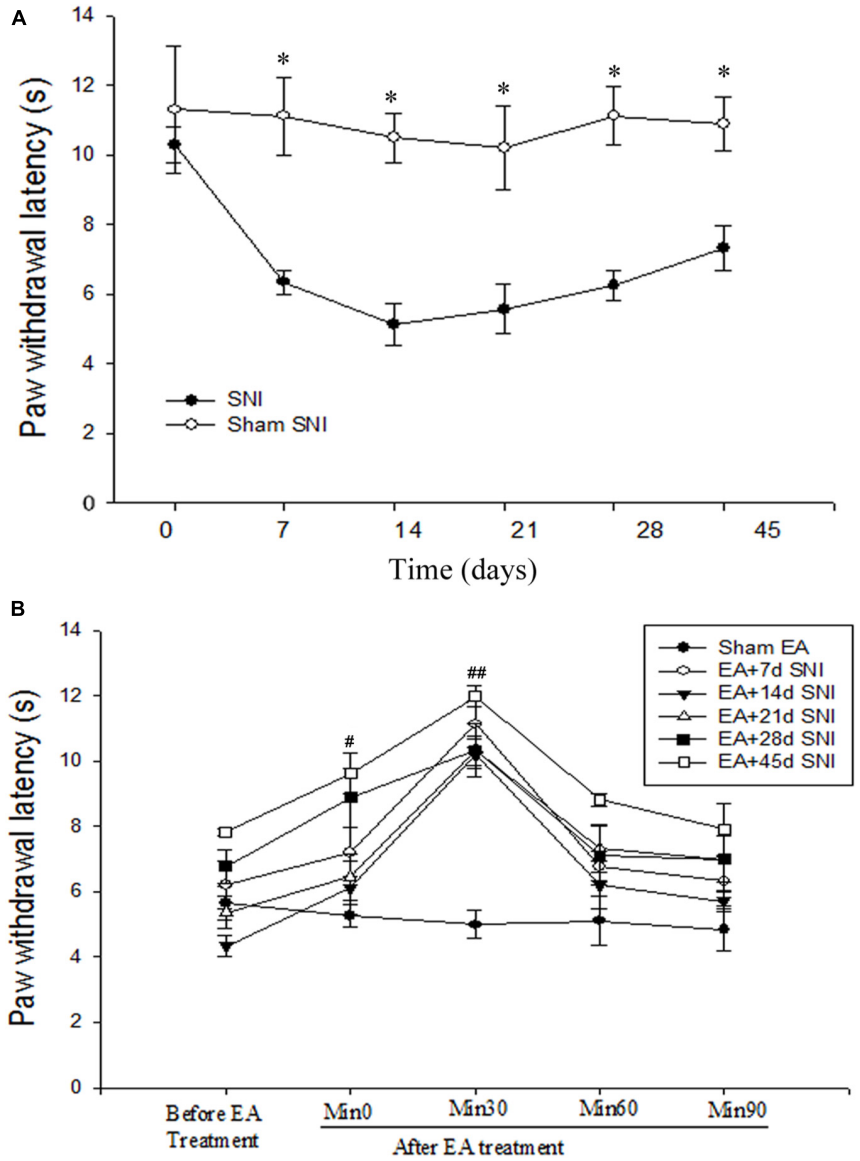

FIGURE 1 | Immediate antihyperalgesic effects of EA at the different stages of spare nerve injury (SNI). **(A)** Thermal hyperalgesia during 45 days after the SNI operation. $^{*}p < 0.01$. **(B)** Immediate effects of single EA on thermal hyperalgesia during the different stages of SNI. $^{\#}p < 0.05$; $^{\#\#}p < 0.01$ vs. PWL scores before EA stimulation. There were no significant differences in PWL scores before and after Sham EA ($p > 0.05$).

orexin neurons in the NAc shell compared with the control and the SNI groups (Fisher's LSD test; $p < 0.05$; **Figure 6C**). No significant difference was observed among the different groups in CTb neurons in the NAc shell [$F(2,9) = 0.66$, $p > 0.05$].

Microinjection of SB334867 Into the Nucleus Accumbens Shell Ablates Electroacupuncture-Induced Conditioned Place Preference in Spared Nerve Injury Rats

Next, we further characterized NAc shell as a critical site of orexin actions during the reward effects of pain relief induced by EA. The rats were implanted with cannulae in the NAc shell as described in the experimental techniques. The rats were given one week of recovery time after the surgery before CPP conditioning and testing. Thereafter, the rats were given an injection of SB or vehicle (DMSO) in each NAc shell 30 min prior to being placed in the CPP test (**Figure 7A**). Significant differences were found among the various groups in the preference scores [$F(3,18) = 3.83$; $p = 0.03$, **Figure 7**]. The SNI + EA group displayed a significant preference for the EA-paired chamber compared with the SNI group ($p < 0.01$). NAc shell microinjection of SB334867 significantly reduced the preference scores relative to the rats in the SNI + EA group ($p < 0.05$).

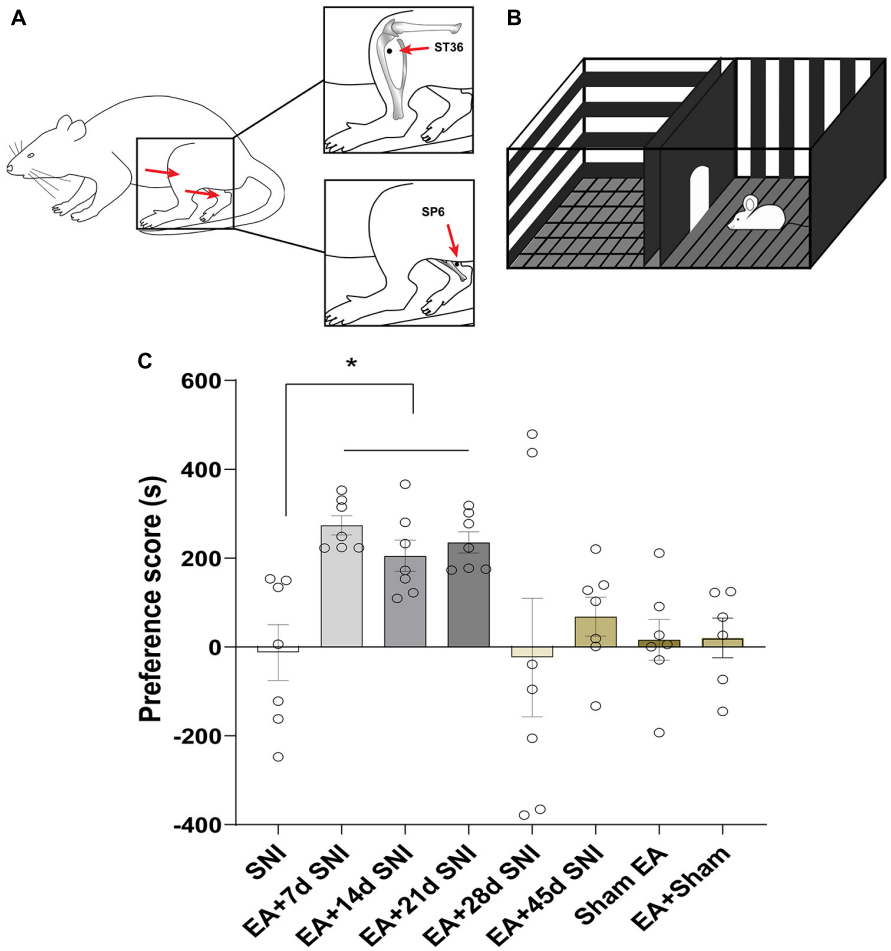

FIGURE 2 | Electroacupuncture induced CPP at the early phase of chronic pain but not at the late phase. **(A)** Placement of EA stimulation. EA was performed at the acupuncture points ST36 and SP6 (solid circle). **(B)** A standard two-chamber for CPP conditioning and test. **(C)** The preference scores among the various groups. *$p < 0.01$ vs. SNI group.

Effects of Combined Electroacupuncture and Low-Dose Orexin-A Treatment on the Thermal Hyperalgesia and Conditioned Place Preference Scores

We next investigated the immediate effect of EA and low-dose orexin-A on thermal hyperalgesia and the CPP scores. According to Bingham et al.'s (2001) study, orexin-A significantly increased the latency to response in a dose-dependent manner (1, 3, 10, and 30 mg/kg) when given intravenously 5 min pretest in rats. We, therefore, selected 1 mg/kg orexin-A (ORXA, i.v. injection) for the present study. The rats were divided into the following groups (n = 6–8 per group): (a) SNI, (b) EA + ORXA, (c) EA + saline, (d) Sham EA + ORXA. The ANOVA analysis showed significant differences in the PWL scores among the different groups [$F(3,38) = 8.03$; $p < 0.001$, **Figure 8**]. The EA + ORXA, EA + saline, and Sham EA + ORXA groups displayed increased PWL scores compared with the SNI group ($p < 0.01$). However, the combination of EA and orexin-A (EA + ORXA group) showed markedly higher PWL scores than those of the EA + saline and Sham EA + ORXA groups ($p < 0.05$). We also found significant differences among the various groups in the preference scores [$F(3,18) = 13.77$, $p < 0.001$; **Figure 8B**]. Additionally, compared with the SNI and Sham EA + ORXA animals, EA + ORXA and EA + saline rats exhibited a preference for the EA-paired chamber compared with the SNI and Sham EA + ORXA animals ($p < 0.05$). The combination of EA and orexin-A (EA + ORXA group) was found to induce higher CPP scores compared with EA + saline group ($p < 0.05$).

DISCUSSION

The aim of the present study was to determine whether acupuncture induces rewards of pain relief, together with investigating whether the orexin neurons in the LH are involved in this process. Using the CPP paradigm, we found that EA was indeed able to induce the reward effects of pain relief at an early phase of chronic pain but not at a late phase, which

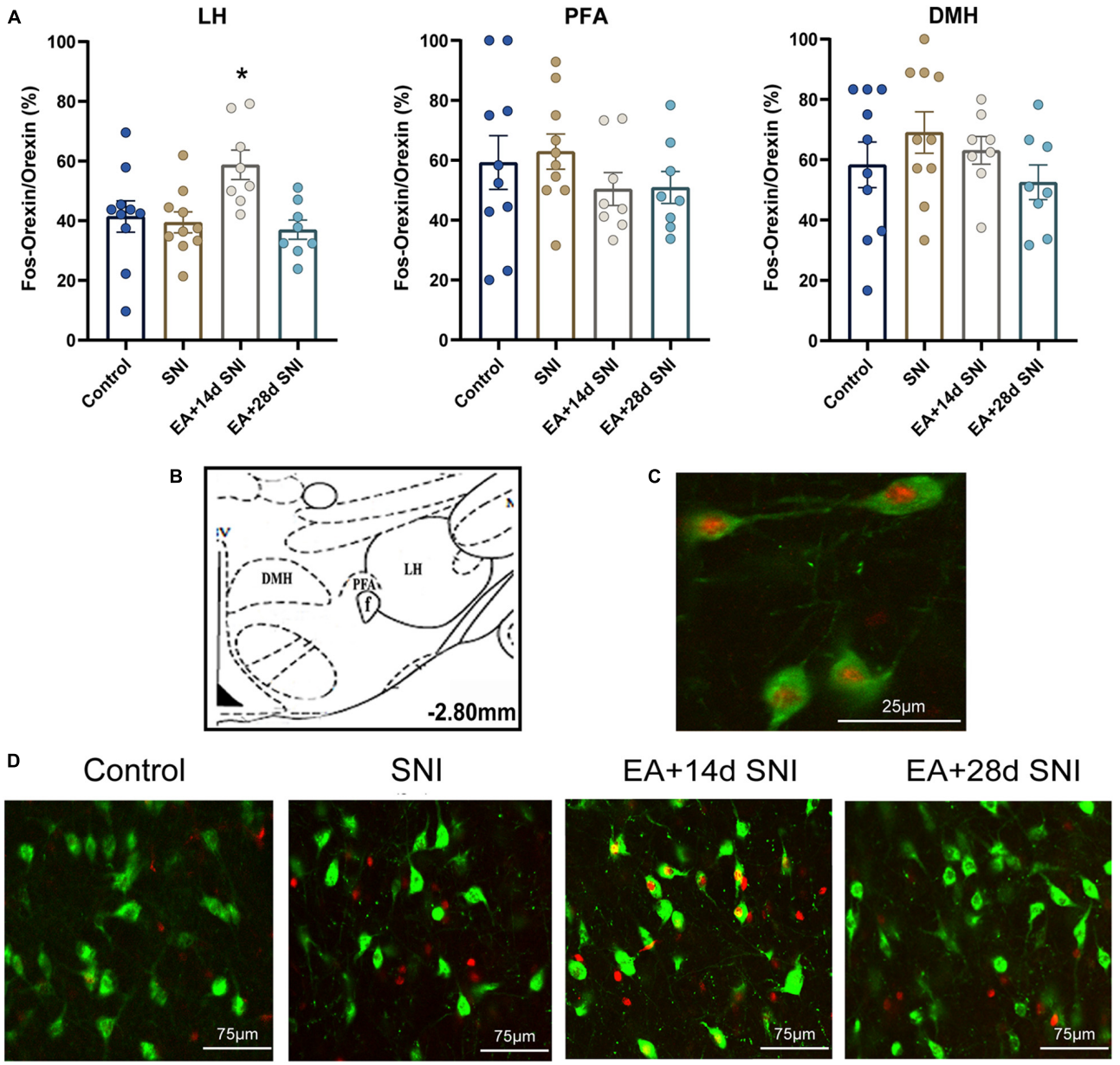

FIGURE 3 | The reward effects of pain relief induced by EA-induced activation of the c-Fos-positive orexin neurons in the LH. **(A)** The percentages of orexin neurons that were observed to be c-Fos positive in the LH, PFA and DMH. *$p < 0.01$ vs. SNI group, control group, and EA + 28 days SNI. **(B)** Schematic coronal section through the hypothalamic subregions where stained nuclei were counted. **(C)** Double-labeled orexin (green) + c-Fos-positive (red) neurons (×40) in the LH. **(D)** Representative photomicrograph showing orexin/c-Fos immunoreactivity in the LH. Scale bar, 75 μm.

was different from the antihyperalgesic effect of EA observed during the different stages. The EA-induced reward effects of pain relief activated the c-Fos-positive orexin neurons in the LH. Thereafter, by using CTb combined with Fos detection, we found that LH-projecting orexin neurons in the NAc shell were substantially activated during CPP induced by EA. Moreover, microinjection of the orexin-A antagonist in the LH and NAc shell blocked EA reward induction. A combination of both EA and low-dose orexin-A produced a greater antihyperalgesia effect and higher CPP scores. Taken together, these findings clearly demonstrate that orexin signaling in the LH can play a pivotal role in EA-induced reward effects of pain relief.

Pain relief can produce substantial negative reinforcement and is thus considered to be a potential reward. Similar to observations in humans, reward from pain relief can be demonstrated by the measurement of motivated behavior in different animals using various classically established models (for example, the CPP paradigm; Navratilova et al., 2012, 2015; Porreca and Navratilova, 2017). Our results showed that EA induced a significant preference for the EA paired chamber in

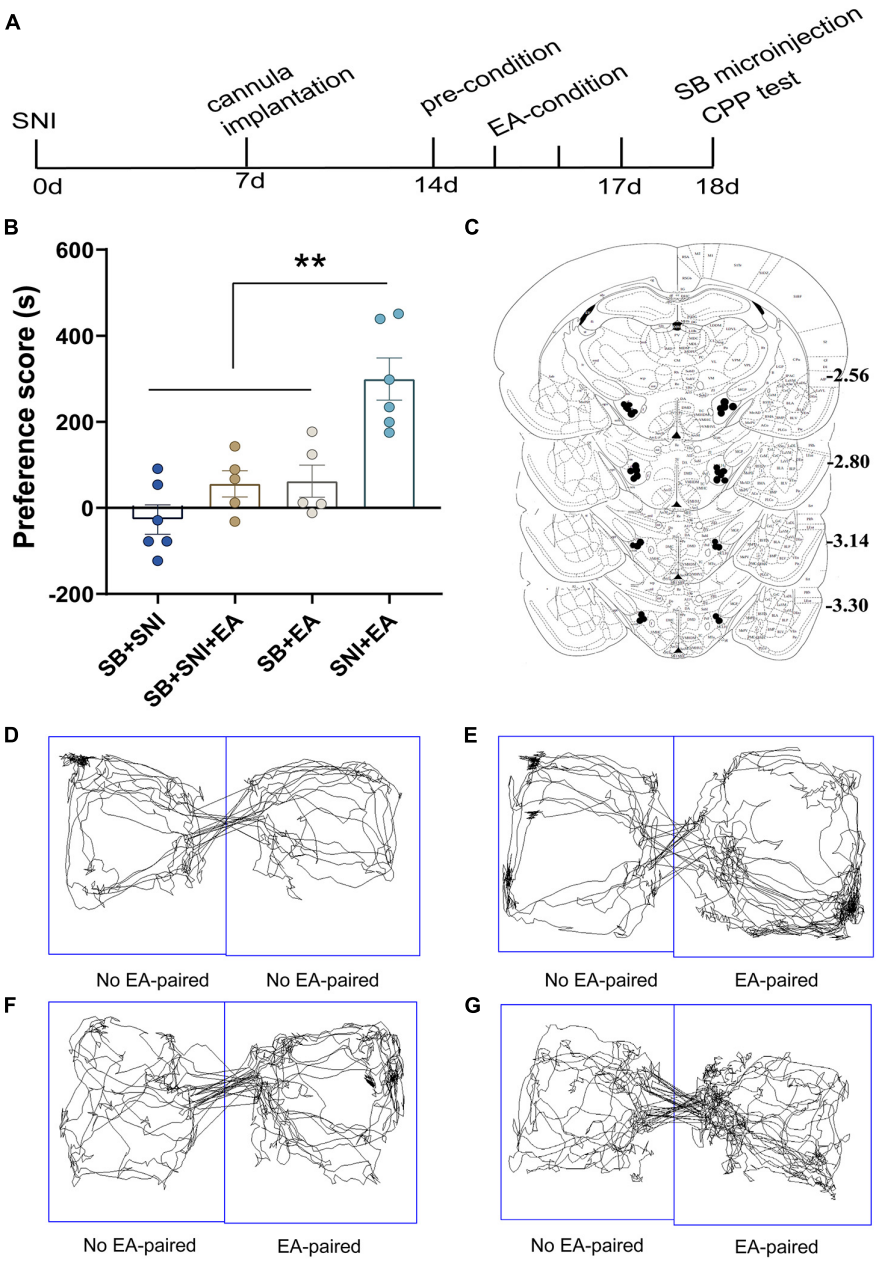

FIGURE 4 | Microinjection of orexin antagonist SB334867 into the LH can significantly attenuate EA-induced CPP in SNI rats. **(A)** A timeline of SNI modeling, EA-induced CPP, SB microinjection, and CPP test. **(B)** The preference scores after CPP testing among the different groups. $^{**}p < 0.01$ vs. SB + SNI group, SB + SNI + EA group, and SB + EA group. **(C)** Microinfusion cannula placements. The numbers indicate distance from Bregma in millimeters. Real-time movement traces among the groups during CPP test: **(D)** SB + SNI group; **(E)** SB + SNI + EA group; **(F)** SB + EA group; and **(G)** SNI + EA group.

the CPP test, thereby clearly indicating the reward of pain relief by EA in chronic pain. This finding is consistent with our clinical observations that the expectation and pleasure of pain relief could be induced by acupuncture and EA in many patients with chronic pain (data not shown here). Several previous studies related to acupuncture analgesia have largely focused on nociception (Vickers et al., 2018). However, given that acupuncture-induced reward of pain relief is clinically significant, targeting the reward mechanisms of pain relief induced by EA might offer a new prospect for a better understanding of the effects of acupuncture analgesia. Furthermore, analgesic agents can also significantly reverse evoked tactile allodynia and concomitantly produce CPP (King et al., 2009). Therefore, our data also provided conclusive evidence that EA can produce significant therapeutic effects in the treatment of chronic pain.

Chronic pain can last for weeks, months, or even years. Moreover, consistent with previous studies (Decosterd and Woolf, 2000; Boccella et al., 2018), we found that the SNI group

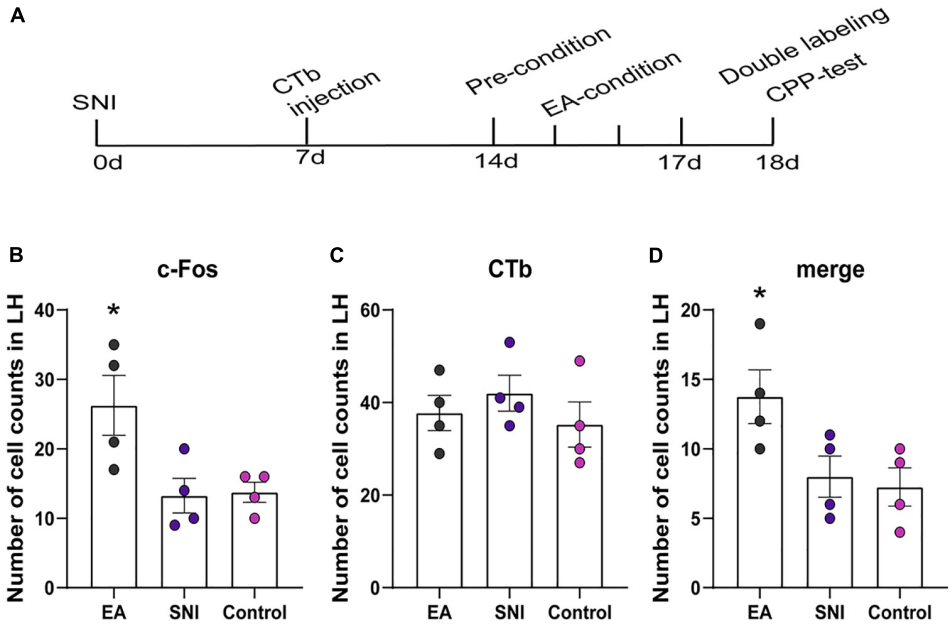

FIGURE 5 | The orexinergic neural pathway from the LH to the NAc shell was activated by EA-induced CPP. **(A)** A timeline of SNI modeling, CTb microinjection, EA induced CPP conditioning and testing. **(B–D)** The number of the c-Fos positive neurons, CTb stained neurons, and double-labeled CTb/Fos neurons in the NAc shell. *$p < 0.01$ vs. SNI group and control group.

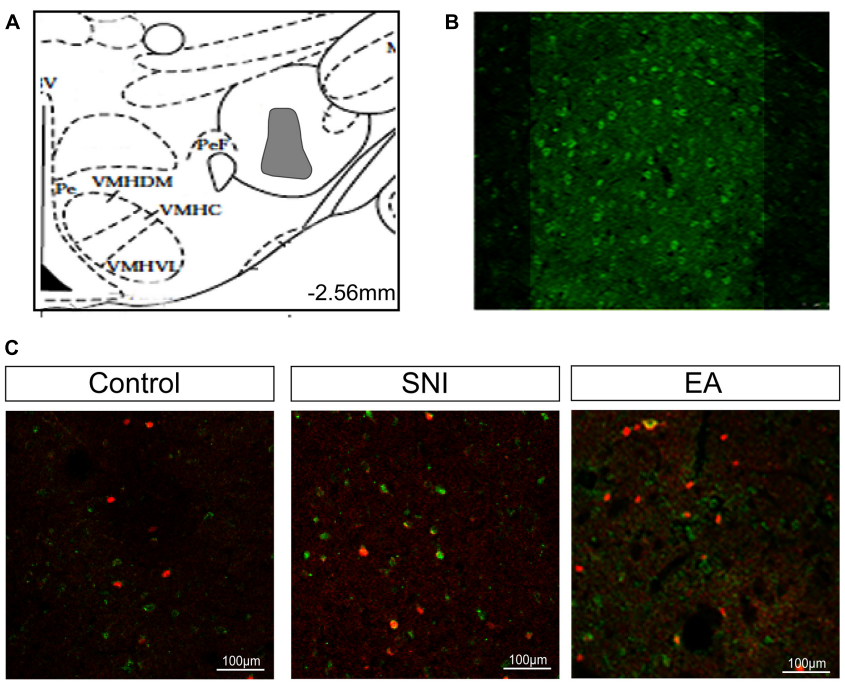

FIGURE 6 | Activated afferents from the LH to the NAc shell using CTb/c-Fos double immunohistochemistry after EA induced CPP. **(A)** The maximum extent of CTb-IR (indicated gray area) in the LH. **(B)** Fluorescent photomicrographs of representative injection sites of 30 nL of CTb in the LH. **(C)** Representative immunofluorescence images for CTb/c-Fos in the NAc shell. Scale bar, 100 μm.

developed thermal hyperalgesia from days 1 to 7 after surgery that lasted for at least 45 days. EA showed significant immediate antihyperalgesic effects at the different stages of chronic pain. Notably, the EA-treated rats exhibited marked preferences for the EA-paired chamber on days 7, 14, and 21 after SNI surgery (early stage). However, EA did not significantly increase the

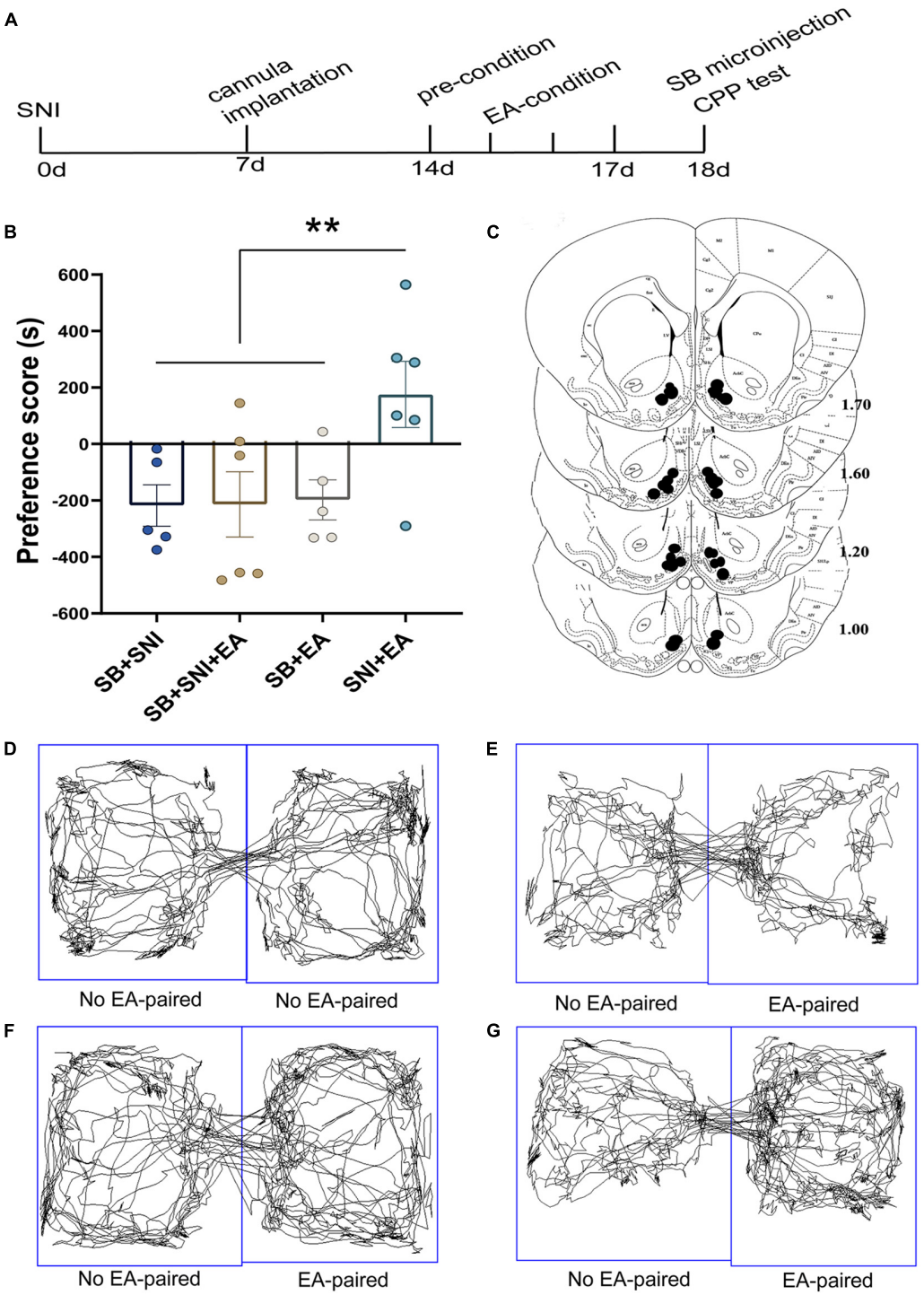

FIGURE 7 | Microinjection of orexin antagonist SB334867 into the NAc can markedly ablate EA induced CPP in SNI rats. **(A)** A timeline of SNI modeling, EA-induced CPP, SB microinjection and CPP test. **(B)** The preference scores after CPP testing among the various groups. $^{**}p < 0.01$ vs. SB + SNI group, SB + SNI + EA group and SB + EA group. **(C)** Microinfusion cannula placements. The numbers indicate distance from Bregma in millimeters. Real-time movement traces among the different groups during CPP test: **(D)** SB + SNI group; **(E)** SB + SNI + EA group; **(F)** SB + EA group; **(G)** SNI + EA group.

CPP scores on days 28 and 45 after SNI surgery (late stage). These findings suggested that there were at least two distinct stages (early stage and late stage), which might be involved in two different mechanisms mediating the reward effects of pain relief induced by EA. The reward effect of EA was found to be directly correlated with the time window of chronic pain.

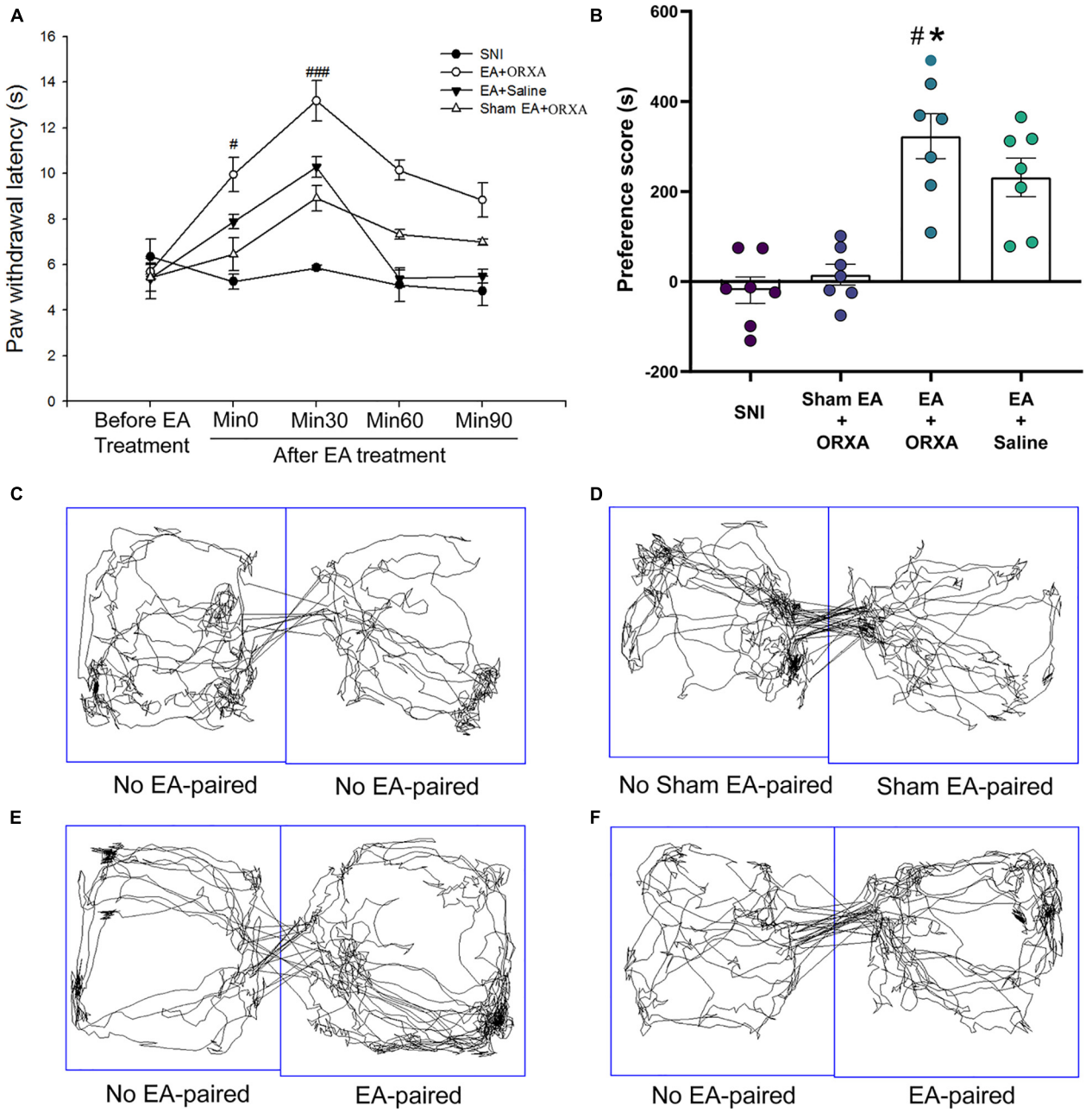

FIGURE 8 | The potential effects of combinations of EA and low-dose orexin-A on the thermal hyperalgesia and CPP scores. **(A)** Immediate effects of EA and low-dose orexin-A on the thermal hyperalgesia among the various groups. $^{###}p < 0.05$ vs. SNI group, EA + Saline, and Sham EA + ORXA group. **(B)** The preference scores after CPP testing among the different groups. $^{\#}p < 0.01$ vs. the SNI group; $^{*}p < 0.05$ vs. the EA + saline group. Real-time movement traces during CPP test: **(C)** SNI group; **(D)** Sham EA + ORXA group; **(E)** EA + ORXA group; and **(F)** EA + saline group.

Earlier studies have shown that chronic pain can induce long-term plasticity, substantially alter brain structural features, and also affect brain functional activity (Baliki et al., 2012; Hashmi et al., 2013). It has been suggested that long-term plasticity in the brain may induce the distinct reward effects of EA during the different stages of chronic pain. In addition, the combination of EA and low-dose orexin-A on the thermal hyperalgesia and CPP scores in the present study focused only on the single and immediate antihyperalgesic effects, which might provide a novel therapeutic option for the clinical use of an EA/orexin-A combination for pain relief in patients with chronic pain. Of course, further repeated combination treatments need to be tested in future studies.

A great deal of data has indicated the potential role of hypothalamic orexin neurons in pain modulation and the reward process. Orexin-A microinjection into the posterior

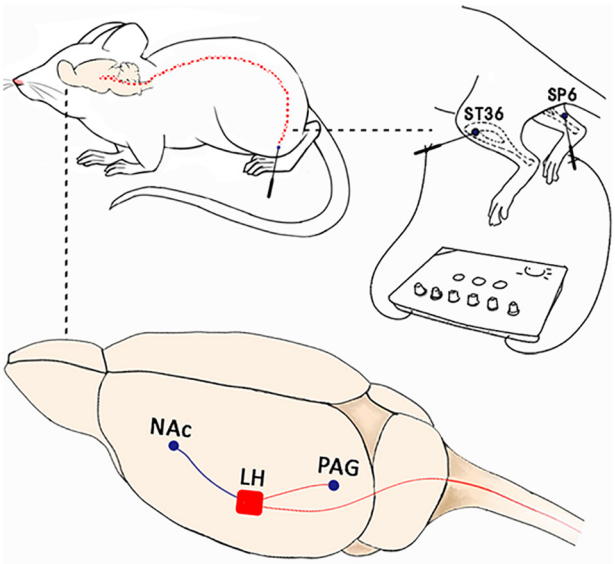

FIGURE 9 | The possible mechanism involved in orexin signals in the lateral hypothalamus for acupuncture analgesia. Acupuncture signals at various acupuncture points can travel through the spinal cord to the hypothalamus. The LH orexin system is a central hub that can integrate outputs to various brain areas that can actively participate in acupuncture or EA analgesia. The projections to orexin signals in the spinal cord and PAG (descending circuits) were involved in EA-induced pain inhibition. The orexin signals in the NAc shell were found to be involved in EA-induced reward effects and inhibition of the affective component of pain.

hypothalamus can effectively decrease the response of facial A- and C-fibers to heat and electrical stimulation (Bartsch et al., 2004). Moreover, Zhou et al. (2018) found that the orexin system facilitated both anesthesia emergence and pain control (Watanabe et al., 2005; Fakhoury et al., 2020). Significant hyperalgesia was observed in prepro-orexin knockout mice (Watanabe et al., 2005). Interestingly, the orexin system has also been reported to be involved in EA-induced analgesia (Chen et al., 2020). Acupuncture at PC6 acupuncture points significantly enhanced hypothalamic c-Fos–positive orexin neuronal numbers and induced higher orexin-A in the ventrolateral PAG in chronic constriction nerve injury and acute thermal nociception animal models (Chen et al., 2018). In the present study, we provide the first evidence that orexin system function can functionally extend beyond acupuncture analgesia to the reward effects of pain relief induced by EA. Hypothalamic neuropeptides can be mainly divided into two distinct types, namely, orexin-A and orexin-B. The selective orexin-A antagonist SB-334867 and orexin-A were used in the present study. A significant body of literature has indicated that the administration of orexin-A receptor antagonists, either systemically or locally into reward regions, attenuates a broad range of drug-seeking behaviors (Harris et al., 2005; Bentzley and Aston-Jones, 2015; Fragale et al., 2019; James et al., 2019). Similar to above results, our data clearly indicated the involvement of the orexin system in reward induced by EA analgesia. Orexin neurons can elicit their effects *via* affecting the orexin-A and orexin-B receptors (Sakurai et al., 1998; Harris and Aston-Jones, 2006). It is generally accepted that the orexin-A receptor is primarily involved in motivation and reward and the orexin-B receptor in the modulation of sleep/wake cycle and energy homeostasis (Tsujino and Sakurai, 2009; Jupp et al., 2011; Perrey and Zhang, 2020). Given that SB334867 is an orexin-A receptor antagonist, our findings suggested that the orexin-A receptor may be involved in the rewards of pain relief induced by EA. Our results also provided evidence that the LH orexin system is an essential part of the circuitry that can effectively integrate cues with EA-induced reward of pain relief. This view is consistent with the observed roles of orexin neurons in drug and food rewards (Harris et al., 2005; Moorman and Aston-Jones, 2009; Sartor and Aston-Jones, 2012). Whether orexin-B might also be involved in EA-induced rewards requires further clarification. Notably, acupuncture activates orexin neurons in several specific hypothalamus subregions, including the LH and the PFA (Chen et al., 2018). We found that EA induced a significant increase in c-Fos-positive orexin neurons only in the LH subregion, but not in the PFA and the DMH after the EA-induced preference test. This discrepancy might be possibly explained by functionally dichotomous orexin neurons present in the different hypothalamic subregions. As reviewed by Harris and Aston-Jones (2006) previously, orexins are functionally dichotomous, and orexin neurons in the LH are primarily involved in reward processing, whereas those in the PeF and DMH can effectively mediate the arousal and stress functions previously found to be associated with these peptides (Harris et al., 2005; Harris and Aston-Jones, 2006; Gao and Hermes, 2015). Orexin neurons in the LH, but not in the PeF and DMH, were noted to be stimulated by drug-conditioned contextual stimuli on the drug-free CPP test day (Harris et al., 2005). Our results are also consistent with these observations and support the view that the rewards induced by EA stimulation might be primarily associated with LH orexin cells.

Orexin neurons in the LH can innervate broadly in the various brain areas. Some studies have suggested that orexin might be involved in mediating the analgesic effect of EA at the spinal cord and supraspinal cord levels (Chen et al., 2020). For instance, one study showed that EA could significantly alleviate pain through modulating spinal orexin-A and its receptor interactions independent of the opioid system (Feng et al., 2012). Chen et al. (2018) focused on the PAG region and found that EA at PC6 can stimulate the release of orexin from the hypothalamus to markedly inhibiting pain responses through an endocannabinoid receptor that can reduce the inhibitory control in the PAG. We found in the present study that orexinergic neural pathway from the LH to the NAc shell could be activated by EA-induced rewards of pain relief. LH orexin neurons can heavily innervate the NAc, and the orexin-A receptor is highly expressed in this area (Trivedi et al., 1998; Marcus et al., 2001). Orexin microinjection in the NAc shell has been reported to activate NAc GABAergic and dopaminergic cells (Vittoz and Berridge, 2006; Morales-Mulia et al., 2020). In addition, orexin-A infusions into the NAc can also activate morphine-induced preferences and the injection of orexin-A antagonist into the NAc reduced the CPP for morphine (Harris et al., 2005). These results clearly indicated that orexin release in the NAc was necessary for

reward effects (Taslimi et al., 2012; Sadeghzadeh et al., 2016; Assar et al., 2019). Notably, the LH-NAc pathway also plays an important role in pain modulation (Azhdari-Zarmehri et al., 2013; Yazdi et al., 2016). Chronic pain is often associated with various structural and functional abnormalities in the NAc. The offset of acute thermal stimulus can functionally increase NAc activity in healthy subjects (Baliki et al., 2010). It has been found that administration of SB334867 into the NAc dose-dependently decreased antinociception (Jahangirvand et al., 2016). A previous study has also demonstrated that the NAc appears to encode the affective value and saliency of the stimulus (Schultz, 2013; Navratilova and Porreca, 2014). In addition, fMRI studies have demonstrated that significant functional responses in the NAc were associated with acupuncture analgesia (Wang Z. et al., 2017; Yu et al., 2020b). Hence, we have suggested that the various acupuncture signals at acupuncture points can travel through the spinal cord to the hypothalamus. The LH orexin system is a central hub that can integrate outputs to several other brain areas participating in acupuncture or EA analgesia. Moreover, various projections to orexin signals in the spinal cord and PAG (descending circuits) are involved in EA-induced pain inhibition. Orexin signals in the NAc shell are also involved in EA-induced reward effects and the potential inhibition of the affective component of pain (**Figure 9**). The present study extends our understanding of LH orexin signaling on EA-induced rewards and provides new insights into mechanisms of acupuncture analgesia.

Clinical Implications

Chronic pain has the potential to induce long-term plasticity in the central nervous system during the course of a disease, which can link various modulatory factors to cause a change in both perception and behavior. The findings that EA induced the preference for cues associated with EA-induced pain relief at an early phase of chronic pain but not at the late phase could help to provide novel therapeutic options in the management of patients with chronic pain. The therapeutic effects of EA may be directly correlated with the time window of chronic pain. In addition, the combination of EA and low-dose orexin-A treatments produced significantly greater antihyperalgesia effects and CPP scores. Thus, it might provide a novel therapeutic strategy for the clinical application of the EA/orexin-A combination for pain relief in patients with chronic pain.

DATA AVAILABILITY STATEMENT

The raw data supporting the conclusions of this article will be made available by the authors, without undue reservation.

ETHICS STATEMENT

The animal study was reviewed and approved by the Shanghai University of TCM Animal Ethics Committee.

AUTHOR CONTRIBUTIONS

SL designed the experiment. CW, MC, CQ, XS, and SL contributed to writing and editing. CW, MC, CQ, and XQ performed the experiments and analyzed the data. XS, XQ, and SL supervised the research. All authors contributed to the article and approved the submitted version.

FUNDING

This work was supported by the National Natural Science Foundation of China (81873379 and 82104990).

ACKNOWLEDGMENTS

We thank Chunlei Shan for his helpful comments on the manuscript. We would like to thank all the reviewers who participated in the review and MJEditor (www.mjeditor.com) for its linguistic assistance during the preparation of this manuscript.

REFERENCES

Assar, N., Mahmoudi, D., Mousavi, Z., Zarrabian, S., and Haghparast, A. (2019). Role of orexin-1 and −2 receptors within the nucleus accumbens in the acquisition of sensitization to morphine in rats. *Behav. Brain Res.* 373:112090. doi: 10.1016/j.bbr.2019.112090

Azhdari-Zarmehri, H., Reisi, Z., Vaziri, A., Haghparast, A., Shaigani, P., and Haghparast, A. (2013). Involvement of orexin-2 receptors in the ventral tegmental area and nucleus accumbens in the antinociception induced by the lateral hypothalamus stimulation in rats. *Peptides* 47, 94–98. doi: 10.1016/j.peptides.2013.07.012

Baliki, M. N., Geha, P. Y., Fields, H. L., and Apkarian, A. V. (2010). Predicting value of pain and analgesia: nucleus accumbens response to noxious stimuli changes in the presence of chronic pain. *Neuron* 66, 149–160. doi: 10.1016/j.neuron.2010.03.002

Baliki, M. N., Petre, B., Torbey, S., Herrmann, K. M., Huang, L., Schnitzer, T. J., et al. (2012). Corticostriatal functional connectivity predicts transition to chronic back pain. *Nat. Neurosci.* 15, 1117–1119. doi: 10.1038/nn.3153

Bartsch, T., Levy, M. J., Knight, Y. E., and Goadsby, P. J. (2004). Differential modulation of nociceptive dural input to [hypocretin] orexin A and B receptor activation in the posterior hypothalamic area. *Pain* 109, 367–378. doi: 10.1016/j.pain.2004.02.005

Bentzley, B. S., and Aston-Jones, G. (2015). Orexin-1 receptor signaling increases motivation for cocaine-associated cues. *Eur. J. Neurosci.* 41, 1149–1156. doi: 10.1111/ejn.12866

Bingham, S., Davey, P. T., Babbs, A. J., Irving, E. A., Sammons, M. J., Wyles, M., et al. (2001). Orexin-A, an hypothalamic peptide with analgesic properties. *Pain* 92, 81–90. doi: 10.1016/s0304-3959(00)00470-x

Boccella, S., Guida, F., Palazzo, E., Marabese, I., de Novellis, V., Maione, S., et al. (2018). Spared Nerve Injury as a Long-Lasting Model of Neuropathic Pain. *Methods Mol. Biol.* 1727, 373–378. doi: 10.1007/978-1-4939-7571-6_28

Burdakov, D. (2020). How orexin signals bias action: Hypothalamic and accumbal circuits. *Brain Res.* 1731:145943. doi: 10.1016/j.brainres.2018.09.011

Chen, T., Zhang, W. W., Chu, Y. X., and Wang, Y. Q. (2020). Acupuncture for Pain Management: Molecular Mechanisms of Action. *Am. J. Chin. Med.* 48, 793–811. doi: 10.1142/s0192415x20500408

Chen, Y. H., Lee, H. J., Lee, M. T., Wu, Y. T., Lee, Y. H., Hwang, L. L., et al. (2018). Median nerve stimulation induces analgesia via orexin-initiated endocannabinoid disinhibition in the periaqueductal gray. *Proc. Natl. Acad. Sci. U S A* 115, E10720–E10729. doi: 10.1073/pnas.1807991115

Decosterd, I., and Woolf, C. J. (2000). Spared nerve injury: an animal model of persistent peripheral neuropathic pain. *Pain* 87, 149–158. doi: 10.1016/s0304-3959(00)00276-1

DosSantos, M. F., Moura, B. S., and DaSilva, A. F. (2017). Reward Circuitry Plasticity in Pain Perception and Modulation. *Front. Pharmacol.* 8:790. doi: 10.3389/fphar.2017.00790

Duanmu, C. L., Feng, X. M., Yan, Y. X., Wang, J. Y., Gao, Y. H., Qiao, L. N., et al. (2017). Effect of Electroacupuncture Intervention on Expression of Synaptic Plasticity-related Molecules in Amygdala in Chronic Pain-negative Affection Rats. *Zhen Ci Yan Jiu* 42, 1–8.

Elman, I., and Borsook, D. (2016). Common Brain Mechanisms of Chronic Pain and Addiction. *Neuron* 89, 11–36. doi: 10.1016/j.neuron.2015.11.027

Fakhoury, M., Salman, I., Najjar, W., Merhej, G., and Lawand, N. (2020). The Lateral Hypothalamus: An Uncharted Territory for Processing Peripheral Neurogenic Inflammation. *Front. Neurosci.* 14:101. doi: 10.3389/fnins.2020.00101

Feng, X. M., Mi, W. L., Xia, F., Mao-Ying, Q. L., Jiang, J. W., Xiao, S., et al. (2012). Involvement of spinal orexin A in the electroacupuncture analgesia in a rat model of post-laparotomy pain. *BMC Complement Altern. Med.* 12:225. doi: 10.1186/1472-6882-12-225

Fragale, J. E., Pantazis, C. B., James, M. H., and Aston-Jones, G. (2019). The role of orexin-1 receptor signaling in demand for the opioid fentanyl. *Neuropsychopharmacology* 44, 1690–1697. doi: 10.1038/s41386-019-0420-x

Gao, X. B., and Hermes, G. (2015). Neural plasticity in hypocretin neurons: the basis of hypocretinergic regulation of physiological and behavioral functions in animals. *Front. Syst. Neurosci.* 9:142. doi: 10.3389/fnsys.2015.00142

George, P., and Charles, W. (1986). *The Rat Brain in Stereotaxic Coordinates*. London: Academic.

Hamlin, A. S., Clemens, K. J., and McNally, G. P. (2008). Renewal of extinguished cocaine-seeking. *Neuroscience* 151, 659–670. doi: 10.1016/j.neuroscience.2007.11.018

Harris, G. C., and Aston-Jones, G. (2006). Arousal and reward: a dichotomy in orexin function. *Trends Neurosci.* 29, 571–577. doi: 10.1016/j.tins.2006.08.002

Harris, G. C., Wimmer, M., and Aston-Jones, G. (2005). A role for lateral hypothalamic orexin neurons in reward seeking. *Nature* 437, 556–559. doi: 10.1038/nature04071

Hashmi, J. A., Baliki, M. N., Huang, L., Baria, A. T., Torbey, S., Hermann, K. M., et al. (2013). Shape shifting pain: chronification of back pain shifts brain representation from nociceptive to emotional circuits. *Brain* 136(Pt 9), 2751–2768. doi: 10.1093/brain/awt211

Hou, Y., Chen, M., Wang, C., Liu, L., Mao, H., Qu, X., et al. (2021). Electroacupuncture Attenuates Anxiety-Like Behaviors in a Rat Model of Post-traumatic Stress Disorder: the Role of the Ventromedial Prefrontal Cortex. *Front. Neurosci.* 15:690159. doi: 10.3389/fnins.2021.690159

Jahangirvand, M., Yazdi, F., Moradi, M., and Haghparast, A. (2016). Intra-accumbal Orexin-1 Receptors are Involved in Antinociception Induced by Stimulation of the Lateral Hypothalamus in the Formalin Test as an Animal Model of Persistent Inflammatory Pain. *Iran J. Pharm. Res.* 15, 851–859.

James, M. H., Stopper, C. M., Zimmer, B. A., Koll, N. E., Bowrey, H. E., and Aston-Jones, G. (2019). Increased Number and Activity of a Lateral Subpopulation of Hypothalamic Orexin/Hypocretin Neurons Underlies the Expression of an Addicted State in Rats. *Biol. Psychiatry* 85, 925–935. doi: 10.1016/j.biopsych.2018.07.022

Jupp, B., Krivdic, B., Krstew, E., and Lawrence, A. J. (2011). The orexin1 receptor antagonist SB-334867 dissociates the motivational properties of alcohol and sucrose in rats. *Brain Res.* 1391, 54–59. doi: 10.1016/j.brainres.2011.03.045

Khosrowabadi, E., Karimi-Haghighi, S., Jamali, S., and Haghparast, A. (2020). Differential Roles of Intra-accumbal Orexin Receptors in Acquisition and Expression of Methamphetamine-Induced Conditioned Place Preference in the Rats. *Neurochem. Res.* 45, 2230–2241. doi: 10.1007/s11064-020-03084-1

King, T., Vera-Portocarrero, L., Gutierrez, T., Vanderah, T. W., Dussor, G., Lai, J., et al. (2009). Unmasking the tonic-aversive state in neuropathic pain. *Nat. Neurosci.* 12, 1364–1366. doi: 10.1038/nn.2407

Kong, J., Kaptchuk, T. J., Polich, G., Kirsch, I., Vangel, M., Zyloney, C., et al. (2009). An fMRI study on the interaction and dissociation between expectation of pain relief and acupuncture treatment. *Neuroimage* 47, 1066–1076. doi: 10.1016/j.neuroimage.2009.05.087

Koo, S. T., Park, Y. I., Lim, K. S., Chung, K., and Chung, J. M. (2002). Acupuncture analgesia in a new rat model of ankle sprain pain. *Pain* 99, 423–431. doi: 10.1016/s0304-3959(02)00164-1

Latremoliere, A., and Woolf, C. J. (2009). Central sensitization: a generator of pain hypersensitivity by central neural plasticity. *J. Pain* 10, 895–926. doi: 10.1016/j.jpain.2009.06.012

Leknes, S., Brooks, J. C., Wiech, K., and Tracey, I. (2008). Pain relief as an opponent process: a psychophysical investigation. *Eur. J. Neurosci.* 28, 794–801. doi: 10.1111/j.1460-9568.2008.06380.x

Li, Y., Yin, C., Li, X., Liu, B., Wang, J., Zheng, X., et al. (2019). Electroacupuncture Alleviates Paclitaxel-Induced Peripheral Neuropathic Pain in Rats via Suppressing TLR4 Signaling and TRPV1 Upregulation in Sensory Neurons. *Int. J. Mol. Sci.* 2019:20. doi: 10.3390/ijms20235917

Makary, M. M., Polosecki, P., Cecchi, G. A., DeAraujo, I. E., Barron, D. S., Constable, T. R., et al. (2020). Loss of nucleus accumbens low-frequency fluctuations is a signature of chronic pain. *Proc. Natl. Acad. Sci. U S A* 117, 10015–10023. doi: 10.1073/pnas.1918682117

Marchant, N. J., Hamlin, A. S., and McNally, G. P. (2009). Lateral hypothalamus is required for context-induced reinstatement of extinguished reward seeking. *J. Neurosci.* 29, 1331–1342. doi: 10.1523/jneurosci.5194-08.2009

Marchant, N. J., Millan, E. Z., and McNally, G. P. (2012). The hypothalamus and the neurobiology of drug seeking. *Cell Mol. Life Sci.* 69, 581–597. doi: 10.1007/s00018-011-0817-0

Marcus, J. N., Aschkenasi, C. J., Lee, C. E., Chemelli, R. M., Saper, C. B., Yanagisawa, M., et al. (2001). Differential expression of orexin receptors 1 and 2 in the rat brain. *J. Comp. Neurol.* 435, 6–25. doi: 10.1002/cne.1190

Massaly, N., Copits, B. A., Wilson-Poe, A. R., Hipólito, L., Markovic, T., Yoon, H. J., et al. (2019). Pain-Induced Negative Affect Is Mediated via Recruitment of The Nucleus Accumbens Kappa Opioid System. *Neuron* 102, 564.e–573.e. doi: 10.1016/j.neuron.2019.02.029

Millan, E. Z., Furlong, T. M., and McNally, G. P. (2010). Accumbens shell-hypothalamus interactions mediate extinction of alcohol seeking. *J. Neurosci.* 30, 4626–4635. doi: 10.1523/jneurosci.4933-09.2010

Moorman, D. E., and Aston-Jones, G. (2009). Orexin-1 receptor antagonism decreases ethanol consumption and preference selectively in high-ethanol–preferring Sprague–Dawley rats. *Alcohol* 43, 379–386. doi: 10.1016/j.alcohol.2009.07.002

Morales-Mulia, S., Magdaleno-Madrigal, V. M., Nicolini, H., Genis-Mendoza, A., and Morales-Mulia, M. (2020). Orexin-A up-regulates dopamine D2 receptor and mRNA in the nucleus accumbens Shell. *Mol. Biol. Rep.* 47, 9689–9697. doi: 10.1007/s11033-020-05979-2

Narita, M., Nagumo, Y., Hashimoto, S., Narita, M., Khotib, J., Miyatake, M., et al. (2006). Direct involvement of orexinergic systems in the activation of the mesolimbic dopamine pathway and related behaviors induced by morphine. *J. Neurosci.* 26, 398–405. doi: 10.1523/jneurosci.2761-05.2006

Navratilova, E., Atcherley, C. W., and Porreca, F. (2015). Brain Circuits Encoding Reward from Pain Relief. *Trends Neurosci.* 38, 741–750. doi: 10.1016/j.tins.2015.09.003

Navratilova, E., and Porreca, F. (2014). Reward and motivation in pain and pain relief. *Nat. Neurosci.* 17, 1304–1312. doi: 10.1038/nn.3811

Navratilova, E., Xie, J. Y., Okun, A., Qu, C., Eyde, N., Ci, S., et al. (2012). Pain relief produces negative reinforcement through activation of mesolimbic reward-valuation circuitry. *Proc. Natl. Acad. Sci. U S A* 109, 20709–20713. doi: 10.1073/pnas.1214605109

Ossipov, M. H., Dussor, G. O., and Porreca, F. (2010). Central modulation of pain. *J. Clin. Invest.* 120, 3779–3787. doi: 10.1172/jci43766

Patyal, R., Woo, E. Y., and Borgland, S. L. (2012). Local hypocretin-1 modulates terminal dopamine concentration in the nucleus accumbens shell. *Front. Behav. Neurosci.* 6:82. doi: 10.3389/fnbeh.2012.00082

Perrey, D. A., and Zhang, Y. (2020). Therapeutics development for addiction: Orexin-1 receptor antagonists. *Brain Res.* 1731:145922. doi: 10.1016/j.brainres.2018.08.025

Petrovich, G. D., Hobin, M. P., and Reppucci, C. J. (2012). Selective Fos induction in hypothalamic orexin/hypocretin, but not melanin-concentrating hormone neurons, by a learned food-cue that stimulates feeding in sated rats. *Neuroscience* 224, 70–80. doi: 10.1016/j.neuroscience.2012.08.036

Porreca, F., and Navratilova, E. (2017). Reward, motivation, and emotion of pain and its relief. *Pain* 1(Suppl. 1), S43–S49. doi: 10.1097/j.pain.0000000000000798

Sadeghzadeh, F., Namvar, P., Naghavi, F. S., and Haghparast, A. (2016). Differential effects of intra-accumbal orexin-1 and -2 receptor antagonists on the expression and extinction of morphine-induced conditioned place preference in rats. *Pharmacol. Biochem. Behav.* 142, 8–14. doi: 10.1016/j.pbb.2015.12.005

Sakurai, T., Amemiya, A., Ishii, M., Matsuzaki, I., Chemelli, R. M., Tanaka, H., et al. (1998). Orexins and orexin receptors: a family of hypothalamic neuropeptides and G protein-coupled receptors that regulate feeding behavior. *Cell* 92:1. doi: 10.1016/s0092-8674(02)09256-5

Sartor, G. C., and Aston-Jones, G. S. (2012). A septal-hypothalamic pathway drives orexin neurons, which is necessary for conditioned cocaine preference. *J. Neurosci.* 32, 4623–4631. doi: 10.1523/jneurosci.4561-11.2012

Schultz, W. (2013). Updating dopamine reward signals. *Curr. Opin. Neurobiol.* 23, 229–238. doi: 10.1016/j.conb.2012.11.012

Serafini, R. A., Pryce, K. D., and Zachariou, V. (2020). The Mesolimbic Dopamine System in Chronic Pain and Associated Affective Comorbidities. *Biol. Psychiatry* 87, 64–73. doi: 10.1016/j.biopsych.2019.10.018

Shields, S. D., Eckert, W. A. III, and Basbaum, A. I. (2003). Spared nerve injury model of neuropathic pain in the mouse: a behavioral and anatomic analysis. *J. Pain* 4, 465–470. doi: 10.1067/s1526-5900(03)00781-8

Taslimi, Z., Arezoomandan, R., Omranifard, A., Ghalandari-Shamami, M., Riahi, E., Vafaei, A. A., et al. (2012). Orexin A in the ventral tegmental area induces conditioned place preference in a dose-dependent manner: involvement of D1/D2 receptors in the nucleus accumbens. *Peptides* 37, 225–232. doi: 10.1016/j.peptides.2012.07.023

Trivedi, P., Yu, H., MacNeil, D. J., Van der Ploeg, L. H., and Guan, X. M. (1998). Distribution of orexin receptor mRNA in the rat brain. *FEBS Lett.* 438, 71–75. doi: 10.1016/s0014-5793(98)01266-6

Truini, A., Garcia-Larrea, L., and Cruccu, G. (2013). Reappraising neuropathic pain in humans–how symptoms help disclose mechanisms. *Nat. Rev. Neurol.* 9, 572–582. doi: 10.1038/nrneurol.2013.180

Tsujino, N., and Sakurai, T. (2009). Orexin/hypocretin: a neuropeptide at the interface of sleep, energy homeostasis, and reward system. *Pharmacol. Rev.* 61, 162–176. doi: 10.1124/pr.109.001321

Vickers, A. J., and Linde, K. (2014). Acupuncture for chronic pain. *Jama* 311, 955–956. doi: 10.1001/jama.2013.285478

Vickers, A. J., Vertosick, E. A., Lewith, G., MacPherson, H., Foster, N. E., Sherman, K. J., et al. (2018). Acupuncture for Chronic Pain: update of an Individual Patient Data Meta-Analysis. *J. Pain* 19, 455–474. doi: 10.1016/j.jpain.2017.11.005

Vittoz, N. M., and Berridge, C. W. (2006). Hypocretin/orexin selectively increases dopamine efflux within the prefrontal cortex: involvement of the ventral tegmental area. *Neuropsychopharmacology* 31, 384–395. doi: 10.1038/sj.npp.1300807

Wang, X., Zhang, B., Zhang, L., and Liu, S. (2017). Electroacupuncture suppresses morphine reward-seeking behavior: Lateral hypothalamic orexin neurons implicated. *Neurosci. Lett.* 661, 84–89. doi: 10.1016/j.neulet.2017.09.057

Wang, Z., Wang, X., Liu, J., Chen, J., Liu, X., Nie, G., et al. (2017). Acupuncture treatment modulates the corticostriatal reward circuitry in major depressive disorder. *J. Psychiatr. Res.* 84, 18–26. doi: 10.1016/j.jpsychires.2016.09.014

Watanabe, M., and Narita, M. (2018). Brain Reward Circuit and Pain. *Adv. Exp. Med. Biol.* 1099, 201–210. doi: 10.1007/978-981-13-1756-9_17

Watanabe, S., Kuwaki, T., Yanagisawa, M., Fukuda, Y., and Shimoyama, M. (2005). Persistent pain and stress activate pain-inhibitory orexin pathways. *Neuroreport* 16, 5–8. doi: 10.1097/00001756-200501190-00002

Yazdi, F., Jahangirvand, M., Ezzatpanah, S., and Haghparast, A. (2016). Role of orexin-2 receptors in the nucleus accumbens in antinociception induced by carbachol stimulation of the lateral hypothalamus in formalin test. *Behav. Pharmacol.* 27, 431–438. doi: 10.1097/fbp.0000000000000216

Yu, S., Li, W., Shen, W., Edwards, R. R., Gollub, R. L., Wilson, G., et al. (2020a). Impaired mesocorticolimbic connectivity underlies increased pain sensitivity in chronic low back pain. *Neuroimage* 218:116969. doi: 10.1016/j.neuroimage.2020.116969

Yu, S., Ortiz, A., Gollub, R. L., Wilson, G., Gerber, J., Park, J., et al. (2020b). Acupuncture Treatment Modulates the Connectivity of Key Regions of the Descending Pain Modulation and Reward Systems in Patients with Chronic Low Back Pain. *J. Clin. Med.* 9:6. doi: 10.3390/jcm9061719

Zhang, R., Lao, L., Ren, K., and Berman, B. M. (2014). Mechanisms of acupuncture-electroacupuncture on persistent pain. *Anesthesiology* 120, 482–503. doi: 10.1097/aln.0000000000000101

Zhang, Y., Meng, X., Li, A., Xin, J., Berman, B. M., Lao, L., et al. (2012). Electroacupuncture alleviates affective pain in an inflammatory pain rat model. *Eur. J. Pain* 16, 170–181. doi: 10.1016/j.ejpain.2011.07.002

Zhou, W., Cheung, K., Kyu, S., Wang, L., Guan, Z., Kurien, P. A., et al. (2018). Activation of orexin system facilitates anesthesia emergence and pain control. *Proc. Natl. Acad. Sci. U S A* 115, E10740–E10747. doi: 10.1073/pnas.1808622115

Conflict of Interest: The authors declare that the research was conducted in the absence of any commercial or financial relationships that could be construed as a potential conflict of interest.

Publisher's Note: All claims expressed in this article are solely those of the authors and do not necessarily represent those of their affiliated organizations, or those of the publisher, the editors and the reviewers. Any product that may be evaluated in this article, or claim that may be made by its manufacturer, is not guaranteed or endorsed by the publisher.

frontiers | Frontiers in Molecular Neuroscience

ORIGINAL RESEARCH
published: 26 April 2022
doi: 10.3389/fnmol.2022.842674

Acupuncture Modulates the Spontaneous Activity and Functional Connectivity of Calcarine in Patients With Chronic Stable Angina Pectoris

Lei Lan[1,2†], Tao Yin[1,2†], Zilei Tian[1,2†], Ying Lan[3], Ruirui Sun[1,2], Zhengjie Li[1,2], Miaomiao Jing[4], Qiao Wen[1,2], Shenghong Li[5], Fanrong Liang[1,6] and Fang Zeng[1,2,6*]*

[1] Acupuncture and Tuina School, The 3rd Teaching Hospital, Chengdu University of Traditional Chinese Medicine, Chengdu, China, [2] Acupuncture and Brain Science Research Center, Chengdu University of Traditional Chinese Medicine, Chengdu, China, [3] Hospital of Chengdu University of Traditional Chinese Medicine, Chengdu, China, [4] Gansu Provincial Hospital of Traditional Chinese Medicine, Lanzhou, China, [5] State Key Laboratory of Southwestern Chinese Medicine Resources, Innovative Institute of Chinese Medicine and Pharmacy, Chengdu University of Traditional Chinese Medicine, Chengdu, China, [6] Key Laboratory of Sichuan Province for Acupuncture and Chronobiology, Chengdu, China

Background: Acupuncture is an effective adjunctive therapy for chronic stable angina pectoris (CSAP), while the underlying mechanism is unclear. This study aimed to investigate the central pathophysiology of CSAP and explore the mechanism of different acupoint prescriptions for CSAP from the perspective of brain-heart interaction.

Methods: Thirty-seven CSAP patients and sixty-five healthy subjects (HS) were enrolled, and thirty CSAP patients were divided into two acupoint prescriptions groups (Group A: acupoints on the meridian directly related to the *Heart*; Group B: acupoints on the meridian indirectly related to the *Heart*). The Magnetic Resonance Imaging data and clinical data were collected at baseline and after treatment. The comparisons of brain spontaneous activity patterns were performed between CSAP patients and HS, as well as between baseline and after treatment in CSAP patients. Then, the changes in resting-state functional connectivity before and after treatment were compared between the two acupoint prescriptions.

Results: Chronic stable angina pectoris patients manifested higher spontaneous activity on the bilateral calcarine, left middle occipital gyrus, right superior temporal gyrus, and right postcentral gyrus. After acupuncture treatment, the spontaneous activity of the left calcarine, left cuneus, and right orbitofrontal gyrus was decreased. The left calcarine was identified as region-of-interest for functional connectivity analysis. Compared with group B, CSAP patients in group A had significantly increased functional connectivity between left calcarine and the left inferior temporal gyrus/cerebellum crus 1, left hippocampus, left thalamus, and left middle cingulate cortex after treatment. Thresholds for all comparisons were $p < 0.05$, Gaussian Random Field corrected.

OPEN ACCESS

Edited by:
Binlong Zhang, Guang'anmen Hospital, China Academy of Chinese Medical Sciences, China

Reviewed by:
Long Jiang Zhang, Nanjing General Hospital of Nanjing Military Command, China
Haiqing Song, Capital Medical University, China
Wuhai Tao, Shenzhen University, China

***Correspondence:**
Fanrong Liang
lfr@cdutcm.edu.cn
Fang Zeng
zengfang@cdutcm.edu.cn

† These authors have contributed equally to this work and share first authorship

Specialty section:
This article was submitted to Neuroplasticity and Development, a section of the journal Frontiers in Molecular Neuroscience

Received: *24 December 2021*
Accepted: *05 April 2022*
Published: *26 April 2022*

Citation:
Lan L, Yin T, Tian Z, Lan Y, Sun R, Li Z, Jing M, Wen Q, Li S, Liang F and Zeng F (2022) Acupuncture Modulates the Spontaneous Activity and Functional Connectivity of Calcarine in Patients With Chronic Stable Angina Pectoris. Front. Mol. Neurosci. 15:842674. doi: 10.3389/fnmol.2022.842674

Conclusion: Regulating the aberrant spontaneous activity of the calcarine might be an underlying mechanism of acupuncture for CSAP. The multi-threaded modulation of functional connectivity between calcarine and multiple pain-related brain regions might be a potential mechanism for better efficacy of acupuncture at points on the meridian directly related to the *Heart*.

Keywords: coronary artery disease, angina, brain-heart interaction, fractional amplitude of low-frequency fluctuations, functional connectivity, acupuncture

INTRODUCTION

Chronic stable angina pectoris (CSAP) is a clinical syndrome characterized by constricting discomfort in the chest, jaw, shoulder, or back, typically aggravated by exertion or emotional stress (Piccolo et al., 2015). As the most common manifestation of coronary artery disease (CAD; Benjamin et al., 2017), CSAP has been identified as a predominant risk of major cardiovascular events and sudden cardiac death, and brings a significant impact on functional capacity and quality of life of patients (Chaitman and Laddu, 2011). Therefore, searching for the effective management of CSAP to reduce the frequency of angina attacks is of great value. Acupuncture is a widely used traditional practice for the prevention and treatment of angina and has been identified as a safe and effective adjunctive therapy for CSAP in several high-quality clinical trials (Zhao et al., 2019, 2021; Huang et al., 2021). It was reported that acupuncture could effectively alleviate symptoms, reduce the frequency of angina attacks, and decrease nitroglycerin use in CSAP patients (Shen et al., 2021). However, the underlying mechanism of acupuncture for CSAP was still unclear.

Recently, the proposal of brain-heart interaction theory (Silvani et al., 2016) provides a new perspective to explore the pathogenesis of cardiovascular diseases and explain the mechanism of intervention. For example, evidence from functional Magnetic Resonance Imaging (fMRI) demonstrated that the dysfunction of autonomic-limbic integration might be the important pathophysiology of takotsubo syndrome (Templin et al., 2019), and the hyperactivity of the temporal gyrus, parahippocampus, fusiform gyrus, and cerebellum played a critical role in pain perception response in CAD patients (Wittbrodt et al., 2020). Furthermore, during the dobutamine-induced angina task, patients with angina manifested increased regional cerebral blood flow in the thalamus, periaqueductal gray, prefrontal cortex, and anterior cingulate cortex (Rosen et al., 1994). These regions overlapped highly with the findings of previous neuroimaging studies about pain (Davis et al., 2017; Mouraux and Iannetti, 2018), which suggested that angina pain, a typical kind of visceral nociception, might share the similarity in pain processing with somatalgia. As an increasing number of studies have detected that acupuncture could modulate the activities of pain processing-related regions, including the thalamus (Chu et al., 2012), hippocampus (Ma et al., 2020), medulla oblongata-brainstem (Chang et al., 2021), middle temporal gyrus (Yu et al., 2019), and occipital gyrus (Ma et al., 2020) in patients with chronic pain, it was necessary and feasible to explore the mechanism of acupuncture for treating CSAP by functional neuroimaging techniques.

Therefore, this resting-state fMRI study was conducted, with the following three aims: (1) comparing the brain spontaneous activity patterns between CSAP patients and healthy subjects (HS), and (2) investigating how acupuncture modulates the abnormal activity pattern of CSAP patients, and (3) exploring the differences of two acupoint prescriptions on regulating resting-state functional connectivity (rsFC) of CSAP patients. We hypothesized that CSAP patients had aberrant functional activity in these brain regions closely associated with pain processing, which could be significantly modulated by acupuncture treatment, and that different acupoint prescriptions had different regulating effects on rsFC of CSAP patients.

MATERIALS AND METHODS

Study Design

This trial consisted of a 2-week baseline phase and a 2-week treatment phase. CSAP patients underwent clinical evaluation and MRI scans at the baseline and end of the treatment phase. HS underwent evaluation and MRI scans at the baseline. The flowchart of the study is shown in **Figure 1**.

Ethical Approval and Trial Registration

This study was approved by the Sichuan Traditional Chinese Medicine Regional Ethics Committee (No. 2013KL-14) and was registered on ChiCTR (No. ChiCTR-TRC-13003265). The study was conducted in accordance with the Declaration of Helsinki. All the participants provided written informed consent.

Participants

A total of 37 CSAP patients and 65 healthy subjects (HS) were enrolled in this study. The patients were recruited from the Third Teaching Hospital of Chengdu University of Traditional Chinese Medicine and Sichuan Second Hospital of Traditional Chinese Medicine. HS came from the nearby communities.

The diagnostic criteria of CSAP followed the guidelines for the management of patients with chronic stable angina of the American College of Cardiology/American Heart Association (Fraker et al., 2007) and the Chinese Society of Cardiology (Chinese Society of Cardiology, Chinese Medical Association, and Editorial Board of Chinese Journal of Cardiology, 2007). Patients were included if they fulfilled all of the following items: (1) aged from 45 to 80 years old; (2) right-handedness;

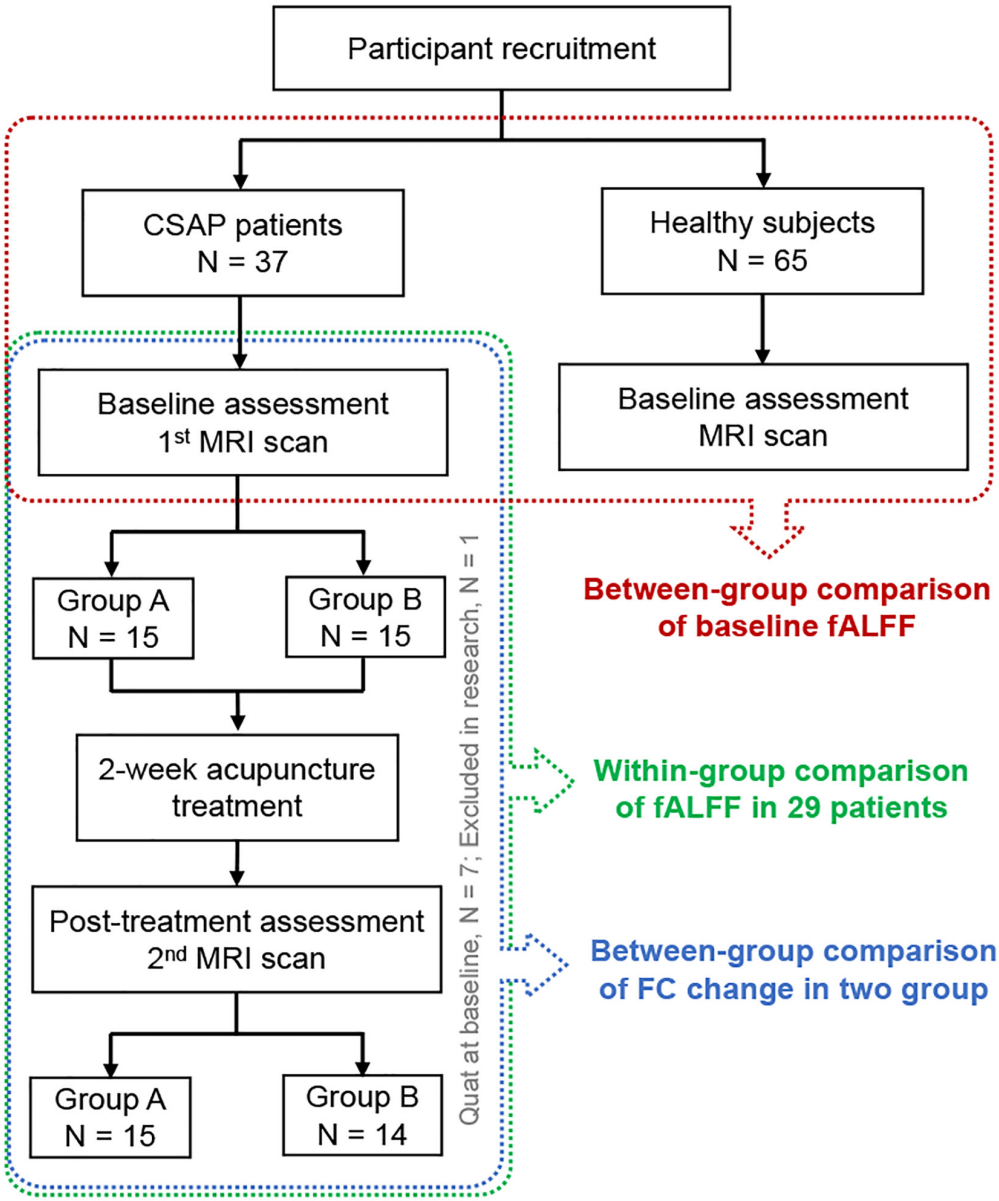

FIGURE 1 | The flowchart of the study. CSAP, chronic stable angina pectoris; MRI, Magnetic Resonance Imaging; fALFF, fractional Amplitude of Low-Frequency Fluctuation; FC, functional connectivity.

(3) met the diagnostic criteria; (4) graded as level 1 or 2 of angina based on the angina grading system of the Canadian Cardiovascular Society (Smith, 2002); (5) coronary artery stenosis ≥50% on coronary angiography; (6) the duration of disease was longer than 3 months; (7) the frequency of angina attacks was more than twice a week. The patients were excluded if they matched one of the following items: (1) had an acute coronary syndrome, malignant arrhythmia, or myocardial infarction within the last 3 months; (2) suffered from other severe psychiatric, neurological, cardiovascular, respiratory, or renal disorders; (3) had a diagnosis of diabetes or impaired glucose tolerance; (4) suffered from other chronic pain disorders or having a history of head trauma; (5) had any contraindication to MRI scanning, such as claustrophobia; (6) the Zung Self-Rating Anxiety Scale (SAS) or Self-Rating Depression Scale (SDS) ≥50; (7) participated in other clinical trials within 3 months; (8) received acupuncture treatment in the past 3 months.

Healthy subjects should meet the following criteria for inclusion: (1) aged from 45 to 80 years old; (2) right-handedness; (3) had no CSAP or other physical or psychological diseases. The exclusion criteria of HS were as follows: (1) had any contraindication to MRI scanning, such as claustrophobia; (2) participated in other clinical trials within 3 months; (3) received acupuncture treatment in the past 3 months.

All participants underwent clinical assessment, physical examination, and laboratory tests after recruitment. The

cardiologists from Chengdu University of Traditional Chinese Medicine determined whether a participant could be included based on the inclusion criteria and physical examination results.

Intervention

Patients willing to receive acupuncture treatment were assigned into two groups randomly using a random number table. The acupoint prescriptions were as follows: Group A (acupoints on the meridian directly related to the *Heart*): bilateral *Neiguan* (PC6) and bilateral *Tongli* (HT5); Group B (acupoints on the meridian indirectly related to the *Heart*): bilateral *Yangxi* (LI5) and bilateral *Pianli* (LI6). The location of these acupoints is provided in **Supplementary Figure 1**. All acupoints were stimulated with the 1.5 *cun* (diameter 0.25 mm, length 40 mm) filiform acupuncture needles. One licensed acupuncturist with more than 5 years of clinical experience administered all the acupuncture manipulation. First, the needles were inserted into the acupoints 5–15 mm perpendicularly. Then the acupuncturist lifted and thrusted the needles with an amplitude of 3–5 mm, twirled the needles in 90–180° to achieve *deqi* sensation. The needles were retained in the acupoints for 30 min, during which the needles were manipulated every 10 min for 2 times, with each time taking 10–15 s.

The treatment sessions lasted for 2 weeks, with five consecutive days per week followed by 2 days off for a total of 10 acupuncture treatments. During the treatment, the regular use of aspirin, clopidogrel, beta-adrenergic blocking agents, statins, angiotensin-converting enzyme inhibitors were allowed as basic management for all CSAP patients (Fraker et al., 2007). HS received no acupuncture treatment.

Outcome Measurements

The primary outcome was the frequency of angina attacks for 2 weeks, and the secondary outcomes included the McGill pain score, SAS, and SDS. The McGill Pain Questionnaire is a personalized measurement tool for pain experience (Melzack, 1975), which could be used to monitor the pain intensity and affectivity, and to determine the effectiveness of interventions. The SAS and SDS are self-reported scales for evaluating patients' anxiety and depression status.

Statistical Analysis

All the clinical data were analyzed with SPSS 20 software (IBM, Armonk, NY, United States). Shapiro–Wilk test was used to evaluate the normality of the data. The comparisons between the demographic characteristics of CSAP patients and HS, as well as between symptom improvements of Group A and Group B were performed with the two-sample *t*-tests or *Chi-square* tests. The comparisons of clinical outcomes within the pre- and post-treatment were conducted with the paired *t*-test. All the statistical thresholds were set at $p < 0.05$, two-tailed.

Magnetic Resonance Imaging Scans

Magnetic resonance imaging data were collected using a 3.0T MRI scanner (Siemens, Munich, Germany) with an eight-channel phased-array head coil at the West China Hospital of Sichuan University. Each scanning session included a T1-weighted imaging scan and a resting-state blood oxygen level-dependent (BOLD) imaging scan.

Participants were required to stay awake and keep their heads still during the scan, with their eyes closed and ears plugged. The T1 image were obtained using a fast spoiled gradient recalled sequence (slice thickness = 1 mm, repetition time = 2700 ms, echo time = 3.39 ms, field of view = 256 mm, flip angle = 7°, matrix = 256 × 256). The BOLD image was obtained using the echo-planar imaging (slice number = 30, total volumes: 180, slice thickness = 5 mm, repetition time = 2000 ms, echo time = 30 ms, field of view = 240 mm, flip angle = 90°, matrix = 64 × 64).

Magnetic Resonance Imaging Data Processing

Data Preprocessing

Magnetic resonance imaging data were preprocessed with the DPABI toolbox (Yan et al., 2016)[1]. The data preprocessing included the following steps: (1) discarding of the first ten time points; (2) slice timing correction; (3) realignment and head motion correction; (4) excluding participants with excessive head motion [mean framewise displacement (Jenkinson et al., 2002) >0.2]; (5) spatial normalization into Montreal Neurological Institute space through Diffeomorphic Anatomical Registration Through Exponentiated Lie Algebra (Ashburner, 2007); (6) spatial smoothing with 4 mm full width half maximum Gaussian; (7) regression of confounding factors (white matter, cerebrospinal fluid, and linear and quadratic trends); (8) temporal filtering (0.01–0.1 Hz) of the time series was performed after the fractional Amplitude of Low-Frequency Fluctuation (fALFF) analysis.

Fractional Amplitude of Low-Frequency Fluctuation Analysis

After checking the quality of images, the whole-brain fALFF was calculated for every participant. In the first part of analysis, a two-sample *t*-test was performed to compare the between-group difference of the baseline fALFF in CSAP patients and HS, with the age, gender, education level, Body Mass Index (BMI), and mean framewise displacement as covariances. In the second part of analysis, a paired *t*-test was conducted between the pre- and post-treatment fALFF of all CSAP patients to investigate the modulating effects of acupuncture. The threshold of these comparisons was set to $p < 0.05$ (two-tailed) at both voxel level and cluster level, corrected with the Gaussian Random Field (GRF) method.

Subsequently, the results of the first and second part of analysis were overlapped, to extract the key region that participates both in the neuropathology and acupuncture treatment effects of CSAP. Then, the partial correlation analyses between the baseline fALFF of the overlapping region and the baseline clinical symptoms, as well as between the fALFF change of this region and the clinical measures improvements after treatment were performed in CSAP patients, with age, gender, education level, BMI, and head motion as covariates. The statistical threshold for correlation analyses was set at $p < 0.05$.

[1] http://rfmri.org/dpabi

Resting-State Functional Connectivity Analysis

The overlapping region identified above was set as region-of-interest (ROI), and the ROI-to-voxel rsFC maps were calculated for all patients. To investigate the specific effects of different acupoint prescriptions for the rsFC of CSAP patients, the within-group comparisons between the pre- and post-treatment rsFC maps in Group A and Group B, as well as the between-group comparison of the rsFC maps change between Group A and B were performed. The within-group comparisons were conducted with the paired *t*-test. The between-group comparison was performed with the two-sample *t*-test, using age, gender, education level, and BMI as covariates. The threshold of these comparisons was set to voxel-level $p < 0.05$ and cluster-level *p-GRF* < 0.05, two-tailed. Furthermore, the Spearman correlation analyses between rsFC change and clinical measures improvements after acupuncture treatment in Group A, Group B, and all the patients were also performed for the non-normal distribution of clinical data in both group A and B. The statistical threshold for correlation analyses was set at $p < 0.05$.

RESULTS

Demographic and Clinical Characteristics of Chronic Stable Angina Pectoris Patients and Healthy Subjects

In total, 37 CSAP patients and 65 HS were included. The age of CSAP patients was higher than HS. There was no statistical difference in gender, BMI, and education level between CSAP patients and HS (**Table 1**). No statistical difference in mean framewise displacement was found between CSAP patients (0.12 ± 0.06) and HS (0.10 ± 0.05). And there were no significant pharmacological intervention differences or baseline characteristic differences between Group A and Group B (**Table 2**).

Baseline Comparison of the Fractional Amplitude of Low-Frequency Fluctuation Between Chronic Stable Angina Pectoris Patients and Healthy Subjects

Chronic stable angina pectoris patients had significantly higher fALFF in the bilateral calcarine, left middle occipital gyrus (MOG), right superior temporal gyrus, and right postcentral gyrus, while no region with lower fALFF than HS (voxel-level $p < 0.05$, cluster-level *p-GRF* < 0.05) (**Figure 2A** and **Supplementary Table 1**).

Acupuncture Effects on the Clinical Symptoms of Chronic Stable Angina Pectoris Patients

Seven CSAP patients were unwilling to receive acupuncture treatment and quit at the baseline. One CSAP patient was excluded due to the excessive head motion in the second scan. Therefore, 29 CSAP patients (15 patients in group A and 14 patients in group B) with eligible clinical and imaging data were retained for the following analysis.

The within-group analysis among these 29 patients demonstrated that acupuncture treatment could significantly improve the McGill pain score ($p < 0.001$) and SAS score ($p < 0.05$). Patients in Group A had significant improvements in the frequency of angina attacks ($p < 0.05$), McGill pain scale ($p < 0.01$), and SAS score ($p < 0.05$), while patients in Group B only had a significant improvement in McGill pain scale ($p < 0.001$) after acupuncture treatment. There was no significant between-group difference in these 4 metrics in Group A and Group B ($p > 0.05$) (**Table 3**).

Acupuncture Effects on the Fractional Amplitude of Low-Frequency Fluctuation of Chronic Stable Angina Pectoris Patients

After acupuncture treatment, CSAP patients manifested significantly increased fALFF in the brain stem, hippocampus, and parahippocampus, as well as decreased fALFF in the left calcarine, left cuneus, right middle orbitofrontal gyrus, and right median orbitofrontal gyrus (voxel-level $p < 0.05$, cluster-level *p-GRF* < 0.05) (**Figure 2B** and **Supplementary Table 2**). In addition, **Supplementary Figure 2** and **Supplementary Table 3** displayed the between-group differences of fALFF changes in these two groups.

Regulation of Acupuncture on the Aberrant Fractional Amplitude of Low-Frequency Fluctuation in Chronic Stable Angina Pectoris Patients

This study further performed an overlapping analysis between regions that survived in the baseline comparison and regions that changed after treatment in CSAP patients, finding that the overlapping region was located at the left calcarine (cluster size = 41) (**Figure 3A**). There were significant differences in fALFF of this region between CSAP patients and HS, as well as between the baseline and after treatment in CSAP patients (**Figure 3B**). In addition, the baseline fALFF of this region was significantly correlated with the baseline McGill pain score of CSAP patients ($r = -0.446$, $p = 0.010$) (**Figure 3C**). The change in fALFF of this region was significantly correlated with the improvement of McGill pain score ($r = 0.464$, $p = 0.011$), SAS score ($r = 0.563$, $p = 0.001$), and SDS score ($r = 0.439$, $p = 0.017$) in CSAP patients (**Figures 3D–F**).

Variation of Different Prescriptions on the Modulation of Resting-State Functional Connectivity in Chronic Stable Angina Pectoris Patients

The overlapping region (the left calcarine) was set as the ROI for the ROI-voxel rsFC analysis. Patients in Group A manifested increased rsFC between ROI and the left cerebellum crus 1, left fusiform gyrus, and right supramarginal gyrus, while no

TABLE 1 | The demographic and clinical characteristics of CSAP patients and HS.

	CSAP (n = 37) (mean ± SD)	HS (n = 65) (mean ± SD)	Statistic value	p value
Age (Years)	65.05 ± 7.23	56.71 ± 5.49	$t = 6.092$	<0.001***
Gender (M/F)	20/17	26/39	$x^2 = 0.342$	0.559
BMI (Kg/m^2)	24.42 ± 2.67	23.35 ± 2.72	$t = 1.911$	0.059
Education level (primary/middle school/college)	6/22/9	8/40/17	$x^2 = 0.310$	0.856
Duration (Month)	57.92 ± 56.78	/	/	/
Frequency of angina attacks	5.89 ± 4.38	/	/	/
McGill pain scale	10.46 ± 3.82	/	/	/
SAS score	32.97 ± 4.51	/	/	/
SDS score	30.95 ± 4.70	/	/	/

*CSAP, chronic stable angina pectoris; HS, healthy subjects; M/F, male/female; BMI, Body Mass Index; SAS, self-rating anxiety scale; SDS, self-rating depression scale. ***$p < 0.001$.*

TABLE 2 | The between-group comparison of demographic characteristics and baseline conditions of CSAP patients in these two acupuncture groups.

	Group A (n = 15) (mean ± SD)	Group B (n = 14) (mean ± SD)	Statistic value	p value
Age (Years)	65.20 ± 5.967	65.86 ± 7.675	$t = -0.258$	0.189
Gender (M/F)	6/9	8/6	$x^2 = 0.852$	0.356
BMI (Kg/m^2)	25.05 ± 2.94	24.56 ± 2.56	$t = 0.478$	0.593
Education level (primary/middle school/college)	3/10/2	2/8/4	$x^2 = 1.056$	0.590
Duration (Month)	62.33 ± 52.64	59.79 ± 71.46	$t = 0.110$	0.913
Frequency of angina attacks	5.53 ± 3.60	5.43 ± 4.85	$t = 0.689$	0.414
McGill pain score	10.73 ± 4.76	9.57 ± 2.64	$t = 0.363$	0.552
SAS score	33.58 ± 3.83	32.68 ± 5.32	$t = 0.024$	0.877
SDS score	31.93 ± 5.02	30.36 ± 5.08	$t = 0.211$	0.650
Drug use				
Antiplatelet drugs (Y/N)	10/5	8/6	$x^2 = 0.279$	0.597
ACEI/ARB (Y/N)	4/11	3/11	$x^2 = 0.109$	0.742
Beta-adrenergic blocking agents (Y/N)	5/10	6/8	$x^2 = 0.279$	0.597
Statins	11/4	9/5	$x^2 = 0.277$	0.599

M/F, male/female; BMI, Body Mass Index; SAS, self-rating anxiety scale; SDS, self-rating depression scale; Y/N, Yes/No; ACEI, angiotensin-converting enzyme inhibitors; ARB, angiotensin receptor Blocker.

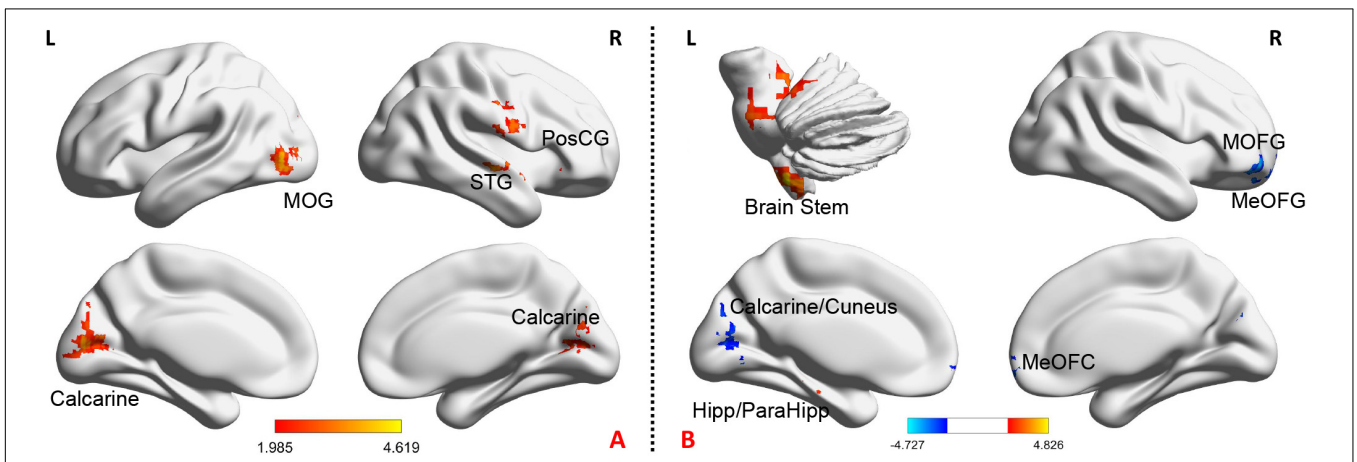

FIGURE 2 | The baseline and the change of fALFF after treatment in CSAP patients. **(A)** Illustrates the baseline comparison of fALFF between CSAP patients and HS. The warm tone indicates CSAP patients >HS. **(B)** Illustrates acupuncture effects on the fALFF of CSAP patients. The warm tone indicates increased fALFF after treatment while the cool tone indicates decreased fALFF after treatment. Threshold: voxel-level $p < 0.05$, cluster-level p-$GRF < 0.05$. MOG, middle occipital gyrus; PosCG, postcentral gyrus; STG, superior temporal gyrus; MOFG, middle orbitofrontal gyrus; MeOFG, median orbitofrontal gyrus; ParaHipp, parahippocampus; Hipp, hippocampus; L, left; R, right.

TABLE 3 | The clinical effects of acupuncture in CSAP patients.

	Pre (mean ± SD)	Pos (mean ± SD)	Within-group comparison		Between-group comparison [(A_{pos} – A_{pre}) vs. (B_{pos} – B_{pre})]	
			t value	*p* value	*t* value	*p* value
Frequency of angina attacks						
All patients	5.48 ± 4.17	4.45 ± 3.73	1.240	0.225		
Group A ($n = 15$)	5.53 ± 3.60	3.93 ± 3.26	1.964	0.049*	0.689	0.414
Group B ($n = 14$)	5.43 ± 4.85	5.00 ± 4.22	0.528	0.598		
McGill pain score						
All patients	10.17 ± 3.86	6.36 ± 2.95	6.101	<0.001***		
Group A ($n = 15$)	10.73 ± 4.76	6.87 ± 2.61	3.665	0.003**	0.363	0.552
Group B ($n = 14$)	9.57 ± 2.64	5.82 ± 3.28	5.557	<0.001***		
SAS score						
All patients	33.15 ± 4.55	31.19 ± 4.55	2.328	0.027*		
Group A ($n = 15$)	33.58 ± 3.83	31.29 ± 4.64	2.427	0.029*	0.024	0.877
Group B ($n = 14$)	32.68 ± 5.32	31.07 ± 4.62	1.104	0.290		
SDS score						
All patients	31.17 ± 5.02	30.52 ± 5.13	0.674	0.506		
Group A ($n = 15$)	31.93 ± 5.02	30.50 ± 5.51	1.264	0.227	0.211	0.650
Group B ($n = 14$)	30.36 ± 5.08	30.54 ± 4.90	−0.110	0.914		

Pre, Pre-treatment; Pos, Pos-treatment; SD, standard deviation; SAS, self-rating anxiety scale; SDS, self-rating depression scale.
**p < 0.05; **p < 0.01; ***p < 0.001.*

significant rsFC change was found in Group B after treatment (**Figure 4A** and **Supplementary Table 4**).

Compared to group B, CSAP patients in group A had significantly increased rsFC between ROI and the left inferior temporal gyrus (ITG)/cerebellum crus 1, left hippocampus/thalamus, and left middle cingulate cortex (MCC) after acupuncture treatment (voxel-level $p < 0.05$, cluster-level *p-GRF* < 0.05) (**Figures 4B,C** and **Supplementary Table 5**).

The rsFC change between the ROI and left ITG/cerebellum crus 1 was significantly correlated with McGill pain score improvement ($r = 0.561$, $p = 0.030$) and SDS score improvement in Group A ($r = 0.650$, $p = 0.009$) (**Figure 4D**), while no significant correlation in group B or in all 29 patients.

DISCUSSION

To the best of our knowledge, this was the first study to investigate the aberrant brain spontaneous activity patterns of CSAP patients and explore the modulating effects of acupuncture for functional brain activity as well as rsFC in CSAP patients. The findings demonstrated that acupuncture could significantly decrease the elevated spontaneous activity of the left calcarine in CSAP patients. Compared with the acupoints on the meridian indirectly related to the *Heart*, acupuncturing at the points on the meridians directly related to the *Heart* had a remarkable effect on the regulation of rsFC between the calcarine and the ITG, cerebellum crus 1, hippocampus, thalamus, and MCC.

Brain-heart interaction plays an important role in the pathophysiology and treatment of cardiovascular diseases (Silvani et al., 2016). On the one hand, the heart receives signals from the brain via the sympathetic and parasympathetic nerves which are controlled by the central autonomic network (Benarroch, 1993). On the other hand, the noxious pain stimulus of angina is mediated by coronary chemoreceptors and transmitted to the brain via vagal afferent nerves, and finally integrated and processed in the cerebral cortex. The current study demonstrated that CSAP patients manifested higher spontaneous activity on the calcarine, MOG, and postcentral gyrus, and that the abnormally elevated functional activity of the calcarine was positively correlated with the McGill pain score in patients. The postcentral gyrus is the cortex center of somatic sensation perception and the crucial part of the pain neural matrix, which is responsible for the adjustment of pain perception, including the positioning and recognition of pain intensity (Mouraux and Iannetti, 2018). Calcarine and MOG are important components of the primary visual cortex and are traditionally thought to be primarily involved in visual processing (Thiebaut de Schotten et al., 2014). However, there is growing evidence in recent years found that several components of the visual cortex, including the calcarine and MOG, were also involved in the processing of pain signals. Results of several fMRI studies have indicated that patients with chronic pain, such as migraine (Wei et al., 2019), low back pain (Bush et al., 2021), and persistent somatoform pain disorder (Liu et al., 2019), exhibited atypical functional activity patterns in the occipital gyrus. For example, (Wei et al., 2019) demonstrated that migraine patients had aberrant spontaneous activity and regional homogeneity in calcarine, as well as atypical rsFC between calcarine and the thalamus, the relay station of sensory signaling. Moreover, these abnormalities of calcarine activity and connectivity patterns were significantly correlated with the pain intensity and affective condition of patients (Wei et al., 2019, 2021). This evidence indicated that calcarine was involved in the processing of pain perception

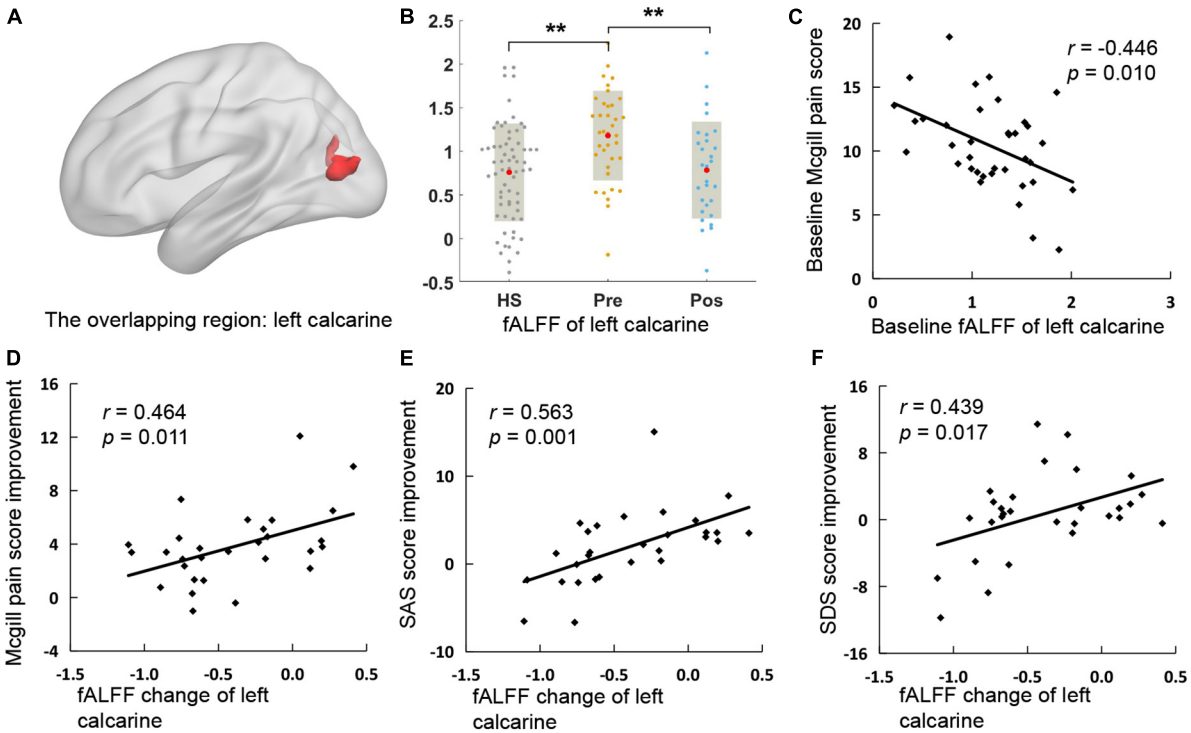

FIGURE 3 | The overlapping region and its correlation with clinical symptoms. **(A)** Is the location of the overlapping region. **(B)** Is the comparison of fALFF of the overlapping region among HS and the baseline and after treatment of CSAP patients. **(C)** Illustrates the correlation between the baseline fALFF of the overlapping region and the baseline McGill pain score in CSAP patients. **(D–F)** Illustrate the correlations between the fALFF change of the overlapping region and improvements of clinical symptoms after treatment. HS, healthy subjects; pre, pre-treatment; pos, post-treatment; fALFF, fractional Amplitude of Low-Frequency Fluctuation; SAS, self-rating anxiety scale; SDS, self-rating depression scale. $^{*}p < 0.05$; $^{**}p < 0.01$; $^{***}p < 0.001$.

and pain affectivity (Schwedt et al., 2015). In addition to the somatalgia, patients with chronic visceral pain (e.g., irritable bowel syndrome) also exhibited higher spontaneous activity and regional homogeneity in calcarine at resting-state (Chen et al., 2021), and increased activity in the visual cortex during the expectation of rectal pain. These findings suggested that the calcarine was not only associated with pain perception and pain affectivity but was also involved in hypervigilance to pain anticipation (Lee et al., 2012). The typical symptom of CSAP is prolonged, episodic chest dullness and crushing pain. This noxious pain stimulation as well as alertness and excessive fear of angina attacks lead to the hypersensitization of calcarine, manifested as symptoms-associated hyperactivity of the calcarine in CSAP patients.

After acupuncture treatment, the pain experience and anxiety condition were significantly improved, the abnormally elevated functional activity of the calcarine was significantly normalized in CSAP patients, and there were positive correlations between fALFF change in calcarine and improvements of McGill pain, SAS, and SDS score in patients. These findings reverified that acupuncture was an effective adjunctive therapy for CSAP, which was consisted with the previous multicenter randomized controlled trial (Zhao et al., 2019), and suggested that the effects of acupuncture in improving the pain experience of CSAP patients were closely related to the modulation of calcarine activity. In addition, this study also found that acupuncture treatment could significantly regulate the spontaneous activity of the brainstem, hippocampus, parahippocampus, and orbitofrontal cortex in CSAP patients, which were closely related to the transmission, perception, attention, and cognition of pain (Bushnell et al., 2013). These findings indicated that acupuncture for analgesia was not single-targeted. The improvements of symptoms in CSAP patients induced by acupuncture were associated with its multi-targeted modulations of the pain process. These similar results have also been observed in acupuncture treatment of other visceral pains and somatalgia (Ma et al., 2020, 2021; Wen et al., 2021).

Another important finding of this study was the difference in clinical efficacy and modulation of rsFC patterns between acupuncture at points on the meridian indirectly and directly related to the *Heart*. These results supported the classic acupuncture theory "selecting acupoints along the meridian" (Xing et al., 2013) and explained the potential mechanism of better effects of acupoints on the meridian directly related to the *Heart* for CSAP from the perspective of brain-heart interaction. This study compared the differences of ROI-voxel rsFC change between these two acupoint prescriptions, finding that acupuncturing at points on the meridian directly related to the *Heart* could significantly increase the rsFC between the calcarine and the thalamus, hippocampus, MCC, and

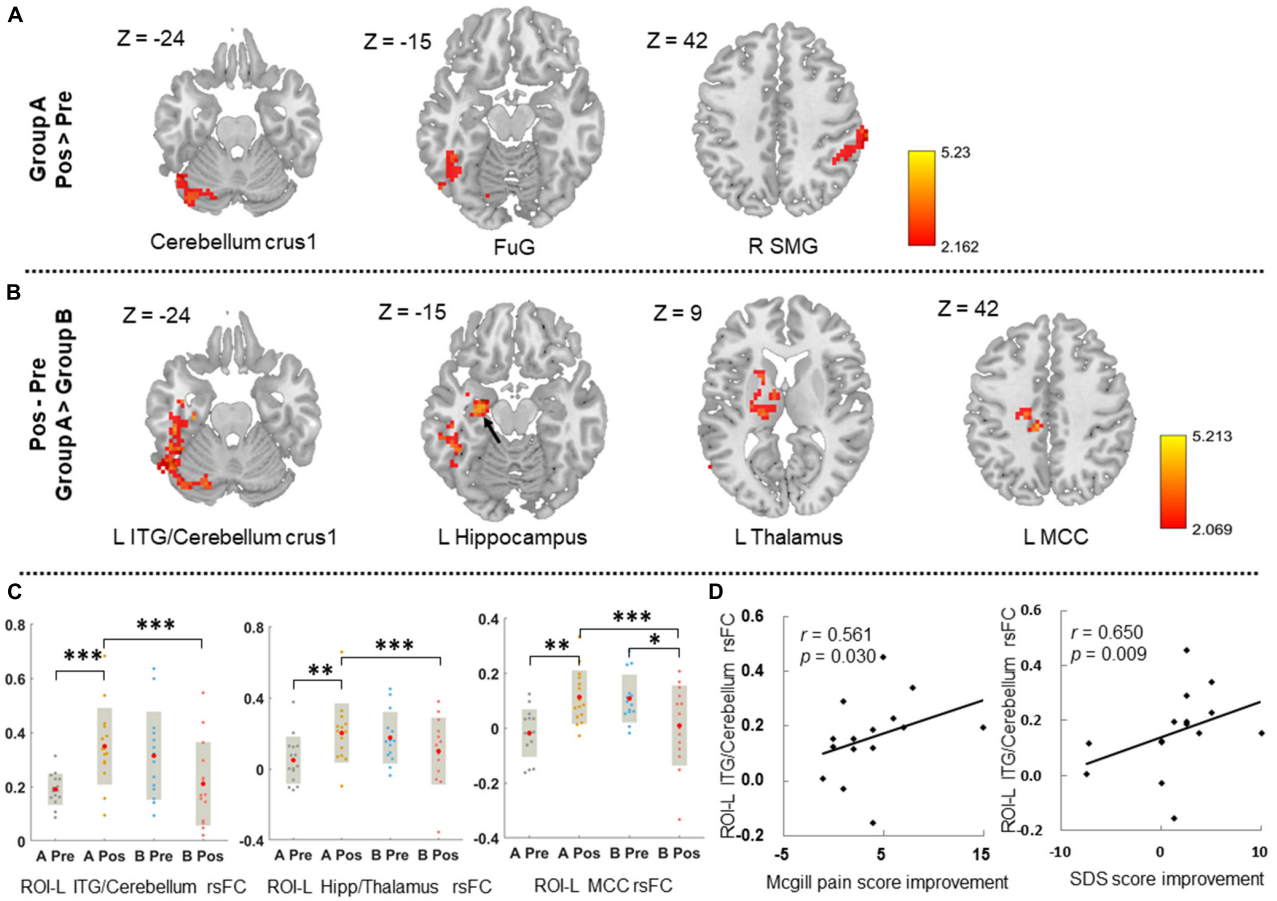

FIGURE 4 | The ROI-based rsFC change after treatment and its correlations with clinical symptoms improvements. **(A)** Displays the ROI-based rsFC change after treatment in group A. Threshold: voxel-level $p < 0.05$, cluster-level *p-GRF* < 0.05. **(B)** Displays the between-group difference of ROI-based rsFC change after treatment in groups A and B. Threshold: voxel-level $p < 0.05$, cluster-level *p-GRF* < 0.05. **(C)** Illustrates the comparisons of ROI-based rsFC values of the survival regions at pre- and post-treatment in those two groups. **(D)** Illustrates the correlations between ROI-based rsFC change of the survival regions and clinical symptoms improvements in group A. L, left; R, right; FuG, fusiform gyrus; SMG, supramarginal gyrus; ITG, inferior temporal gyrus; MCC, middle cingulate cortex; Hipp, hippocampus; ROI, region-of-interest; rsFC, resting-state functional connectivity; SDS, self-rating depression scale; $*p < 0.05$; $**p < 0.01$; $***p < 0.001$. The black arrow indicates the location of the left hippocampus.

ITG/Cerebellum crus 1 than acupoints on the meridian indirectly related to the *Heart*. Pain is a multidimensional and complex experience involving sensory, cognitive, and affective aspects (Fitzcharles et al., 2021). The thalamus is a pivotal node for pain transmission and mediation, the hippocampus and cingulate cortex are responsible for the processing and encoding of pain cognition and affectivity, while the cerebellum and ITG play an important role in pain visual perception and multimodal sensory integration (Saab, 2012; Bushnell et al., 2013; Finnerup et al., 2021). Therefore, the current findings, while confirming the specificity of the acupoint effects, also suggested that better improvement of CSAP symptoms by acupuncturing at points on the meridian directly related to the *Heart* might be correlated with their multi-threaded modulations to the pain network.

Several limitations should be concerned in this study. First, the sample size was smaller in each acupuncture treatment group. Second, the intervention phase was short. These two factors may account for the non-significant difference in clinical efficacy between two acupoint prescriptions. Third, to be consistent with clinical practice, patients in this study are allowed to receive recommended pharmacological interventions. Therefore, the effects of drugs on functional brain activity are difficult to exclude.

CONCLUSION

The current study provided neuroimaging evidence for understanding the central pathophysiology of CSAP patients and the mechanism of acupuncture for CSAP. These findings suggested that the elevated spontaneous activity of the calcarine was an important central pathological characteristic of CSAP, and regulation of the aberrant spontaneous activity of the calcarine might be an underlying mechanism of acupuncture treatment for CSAP patients. The multi-threaded modulation of rsFC between calcarine and multiple pain-related brain regions might be a potential mechanism for better efficacy of acupuncture at points on the meridian directly related to the *Heart*.

DATA AVAILABILITY STATEMENT

The raw data supporting the conclusions of this article will be made available by the authors, without undue reservation.

ETHICS STATEMENT

The studies involving human participants were reviewed and approved by the Sichuan Traditional Chinese Medicine Regional Ethics Committee. The patients/participants provided their written informed consent to participate in this study.

AUTHOR CONTRIBUTIONS

FL and FZ conceived and designed the study. YL, RS, ZL, MJ, and QW recruited the participants. TY and ZT analyzed the data. LL drafted the manuscript. SL, FL, and FZ revised the manuscript. All authors contributed to the article and approved the submitted version.

FUNDING

This study was financially supported by the National Key R&D Program of China (Nos. 2018YFC1704600 and 2018YFC1704605), State Key Program for Basic Research of China (2012CB518501), and National Natural Science Foundation of China (Nos. 81590950, 81273154, and 81473602).

ACKNOWLEDGMENTS

We thank various people for their contribution to this project and their families.

SUPPLEMENTARY MATERIAL

The Supplementary Material for this article can be found online at: https://www.frontiersin.org/articles/10.3389/fnmol.2022.842674/full#supplementary-material

REFERENCES

Ashburner, J. (2007). A fast diffeomorphic image registration algorithm. *Neuroimage* 38, 95–113. doi: 10.1016/j.neuroimage.2007.07.007

Benarroch, E. E. (1993). The central autonomic network: functional organization, dysfunction, and perspective. *Mayo Clin. Proc.* 68, 988–1001. doi: 10.1016/s0025-6196(12)62272-1

Benjamin, E. J., Blaha, M. J., Chiuve, S. E., Cushman, M., Das, S. R., Deo, R., et al. (2017). Heart Disease and Stroke Statistics-2017 Update: a Report From the American Heart Association. *Circulation* 135, e146–e603. doi: 10.1161/cir.0000000000000485

Bush, N. J., Schneider, V., Sevel, L., Bishop, M. D., and Boissoneault, J. (2021). Associations of Regional and Network Functional Connectivity With Exercise-Induced Low Back Pain. *J. Pain* 22, 1606–1616. doi: 10.1016/j.jpain.2021.05.004

Bushnell, M. C., Ceko, M., and Low, L. A. (2013). Cognitive and emotional control of pain and its disruption in chronic pain. *Nat. Rev. Neurosci.* 14, 502–511. doi: 10.1038/nrn3516

Chaitman, B. R., and Laddu, A. A. (2011). Stable angina pectoris: antianginal therapies and future directions. *Nat. Rev. Cardiol.* 9, 40–52. doi: 10.1038/nrcardio.2011.129

Chang, C. M., Yang, C. P., Yang, C. C., Shih, P. H., and Wang, S. J. (2021). Evidence of Potential Mechanisms of Acupuncture from Functional MRI Data for Migraine Prophylaxis. *Curr. Pain Headache Rep.* 25:49. doi: 10.1007/s11916-021-00961-4

Chen, X. F., Guo, Y., Lu, X. Q., Qi, L., Xu, K. H., Chen, Y., et al. (2021). Aberrant Intraregional Brain Activity and Functional Connectivity in Patients With Diarrhea-Predominant Irritable Bowel Syndrome. *Front. Neurosci.* 15:721822. doi: 10.3389/fnins.2021.721822

Chinese Society of Cardiology, Chinese Medical Association, and Editorial Board of Chinese Journal of Cardiology (2007). Guideline for diagnosis and treatment of patients with chronic stable angina. *Chin. J. Cardiol.* 35, 195–206. doi: 10.3760/j.issn:0253-3758.2007.03.002

Chu, W. C., Wu, J. C., Yew, D. T., Zhang, L., Shi, L., Yeung, D. K., et al. (2012). Does acupuncture therapy alter activation of neural pathway for pain perception in irritable bowel syndrome?: a comparative study of true and sham acupuncture using functional magnetic resonance imaging. *J. Neurogastroenterol. Motil.* 18, 305–316. doi: 10.5056/jnm.2012.18.3.305

Davis, K. D., Flor, H., Greely, H. T., Iannetti, G. D., Mackey, S., Ploner, M., et al. (2017). Brain imaging tests for chronic pain: medical, legal and ethical issues and recommendations. *Nat. Rev. Neurol.* 13, 624–638. doi: 10.1038/nrneurol.2017.122

Finnerup, N. B., Kuner, R., and Jensen, T. S. (2021). Neuropathic Pain: from Mechanisms to Treatment. *Physiol. Rev.* 101, 259–301. doi: 10.1152/physrev.00045.2019

Fitzcharles, M. A., Cohen, S. P., Clauw, D. J., Littlejohn, G., Usui, C., and Häuser, W. (2021). Nociplastic pain: towards an understanding of prevalent pain conditions. *Lancet* 397, 2098–2110. doi: 10.1016/s0140-6736(21)00392-5

Fraker, T. D. Jr., Fihn, S. D., 2002 Chronic Stable Angina Writing Committee, American College of Cardiology, American Heart Association, Gibbons, R. J., et al. (2007). 2007 chronic angina focused update of the ACC/AHA 2002 guidelines for the management of patients with chronic stable angina: a report of the American College of Cardiology/American Heart Association Task Force on Practice Guidelines Writing Group to develop the focused update of the 2002 guidelines for the management of patients with chronic stable angina. *J. Am. Coll. Cardiol.* 50, 2264–2274. doi: 10.1016/j.jacc.2007.08.002

Huang, S., Li, L., Liu, J., Li, X., Shi, Q., Li, Y., et al. (2021). The Preventive Value of Acupoint Sensitization for Patients with Stable Angina Pectoris: a Randomized, Double-Blind, Positive-Controlled, Multicentre Trial. *Evid. Based Complement. Alternat. Med.* 2021:7228033. doi: 10.1155/2021/7228033

Jenkinson, M., Bannister, P., Brady, M., and Smith, S. (2002). Improved optimization for the robust and accurate linear registration and motion correction of brain images. *Neuroimage* 17, 825–841. doi: 10.1016/s1053-8119(02)91132-8

Lee, H. F., Hsieh, J. C., Lu, C. L., Yeh, T. C., Tu, C. H., Cheng, C. M., et al. (2012). Enhanced affect/cognition-related brain responses during visceral placebo analgesia in irritable bowel syndrome patients. *Pain* 153, 1301–1310. doi: 10.1016/j.pain.2012.03.018

Liu, Q., Zeng, X. C., Jiang, X. M., Zhou, Z. H., and Hu, X. F. (2019). Altered Brain Functional Hubs and Connectivity Underlie Persistent Somatoform Pain Disorder. *Front. Neurosci.* 13:415. doi: 10.3389/fnins.2019.00415

Ma, K., Liu, Y., Shao, W., Sun, J., Li, J., Fang, X., et al. (2020). Brain Functional Interaction of Acupuncture Effects in Diarrhea-Dominant Irritable Bowel Syndrome. *Front. Neurosci.* 14:608688. doi: 10.3389/fnins.2020.608688

Ma, P., Dong, X., Qu, Y., He, Z., Yin, T., Cheng, S., et al. (2021). A Narrative Review of Neuroimaging Studies in Acupuncture for Migraine. *Pain Res. Manag.* 2021:9460695. doi: 10.1155/2021/9460695

Melzack, R. (1975). The McGill Pain Questionnaire: major properties and scoring methods. *Pain* 1, 277–299. doi: 10.1016/0304-3959(75)90044-5

Mouraux, A., and Iannetti, G. D. (2018). The search for pain biomarkers in the human brain. *Brain* 141, 3290–3307. doi: 10.1093/brain/awy281

Piccolo, R., Giustino, G., Mehran, R., and Windecker, S. (2015). Stable coronary artery disease: revascularisation and invasive strategies. *Lancet* 386, 702–713. doi: 10.1016/s0140-6736(15)61220-x

Rosen, S. D., Paulesu, E., Frith, C. D., Frackowiak, R. S., Davies, G. J., Jones, T., et al. (1994). Central nervous pathways mediating angina pectoris. *Lancet* 344, 147–150. doi: 10.1016/s0140-6736(94)92755-3

Saab, C. Y. (2012). Pain-related changes in the brain: diagnostic and therapeutic potentials. *Trends Neurosci.* 35, 629–637. doi: 10.1016/j.tins.2012.06.002

Schwedt, T. J., Chiang, C. C., Chong, C. D., and Dodick, D. W. (2015). Functional MRI of migraine. *Lancet Neurol.* 14, 81–91. doi: 10.1016/s1474-4422(14)70193-0

Shen, M., Huang, J., and Qiu, T. (2021). Quality of the Evidence Supporting the Role of Acupuncture for Stable Angina Pectoris: an Umbrella Review of Systematic Reviews. *Front. Cardiovasc. Med.* 8:732144. doi: 10.3389/fcvm.2021.732144

Silvani, A., Calandra-Buonaura, G., Dampney, R. A., and Cortelli, P. (2016). Brain-heart interactions: physiology and clinical implications. *Philos. Trans. A Math. Phys. Eng. Sci.* 374:20150181. doi: 10.1098/rsta.2015.0181

Smith, E. R. (2002). The angina grading system of the Canadian Cardiovascular Society. *Can. J. Cardiol.* 18, 439–442.

Templin, C., Hänggi, J., Klein, C., Topka, M. S., Hiestand, T., Levinson, R. A., et al. (2019). Altered limbic and autonomic processing supports brain-heart axis in Takotsubo syndrome. *Eur. Heart J.* 40, 1183–1187. doi: 10.1093/eurheartj/ehz068

Thiebaut de Schotten, M., Urbanski, M., Valabregue, R., Bayle, D. J., and Volle, E. (2014). Subdivision of the occipital lobes: an anatomical and functional MRI connectivity study. *Cortex* 56, 121–137. doi: 10.1016/j.cortex.2012.12.007

Wei, H. L., Li, J., Guo, X., Zhou, G. P., Wang, J. J., Chen, Y. C., et al. (2021). Functional connectivity of the visual cortex differentiates anxiety comorbidity from episodic migraineurs without aura. *J. Headache Pain* 22:40. doi: 10.1186/s10194-021-01259-x

Wei, H. L., Zhou, X., Chen, Y. C., Yu, Y. S., Guo, X., Zhou, G. P., et al. (2019). Impaired intrinsic functional connectivity between the thalamus and visual cortex in migraine without aura. *J. Headache Pain* 20:116. doi: 10.1186/s10194-019-1065-1

Wen, Q., Ma, P., Dong, X., Sun, R., Lan, L., Yin, T., et al. (2021). Neuroimaging Studies of Acupuncture on Low Back Pain: a Systematic Review. *Front. Neurosci.* 15:730322. doi: 10.3389/fnins.2021.730322

Wittbrodt, M. T., Moazzami, K., Shah, A. J., Lima, B. B., Hammadah, M., Mehta, P. K., et al. (2020). Neural responses during acute mental stress are associated with angina pectoris. *J. Psychosom. Res.* 134:110110. doi: 10.1016/j.jpsychores.2020.110110

Xing, J. J., Zeng, B. Y., Li, J., Zhuang, Y., and Liang, F. R. (2013). Acupuncture point specificity. *Int. Rev. Neurobiol.* 111, 49–65. doi: 10.1016/b978-0-12-411545-3.00003-1

Yan, C. G., Wang, X. D., Zuo, X. N., and Zang, Y. F. (2016). DPABI: data Processing & Analysis for (Resting-State) Brain Imaging. *Neuroinformatics* 14, 339–351. doi: 10.1007/s12021-016-9299-4

Yu, S. W., Lin, S. H., Tsai, C. C., Chaudhuri, K. R., Huang, Y. C., Chen, Y. S., et al. (2019). Acupuncture Effect and Mechanism for Treating Pain in Patients With Parkinson's Disease. *Front. Neurol.* 10:1114. doi: 10.3389/fneur.2019.01114

Zhao, L., Li, D., Zheng, H., Chang, X., Cui, J., Wang, R., et al. (2019). Acupuncture as Adjunctive Therapy for Chronic Stable Angina: a Randomized Clinical Trial. *JAMA Intern. Med.* 179, 1388–1397. doi: 10.1001/jamainternmed.2019.2407

Zhao, L., Song, Q., Wu, H., Wang, Y., Wu, J., Fang, J., et al. (2021). Acupuncture as Adjuvant Therapy for Treating Stable Angina Pectoris with Moderate Coronary Artery Lesions and the Mechanism of Heart-Brain Interactions: a Randomized Controlled Trial Protocol. *Evid. Based Complement. Alternat. Med.* 2021:6634404. doi: 10.1155/2021/6634404

Conflict of Interest: The authors declare that the research was conducted in the absence of any commercial or financial relationships that could be construed as a potential conflict of interest.

frontiers | Frontiers in Molecular Neuroscience

ORIGINAL RESEARCH
published: 03 May 2022
doi: 10.3389/fnmol.2022.869799

Environmental Enrichment and Estrogen Upregulate Beta-Hydroxybutyrate Underlying Functional Improvement

*Soonil Pyo [1,2], Joohee Kim [1,2], Jihye Hwang [1], Jeong Hyun Heo [1,3,4], Kyungri Kim [1,2] and Sung-Rae Cho [1,2,3,5]**

[1] Department and Research Institute of Rehabilitation Medicine, Yonsei University College of Medicine, Seoul, South Korea, [2] Brain Korea 21 Plus Project for Medical Sciences, Yonsei University College of Medicine, Seoul, South Korea, [3] Graduate Program of Biomedical Engineering, Yonsei University College of Medicine, Seoul, South Korea, [4] Department of Physiology, Yonsei University College of Medicine, Seoul, South Korea, [5] Rehabilitation Institute of Neuromuscular Disease, Yonsei University College of Medicine, Seoul, South Korea

OPEN ACCESS

Edited by:
Pedro Rojas-Morales,
National Autonomous University of Mexico, Mexico

Reviewed by:
Alessandro Ieraci,
University of Milan, Italy
Cheong Hoon Seo,
Hallym University, South Korea
Sung Hoon Kim,
Yonsei University, South Korea

***Correspondence:**
Sung-Rae Cho
srcho918@yuhs.ac

Specialty section:
This article was submitted to Neuroplasticity and Development, a section of the journal Frontiers in Molecular Neuroscience

Received: 05 February 2022
Accepted: 21 March 2022
Published: 03 May 2022

Citation:
Pyo S, Kim J, Hwang J, Heo JH, Kim K and Cho S-R (2022) Environmental Enrichment and Estrogen Upregulate Beta-Hydroxybutyrate Underlying Functional Improvement. Front. Mol. Neurosci. 15:869799. doi: 10.3389/fnmol.2022.869799

Environmental enrichment (EE) is a promising therapeutic strategy in improving metabolic and neuronal responses, especially due to its non-invasive nature. However, the exact mechanism underlying the sex-differential effects remains unclear. The aim of the current study was to investigate the effects of EE on metabolism, body composition, and behavioral phenotype based on sex. Long-term exposure to EE for 8 weeks induced metabolic changes and fat reduction. In response to the change in metabolism, the level of βHB were influenced by sex and EE possibly in accordance to the phases of estrogen cycle. The expression of β-hydroxybutyrate (βHB)-related genes and proteins such as monocarboxylate transporters, histone deacetylases (HDAC), and brain-derived neurotrophic factor (BDNF) were significantly regulated. In cerebral cortex and hippocampus, EE resulted in a significant increase in the level of βHB and a significant reduction in HDAC, consequently enhancing BDNF expression. Moreover, EE exerted significant effects on motor and cognitive behaviors, indicating a significant functional improvement in female mice under the condition that asserts the influence of estrogen cycle. Using an ovariectomized mice model, the effects of EE and estrogen treatment proved the hypothesis that EE upregulates β-hydroxybutyrate and BDNF underlying functional improvement in female mice. The above findings demonstrate that long-term exposure to EE can possibly alter metabolism by increasing the level of βHB, regulate the expression of βHB-related proteins, and improve behavioral function as reflected by motor and cognitive presentation following the changes in estrogen level. This finding may lead to a marked improvement in metabolism and neuroplasticity by EE and estrogen level.

Keywords: environmental enrichment (EE), sex, beta-hydroxybutyrate (β-HB), estrogen, female, functional improvement, brain derived neurotrophic factor (BDNF), neuroplasticity

INTRODUCTION

Sex differences in metabolic responses to exercise have been presented in many previous studies (Davis et al., 2000; Kang et al., 2006; Vislocky et al., 2008; Hagobian et al., 2009; Isacco and Miles-Chan, 2018). During a prolonged exercise, females oxidize more lipids and fewer carbohydrate than males oxidize, resulting in greater lipolysis (Tarnopolsky, 2008; Henderson, 2014; Maunder et al., 2018; Allman et al., 2019). These differences are partially due to the higher circulating concentrations of estrogen in females (Gavin et al., 2013; Brockman and Yardley, 2018). Estrogen controls lipolysis in various tissues, and its beneficial effect on whole-body fat reduction has been reported (Pedersen et al., 2004; D'eon et al., 2005; Gavin et al., 2013). At a rate proportional to fat oxidation, ketogenesis occurs mainly in the mitochondria of liver cells (Lopes-Cardozo et al., 1975). It is caused by nutrient-deficient conditions such as caloric restriction (Lin et al., 2015), fasting (Balasse and Fery, 1989; Higashino-Matsui et al., 2012), and prolonged exercise (Phinney, 2004; Hargreaves and Spriet, 2020), which breaks down free fatty acids to produce ketone bodies such as acetoacetate and β-hydroxybutyrate (βHB; Dhillon and Gupta, 2020).

Environmental enrichment (EE) is a method of raising rodents in a huge cage, with novel objects and running wheels, and allowing numerous social interactions (Nithianantharajah and Hannan, 2006). Previous studies have demonstrated that exposure to EE can elicit energetic stress with diverse cellular responses to maintain energy homeostasis (Goodpaster and Sparks, 2017; De Souza et al., 2019; Queen et al., 2020) and modulate systemic metabolism, increase the rate of metabolic processes, and modulate levels of various metabolites (Fery and Balasse, 1983; Mika et al., 2019; Thyfault and Bergouignan, 2020). EE exerts beneficial effects on behaviors and emotions in various rodent models (Matsumori et al., 2006; Nithianantharajah and Hannan, 2006; Madronal et al., 2010) via improvement of brain metabolism (Takimoto and Hamada, 2014; Matsui et al., 2017; Puchalska and Crawford, 2017). Moreover, these beneficial effects of EE are highly influenced by biological sex (Davis et al., 2000; Lin et al., 2011; Kiss et al., 2013; Chamizo et al., 2016).

Under nutritional stress after starvation or exercise, the synthesis and utilization of ketone bodies in hepatic mitochondria through free fatty acid metabolism can produce necessary nutrients to extrahepatic tissues such as the brain (Evans et al., 2017; Puchalska and Crawford, 2017). Endogenous βHB can easily cross the blood-brain barrier (Hasselbalch et al., 1995). However, the permeability of βHB in neuronal cells is dependent on the expression of monocarboxylate transporters (MCTs; Pierre and Pellerin, 2005; Vijay and Morris, 2014), and the permeated βHB is further catalyzed by 3-hydroxybutyrate dehydrogenase as the first stage of βHB oxidation (Evans et al., 2017). Among the endogenous ketone bodies, βHB can act as an epigenetic regulator through the inhibition of histone deacetylases (HDACs) in the brain, which in turn increases the acetylation of histones occupying loci related to brain-derived neurotrophic factor (BDNF). Previous studies have presented similar results that βHB can act as an epigenetic regulator in various cell types (Dabek et al., 2020; Zhang et al., 2020; Ruppert et al., 2021). More specifically, βHB can modulate the expression of BDNF with histone modifications on several locations (Xie et al., 2016; Hu et al., 2020; Mierziak et al., 2021). Mounting evidence suggests that changes in the level of βHB following EE and estrogen may regulate BDNF level in an epigenetic manner.

Although several studies have examined the metabolic and neuronal responses to EE, less attention has been paid to the mechanism underlying the effects of EE on metabolism and its brain function under the influence of estrogen cycle. Therefore, the purpose of this study is to determine whether EE exerts effects on metabolism under the influence of estrogen.

MATERIALS AND METHODS

Ethics Statement and Experimental Animals

All procedures were reviewed and approved by the Association for Assessment and Accreditation of Laboratory Animal Care and the Institutional Animal Care and Use Committee of the Yonsei University Health System (permit number: 2018-0110, 2019-0336, and 2020-0054). All procedures were in accordance with the guidelines of the National Institutes of Health's Guide for the Care and Use of Laboratory Animals. These regulations, notifications, and guidelines originated and were modified from the Animal Protection Law (2008), Laboratory Animal Act (2008), and Eighth Edition of the Guide for the Care and Use of Laboratory Animals (NRC 2011). Mice were provided food and water *ad libitum* under a 12-h light/dark cycle, according to animal protection regulations. They were sacrificed at 8 weeks after the special housing conditions under anesthesia induced by intraperitoneal injection of ketamine (100 mg/kg) and xylazine (10 mg/kg) anesthesia by intraperitoneal injection. All efforts were made to minimize animal suffering.

Experimental Procedures and Cage Condition

At 6 weeks of age, a total of 104 (52 male and 52 female) ICR/CD-1 mice were randomly housed in either standard conditions (SC, $n = 26$ per sex) or an enriched environment (EE, $n = 26$ per sex). Additionally, a total of 70 mice underwent ovariectomy [OVX group, $n = 24$; OVX + Estradiol (E2) group, $n = 15$; OVX + EE group, $n = 14$; and OVX + E2/EE, $n = 17$]. The subcutaneous injection of E2 treatment (5 μg E2/corn oil) was administered every 3–4 days. The treatments (E2 and/or EE) for each group lasted until 14 weeks of age, as previously described (Seo et al., 2018). All mice were fed a normal chow diet, and vaginal cytology was conducted for all female mice immediately before sacrifice, as previously described (Byers et al., 2012).

Dual Energy X-Ray Absorptiometry

Dual Energy X-Ray Absorptiometry (DXA) is a method to assess *in vivo* body composition in humans and animals, and can differentiate between fat and non-fat tissues. DXA was performed at 14 weeks of age to determine the whole-body composition of each group of mice. Each mouse was anesthetized with a mixture

of xylazine and ketamine, transferred, and correctly positioned in the DXA chamber, and bone mineral content, fat, and lean body mass were measured.

Blood Biochemical Testing

All mice went through fasting process for 5–6 h before blood collection. Blood was drawn into BD Microtainer® blood collection tubes (USA). Blood samples were centrifuged for 10 min at 300 g, and serum supernatants were collected and transferred to other tubes. Total protein, total cholesterol, high-density lipoprotein, triglyceride, and lactate dehydrogenase levels were measured using DRI-CHEM 4000i (Fuji).

Indirect Calorimetry

To investigate the effect of EE on metabolism and physiology under the influence of estrogen, a total of 12 mice ($n = 3$ per group) for the normal model and a total of 22 OVX mice (OVX group, $n = 6$, OVX + E2 group, $n = 6$; OVX + EE group, $n = 5$, OVX + E2/EE, $n = 5$) were housed in metabolic automatic cages (Phenomaster, TSE systems) at 14 weeks of age. After 2 days of acclimation, measurements of energy expenditure, respiratory exchange ratio, and core temperature were taken at 9-min intervals for a total of 5 days.

βHB Assay

βHB levels were measured in the blood serum and brain tissue extracts using the βHB assay kit from Sigma-Aldrich (MAK041-1KT) following the manufacturer's instructions. The values were obtained at 1:40 dilution and expressed as pmol/well, unless noted otherwise; each well contained a total volume of 200 μL.

Quantitative Real-Time PCR

Total RNA was prepared in the interested brain tissue lysates using TRIzol reagent (Invitrogen Life Technologies, Carlsbad, CA, USA) according to the manufacturer's instructions. A nanodrop spectrophotometer (Thermo Fisher Scientific, Waltham, MA, USA) was used to confirm the quality and quantity of extracted RNA. Differentially expressed genes of interest from cerebral cortex and hippocampus were selected to validate by Quantitative Real-Time PCR (qRT-PCR). ReverTra Ace® qPCR RT Master Mix with gDNA Remover (Toyobo, Osaka, Japan) was used to synthesize cDNA with total RNA. Then, 2 μl of cDNA in a total volume of 20 μl was used in the following reaction. The qRT-PCR was performed in triplicate on a Light Cycler 480 (Roche Applied Science, Mannheim, Germany) using the Light Cycler 480 SYBR Green master mix (Roche), with thermocycler conditions as follows: amplifications were performed starting with a 300 s template preincubation step at 95°C, followed by 45 cycles at 95°C for 10 s, 60°C for 10 s, and 72°C for 10 s. The melting curve analysis began at 95°C for 5 s, followed by 1 min at 60°C. The specificity of the produced amplification product was confirmed by the examination of a melting curve analysis and showed a distinct single sharp peak with the expected Tm for all samples. A distinct single peak indicates that a single DNA sequence was amplified during qRT-PCR. The detail sequence of the primers is listed in **Supplementary Table 1**. Primers were designed using the NCBI primer blast with the parameters set to a product of 150–200 bp within the region surrounding the identified translocation. The expression of each gene of interest was obtained using the $2^{-\Delta\Delta CT}$ method. The expression level of each gene of interest was obtained using the $2^{-\Delta\Delta CT}$ method. Target-gene expression was normalized relative to the expression of GAPDH and represented as fold change relative to the male control group.

Western Blot

Brain lysates were isolated from cerebral cortex and hippocampus. To assess the protein expression of MCT1, MCT2, MCT4, HDAC1, HDAC2, HDAC3, BDNF in cerebral cortex and hippocampus, total protein was extracted from all mice and dissolved in sample buffer (60 mM Tris–HCl, pH 6.8, 14.4 mM b-mercaptoethanol, 25% glycerol, 2% SDS, and 0.1% bromophenol blue; Invitrogen), incubated for 10 min at 70°C, and separated on a 10% SDS reducing polyacrylamide gel (Invitrogen). Twenty microgram of Protein samples were separated with SDS-polyacrylamide gel electrophoresis (PAGE) on a 4–12% gradient Bis-Tris gel and Tris-Acetate gel (Invitrogen, Carlsbad, CA, USA). The separated proteins were further transferred onto a 0.45 μm Invitrolon™ polyvinylidene difluoride (PVDF) filter paper sandwich using a XCell II™ Blot Module (Invitrogen, Life Technologies, Carlsbad, CA, USA). The membranes were blocked for 1 h in Tris-buffered saline (TBS) (10 mM Tris-HCl, pH 7.5, 150 mM NaCl) plus 0.05% Tween 20 (TBST) containing 5% non-fat dry milk (Bio-Rad, Hercules, CA, USA) at room temperature, washed three times with TBST, and incubated at 4°C overnight with the following primary antibodies; anti-MCT1 (1:500, Abcam), anti-MCT2 (1:200, Santa Cruz), anti-MCT4 (1:200, Santa Cruz), anti-HDAC1 (1:500, Santa Cruz), anti-HDAC2 (1:200, Santa Cruz), anti-HDAC3 (1:1,000, Santa Cruz), anti-BDNF (1:1,000, Abcam), and anti-β-Actin (1:5,000, Abcam). After washing the blots three times with TBST, the blots were incubated for 1 h with horseradish peroxidase-conjugated secondary antibodies (1:5,000; Santa Cruz, CA, USA) at room temperature. The proteins were further washed three times with TBST and visualized with an enhanced chemiluminescence (ECL) detection system (Amersham Pharmacia Biotech, Little Chalfont, UK). Using ImageQuant™ LAS 4000 software (GE Healthcare Life Science, Chicago, IL, USA), western blot results were saved into TIFF image files, and then the images and the density of the band were analyzed and expressed as the ratio relative to the control band density using Multi-Gauge (Fuji Photo Film, version 3.0, Tokyo, Japan). To normalize the values of all samples to account for band intensity, the average band intensity for each mouse group was first calculated. The samples were normalized to the group average of controls, and target protein expressions were normalized relative to the internal expression of β-Actin. The value of the male control group was set to 1 and was divided by the value of each individual mouse.

Immunohistochemistry

The brain tissues were frozen in Surgipath FSC 22 clear frozen section compound (Leica Microsystems) using dry ice and isopentane. The harvested brain tissues were cryosectioned into 16-μm-thick sections along the coronal plane, and

immunohistochemical staining was performed as previously described. Eight weeks after EE, to confirm the endogenous expression of MAP2 (1:400, Abcam), GFAP (1:400, Neuromics), MCT2 (1:400, Santa Cruz), and MCT4 (1:400, Santa Cruz), the brain sections of the cerebral cortex and hippocampus were immunostained. The sections were incubated with Alexa Fluor® 488 goat anti-rabbit (1:400, Invitrogen) and Alexa Fluor® 594 goat anti-mouse (1:400, Invitrogen) secondary antibodies, and then covered with Vectashield® mounting medium with 4C, 6-diamidino-2-phenylindole (Vector, Burlingame, CA, USA). The stained sections were analyzed using an LSM 700 confocal microscope (Zeiss, Gottingen, Germany). The z-stack confocal analysis was used to measure the colocalization of MAP2 with MCT2 and GFAP with MCT4 and to create Maximum Intensity Projection (MIP) and Ortho (2.5D) images for further colocalization clarification.

Behavioral Assessments

Rotarod Test

A rotarod test was used to assess motor coordination and locomotor function. All animals received a pretreatment performance evaluation at 6 weeks of age. For this assessment, mice were placed on a rotarod treadmill [Ugo Basile, Gemonio (VA), Italy], and the latency to fall, which is the length of time that the animals remained on the rolling rod, was measured. Rotarod tests were then performed at a 2-week interval until 14 weeks of age after the commencement of the treatment at an accelerating speed (4–80 rpm) and a constant speed (32, 64 rpm). The latency period was measured twice for each test, and individual tests were terminated at a maximum latency of 300 s.

Y-Maze Test

Y-maze test is to evaluate cognition and short-term spatial memory (Wahl et al., 1992). This test was carried out in an enclosed "Y" shaped maze (Jeung Do B&P). Normal mice tend to visit the arms of the maze one after the other. This behavior is called spontaneous alternation and used to assess short-term spatial memory in a new environment (Wahl et al., 1992). The number of each arm entries, spontaneous alternation, and percent alternation were recorded for 8 min. The percent alternation was calculated as follows: [Number of spontaneous alternation/(Number of total arm entries – 2)] × 100. At the end of each trial the maze was cleaned of urine and feces with 70% ethanol.

Hanging Wire Test

Hanging wire test is designed to assess both limb strength and balance (Manwani et al., 2011). Mice were tested for their ability to hang from a thick metallic wire, which was secured to two vertical stands. To avoid any vibration, the wire was tightly attached to the plastic frame. The wire was secured 35 cm above the bedding cage to prevent falling injury. Each mouse was put on three trials. Latency to fall from the wire was recorded, and the maximum latency period was 300 s.

Open Field Test

Open field test is generally used to evaluate locomotor activity and anxiety behaviors in a novel environment (Kraeuter et al., 2019). Activity monitoring was conducted on a premise of square area measuring 30 × 30.5 × 31 cm^3. The dimension of the premise was divided into 16 sectors. The 4 inner sectors were marked as the center, while the 12 outer sectors were defined as the periphery. Total spent time in the periphery was recorded as an index of anxiety. Mice were placed individually into the periphery of the area and could explore freely for 25 min while being monitored with a video camera. The data were analyzed using the video tracking system Smart Vision 2.5.21 (Panlab, Barcelona, Spain).

Statistical Analysis

Statistical analyses were performed using the Statistical Package for Social Sciences software (version 25.0; IBM Corporation, Armonk, NY, USA). Levene's test was applied for the homogeneity of variance of the data. A two-way analysis of variance (ANOVA) test was used to examine the primary effects (Sex or Period or Housing) and interaction effects (Sex × Housing or Period × Housing), followed by Tukey's *post-hoc* test for comparisons within sex or period and between housing conditions under significant interaction. A two-way repeated measure ANOVA test was used to examine the primary and interaction effects within and between groups (5 × 4 factorial design) for the rotarod test. *Post-hoc* analysis was used to find where the significant differences were, and was identified at $p < 0.01$ using a Bonferroni adjustment as a multiple pairwise comparison. For the comparison of the OVX groups, a one-way ANOVA followed by Tukey's multiple comparison test was used. The data are expressed as the mean ± standard error of the mean (SEM), and all graphical artworks were produced using GraphPad Prism version 9.

RESULTS

EE Induces Metabolic Changes and Fat Reduction

For 8 weeks from 6 weeks of age, normal mice were exposed to either control cages or EE cages (**Supplementary Figure 1A**); the experimental scheme for normal models is shown in **Figures 1A,C,D**, and body weight change is noted in **Figure 1B**. Representative DXA images from each group are shown in **Figure 1E**. In DXA images, red dots indicate fat tissues, blue dots indicate non-fat tissues, and white dots indicate bone tissues. Significant housing effect was observed, indicating that fat reduction occurred after exposure to EE regardless of sex (**Figure 1F**). In blood biochemical analysis, significant gender effect and housing effect were noted in serum triglyceride (TG), indicating that EE mice have lower TG level than control mice regardless of sex, while female mice showed a higher TG level than male mice regardless of housing condition (**Figure 1G**). A significant housing effect in serum total cholesterol (TCHO) was also observed, indicating that exposure to EE can decrease TCHO level regardless of sex (**Figure 1H**). Metabolic cage analysis showed a significant housing effect in the respiratory exchange

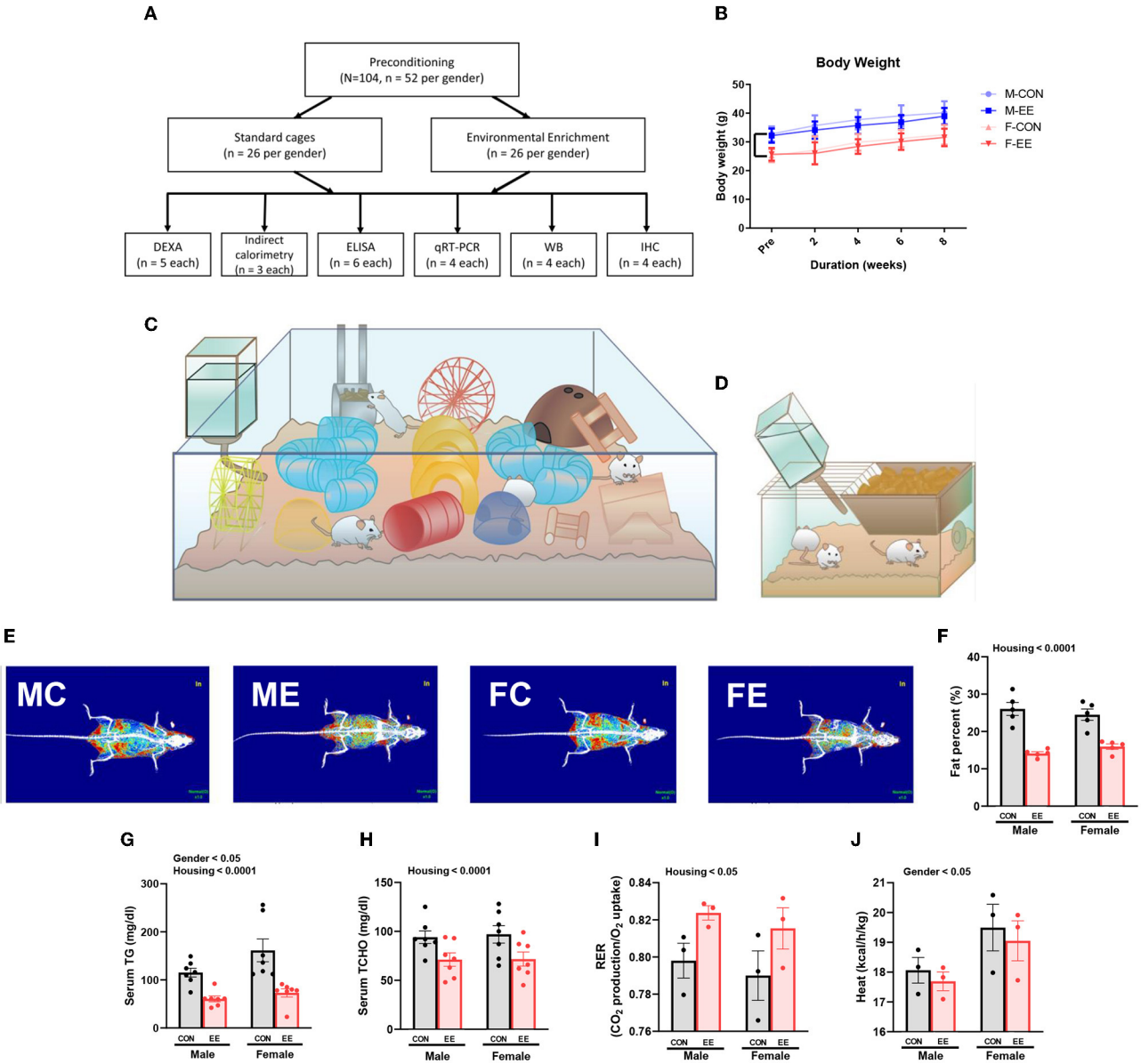

FIGURE 1 | Differential metabolic change by sex sensitivity and exposure to EE in normal models. **(A)** The experimental scheme for normal models. **(B)** Body weight change at 2-week interval ($n = 26$ per group). The representative figures of **(C)** EE cage and **(D)** control cage. **(E)** The representative DXA image of each group. **(F)** Percentage fat in male and female mice exposed to control (CON) or enriched (EE) cages ($n = 5$ per group). After exposure to EE or control cage, blood biochemical analysis ($n = 7$ per group) and indirect calorimetry ($n = 3$ per group) were conducted. **(G)** Serum triglyceride. **(H)** Serum total cholesterol. **(I)** Respiratory exchange ratio. **(J)** Heat. Two-way ANOVA with Tukey multiple comparison test. Significant sex effect, significant housing effect, and the significant interaction between sex and housing were noted with p-value. Data are means ± SEM.

ratio, indicating that EE mice have higher RER ratio than control mice regardless of sex (**Figure 1I**) and significant sex effect on heat, indicating that female mice have higher heat than male mice regardless of housing condition (**Figure 1J**). Collectively, these data imply that female mice have different body composition compared to male mice, and long-term exposure to EE can induce fat reduction and change body composition, with resultant metabolic changes in both sexes of mice.

The Level of βHB Were Influenced by Sex and EE in Normal Mice

βHB enzyme-linked immunosorbent assay (ELISA) analysis indicated significant housing and sex effects on serum βHB levels (**Figure 2A**), indicating that female mice have higher βHB level than male mice regardless of housing, and EE mice have higher βHB level than control mice regardless of sex. Further analysis based on the estrus cycle indicated a trend on the interaction between housing and period ($P =$

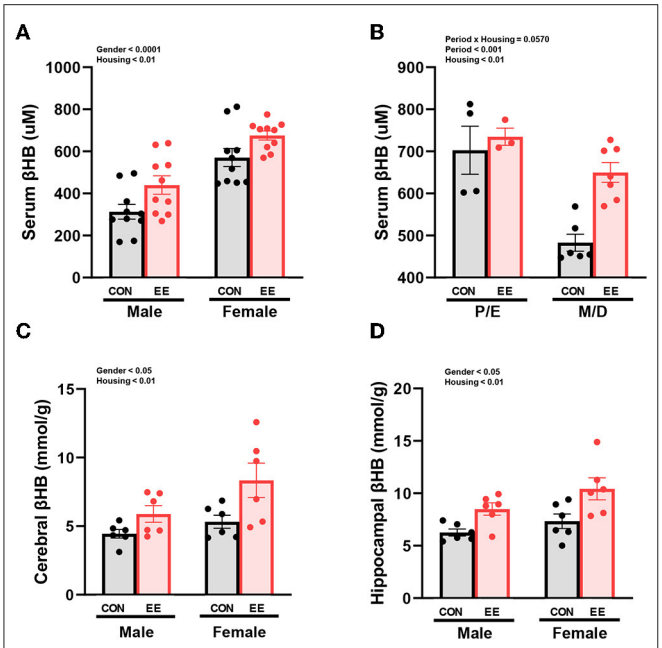

FIGURE 2 | Differential βHB level by sex and exposure to EE in normal models. βHB enzyme-linked immunosorbent assay (ELISA) was conducted in serum (n = 10 per group), cerebral cortex (n = 6 per group), and hippocampus (n = 6 per group). **(A)** Serum βHB levels. **(B)** Further female subgroup analysis based on estrus cycle in serum βHB. **(C)** Cerebral cortex βHB and **(D)** Hippocampus βHB. Two-way ANOVA with Tukey multiple comparison test. Significant sex effect, significant housing effect, and the significant interaction between sex and housing were noted with p-value. Data are means ± SEM.

0.0570). Significant housing effect and period effect on serum βHB levels in female mice were observed, indicating that serum βHB levels in proestrus and estrus (P/E) stage were higher than in metestrus and diestrus (M/D) stage regardless of housing, and EE mice have higher serum βHB levels than control mice regardless of period (**Figure 2B**). The stage of the estrus cycle was determined through vaginal cytology (**Supplementary Figure 1B**). Moreover, significant housing and sex effects were also indicated on βHB levels in the cerebral cortex and hippocampus, respectively (**Figures 2C,D**). This indicates that female mice have higher βHB levels than male mice regardless of housing, and EE mice have higher βHB levels than control mice regardless of sex. These data demonstrate that the baseline level of βHB is different between sexes, and EE can induce metabolic changes and alter body composition. The changes in female mice are due to the influence of the estrus cycle in response to the increased rate of lipolysis.

The Expression of βHB-Related Genes and Proteins Were Influenced by Sex and EE

To examine the expression of βHB-related genes, qRT-PCR was conducted in the cerebral cortex (**Figures 3A1–G1**) and hippocampus (**Figures 3A2–G2**). There was a significant interaction between housing and gender in MCT2 [$F_{(1,44)}$ = 36.18, P = 0.0001], HDAC3 [$F_{(1,44)}$ = 10.96, P = 0.0019], and BDNF [$F_{(1,44)}$ = 20.85, P = 0.0001] in cerebral cortex. Moreover, there was a significant interaction between housing and gender in MCT2 [$F_{(1,44)}$ = 11.38, P = 0.0016], MCT4 [$F_{(1,44)}$ = 8.822, P = 0.0048], HDAC1 [$F_{(1,44)}$ = 42.80, P = 0.0001], HDAC2 [$F_{(1,44)}$ = 5.344, P = 0.0255], and BDNF [$F_{(1,44)}$ = 29.65, P = 0.0001] in hippocampus. Significant housing effects and sex effects are noted in the figures. Western blotting was conducted to examine the expression of βHB-related proteins in cerebral cortex (**Figures 4A1–H1**) and hippocampus (**Figures 4A2–H2**), and representative images are shown in **Figures 4A1,A2**, respectively. Significant housing or sex effect was noted in βHB-related proteins. Collectively, these data indicate that the expression of βHB-related genes and proteins was significantly regulated by EE and sex. In cerebral cortex and hippocampus, EE led to a significant increase in the level of βHB and a significant reduction in the level of HDAC, which consequently enhanced BDNF expression under the influence of sex.

EE Induces Higher βHB Uptake of the Brain by Both Astrocytes and Neurons

To examine the uptake of βHB in cerebral cortex and hippocampus, histological assessments with GFAP, MCT4, MAP-2, and MCT2 were conducted. The representative images of GFAP and MCT4 in the cerebral cortex and hippocampus are shown in **Figures 5A1,A2**, respectively. The representative images of MAP-2 and MCT2 in the cerebral cortex and hippocampus are shown in **Figures 5B1,B2**, respectively. Significant sex and housing effect were noted both in the colocalization of GFAP and MCT4 in cerebral cortex (**Figure 5C1**) and the colocalization of MAP2 and MCT2 in hippocampus (**Figure 5D1**), indicating that female mice have the higher colocalization than male mice regardless of housing, and EE mice have the higher colocalization than control mice regardless of sex. Significant housing effect was noted in the colocalization of GFAP and MCT4 in cerebral cortex (**Figure 5C2**) and in the colocalization of MAP2 and MCT2 in hippocampus (**Figure 5D2**), implying that EE mice have higher colocalization than control mice regardless of sex. Raw intensity of GFAP and MAP2 for cerebral cortex and hippocampus are shown in **Figures 5E1,F1,E2,F2**. Significant housing effect was observed in raw MAP2 expression, demonstrating that EE mice showed a higher expression of MAP2 than control mice regardless of sex in cerebral cortex and hippocampus. Significant gender effect was observed in raw GFAP expression, indicating that female mice showed higher expression of GFAP than male mice regardless of housing in hippocampus. These combined data indicate that long-term exposure to EE can induce the higher βHB uptake as indicated by the higher colocalization rate in cerebral cortex and hippocampus by astrocytes and neurons.

EE Improves the Motor and Cognitive Functions in Normal Mice

To examine motor and cognitive function of normal mice, rotarod test and Y-maze test were conducted. In rotarod test, female EE mice significantly outperformed the other groups of

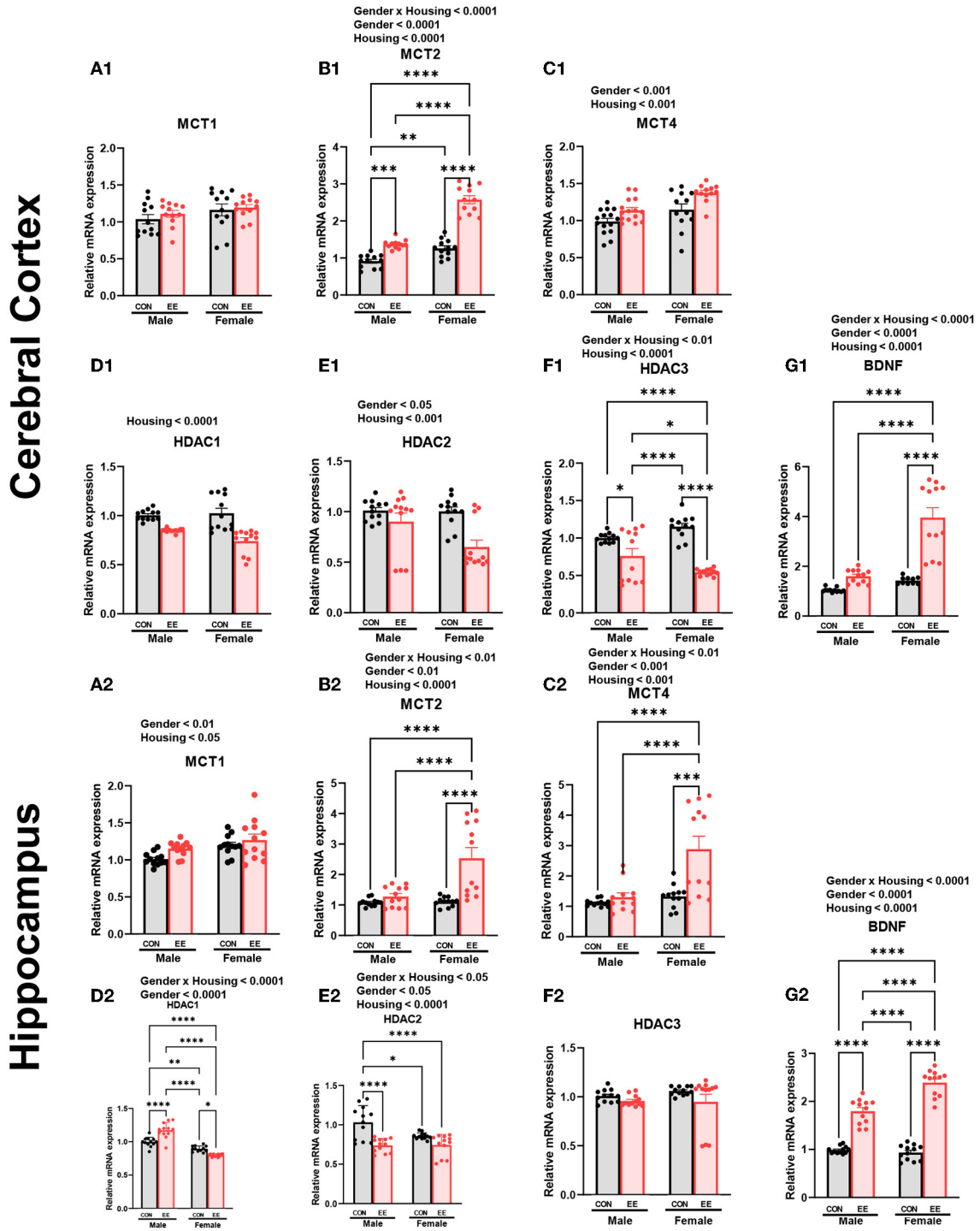

FIGURE 3 | Effects of EE on the expression of βHB-related genes under the influence of estrogen by qRT-PCR. **(A1–G1)** Cerebral cortex and **(A2–G2)** hippocampus mRNA levels for βHB-related genes measured using qRT-PCR ($n = 4$ per group). All samples were run in triplicate. Two-way ANOVA with Tukey multiple comparison test. Significant sex effect, significant housing effect, and the significant interaction between sex and housing were noted with p-value. Data are means ± SEM. $^{*}p < 0.05$, $^{**}p < 0.01$, $^{***}p < 0.001$, and $^{****}p < 0.0001$.

mice at accelerating speed 4–80 rpm (**Figure 6A**), constant 48 rpm (**Figure 6B**), and constant 64 rpm (**Figure 6C**). Specifically, rotarod performance was significantly improved in EE mice from 2 to 8 weeks after EE treatment. In Y-maze test, significant housing effect was observed in the number of alterative behaviors (**Figure 6D**) and the number of entries (**Figure 6E**),

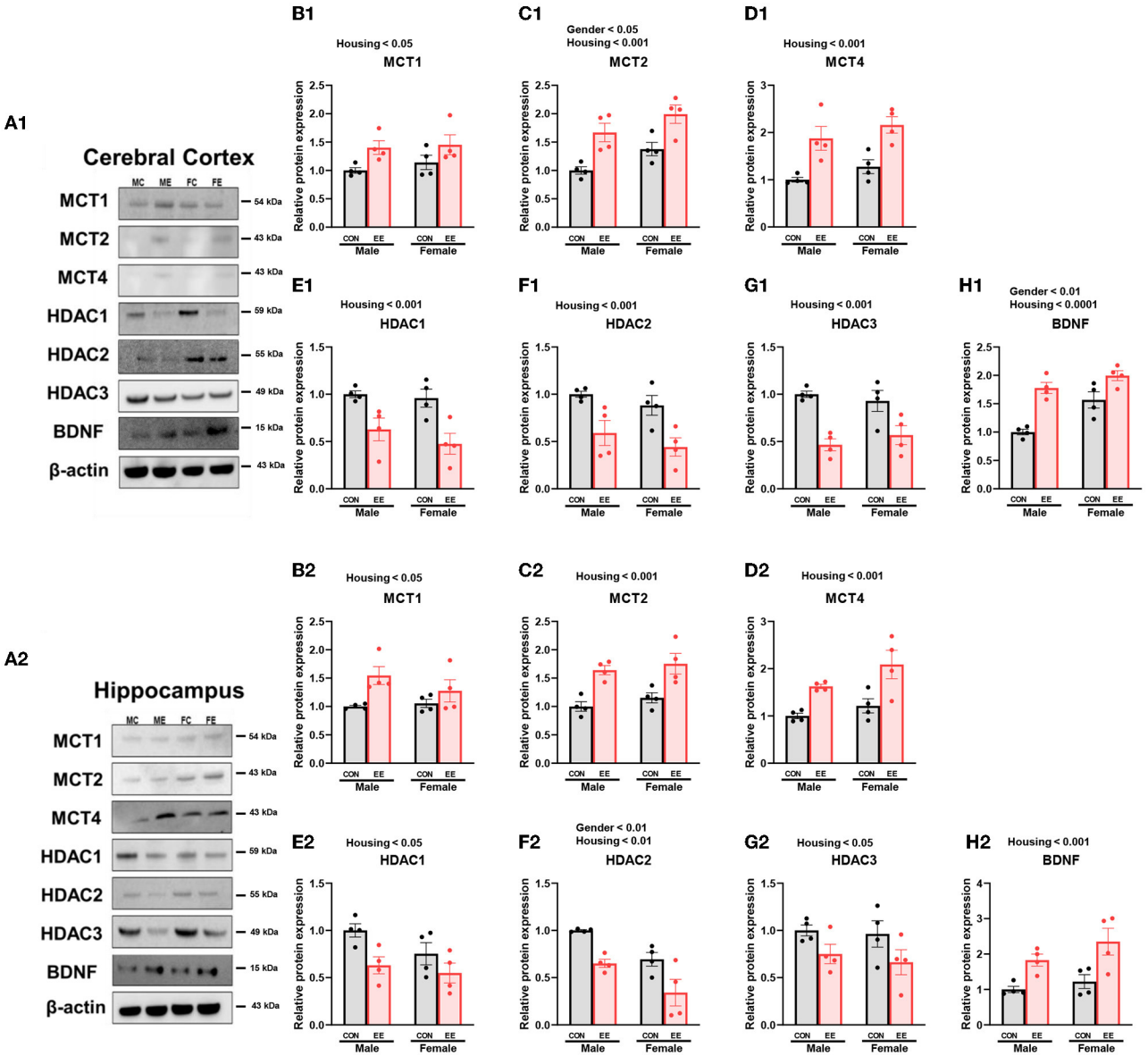

FIGURE 4 | Effects of EE on the expression of βHB-related proteins under the influence of estrogen by western blot. **(A1–H1)** Cerebral cortex and **(A2–H2)** hippocampus protein levels for βHB-related proteins measured using western blot ($n = 4$ per group). Two-way ANOVA with Tukey multiple comparison test. Significant sex effect, significant housing effect, and the significant interaction between sex and housing were noted with p-value. Data represented are means ± SEM.

demonstrating that the raw number of alternation and total entries were significantly decreased in EE mice compared to control mice regardless of gender. Significant housing effect was observed in the percentage of alternation, indicating that EE mice have higher percentage of alternation than control mice regardless of gender (**Figure 6F**). These data indicated that exposure to EE improves cognitive function. These combined data indicate that long-term exposure to EE improves motor and cognitive function.

EE and Estrogen Treatment Can Induce Lipolysis and Metabolic Changes in OVX Mice

To produce an estrogen-deficient model, OVX was conducted at 6 weeks of age (**Supplementary Figure 1C**), and the experimental scheme for OVX models is shown in **Figure 7A**. Body weight measurement for OVX group, OVX + E2 group, OVX + EE group, and OVX + E2/EE group is noted in **Figure 7B**, and the body weight was significantly decreased by

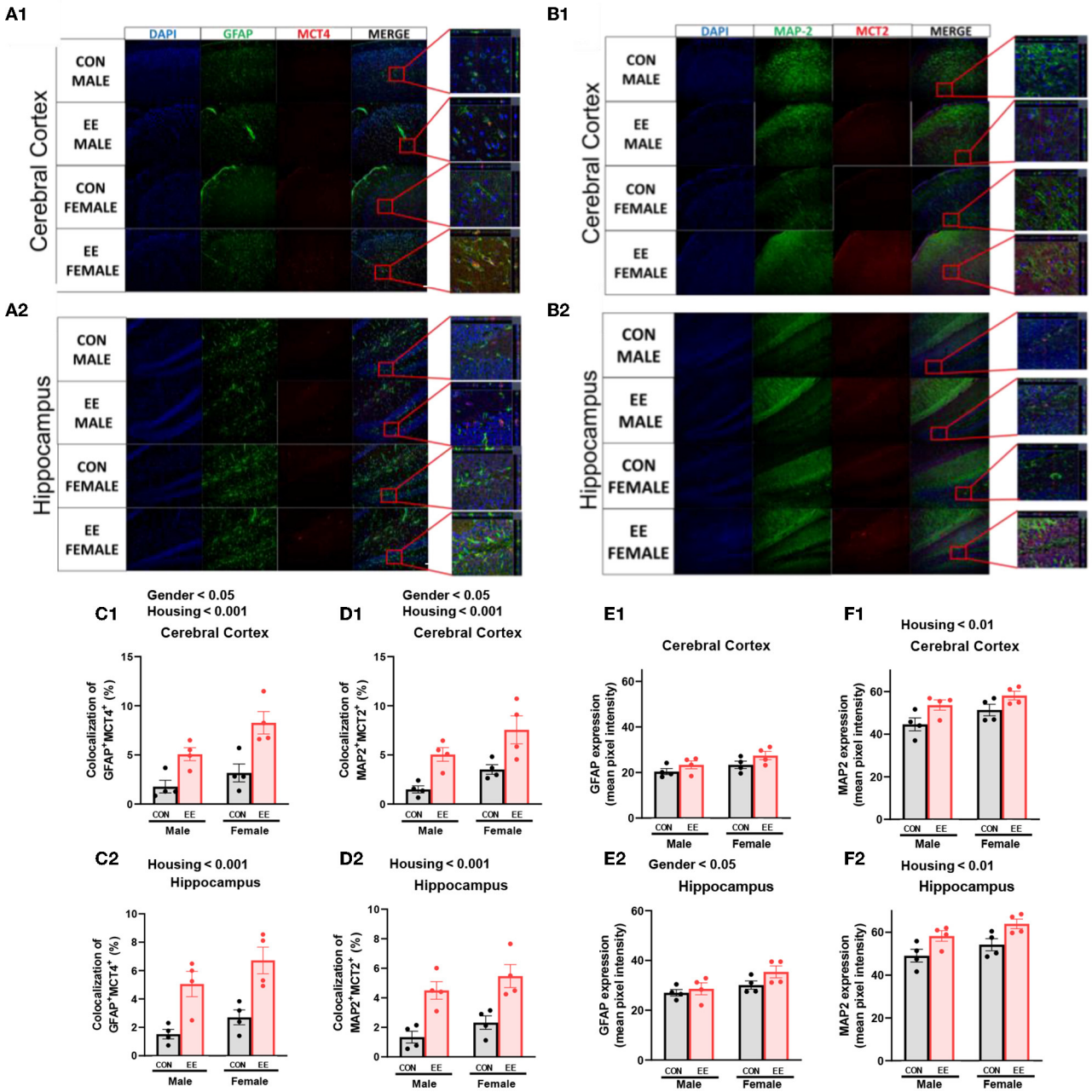

FIGURE 5 | Effects of EE on the uptake of βHB in cerebral cortex and hippocampus under the influence of estrogen. Representative IHC images of **(A1,A2)** $GFAP^+MCT4^+$ in cerebral cortex and hippocampus and **(B1,B2)** $MAP2^+MCT2^+$ in the cerebral cortex and hippocampus ($n = 4$ per group). **(C1–F1)** Quantification of $GFAP^+MCT4^+$ and $MAP2^+MCT2^+$ in the cerebral cortex and hippocampus. **(C2–F2)** Raw intensity of GFAP and MAP2 in cerebral cortex and hippocampus. Two-way ANOVA with Tukey multiple comparison test. Significant sex effect, significant housing effect, and the significant interaction between sex and housing were noted with *p*-value. Data are means ± SEM.

exposure to EE and the synergistic effect of EE and E2. The level of 17β-estradiol was significantly increased by estrogen treatment and exposure to EE (**Figure 7C**). The representative DEXA images from each group are shown in **Figure 7D**, and significant fat reduction following estrogen treatment and exposure to EE was observed (**Figure 7E**). Moreover, in blood biochemical analysis, the synergistic effect of estrogen and exposure to EE was observed in serum TG (**Figure 7F**), decreasing the level of TG compared to OVX group but not in serum TCHO (**Figure 7G**). In indirect calorimetry, exposure to EE and estrogen treatment significantly increase RER (**Figure 7H**) and heat (**Figure 7I**) in OVX mice, indicating that both treatments can change body composition and induce metabolic changes. Collectively, exposure to EE and estrogen treatment can synergistically increase lipolysis, alter body composition, and metabolic changes in OVX mice.

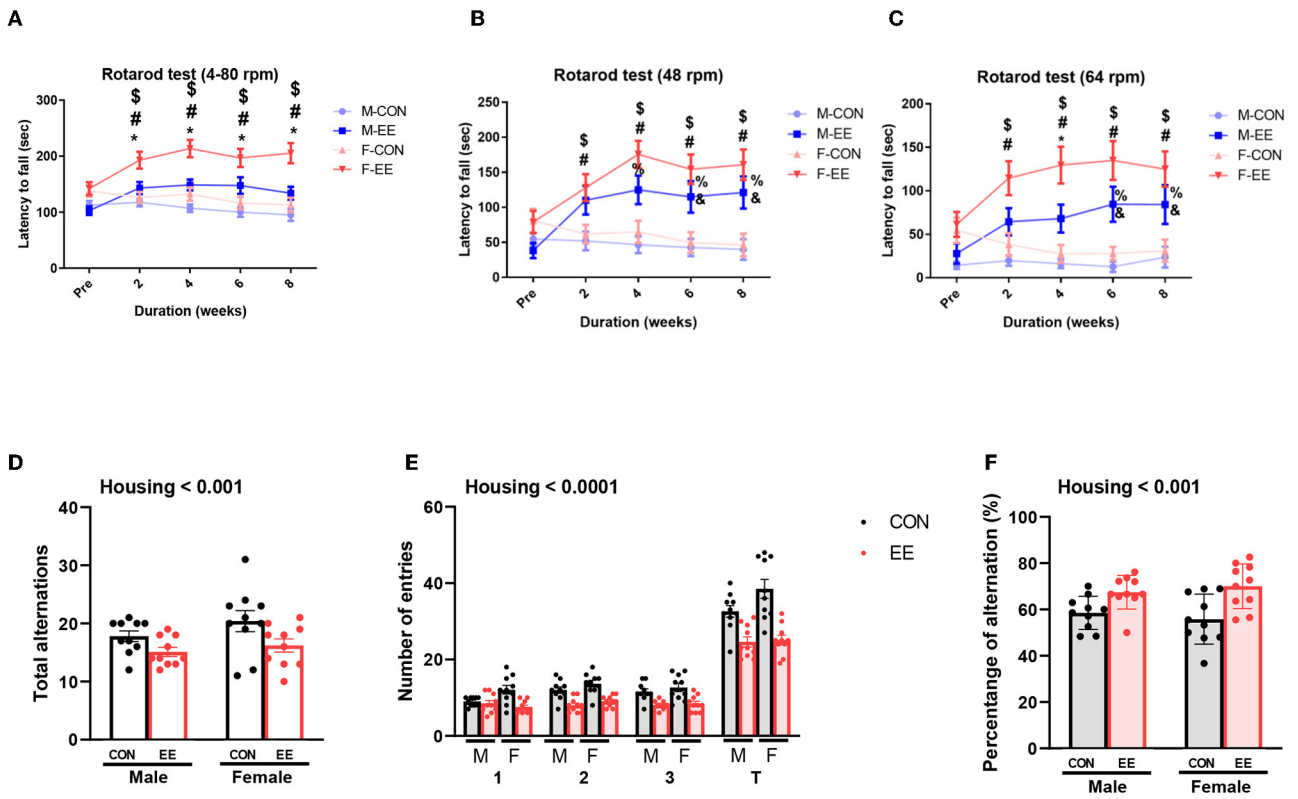

FIGURE 6 | Effects of EE on functional improvement in normal models. Behavioral test assessments conducted for the normal groups. **(A)** Rotarod accelerating from 4 to 80 rpm. **(B)** Rotarod at constant 48 rpm. **(C)** Rotarod at constant 64 rpm ($n = 26$ per group). *F-EE vs. M-EE, $^{\#}$F-EE vs. F-CON, $^{\$}$F-EE vs. M-CON, $^{\%}$M-EE vs. M-CON, and $^{\&}$M-EE vs. F-CON. **(D)** Number of alternative behaviors, **(E)** number of entries, and **(F)** percent alternation of Y-maze test ($n = 10$ per group). Two-way ANOVA with Tukey multiple comparison test. Significant sex effect, significant housing effect, and the significant interaction between sex and housing were noted with p-value. Data represented are means ± SEM. $^{*}p < 0.01$, $^{\#}p < 0.01$, $^{\$}p < 0.01$, $^{\%}p < 0.01$, and $^{\&}p < 0.01$.

EE and Estrogen Treatment Can Reduce Abnormal Lipid Accumulation in Liver and Various Brain Regions in OVX Mice

To examine lipid accumulation in the liver and various brain regions of OVX mice, Oil Red O (ORO) staining, and H&E staining were conducted. The representative images of ORO-stained livers for each group are shown in **Figure 8A**, and the abnormal lipid accumulation was significantly decreased by the synergistic effect of EE and estrogen treatment ($P = 0.0194$, **Figure 8B**). Moreover, hepatic steatosis was observed in the OVX group and was diminished by exposure to EE and/or estrogen treatment (**Figure 8C**). The representative images of ORO-stained cerebral cortex, pia-mater, and subventricular zone (SVZ) are shown in **Figures 8D–F**, respectively. The quantification of ORO-stained cerebral cortex, pia-mater, and SVZ are shown in **Figures 8G–I**. Exposure to EE and estrogen treatment significantly reduced the abnormal accumulation of lipid droplets in cerebral cortex and SVZ. These data indicate that exposure to EE and estrogen treatment can induce lipolysis and reduce abnormal lipid accumulation in the liver and various brain regions.

EE and Estrogen Treatment Can Increase the Level of βHB in OVX Mice

βHB ELISA analysis indicated a significant increase in serum βHB after estrogen treatment and exposure to EE (**Figure 9A**). The synergistic effect of estrogen and EE was observed on the βHB level in the cerebral cortex and hippocampus (**Figures 9B,C**). In response to the increased rate of lipolysis, the level of βHB was significantly increased by EE and estrogen treatment in serum and the brain regions. Particularly, in female mice with EE and estrogen treatment, the level of βHB in cerebral cortex was significantly increased compared with OVX mice ($P = 0.0319$, **Figure 9B**), and the level of hippocampal βHB was significantly increased compared with OVX mice ($P = 0.0014$, **Figure 9C**).

EE and Estrogen Treatment Exerts Synergistic Effects on the Expression of βHB-Related Genes and Proteins in OVX Mice

To examine the expression of βHB-related genes, qRT-PCR was conducted in the cerebral cortex (**Figures 10A1–G1**) and hippocampus (**Figures 10A2–G2**). The significantly synergistic

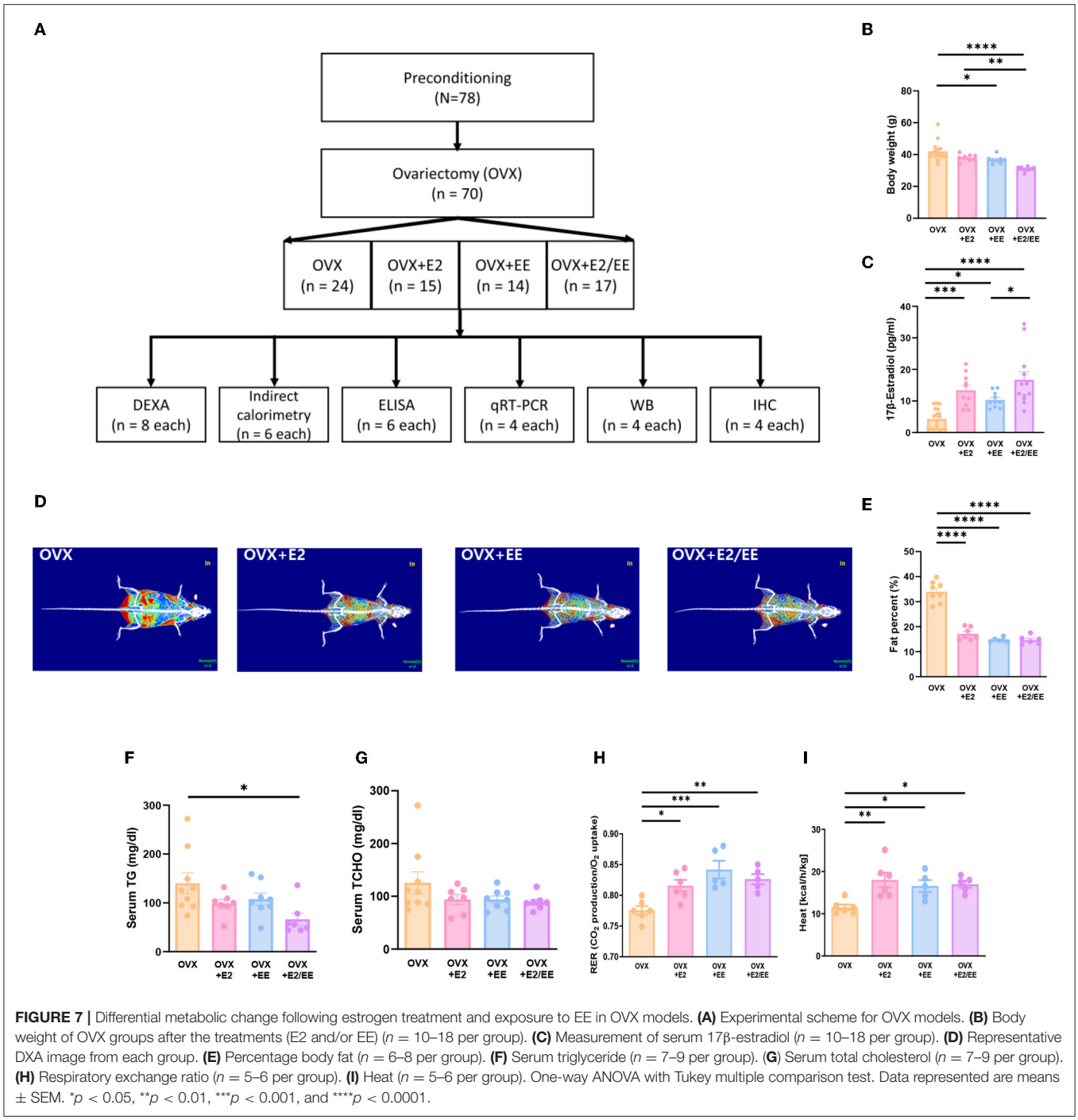

FIGURE 7 | Differential metabolic change following estrogen treatment and exposure to EE in OVX models. **(A)** Experimental scheme for OVX models. **(B)** Body weight of OVX groups after the treatments (E2 and/or EE) (n = 10–18 per group). **(C)** Measurement of serum 17β-estradiol (n = 10–18 per group). **(D)** Representative DXA image from each group. **(E)** Percentage body fat (n = 6–8 per group). **(F)** Serum triglyceride (n = 7–9 per group). (**G**) Serum total cholesterol (n = 7–9 per group). **(H)** Respiratory exchange ratio (n = 5–6 per group). **(I)** Heat (n = 5–6 per group). One-way ANOVA with Tukey multiple comparison test. Data represented are means ± SEM. $^{*}p < 0.05$, $^{**}p < 0.01$, $^{***}p < 0.001$, and $^{****}p < 0.0001$.

effect of EE and estrogen treatment was noted in MCT2, MCT4, HDAC1, HDAC2, HDAC3, and BDNF in both cerebral cortex and hippocampus. To examine the expression of βHB-related proteins, western blotting was conducted. The representative western blot images of βHB-related proteins in cerebral cortex and hippocampus are shown in **Figures 11A1,A2**, respectively. The significantly synergistic effect of EE and estrogen treatment was noted in MCT2, MCT4, HDAC2, HDAC3, and BDNF in cerebral cortex (**Figures 11B1–H1**). Moreover, the significantly synergistic effect of EE and estrogen treatment was noted in MCT2, MCT4, HDAC1, HDAC2, HDAC3, and BDNF in hippocampus (**Figures 11B2–H2**). Collectively, these data indicate that the expression of βHB-related genes and proteins was significantly regulated by exposure to EE and estrogen treatment. Particularly, the expressions of BDNF genes and proteins were significantly enhanced in

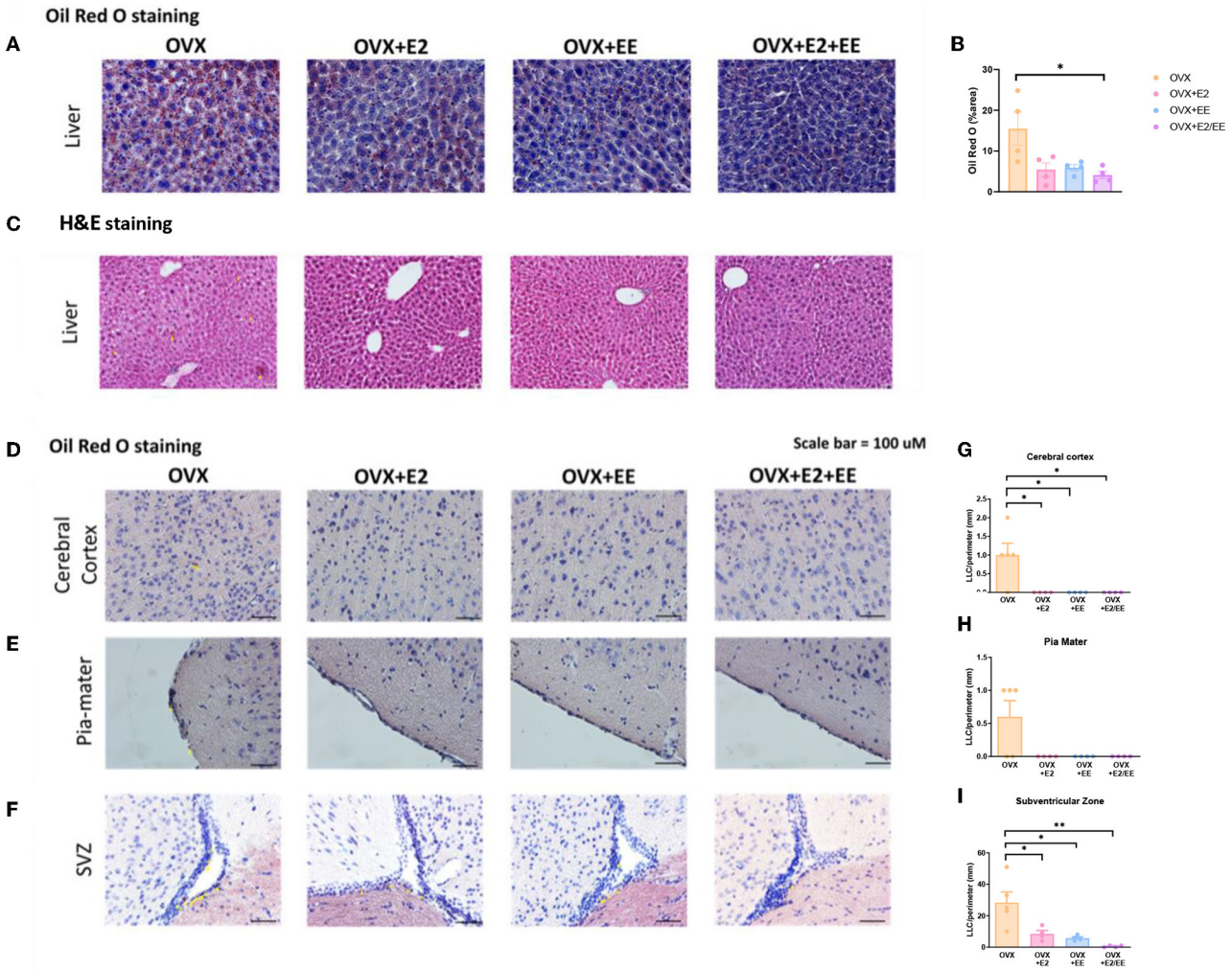

FIGURE 8 | Abnormal lipid accumulation was alleviated by exposure to EE and estrogen treatment in OVX mice. **(A)** The representative images of ORO-stained liver of the OVX groups, and **(B)** quantification thereof. **(C)** The representative images of H&E-stained liver of the OVX groups. The representative images of ORO-stained **(D)** cerebral cortex, **(E)** pia-mater, and **(F)** SVZ, and **(G–I)** quantification thereof, respectively ($n = 4$ per group). One-way ANOVA with Tukey multiple comparison test. Data represented are means ± SEM. $^{*}p < 0.05$ and $^{**}p < 0.01$. White bars = 50 μm.

the cerebral cortex ($P = 0.0004$, **Figure 10G1**; $P = 0.0342$, **Figure 11H1**) and hippocampus ($P < 0.0001$, **Figure 10G2**; $P = 0.0025$, **Figure 11H2**) of the female mice.

EE and Estrogen Treatment Exerts Synergistic Effects on βHB Uptake of the Brain by Both Astrocytes and Neurons in OVX Mice

To examine the uptake of βHB in cerebral cortex and hippocampus, histological assessments with GFAP, MCT4, MAP-2, and MCT2 were conducted. The representative images of GFAP and MCT4 in the cerebral cortex and hippocampus are shown in **Figures 12A1,A2**, respectively. The representative images of MAP-2 and MCT2 in the cerebral cortex and hippocampus are shown in **Figures 12B1,B2**, respectively. The colocalization percent of GFAP with MCT4 ($P < 0.0001$, **Figure 12C1**) and MAP2 with MCT2 ($P < 0.0001$, **Figure 12D1**) in the cerebral cortex was significantly increased in OVX+E2/EE group compared to OVX group. In similar fashion, the colocalization percent of GFAP with MCT4 ($P = 0.0012$, **Figure 12C2**) and MAP2 with MCT2 ($P < 0.0001$, **Figure 12D2**) in the hippocampus was significantly increased in OVX + E2/EE group compared to OVX group (**Figures 12C2,D2**). Raw intensity of GFAP and MAP2 for cerebral cortex and hippocampus are shown in **Figures 12E1,F1,E2,F2**. These combined data indicate that long-term exposure to EE and estrogen treatment can synergistically induce the higher βHB uptake in cerebral cortex and hippocampus by astrocytes and neurons in OVX mice.

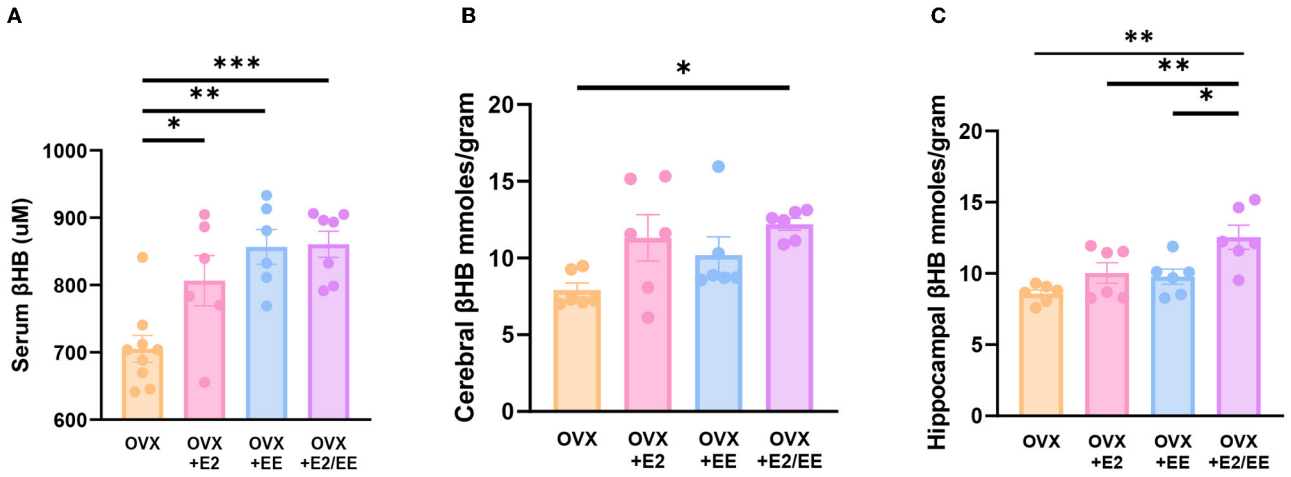

FIGURE 9 | Exposure to EE and estrogen treatment can increase the level of βHB in OVX mice. **(A)** Serum βHB ($n = 6$–9 per group). **(B)** Cerebral cortex βHB ($n = 6$ per group). **(C)** Hippocampus βHB ($n = 6$ per group). One-way ANOVA with Tukey multiple comparison test. Data represented are means ± SEM. $^{*}p < 0.05$, $^{**}p < 0.01$, and $^{***}p < 0.001$.

EE and Estrogen Treatment Synergistically Improve Motor, Emotional, and Cognitive Functions in OVX Mice

To examine motor, emotional, and cognitive function of OVX mice, hanging wire test, open-field test, and Y-maze test were conducted. Significant improvement in motor function following estrogen treatment and exposure to EE was observed in the hanging wire test ($P < 0.0001$, **Figure 13A**). Moreover, a significant reduction in anxiety level ($P = 0.0036$, **Figure 13B**) and cognitive improvement ($P = 0.0001$, **Figure 13E**) were observed in OVX mice after treatment with estrogen and EE. Raw number of alternative behaviors and number of entries in Y-maze are shown in **Figures 13C,D**, respectively. Using an OVX model, these data indicate that EE and estrogen treatment synergistically regulate the expression of βHB-related genes and proteins, thereby improving motor, cognitive, and emotional functions in female mice.

DISCUSSION

EE intervention is a non-invasive strategy for improving metabolic and brain function (Briones et al., 2013; Seo et al., 2018; De Souza et al., 2019; Queen et al., 2020). However, despite its therapeutic potential, many previous studies have reported that a large amount of variation exists in the effects of EE by sex, sex-related differences are observed in metabolic pathways, especially lipid metabolism, under nutrient stress (Mittendorfer et al., 2001; Soeters et al., 2007). Since females generally have more body fat than males do, females have a propensity for the increased oxidation of adiposity, and have more enzymes responsible for β-oxidation (Blaak, 2001; Maher et al., 2010). Since estrogen and exposure to EE are two of the most significant lipolysis factors that influence body composition and metabolism, it is important to consider the interrelated interactions of these factors.

In this study, we investigated metabolic responses after the long-term exposure to EE based on sex. DXA and blood biochemical analyses of fat content indicated that fat reduction occurred after the long-term exposure to EE regardless of sex. Analyses of indirect calorimetry indicated that exposure to EE and estrogen levels can change body composition, consistent with previous studies demonstrating young females have overall higher core temperature than males, which is also influenced by estrogen levels (Heled et al., 2001; Kaciuba-Uscilko and Grucza, 2001; Sanchez-Alavez et al., 2011). Previous results also showed that long-term exposure to EE or prolonged exercise can reduce the fat content in the whole body (Cao et al., 2011; Swift et al., 2014). Although the exact mechanism of EE-induced fat reduction is not clear, enhanced fat oxidation and improved glucose tolerance are responsible for the underlying mechanism (Goodpaster et al., 2003; Solomon et al., 2008). In the estrogen-deficient model, abnormal fat accumulation was observed in liver and brain regions (**Supplementary Figures 2A,B**). This accumulation was significantly alleviated by estrogen and EE exposure.

In response to the fat reduction in both models, the level of βHB was significantly upregulated in both the serum and brain regions by estrogen and EE exposure in this study. Moreover, the expression of βHB-related genes and proteins was significantly modulated by estrogen levels and exposure to EE. This alteration may induce behavioral improvements in motor, cognitive, and emotional functions.

It is important to note that young females utilize larger amounts of fatty acids to produce ketone bodies than their male counterparts under nutritional stress (Marinou et al., 2011; Ballestri et al., 2017). Moreover, in rodent model studies, there were sex-specific and strain-specific effects of calorie restriction on circulating βHB (Mitchell et al., 2016). Our result indicated that circulating βHB concentrations were

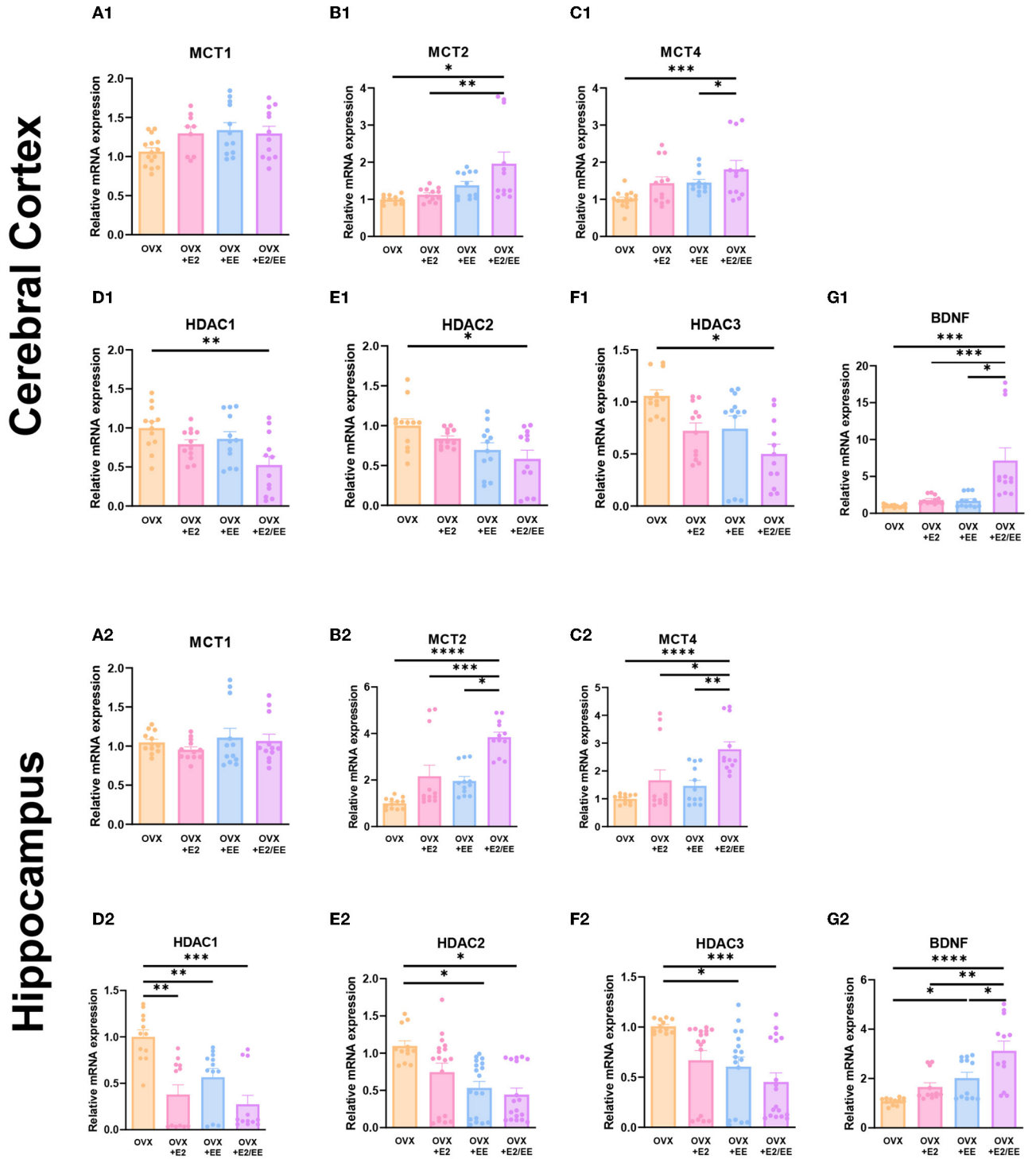

FIGURE 10 | Synergistic effects of estrogen and EE on the expression of ketone-related genes by qRT-PCR. **(A1–G1)** Cerebral cortex and **(A2–G2)** hippocampus mRNA levels for βHB-related genes measured using qRT-PCR ($n = 4$ per group). All samples were run in triplicate. One-way ANOVA with Tukey multiple comparison test. Data represented are means ± SEM. *$p < 0.05$, **$p < 0.01$, ***$p < 0.001$, and ****$p < 0.0001$.

higher in females than in males, regardless of the housing conditions. Interestingly, further subgroup analysis based on estrus cycle in the female group indicated that significantly higher circulating βHB levels following EE exposure at the D/M stage was observed compared to that in female control mice at the D/M stage. Previous studies have shown that

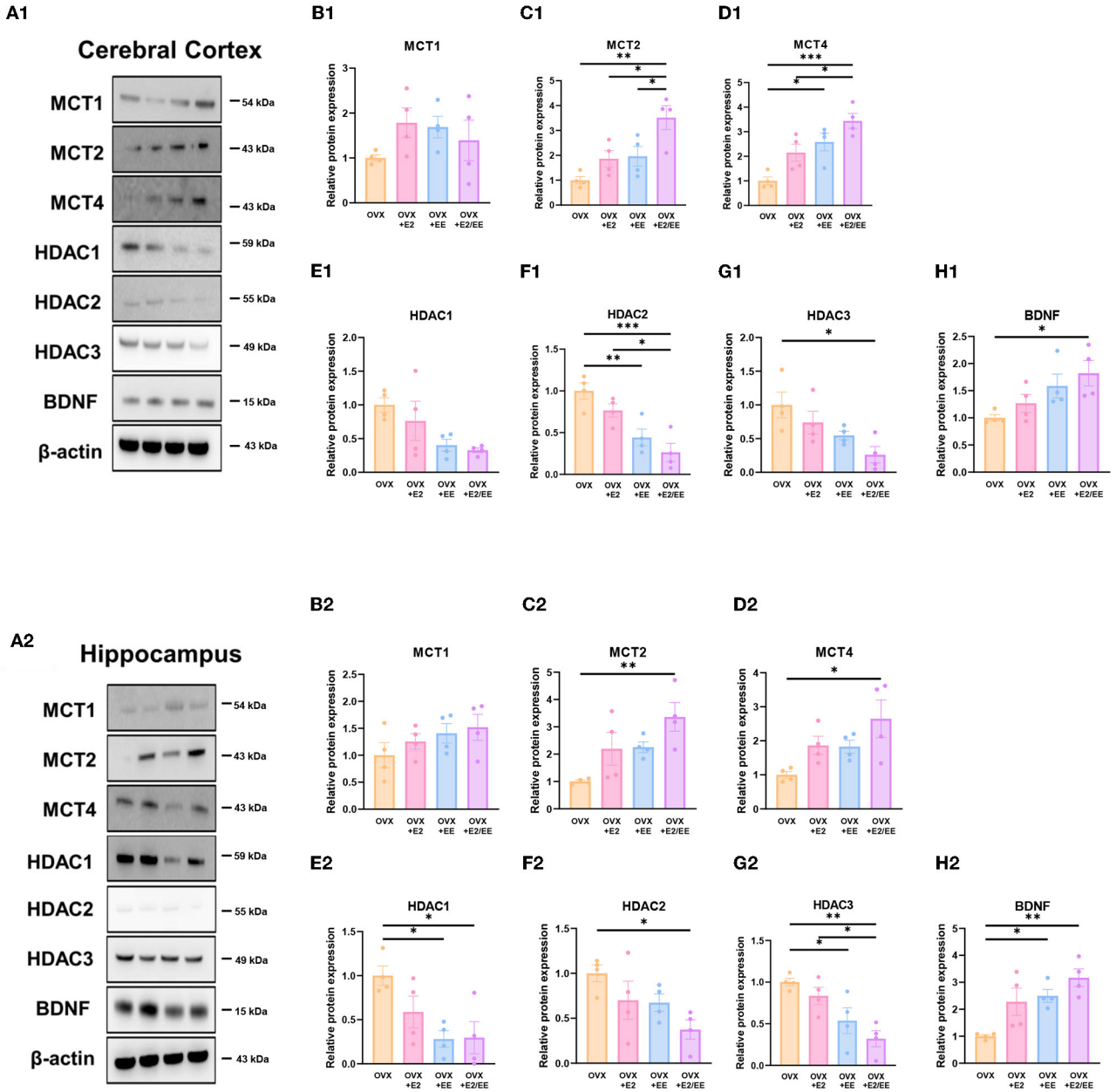

FIGURE 11 | Synergistic effects of estrogen and EE on the expression of ketone-related proteins by western blot. **(A1–H1)** Cerebral cortex and **(A2–H2)** hippocampus protein levels for βHB-related proteins measured using western blot ($n = 4$ per group). One-way ANOVA with Tukey multiple comparison test. Data represented are means ± SEM. $^{*}p < 0.05$, $^{**}p < 0.01$, and $^{***}p < 0.001$.

estrogen levels are closely associated with mitochondrial β-oxidation of fatty acids (Oliveira et al., 2018), and estrogen regulates the level of histone acetylation associated with memory consolidation and increases BDNF promoter acetylation (Fortress et al., 2014). These combined results may suggest the synergistic effect of estrogen and exposure to EE on the utilization of βHB and BDNF, contributing to the effects of EE on metabolism and brain function under the influence of estrogen.

MCTs are solute carrier transporters of alternative metabolites, such as lactate, pyruvate, and ketone bodies (Vijay and Morris, 2014). MCTs are responsible for brain energy metabolism, and three MCT isoforms have been identified in the brain: MCT1, MCT2, and MCT4. MCT1, MCT2 and MCT4 show prominent expression in brain endothelial cells, neurons, and astrocytes, respectively (Pierre and Pellerin, 2005). The expression of these transporters is detectable in varying amounts in the cerebral cortex and

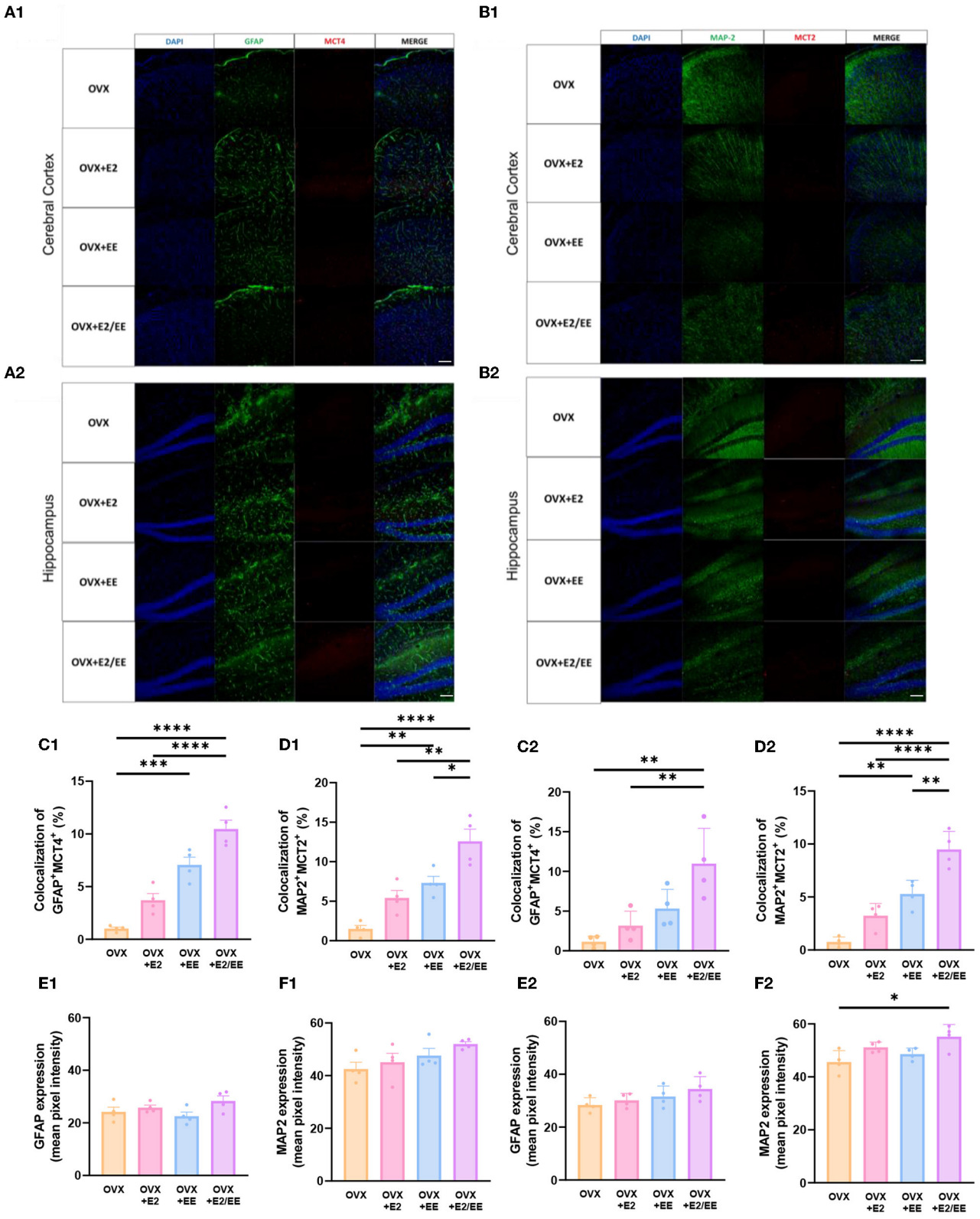

FIGURE 12 | Synergistic effects of estrogen and EE on the uptake of βHB in cerebral cortex and hippocampus. Representative IHC images of **(A1,A2)** $GFAP^+MCT4^+$ in cerebral cortex and hippocampus and **(B1,B2)** $MAP2^+MCT2^+$ in the cerebral cortex and hippocampus ($n = 4$ per group). **(C1–F1)** Quantification of $GFAP^+MCT4^+$ and $MAP2^+MCT2^+$ in the cerebral cortex and hippocampus. **(C2–F2)** Raw intensity of GFAP and MAP2 in cerebral cortex and hippocampus. One-way ANOVA with Tukey multiple comparison test. Data represented are means ± SEM. $^*p < 0.05$, $^{**}p < 0.01$, $^{***}p < 0.001$, and $^{****}p < 0.0001$. A white bar = 50 μm.

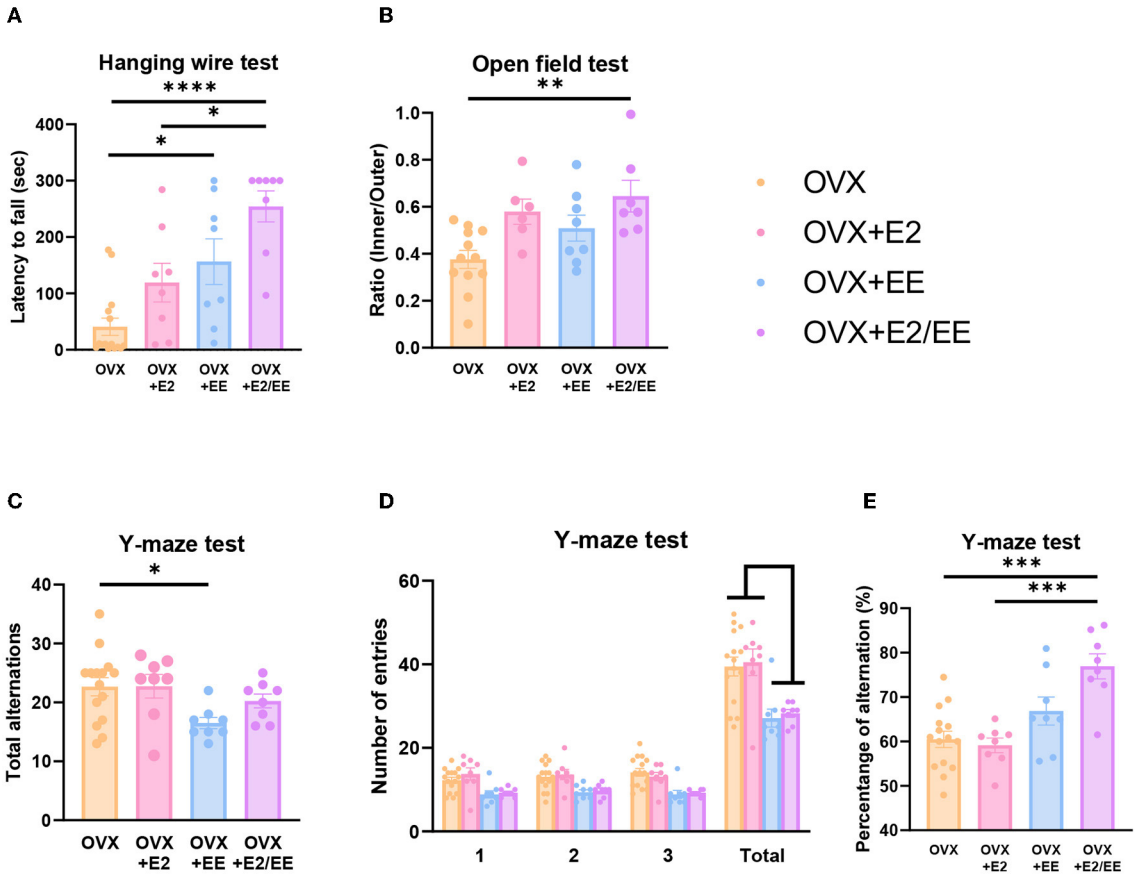

FIGURE 13 | Synergistic effects of estrogen and EE on functional improvement in OVX models. Behavioral test assessments conducted in the OVX groups. **(A)** Hanging wire test, hippocampus ($n = 8$–15 per group). **(B)** Open field test ($n = 6$–12 per group). **(C)** Number of alternative behaviors, **(D)** number of entries, and **(E)** percent alternation of Y-maze test (8–15 per group). One-way ANOVA with Tukey multiple comparison test. Data represented are means ± SEM. $^{*}p < 0.05$, $^{**}p < 0.01$, $^{***}p < 0.001$, and $^{****}p < 0.0001$.

hippocampus (Halestrap, 2012; Halestrap and Wilson, 2012). In this study, the higher colocalization of $MCT2^{+}MAP2^{+}$ and $MCT4^{+}GFAP^{+}$ was observed with exposure to EE and estrogen, and the higher magnification of these images is presented in **Supplementary Figure 2B**. Previous studies have shown a close interrelationship among the levels of βHB, MCTs, HDACs, and BDNF (Robinet and Pellerin, 2011; Halestrap and Wilson, 2012; Takimoto and Hamada, 2014; Sleiman et al., 2016; Achanta and Rae, 2017; Puchalska and Crawford, 2017; Li et al., 2020). Our qRT-PCR and western blotting analyses indicated the synergistic effects of estrogen and EE on the expression of MCT2 and MCT4. Similarly, the expression of HDAC1, 2, and 3 was significantly lower, and the expression of BDNF was significantly higher. The physiological significance of MCT2 and MCT4 on brain energy metabolism and neuroplasticity has been noted in the murine model (Pierre et al., 2002; Pellerin et al., 2005). The inhibition of MCT2 can impair long-term memory, and MCT4 knockout can kill various cancer cells (Newman et al., 2011; Benjamin et al., 2018; Fang et al., 2022).

An estrogen deficient model can be created using ovariectomy (Yokose et al., 1996). Estrogen-deficiency can induce spatial memory impairment, anxious, and depressive behaviors (Lagunas et al., 2010; Djiogue et al., 2018). Short-term estrogen treatment can address these physical and psychological stress-induced cognitive impairments (Khayum et al., 2020; Khaleghi et al., 2021), and prolonged regular (involuntary) exercise can improve estrogen levels in various brain regions and motor coordination performance (Rauf et al., 2015). Exercise also exerts the similar effects of estrogen in terms of lipid oxidation, fat reduction, and inflammation regulation in OVX mice (Jackson et al., 2011; Pighon et al., 2011; Gorres-Martens et al., 2018; Fuller et al., 2021). Moreover, functional locomotor improvement following estrogen treatment was observed in OVX mice. Cognitive deficits induced by decreased BDNF levels can be alleviated by voluntary exercise and estrogen therapy, which regulate the expression of histone deacetylases (Pedram et al., 2013; Rashidy-Pour et al., 2019). These data indicate that estrogen and exercise can improve behavioral functions by enhancing the metabolic phenotype. Using an OVX model in this study, the effect of EE and estrogen treatment proved the hypothesis that EE upregulates βHB and BDNF underlying functional improvement in female mice.

This study has several limitations that some inconsistencies exist in the normal model due to a small size sample, and complexity in defining an absolute EE, which contains complex inanimate and social stimulations. Many components within a complex definition of EE make it difficult to discern which stimulation contributes most to the improvements. Since this study only focused on the effect of EE and estrogen on metabolism, further studies with orchidectomized mice should be conducted to see the holistic sex-specific effect.

In conclusion, this EE exerts an effect on both males and females. However, females have shown significantly differential results in MCT2, HDAC2, and BDNF in cerebral cortex and MCT2, MCT4, HDAC1, HDAC2, BDNF in hippocampus. The level of MCTs, HDACs, and BDNF in the cerebral cortex and hippocampus were regulated by exposure to EE and influenced by the estrogen level. In response to the changed level of βHB, the behavioral improvements in motor and cognition were observed in normal and OVX mice. These combined events showed that EE induces metabolic, molecular, and behavioral changes under the influence of sex, partially by the estrogen level. These findings may be applied to the sex-specific modification of EE and neuroplasticity in female mice from the EE treatment.

DATA AVAILABILITY STATEMENT

The original contributions presented in the study are included in the article/**Supplementary Material**, further inquiries can be directed to the corresponding author/s.

ETHICS STATEMENT

The animal study was reviewed and approved by the Association for Assessment and Accreditation of Laboratory Animal Care and the Institutional Animal Care and Use Committee of the Yonsei University Health System (permit number: 2018-0110, 2019- 0336, and 2020-0054). All procedures were in accordance with the guidelines of the National Institutes of Health's Guide for the Care and Use of Laboratory Animals. These regulations, notifications, and guidelines originated and were modified from the Animal Protection Law (2008), Laboratory Animal Act (2008), and Eighth Edition of the Guide for the Care and Use of Laboratory Animals (NRC 2011).

AUTHOR CONTRIBUTIONS

SP acquired funding for the work, designed the study, developed the setup, drafted the manuscript, and performed the experiments. JK and JH performed experiments and confirmed the accuracy of the data. JHH performed DXA scan and analysis. KK contributed to data validation, data curation, and graphic illustration. S-RC acquired funding for the work, interpreted the data, wrote the manuscript, and conducted study supervision. All authors contributed to the article and approved the submitted version.

FUNDING

This research was supported by the Korean Fund for Regenerative Medicine (KFRM) grant funded by the Korea government (the Ministry of Science and ICT, the Ministry of Health & Welfare). (21A0202L1 and 21C0715L1) to S-RC, a grant from the Korean Health Technology R&D Project through the Korea Health Industry Development Institute (KHIDI), funded by the Ministry of Health & Welfare, Republic of Korea (HI21C1314) to S-RC. SP received funding from Hyundai Motor Chung Mong-Koo Foundation. The funder was not involved in the study design, collection, analysis, interpretation of data, the writing of this article or the decision to submit it for publication.

ACKNOWLEDGMENTS

We would like to thank Editage (www.editage.co.kr) for English language editing.

SUPPLEMENTARY MATERIAL

The Supplementary Material for this article can be found online at: https://www.frontiersin.org/articles/10.3389/fnmol.2022.869799/full#supplementary-material

Supplementary Figure 1 | Experimental methods for the study. **(A)** The real picture of an EE cage and a control cage. **(B)** Determination of estrus cycle by vaginal cytology [(A) proestrus, (B) estrus, (C) diestrus, (D) metestrus]. **(C)** Ovariectomy [(A,B) ovary with fat tissues, (C) unilateral ovariectomy, (D) bilateral ovariectomy].

Supplementary Figure 2 | Higher magnified images of **(A)** MAP-2$^+$MCT2$^+$ and **(B)** GFAP$^+$MCT4$^+$ in the OVX groups.

Supplementary Table 1 | Primer sequences for qRT-PCR.

REFERENCES

Achanta, L. B., and Rae, C. D. (2017). Beta-hydroxybutyrate in the brain: one molecule, multiple mechanisms. *Neurochem. Res.* 42, 35–49. doi: 10.1007/s11064-016-2099-2

Allman, B. R., Morrissey, M. C., Kim, J. S., Panton, L. B., Contreras, R. J., Hickner, R. C., et al. (2019). Fat metabolism and acute resistance exercise in trained women. *J. Appl. Physiol.* 126, 739–745. doi: 10.1152/japplphysiol.00752.2018

Balasse, E. O., and Fery, F. (1989). Ketone body production and disposal: effects of fasting, diabetes, and exercise. *Diabetes Metab. Rev.* 5, 247–270. doi: 10.1002/dmr.5610050304

Ballestri, S., Nascimbeni, F., Baldelli, E., Marrazzo, A., Romagnoli, D., and Lonardo, A. (2017). NAFLD as a sexual dimorphic disease: role of gender and reproductive status in the development and progression of nonalcoholic fatty liver disease and inherent cardiovascular risk. *Adv. Ther.* 34, 1291–1326. doi: 10.1007/s12325-017-0556-1

Benjamin, D., Robay, D., Hindupur, S. K., Pohlmann, J., Colombi, M., El-Shemerly, M. Y., et al. (2018). Dual inhibition of the lactate transporters MCT1 and MCT4 is synthetic lethal with metformin due to NAD+ depletion in cancer cells. *Cell Rep.* 25, 3047–3058.e4. doi: 10.1016/j.celrep.2018.11.043

Blaak, E. (2001). Gender differences in fat metabolism. *Curr. Opin. Clin. Nutr. Metab. Care* 4, 499–502. doi: 10.1097/00075197-200111000-00006

Briones, T. L., Woods, J., and Rogozinska, M. (2013). Decreased neuroinflammation and increased brain energy homeostasis following environmental enrichment after mild traumatic brain injury is associated with improvement in cognitive function. *Acta Neuropathol. Commun.* 1:57. doi: 10.1186/2051-5960-1-57

Brockman, N. K., and Yardley, J. E. (2018). Sex-related differences in fuel utilization and hormonal response to exercise: implications for individuals with type 1 diabetes. *Appl. Physiol. Nutr. Metab.* 43, 541–552. doi: 10.1139/apnm-2017-0559

Byers, S. L., Wiles, M. V., Dunn, S. L., and Taft, R. A. (2012). Mouse estrous cycle identification tool and images. *PLoS ONE* 7:e35538. doi: 10.1371/journal.pone.0035538

Cao, L., Choi, E. Y., Liu, X., Martin, A., Wang, C., Xu, X., et al. (2011). White to brown fat phenotypic switch induced by genetic and environmental activation of a hypothalamic-adipocyte axis. *Cell Metab.* 14, 324–338. doi: 10.1016/j.cmet.2011.06.020

Chamizo, V. D., Rodriguez, C. A., Sanchez, J., and Marmol, F. (2016). Sex differences after environmental enrichment and physical exercise in rats when solving a navigation task. *Learn. Behav.* 44, 227–238. doi: 10.3758/s13420-015-0200-3

Dabek, A., Wojtala, M., Pirola, L., and Balcerczyk, A. (2020). Modulation of cellular biochemistry, epigenetics and metabolomics by ketone bodies. Implications of the ketogenic diet in the physiology of the organism and pathological states. *Nutrients* 12:788. doi: 10.3390/nu12030788

Davis, S. N., Galassetti, P., Wasserman, D. H., and Tate, D. (2000). Effects of gender on neuroendocrine and metabolic counterregulatory responses to exercise in normal man. *J. Clin. Endocrinol. Metab.* 85, 224–230. doi: 10.1210/jc.85.1.224

De Souza, R. M., De Souza, L., Machado, A. E., De Bem Alves, A. C., Rodrigues, F. S., Aguiar, A. S. Jr., et al. (2019). Behavioural, metabolic and neurochemical effects of environmental enrichment in high-fat cholesterol-enriched diet-fed mice. *Behav. Brain Res.* 359, 648–656. doi: 10.1016/j.bbr.2018.09.022

D'eon, T. M., Souza, S. C., Aronovitz, M., Obin, M. S., Fried, S. K., and Greenberg, A. S. (2005). Estrogen regulation of adiposity and fuel partitioning. Evidence of genomic and non-genomic regulation of lipogenic and oxidative pathways. *J. Biol. Chem.* 280, 35983–35991. doi: 10.1074/jbc.M507339200

Dhillon, K. K., and Gupta, S. (2020). *Biochemistry, Ketogenesis.* Treasure Island, FL: StatPearls.

Djiogue, S., Djiyou Djeuda, A. B., Seke Etet, P. F., Ketcha Wanda, G. J. M., Djikem Tadah, R. N., and Njamen, D. (2018). Memory and exploratory behavior impairment in ovariectomized Wistar rats. *Behav. Brain Funct.* 14:14. doi: 10.1186/s12993-018-0146-7

Evans, M., Cogan, K. E., and Egan, B. (2017). Metabolism of ketone bodies during exercise and training: physiological basis for exogenous supplementation. *J. Physiol.* 595, 2857–2871. doi: 10.1113/JP273185

Fang, Y., Liu, W., Tang, Z., Ji, X., Zhou, Y., Song, S., et al. (2022). Monocarboxylate transporter 4 inhibition potentiates hepatocellular carcinoma immunotherapy through enhancing T cell infiltration and immune attack. *Hepatology*. doi: 10.1002/hep.32348. [Epub ahead of print].

Fery, F., and Balasse, E. O. (1983). Ketone body turnover during and after exercise in overnight-fasted and starved humans. *Am. J. Physiol.* 245, E318–E325. doi: 10.1152/ajpendo.1983.245.4.E318

Fortress, A. M., Kim, J., Poole, R. L., Gould, T. J., and Frick, K. M. (2014). 17β-estradiol regulates histone alterations associated with memory consolidation and increases Bdnf promoter acetylation in middle-aged female mice. *Learn. Mem.* 21, 457–467. doi: 10.1101/lm.034033.113

Fuller, K. N. Z., Mccoin, C. S., Von Schulze, A. T., Houchen, C. J., Choi, M. A., and Thyfault, J. P. (2021). Estradiol treatment or modest exercise improves hepatic health and mitochondrial outcomes in female mice following ovariectomy. *Am. J. Physiol. Endocrinol. Metab.* 320, E1020–E1031. doi: 10.1152/ajpendo.00013.2021

Gavin, K. M., Cooper, E. E., Raymer, D. K., and Hickner, R. C. (2013). Estradiol effects on subcutaneous adipose tissue lipolysis in premenopausal women are adipose tissue depot specific and treatment dependent. *Am. J. Physiol. Endocrinol. Metab.* 304, E1167–E1174. doi: 10.1152/ajpendo.00023.2013

Goodpaster, B. H., Katsiaras, A., and Kelley, D. E. (2003). Enhanced fat oxidation through physical activity is associated with improvements in insulin sensitivity in obesity. *Diabetes* 52, 2191–2197. doi: 10.2337/diabetes.52.9.2191

Goodpaster, B. H., and Sparks, L. M. (2017). Metabolic flexibility in health and disease. *Cell Metab.* 25, 1027–1036. doi: 10.1016/j.cmet.2017.04.015

Gorres-Martens, B. K., Field, T. J., Schmidt, E. R., and Munger, K. A. (2018). Exercise prevents HFD- and OVX-induced type 2 diabetes risk factors by decreasing fat storage and improving fuel utilization. *Physiol. Rep.* 6:e13783. doi: 10.14814/phy2.13783

Hagobian, T. A., Sharoff, C. G., Stephens, B. R., Wade, G. N., Silva, J. E., Chipkin, S. R., et al. (2009). Effects of exercise on energy-regulating hormones and appetite in men and women. *Am. J. Physiol. Regul. Integr. Comp. Physiol.* 296, R233–R242. doi: 10.1152/ajpregu.90671.2008

Halestrap, A. P. (2012). The monocarboxylate transporter family–structure and functional characterization. *IUBMB Life* 64, 1–9. doi: 10.1002/iub.573

Halestrap, A. P., and Wilson, M. C. (2012). The monocarboxylate transporter family–role and regulation. *IUBMB Life* 64, 109–119. doi: 10.1002/iub.572

Hargreaves, M., and Spriet, L. L. (2020). Skeletal muscle energy metabolism during exercise. *Nat. Metab.* 2, 817–828. doi: 10.1038/s42255-020-0251-4

Hasselbalch, S. G., Knudsen, G. M., Jakobsen, J., Hageman, L. P., Holm, S., and Paulson, O. B. (1995). Blood-brain barrier permeability of glucose and ketone bodies during short-term starvation in humans. *Am. J. Physiol.* 268, E1161–E1166. doi: 10.1152/ajpendo.1995.268.6.E1161

Heled, Y., Epstein, Y., Shapiro, Y., and Moran, D. (2001). [Thermoregulation in rest and exercise–gender differences]. *Harefuah* 140, 1041–1045.

Henderson, G. C. (2014). Corrigendum: sexual dimorphism in the effects of exercise on metabolism of lipids to support resting metabolism. *Front. Endocrinol.* 5:200. doi: 10.3389/fendo.2014.00200

Higashino-Matsui, Y., Shirato, K., Suzuki, Y., Kawashima, Y., Someya, Y., Sato, S., et al. (2012). Age-related effects of fasting on ketone body production during lipolysis in rats. *Environ. Health Prev. Med.* 17, 157–163. doi: 10.1007/s12199-011-0231-0

Hu, E., Du, H., Shang, S., Zhang, Y., and Lu, X. (2020). Beta-hydroxybutyrate enhances BDNF expression by increasing H3K4me3 and decreasing H2AK119ub in hippocampal neurons. *Front. Neurosci.* 14:591177. doi: 10.3389/fnins.2020.591177

Isacco, L., and Miles-Chan, J. L. (2018). Gender-specific considerations in physical activity, thermogenesis and fat oxidation: implications for obesity management. *Obes. Rev.* 19(Suppl. 1), 73–83. doi: 10.1111/obr.12779

Jackson, K. C., Wohlers, L. M., Valencia, A. P., Cilenti, M., Borengasser, S. J., Thyfault, J. P., et al. (2011). Wheel running prevents the accumulation of monounsaturated fatty acids in the liver of ovariectomized mice by attenuating changes in SCD-1 content. *Appl. Physiol. Nutr. Metab.* 36, 798–810. doi: 10.1139/h11-099

Kaciuba-Uscilko, H., and Grucza, R. (2001). Gender differences in thermoregulation. *Curr. Opin. Clin. Nutr. Metab. Care* 4, 533–536. doi: 10.1097/00075197-200111000-00012

Kang, J., Hoffman, J. R., Chaloupka, E. C., Ratamess, N. A., and Weiser, P. C. (2006). Gender differences in the progression of metabolic responses during incremental exercise. *J. Sports Med. Phys. Fitness* 46, 71–78.

Khaleghi, M., Rajizadeh, M. A., Bashiri, H., Kohlmeier, K. A., Mohammadi, F., Khaksari, M., et al. (2021). Estrogen attenuates physical and psychological stress-induced cognitive impairments in ovariectomized rats. *Brain Behav.* 11:e02139. doi: 10.1002/brb3.2139

Khayum, M. A., Moraga-Amaro, R., Buwalda, B., Koole, M., Den Boer, J. A., Dierckx, R., et al. (2020). Ovariectomy-induced depressive-like behavior and brain glucose metabolism changes in female rats are not affected by chronic mild stress. *Psychoneuroendocrinology* 115:104610. doi: 10.1016/j.psyneuen.2020.104610

Kiss, P., Szabadfi, K., Horvath, G., Tamas, A., Farkas, J., Gabriel, R., et al. (2013). Gender-dependent effects of enriched environment and social isolation in ischemic retinal lesion in adult rats. *Int. J. Mol. Sci.* 14, 16111–16123. doi: 10.3390/ijms140816111

Kraeuter, A. K., Guest, P. C., and Sarnyai, Z. (2019). The open field test for measuring locomotor activity and anxiety-like behavior. *Methods Mol. Biol.* 1916, 99–103. doi: 10.1007/978-1-4939-8994-2_9

Lagunas, N., Calmarza-Font, I., Diz-Chaves, Y., and Garcia-Segura, L. M. (2010). Long-term ovariectomy enhances anxiety and depressive-like behaviors in mice submitted to chronic unpredictable stress. *Horm. Behav.* 58, 786–791. doi: 10.1016/j.yhbeh.2010.07.014

Li, X., Zhan, Z., Zhang, J., Zhou, F., and An, L. (2020). Beta-hydroxybutyrate ameliorates abeta-induced downregulation of TrkA expression by inhibiting HDAC1/3 in SH-SY5Y cells. *Am. J. Alzheimers. Dis. Other Demen.* 35:1533317519883496. doi: 10.1177/1533317519883496

Lin, A. L., Zhang, W., Gao, X., and Watts, L. (2015). Caloric restriction increases ketone bodies metabolism and preserves blood flow in aging brain. *Neurobiol. Aging* 36, 2296–2303. doi: 10.1016/j.neurobiolaging.2015.03.012

Lin, E. J., Choi, E., Liu, X., Martin, A., and During, M. J. (2011). Environmental enrichment exerts sex-specific effects on emotionality in C57BL/6J mice. *Behav. Brain Res.* 216, 349–357. doi: 10.1016/j.bbr.2010.08.019

Lopes-Cardozo, M., Mulder, I., Van Vugt, F., Hermans, P. G., Van Den Bergh, S. G., Klazinga, W., et al. (1975). Aspects of ketogenesis: control and mechanism of ketone-body formation in isolated rat-liver mitochondria. *Mol. Cell. Biochem.* 9, 155–173. doi: 10.1007/BF01751311

Madronal, N., Lopez-Aracil, C., Rangel, A., Del Rio, J. A., Delgado-Garcia, J. M., and Gruart, A. (2010). Effects of enriched physical and social environments on motor performance, associative learning, and hippocampal neurogenesis in mice. *PLoS ONE* 5:e11130. doi: 10.1371/journal.pone.0011130

Maher, A. C., Akhtar, M., Vockley, J., and Tarnopolsky, M. A. (2010). Women have higher protein content of beta-oxidation enzymes in skeletal muscle than men. *PLoS ONE* 5:e12025. doi: 10.1371/journal.pone.0012025

Manwani, B., Liu, F., Xu, Y., Persky, R., Li, J., and Mccullough, L. D. (2011). Functional recovery in aging mice after experimental stroke. *Brain Behav. Immun.* 25, 1689–1700. doi: 10.1016/j.bbi.2011.06.015

Marinou, K., Adiels, M., Hodson, L., Frayn, K. N., Karpe, F., and Fielding, B. A. (2011). Young women partition fatty acids towards ketone body production rather than VLDL-TAG synthesis, compared with young men. *Br. J. Nutr.* 105, 857–865. doi: 10.1017/S0007114510004472

Matsui, T., Omuro, H., Liu, Y. F., Soya, M., Shima, T., Mcewen, B. S., et al. (2017). Astrocytic glycogen-derived lactate fuels the brain during exhaustive exercise to maintain endurance capacity. *Proc. Natl. Acad. Sci. U.S.A.* 114, 6358–6363. doi: 10.1073/pnas.1702739114

Matsumori, Y., Hong, S. M., Fan, Y., Kayama, T., Hsu, C. Y., Weinstein, P. R., et al. (2006). Enriched environment and spatial learning enhance hippocampal neurogenesis and salvages ischemic penumbra after focal cerebral ischemia. *Neurobiol. Dis.* 22, 187–198. doi: 10.1016/j.nbd.2005.10.015

Maunder, E., Plews, D. J., and Kilding, A. E. (2018). Contextualising maximal fat oxidation during exercise: determinants and normative values. *Front. Physiol.* 9:599. doi: 10.3389/fphys.2018.00599

Mierziak, J., Burgberger, M., and Wojtasik, W. (2021). 3-hydroxybutyrate as a metabolite and a signal molecule regulating processes of living organisms. *Biomolecules* 11:402. doi: 10.3390/biom11030402

Mika, A., Macaluso, F., Barone, R., Di Felice, V., and Sledzinski, T. (2019). Effect of exercise on fatty acid metabolism and adipokine secretion in adipose tissue. *Front. Physiol.* 10:26. doi: 10.3389/fphys.2019.00026

Mitchell, S. J., Madrigal-Matute, J., Scheibye-Knudsen, M., Fang, E., Aon, M., Gonzalez-Reyes, J. A., et al. (2016). Effects of sex, strain, and energy intake on hallmarks of aging in mice. *Cell Metab.* 23, 1093–1112. doi: 10.1016/j.cmet.2016.05.027

Mittendorfer, B., Horowitz, J. F., and Klein, S. (2001). Gender differences in lipid and glucose kinetics during short-term fasting. *Am. J. Physiol. Endocrinol. Metab.* 281, E1333–E1339. doi: 10.1152/ajpendo.2001.281.6.E1333

Newman, L. A., Korol, D. L., and Gold, P. E. (2011). Lactate produced by glycogenolysis in astrocytes regulates memory processing. *PLoS ONE* 6:e28427. doi: 10.1371/journal.pone.0028427

Nithianantharajah, J., and Hannan, A. J. (2006). Enriched environments, experience-dependent plasticity and disorders of the nervous system. *Nat. Rev. Neurosci.* 7, 697–709. doi: 10.1038/nrn1970

Oliveira, M. C., Campos-Shimada, L. B., Marcal-Natali, M. R., Ishii-Iwamoto, E. L., and Salgueiro-Pagadigorria, C. L. (2018). A long-term estrogen deficiency in ovariectomized mice is associated with disturbances in fatty acid oxidation and oxidative stress. *Rev. Bras. Ginecol. Obstet.* 40, 251–259. doi: 10.1055/s-0038-1666856

Pedersen, S. B., Kristensen, K., Hermann, P. A., Katzenellenbogen, J. A., and Richelsen, B. (2004). Estrogen controls lipolysis by up-regulating alpha2A-adrenergic receptors directly in human adipose tissue through the estrogen receptor alpha. Implications for the female fat distribution. *J. Clin. Endocrinol. Metab.* 89, 1869–1878. doi: 10.1210/jc.2003-031327

Pedram, A., Razandi, M., Narayanan, R., Dalton, J. T., Mckinsey, T. A., and Levin, E. R. (2013). Estrogen regulates histone deacetylases to prevent cardiac hypertrophy. *Mol. Biol. Cell* 24, 3805–3818. doi: 10.1091/mbc.e13-08-0444

Pellerin, L., Bergersen, L. H., Halestrap, A. P., and Pierre, K. (2005). Cellular and subcellular distribution of monocarboxylate transporters in cultured brain cells and in the adult brain. *J. Neurosci. Res.* 79, 55–64. doi: 10.1002/jnr.20307

Phinney, S. D. (2004). Ketogenic diets and physical performance. *Nutr. Metab.* 1:2. doi: 10.1186/1743-7075-1-2

Pierre, K., Magistretti, P. J., and Pellerin, L. (2002). MCT2 is a major neuronal monocarboxylate transporter in the adult mouse brain. *J. Cereb. Blood Flow Metab.* 22, 586–595. doi: 10.1097/00004647-200205000-00010

Pierre, K., and Pellerin, L. (2005). Monocarboxylate transporters in the central nervous system: distribution, regulation and function. *J. Neurochem.* 94, 1–14. doi: 10.1111/j.1471-4159.2005.03168.x

Pighon, A., Gutkowska, J., Jankowski, M., Rabasa-Lhoret, R., and Lavoie, J. M. (2011). Exercise training in ovariectomized rats stimulates estrogenic-like effects on expression of genes involved in lipid accumulation and subclinical inflammation in liver. *Metab. Clin. Exp.* 60, 629–639. doi: 10.1016/j.metabol.2010.06.012

Puchalska, P., and Crawford, P. A. (2017). Multi-dimensional roles of ketone bodies in fuel metabolism, signaling, and therapeutics. *Cell Metab.* 25, 262–284. doi: 10.1016/j.cmet.2016.12.022

Queen, N. J., Boardman, A. A., Patel, R. S., Siu, J. J., Mo, X., and Cao, L. (2020). Environmental enrichment improves metabolic and behavioral health in the BTBR mouse model of autism. *Psychoneuroendocrinology* 111:104476. doi: 10.1016/j.psyneuen.2019.104476

Rashidy-Pour, A., Bavarsad, K., Miladi-Gorji, H., Seraj, Z., and Vafaei, A. A. (2019). Voluntary exercise and estradiol reverse ovariectomy-induced spatial learning and memory deficits and reduction in hippocampal brain-derived neurotrophic factor in rats. *Pharmacol. Biochem. Behav.* 187:172819. doi: 10.1016/j.pbb.2019.172819

Rauf, S., Soejono, S. K., and Partadiredja, G. (2015). Effects of treadmill exercise training on cerebellar estrogen and estrogen receptors, serum estrogen, and motor coordination performance of ovariectomized rats. *Iran. J. Basic Med. Sci.* 18, 587–592.

Robinet, C., and Pellerin, L. (2011). Brain-derived neurotrophic factor enhances the hippocampal expression of key postsynaptic proteins *in vivo* including the monocarboxylate transporter MCT2. *Neuroscience* 192, 155–163. doi: 10.1016/j.neuroscience.2011.06.059

Ruppert, P. M., Deng, L., Hooiveld, G. J., Hangelbroek, R. W., Zeigerer, A., and Kersten, S. (2021). RNA sequencing reveals niche gene expression effects of beta-hydroxybutyrate in primary myotubes. *Life Sci. Alliance* 4:e202101037. doi: 10.26508/lsa.202101037

Sanchez-Alavez, M., Alboni, S., and Conti, B. (2011). Sex- and age-specific differences in core body temperature of C57Bl/6 mice. *Age* 33, 89–99. doi: 10.1007/s11357-010-9164-6

Seo, J. H., Pyo, S., Shin, Y. K., Nam, B. G., Kang, J. W., Kim, K. P., et al. (2018). The effect of environmental enrichment on glutathione-mediated xenobiotic metabolism and antioxidation in normal adult mice. *Front. Neurol.* 9:425. doi: 10.3389/fneur.2018.00425

Sleiman, S. F., Henry, J., Al-Haddad, R., El Hayek, L., Abou Haidar, E., Stringer, T., et al. (2016). Exercise promotes the expression of brain derived neurotrophic factor (BDNF) through the action of the ketone body beta-hydroxybutyrate. *Elife* 5:e15092. doi: 10.7554/eLife.15092

Soeters, M. R., Sauerwein, H. P., Groener, J. E., Aerts, J. M., Ackermans, M. T., Glatz, J. F., et al. (2007). Gender-related differences in the metabolic response to fasting. *J. Clin. Endocrinol. Metab.* 92, 3646–3652. doi: 10.1210/jc.2007-0552

Solomon, T. P., Sistrun, S. N., Krishnan, R. K., Del Aguila, L. F., Marchetti, C. M., O'carroll, S. M., et al. (2008). Exercise and diet enhance fat oxidation and reduce insulin resistance in older obese adults. *J. Appl. Physiol.* 104, 1313–1319. doi: 10.1152/japplphysiol.00890.2007

Swift, D. L., Johannsen, N. M., Lavie, C. J., Earnest, C. P., and Church, T. S. (2014). The role of exercise and physical activity in weight loss and maintenance. *Prog. Cardiovasc. Dis.* 56, 441–447. doi: 10.1016/j.pcad.2013.09.012

Takimoto, M., and Hamada, T. (2014). Acute exercise increases brain region-specific expression of MCT1, MCT2, MCT4, GLUT1, and COX IV proteins. *J. Appl. Physiol.* 116, 1238–1250. doi: 10.1152/japplphysiol.01288.2013

Tarnopolsky, M. A. (2008). Sex differences in exercise metabolism and the role of 17-beta estradiol. *Med. Sci. Sports Exerc.* 40, 648–654. doi: 10.1249/MSS.0b013e31816212ff

Thyfault, J. P., and Bergouignan, A. (2020). Exercise and metabolic health: beyond skeletal muscle. *Diabetologia* 63, 1464–1474. doi: 10.1007/s00125-020-05177-6

Vijay, N., and Morris, M. E. (2014). Role of monocarboxylate transporters in drug delivery to the brain. *Curr. Pharm. Des.* 20, 1487–1498. doi: 10.2174/13816128113199990462

Vislocky, L. M., Gaine, P. C., Pikosky, M. A., Martin, W. F., and Rodriguez, N. R. (2008). Gender impacts the post-exercise substrate and endocrine response in trained runners. *J. Int. Soc. Sports Nutr.* 5:7. doi: 10.1186/1550-2783-5-7

Wahl, F., Allix, M., Plotkine, M., and Boulu, R. G. (1992). Neurological and behavioral outcomes of focal cerebral ischemia in rats. *Stroke* 23, 267–272. doi: 10.1161/01.STR.23.2.267

Xie, Z., Zhang, D., Chung, D., Tang, Z., Huang, H., Dai, L., et al. (2016). Metabolic regulation of gene expression by histone lysine beta-hydroxybutyrylation. *Mol. Cell* 62, 194–206. doi: 10.1016/j.molcel.2016.03.036

Yokose, S., Ishizuya, T., Ikeda, T., Nakamura, T., Tsurukami, H., Kawasaki, K., et al. (1996). An estrogen deficiency caused by ovariectomy increases plasma levels of systemic factors that stimulate proliferation and differentiation of osteoblasts in rats. *Endocrinology* 137, 469–478. doi: 10.1210/endo.137.2.8593791

Zhang, H., Tang, K., Ma, J., Zhou, L., Liu, J., Zeng, L., et al. (2020). Ketogenesis-generated beta-hydroxybutyrate is an epigenetic regulator of CD8(+) T-cell memory development. *Nat. Cell Biol.* 22, 18–25. doi: 10.1038/s41556-019-0440-0

Conflict of Interest: The authors declare that the research was conducted in the absence of any commercial or financial relationships that could be construed as a potential conflict of interest.

The reviewer SK declared a shared affiliation with the authors to the handling editor at the time of review.

Publisher's Note: All claims expressed in this article are solely those of the authors and do not necessarily represent those of their affiliated organizations, or those of the publisher, the editors and the reviewers. Any product that may be evaluated in this article, or claim that may be made by its manufacturer, is not guaranteed or endorsed by the publisher.

frontiers | Frontiers in Molecular Neuroscience

ORIGINAL RESEARCH
published: 06 May 2022
doi: 10.3389/fnmol.2022.822088

Mechanism of Electroacupuncture Against Cerebral Ischemia–Reperfusion Injury: Reducing Inflammatory Response and Cell Pyroptosis by Inhibiting NLRP3 and Caspase-1

Li Cai[1,2†‡], *Zeng-Yu Yao*[1,2†‡], *Lu Yang*[1,2], *Xiu-Hong Xu*[1], *Meng Luo*[1], *Miao-Miao Dong*[1] and *Guo-Ping Zhou*[1,2*†]

[1] Department of Acupuncture and Massage Rehabilitation, Neuroscience Center, Integrated Hospital of Traditional Chinese Medicine, Southern Medical University, Guangzhou, China, [2] School of Traditional Chinese Medicine, Southern Medical University, Guangzhou, China

Cell pyroptosis is one of the main forms of neuronal injury after cerebral ischemia–reperfusion. It is accompanied by an inflammatory reaction and regulated by the caspase gene family. Electroacupuncture (EA) can reduce neuronal injury caused by cerebral ischemia–reperfusion, and we speculated that EA can prevent neuronal pyroptosis after cerebral ischemia–reperfusion by regulating the nucleotide-binding oligomerization domain-like receptor protein 3 (NLRP3)/caspase-1 pathway. The cerebral ischemia–reperfusion injury model of C57 and caspase-1 gene knockout (Cas-1 ko) mice was established by Longa's method. EA was conducted at acupoints Chize (LU5), Hegu (LI4), Sanyinjiao (SP6), and Zusanli (ST36) for 1.5 h after cerebral ischemia–reperfusion injury for 20 min, and observation was carried out after 24 h. Neurological deficit scores evaluated the neurological function, cerebral infarction volume was observed by triphenyl tetrazolium chloride (TTC) staining, hematoxylin and eosin (H&E) staining, TUNEL and caspase-1 double-labeled fluorescence staining, and NLRP3 and caspase-1 double-labeled immunofluorescence staining that were used to observe the morphology of neurons in hippocampus, and the protein expression of NLRP3, pro-caspase-1, cleaved caspase-1 p20, pro-interleukin-1β (IL-1β), cleaved IL-1β, and GSDMD was detected by Western blot assay. Results showed that EA could reduce the score of neurological deficit, reduce the volume of cerebral infarction and improve the degree of nerve cell injury, and inhibit NLRP3, pro-caspase-1, cleaved caspase-1 p20, pro-IL-1β, cleaved IL-1β, and GSDMD protein expression. In summary, EA plays a neuroprotective role by reducing the pyroptotic neurons that were caspase 1-mediated and inflammatory response after cerebral ischemia–reperfusion.

Keywords: nerve regeneration, cerebral ischemia/reperfusion injury, NLRP3, caspase-1, cell pyroptosis, electroacupuncture

OPEN ACCESS

Edited by:
Binlong Zhang,
China Academy of Chinese Medical Sciences, China

Reviewed by:
Eva Maria Jimenez-Mateos,
Trinity College Dublin, Ireland
Vasantha Kolachala,
Emory University, United States

***Correspondence:**
Guo-Ping Zhou
doctorzgp@sina.com

***ORCID:**
Li Cai
orcid.org/0000-0002-3698-3817
Zeng-Yu Yao
orcid.org/0000-0003-3553-972X
Guo-Ping Zhou
orcid.org/0000-0002-4613-4384

These authors have contributed equally to this work

Specialty section:
This article was submitted to Neuroplasticity and Development, a section of the journal Frontiers in Molecular Neuroscience

Received: *25 November 2021*
Accepted: *04 April 2022*
Published: *06 May 2022*

Citation:
Cai L, Yao Z-Y, Yang L, Xu X-H, Luo M, Dong M-M and Zhou G-P (2022) Mechanism of Electroacupuncture Against Cerebral Ischemia–Reperfusion Injury: Reducing Inflammatory Response and Cell Pyroptosis by Inhibiting NLRP3 and Caspase-1. Front. Mol. Neurosci. 15:822088. doi: 10.3389/fnmol.2022.822088

BACKGROUND

Ischemic stroke is one of the most severe diseases that affect human health and death in the world. It has the characteristics of high morbidity, high disability rate, high mortality, and high recurrence rate (Dabrowska-Bender et al., 2017; Zhou et al., 2019). After a certain period of cerebral ischemia, blood flow is recanalized. However, a large amount of blood oxygen supply can further cause more severe nerve damage and accelerate the death of nerve cells. This phenomenon is called cerebral ischemia/reperfusion injury (Lv et al., 2020). The pathophysiological mechanism of cerebral ischemia/reperfusion injury is a series of complex nerve injury cascade reactions, and the death of nerve cells runs through the whole injury process. Pyroptosis is a programmed cell death with inflammatory response, which has been found and confirmed in recent years. Its classical pathway depends on the activation of caspase-1, and endogenous and exogenous stimulation signals act on inflammatory bodies through different pathways to activate caspase-1. It mediates the swelling and rupture of cell permeability and causes the release of intracellular substances and pro-inflammatory factors, such as interleukin-1β (IL-1β) and IL-18, amplifies local and systemic inflammatory responses, and induces cell pyroptosis (Bergsbaken and Fink, 2009; Doitsh et al., 2014; Jorgensen, 2015).

The activation of inflammatory bodies is a classical pathway for the regulation of cell pyroptosis. Nucleotide-binding oligomerization domain-like receptor protein 3 (NLRP3) recruits caspase-1 through adaptor proteins, such as apoptosis-associated speck-like protein containing CARD (ASC), and induces its precursor protease (pro-caspase-1) to produce autohydration reaction. Activated caspase-1 can effectively trigger downstream components to cause cell pyroptosis (Jin, 2010; Wellington et al., 2014; Rathinam, 2016). NLRP3, as the initiating factor of aseptic inflammatory response of the central nervous system after cerebral ischemia, induces cell pyroptosis, resulting in nerve cell injury, and plays a key role in the inflammatory cascade effect after cerebral ischemia/reperfusion (Fann et al., 2013; Walsh and Muruve, 2014).

Inducing inflammatory response is a major feature of cell pyroptosis different from apoptosis. It is found that the classical caspase-1 signaling pathway mediating pyroptosis is activated in stroke and aggravates brain injury, while inhibiting caspase-1 activation can reduce stroke injury and play a protective role (Kawaguchi et al., 2011; He et al., 2017). Electroacupuncture (EA) is beneficial to improve the symptoms of neurological deficit and restore limb motor function after cerebral ischemia/reperfusion injury. "Chize (LU5), Hegu (LI4)" and "Sanyinjiao (SP6), and Zusanli (ST36)" served as common acupoints in the clinical treatment of stroke and could improve the symptoms of neurological deficit (Zhang et al., 2012; Yang et al., 2015; Wang et al., 2016; Zhu et al., 2017). Our previous studies have found that EA can reduce apoptosis and improve neurological injury after cerebral I/R, but its mechanism needs further investigation (Wu et al., 2015, 2018; Lan et al., 2017).

In this study, the cerebral I/R injury models of C57 and caspase-1 gene knockout (Cas-1 ko) mice were established, and the neurological deficit scores, cerebral infarction area, pyroptosis index, and the expression of NLRP3/caspase-1/IL-1β were analyzed to explore the mechanism of EA on nerve cell protection after cerebral ischemia/reperfusion.

METHODS

Animals

A total of 48 healthy C57BL/6 mice (half male and half female), weighing 20–25 g, and a total of 48 Casp-1 ko mice (half male and half female), weighing 20–25 g, were purchased from Cyagen Biosciences Co. Ltd. (Guangzhou, China; license number: SCXK (Su) 2018-0003). The experimental procedure followed the National Institutes of Health Guide for the Care and Use of Laboratory Animals (NIH Publications No. 8023, revised 1986). The mice were fed standard rodent chow and allowed free access to water. It was approved by the Animal Ethics and Welfare Committee of Southern Medical University of China (approval no. 2021-005). The temperature of the animal house was maintained at a room temperature between 20 and 22°C and a relative humidity of 65–70%. The C57 mice and the caspase knockout mice were randomized into Sham (Sham control) group, I/R (model) group, and EA (I/R + EA) group ($n = 16$ per group).

Establishing Cerebral I/R Injury Mouse Model

The middle cerebral artery of the mice was blocked according to the modified Zea-Longa's method to induce cerebral I/R model (Longa et al., 1989). After anesthetizing the mice with 1% pentobarbital sodium (45 mg/kg) by intraperitoneal injection, the left common carotid artery, left internal carotid artery, external carotid artery, and vagus nerve were carefully exposed through the midline incision under the surgical microscope. A nylon wire of about 11 ± 0.5 mm was introduced into the internal carotid artery to occlude the middle cerebral artery until slight resistance was observed during insertion. After 30 min of occlusion, the blood supply of the ischemic area was restored by slowly drawing the thread, and the reperfusion was achieved. Mice in the Sham group underwent the same procedures, as described previously, but without arterial occlusion. The model evaluation criteria refer to Zea-Longa's 5-point evaluation method (0, no obvious defect; 1, failure to fully extend the contralateral forepaw; 2, circling to the opposite side; 3, falling to the opposite side; 4, loss of walking or consciousness) (Longa et al., 1989). The behavioral evaluation of mice for 2 h after operation, and the score of neurological deficit was 1–3, was included in the follow-up experiment; those that did not meet the above scoring criteria were unconscious and found subarachnoid hemorrhage during brain removal, considering that the model was failed and was not included in the experiment and supplemented randomly.

Electroacupuncture Intervention

The mice in the EA group underwent EA stimulation for 1.5 h after I/R injury. Stainless steel acupuncture needles (diameter: 0.16 × 13 mm^2; Suzhou Universal Acupuncture Medical Devices Co., Ltd., Suzhou, China) were inserted 2–3 mm into LU5, LI4,

ST36, and SP6 acupoints of the paralyzed limb. The selection of acupoints and EA stimulation were made according to "experimental acupuncture" edited by Li (2007). The location of the selected acupoints was as follows: as for LU5, in the depression of the outer end of the transverse cubital crease, an acupuncture needle was inserted perpendicularly to a depth of 3 mm. As for LI4, located between first metacarpal bone and second metacarpal bone, an acupuncture needle was inserted perpendicularly to a depth of 1 mm; as for ST36, located at 5 mm below fibular head at outer lateral posterior knee and puncture, an acupuncture needle was inserted perpendicularly to a depth of 7 mm; as for SP6, located at the tip of the inner ankle of the posterior limb, a needle was inserted upward 10 mm and perpendicularly to a depth of 5 mm. The acupoints were stimulated for 20 min with a dilatational wave of frequency 5/10 Hz and intensity 2 mA using an EA instrument (model KWD-808I, Suzhou Universal Acupuncture Medical Devices Co., Ltd).

Neurological Deficit Scores

At 24 h after the operation (before tissue sampling), the neurological deficit score of mice was evaluated by the Zea-Longa's 5-point evaluation method (Longa et al., 1989). The neurological deficit scores were defined as follows: score 0, no obvious defect; score 1, failure to fully extend the right forepaw; score 2, circling to the contralateral side; score 3, falling to the opposite side; and score 4, not spontaneously walking or loss of consciousness.

Tissue Sampling

The samples were collected for 24 h after I/R injury. After excessive anesthesia (1% pentobarbital sodium, 45 mg/kg), rapid perfusion with 0.9% normal saline (NaCl) and 4% paraformaldehyde in phosphate-buffered saline (PBS) for 3–5 min eliminated the influence of blood factors. Then, the whole brain was dissected out of the cranial cavity immediately. In each group, 4 fresh brain tissues were taken for triphenyl tetrazolium chloride (TTC) staining, 8 tissues were placed in 4% paraformaldehyde solution for hematoxylin and eosin (H&E) and TUNEL staining, and 4 tissues were stored at −80°C in refrigerator for Western blot analysis.

TTC Staining

Fresh brain tissue was stored at −20°C for 20 min and then sectioned every 2 mm in the coronal plane. The slices were placed in 2% TTC phosphate buffer and incubated in a 37°C water bath for 30 min in the dark. Slices were turned evenly every 10 min to make the slices even in contact with the TTC staining solution. After staining, the infarct was stained white, and the normal brain tissue was stained red. The AlphaEaseFC analyzer software (AlphaInnotech, San Leandro, CA, USA) was used to measure the infarct size, and the brain infarct volume percentage (BIVP) was calculated.

Hematoxylin and Eosin Staining

Brain tissue sections were dewaxed with xylene and absolute ethanol two times each and were hydrated. After cleaning, they were stained using hematoxylin (Yuanmu Biotechnology Co., Ltd., Shanghai, China) for 10 min. 1% hydrochloric acid ethanol is used for differentiation, and 1/400 ammonia is used for bluing. After cleaning, they were stained with eosin (Huihong Reagent Co., Ltd., Hunan, China) for 5 min. Ethanol was gradually dehydrated. Xylene was transparent twice and sealed with neutral resin. The morphology of nerve cells in hippocampus under a microscope (Jiangnan Optical Instrument Group, Nanjing, China) was observed to judge the degree of nerve cell injury.

Immunofluorescence Staining

Frozen sections were boiled in ethylenediaminetetraacetic acid (EDTA) antigen repair solution (pH 8.0) (Servicebio, Wuhan, CNH) for antigen retrieval and blocked with 3% bovine serum albumin for 30 min at room temperature. Then, the sections were incubated at 4°C overnight with primary antibodies against caspase-1 (1:50, Servicebio, Wuhan, CNH, GB11383) and NLRP3 (1:100, Servicebio, Wuhan, CNH, GB11300). Then, the sections were incubated with the corresponding secondary antibody at room temperature for 90 min. The sections were washed in PBS 3 times (5 min/time), and 4',6-diamidino-2-phenylindole (DAPI) (Servicebio, Wuhan, CNH, GB1012) was used for staining the dried section for 10 min. Apoptosis was detected by a fluorescein (FITC) TUNEL cell apoptosis detection kit (Servicebio, Wuhan, CNH, G1501-50T). Morphological changes in the cerebral tissues were observed under a microscope (Jiangnan Optical Instrument Group, Nanjing, China), and the images were collected for analysis (AlphaEaseFC). Two 90× fields of view in the hippocampal CA1 area were randomly selected for photography. The number of positive cells was calculated according to the following formula: double-stained cells/total cells × 100%.

Western Blot Assay

Hippocampus tissues were homogenized in Radio Immunoprecipitation Assay (RIPA) lysis buffer, centrifuged at 12,000×*g* for 5 min, and then determined protein concentration in supernatants. Protein lysates were separated by 10% SDS-PAGE gels and then electrophoretically transferred onto polyvinylidene fluoride membranes (Millipore, Boston, USA). The membranes were blocked with 5% nonfat dry milk for 1 h and incubated with primary antibodies, namely, caspase-1 (1:1,000; Servicebio, Wuhan, CNH; GB11383), NLRP3 (1:1,000; Affinity, Wuhan, CNH; DF7438), and IL-1β (1:1,000; Affinity, Wuhan, CNH; AF5103) overnight at 4°C. The membranes were incubated with a corresponding secondary antibody (1:3,000; goat anti-rabbit/mouse IgG; Servicebio, Wuhan, CNH; GB23303) in tris-buffered saline and tween 20 (TBST) for 30 min. The blots were developed using enhanced chemiluminescence, and the intensity of the bands was measured using the AlphaEaseFC analyzer software (AlphaInnotech, San Leandro, CA, USA). The optical density value ratio of the target band to the internal reference served as the relative expression of the target protein.

Statistical Analysis

The SPSS 20.0 software (IBM, Armonk, NY, USA) was used for statistical analysis. Quantitative data are expressed as the mean ± SD. For data conforming to normal distribution and

homogeneity of variance, two-way analysis of variance (ANOVA) is used; during the pairwise comparison between groups, the least significant difference (LSD) is calculated using the *post-hoc* test. If the data do not meet the normal distribution, the Mann–Whitney nonparametric test is used for pairwise comparison, and the Kruskal–Wallis test is used for multiple comparisons. A p-value less than 0.05 was considered statistically significant.

RESULTS

Effect of Electroacupuncture on the Neurological Function After I/R Injury

The neurological deficits of mice in each group were evaluated. There was no nerve injury in the Sham group, but there was an obvious nerve function defect in the I/R and EA groups ($F = 100.942$, $p = 0.026$); in the I/R group, the neurological deficit score of Cas-1 ko mice was lower than that of C57 mice, but there was no significant difference between them in the EA group ($p < 0.05$). The neurological deficit score of the same genotype mice in the EA group was significantly lower than that in the I/R group ($p < 0.05$) (**Figure 1).**

Effect of Electroacupuncture on Cerebral Infarction Volume Ratio After I/R Injury

The TTC staining showed that the brain tissue sections in the Sham group were bright red, and there was no pale infarct; pale infarcts of different sizes were observed in brain tissue sections of the I/R and EA groups ($F = 194.386$, $p < 0.001$). The volume of cerebral infarction in the I/R and EA groups was significantly higher than that in the Sham group, and that in the EA group was lower than that in the I/R group ($p < 0.05$). The cerebral infarction volume of Cas-1 ko mice in the I/R group was lower than that of C57 mice ($p < 0.05$), but there was no significant difference in cerebral infarction volume of different genotypes in the EA group ($P > 0.05$) (**Figure 2**).

Morphological Observation of Electroacupuncture on Neuronal Injury in Hippocampus After I/R Injury

The EA intervention has a cytoprotective effect on neurons in hippocampus after I/R injury. H&E staining showed that after I/R injury, the number of neurons decreased, the arrangement was loose, and vacuole-like changes and irregular nuclear morphology could be observed in the hippocampus. After EA intervention, the pathological changes of neurons in hippocampus were reduced, and less degeneration or necrosis of neurons was observed (**Figure 3A**). TUNEL staining could label the broken DNA fragments in apoptotic or pyroptotic cells (**Figures 3B,D**). In the I/R group, a large number of TUNEL and caspase-1 double-staining neurons were observed in C57 mice. After EA intervention, the positive rates in C57 mice decreased significantly ($p < 0.05$, **Figures 3B,D**). In addition, double-labeled immunofluorescence showed that the expression of caspase-1 and NLRP3 co-localization in neurons in the hippocampus of C57 mice was obvious and evident ($p < 0.05$, **Figures 3C,E**). EA intervention could effectively reduce the number of co-expressed neurons in C57 mice ($p < 0.05$, **Figures 3C,E**). There were no neurons co-expressing caspase-1 and NLRP3 in Cas-1 ko mice of different groups.

Effect of Electroacupuncture on the Expression of Pyroptosis-Related Proteins in Mice After I/R Injury

To explore the effect of EA on neuronal pyroptosis after I/R injury, brain protein was extracted, and the expression of NLRP3, pro-Casp-1, Casp-1 p20, IL-1β, cleaved IL-1β, and GSDMD was evaluated by Western blot. After I/R injury, the expression of NLRP3, pro-Casp-1, Casp-1 p20, IL-1β, cleaved IL-1β, and GSDMD in C57 mice increased significantly, while EA intervention inhibited the expression of those proteins ($p < 0.05$, **Figures 4A,B**). The expression of pro-Casp-1 and Casp-1 p20 of Cas-1 ko mice was absent in different treatment groups, but the trend of other proteins' expression in different treatment groups was similar to those in C57 mice. Furthermore, in the expression of casp-11 protein in Cas-1 ko mice, the results showed that Cas-1 ko mice could express casp-11 (**Figure 4C**).

DISCUSSION

A large number of clinical studies have confirmed that EA stimulation of acupoints can promote the recovery of stroke symptoms and paralyzed limb function, and can significantly improve the cognitive level and motor function of patients with ischemic stroke (Jittiwat, 2019; Nierhaus et al., 2019). Animal experiments showed that after cerebral ischemia, nerve function injury and cell death reached the peak on the first day, and then gradually decreased and stabilized (Kim et al., 2013a). EA intervention in the early stage after cerebral ischemia can increase cerebral blood flow, reduce the degree of cerebral ischemia/reperfusion injury, and expand the treatment time window (Ren et al., 2010; Kim et al., 2013b). This suggests that the best time for acupuncture treatment is within 3 h after ischemia. Therefore, we choose EA for 1.5 h after cerebral ischemia injury and 1 day after cerebral ischemia as the observation time. The neurological deficit score can effectively evaluate the behavioral changes after brain I/R injury, and it is also an important index to judge the recovery of tissue neurological function. Previous studies have shown that EA can improve limb motor function and has a certain neuroprotective effect on cerebral ischemia/reperfusion injury (Xue et al., 2014; Wu et al., 2017). The results of this study show that EA can significantly improve the neurological deficit symptoms after brain I/R injury. In the I/R group, caspase-1 gene mice obtain a lower neurological deficit score than C57 mice, which may be achieved by inhibiting cell death. After EA intervention, there was no difference between C57 mice and caspase-1 gene mice, suggesting that EA may play a neuroprotective role by inhibiting caspase-1. TTC staining of brain sections showed similar results. After brain I/R injury, C57 mice had larger cerebral infarction than Cas-1 ko mice. After EA intervention, the cerebral infarction volume of the two mice was significantly lower than that of the I/R group, and there was no significant difference between the two groups. Relevant

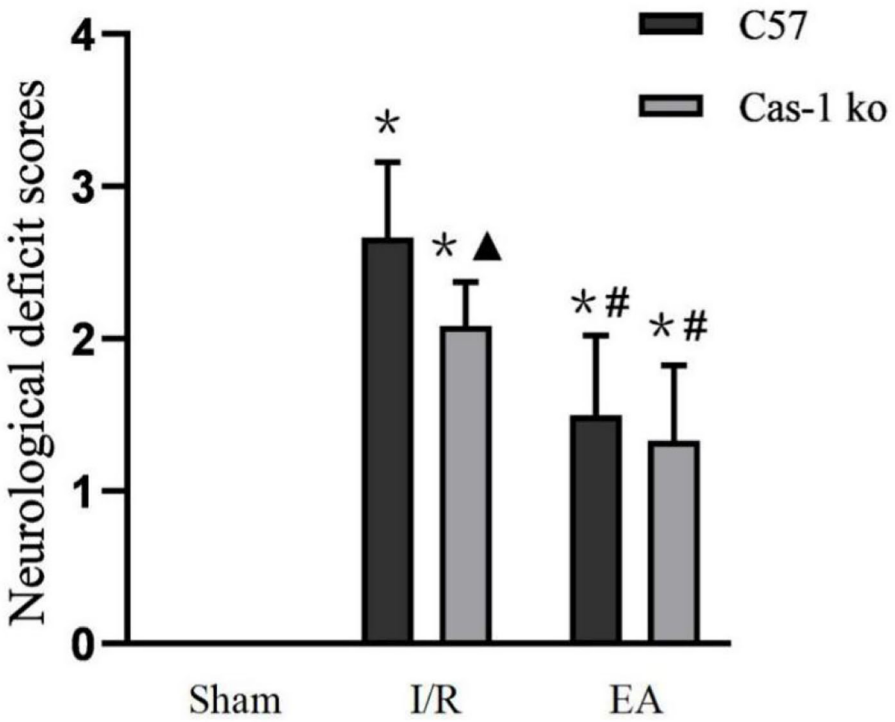

FIGURE 1 | Neurological deficit scores. Comparison within the same genotype: $^{*}p < 0.05$ vs. Sham group; $^{\#}p < 0.05$ vs. I/R group. Comparison within the I/R group: $\blacktriangle p < 0.05$ vs. C57 mice. Data are representative of 12 independent experiments (mean ± SD are representative of values from 12 independent experiments).

studies have shown that inhibiting the expression of caspase-1 can reduce the neuronal injury in the brain after cerebral ischemia/reperfusion and reduce the cerebral infarct area after cerebral ischemia/reperfusion, such as knocking out the caspase-1 gene in mice or using the caspase-1 inhibitor Ac-YVAD = CMK (Liu et al., 2018; Liang et al., 2021). EA may play a similar role.

Under the light microscope, we detected the morphology of nerve cells in hippocampal CA1 area of mice brain by H&E staining, TUNEL+caspase-1 double-labeled staining, and NLRP3+caspase-1 immunofluorescence double staining. Pyroptosis is a form of cell death characterized by both apoptosis and necrosis in morphology and pathophysiology. Its most obvious feature is the rapid formation of plasma membrane pores, cell swelling and osmotic necrosis, and the release of a large number of cell contents and pro-inflammatory mediators to form excessive inflammatory response (Fink and Cookson, 2005). In the I/R group, H&E staining showed the typical characteristics of cell death, loose brain tissue structure, interstitial edema, disordered and swollen nerve cells, pyknosis, and fragmentation of nuclei, and the number of nerve cells decreased significantly. However, in the EA group, the occurrence of this phenomenon was reduced, and only a small amount of nerve cell degeneration and necrosis were observed in the peripheral area of ischemic focus. In TUNEL fluorescence staining, diaminobenzidine (DAB) was used as a marker to detect the active site of peroxidase in cells. Green or brownish-yellow granular precipitates could be formed in apoptotic and focal nuclei, while there was no broken DNA fragment in normal cells and would not react with the marker, so the normal nucleus was blue (Mirzayans and Murray, 2020). In addition, we added caspase-1 staining on the basis of TUNEL in order to identify the pyroptotic neurons which were caspase 1-mediated. In the I/R group, the positive rate of TUNEL and caspase-1 double-stained neurons in C57 mice significantly increased, which suggested that pyroptosis was involved in cerebral ischemia/reperfusion injury. After EA intervention, the positive rate in C57 mice significantly decreased, indicating that EA could reduce the pyroptosis of neurons in hippocampal CA1 area after brain I/R injury, which may be achieved by inhibiting the expression of caspase-1. Previous studies have also shown that acupuncture can inhibit neuronal apoptosis in hippocampus of rats with cerebral ischemia and can promote the recovery of neural cells after cerebral ischemia/reperfusion injury (Wang et al., 2008). Furthermore, double-labeled immunofluorescence showed that NLRP3 and caspase-1 were significantly co-expressed in neurons of C57 mice in the I/R group, which was similar to other studies (Sun et al., 2019; Liu et al., 2021). The number of co-expressed neurons in C57 mice in the EA group was reduced, which suggests that EA intervention may inhibit pyroptosis.

During cerebral ischemia/reperfusion injury, pyroptosis-related inflammatory bodies, such as nlrp1 and NLRP3, are highly expressed in glial cells and neurons. These activated inflammatory bodies activate caspase-1 and induce pyroptosis, which aggravates cerebral ischemia/reperfusion

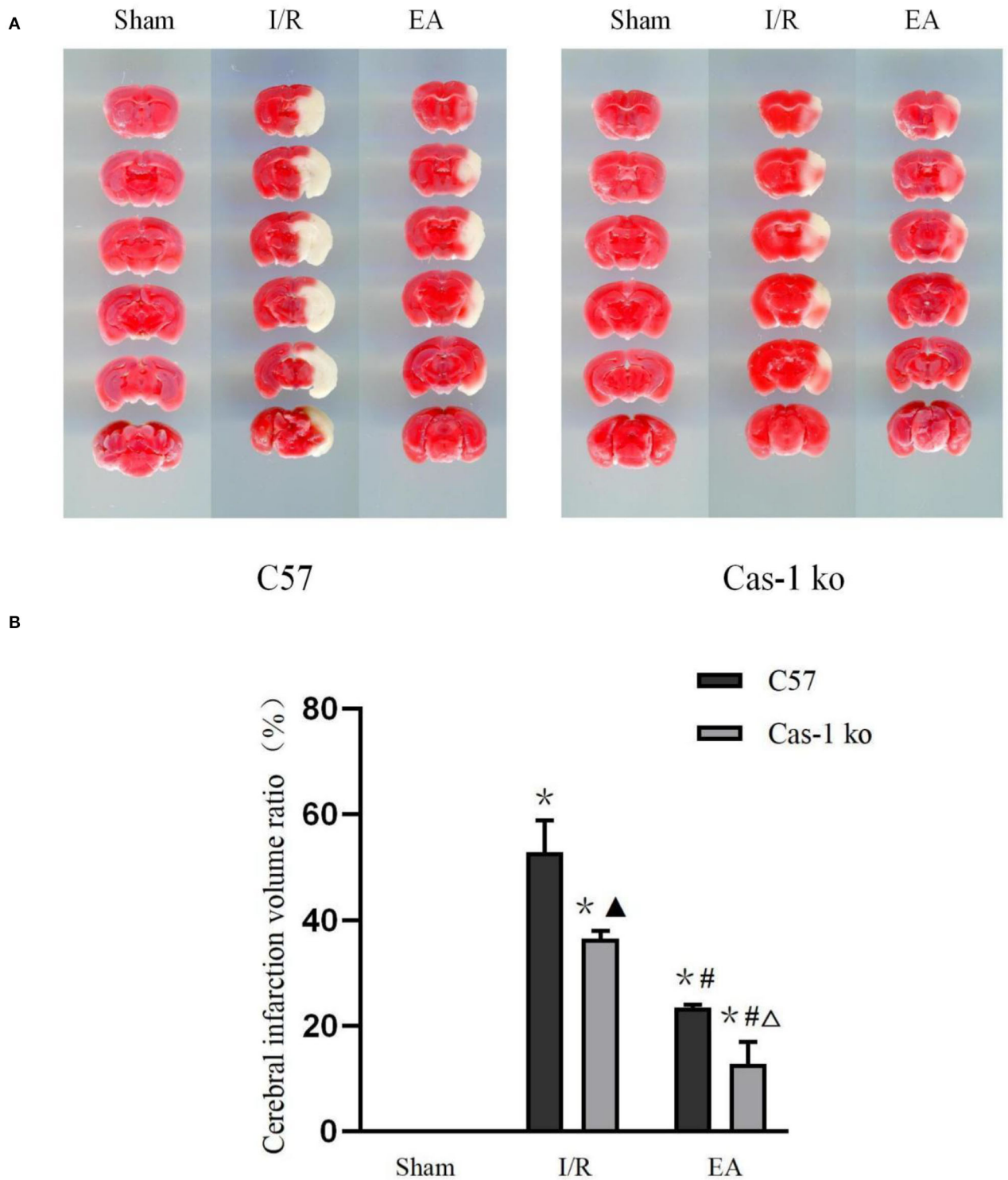

FIGURE 2 | Brain tissue with TTC staining. **(A,B)** TTC staining results of different treatment groups and quantitative analysis of volume ratio. Comparison within the same genotype: $^{*}p < 0.05$ vs. Sham group; $^{\#}p < 0.05$ vs. I/R group. Comparison within the I/R group: $\blacktriangle p < 0.05$ vs. C57 mice. Comparison within the EA group: $\Delta p < 0.05$ vs. C57 mice. Data are representative of four independent experiments [**(A,B)** mean ± SD are representative of values from four independent experiments in **(B)**].

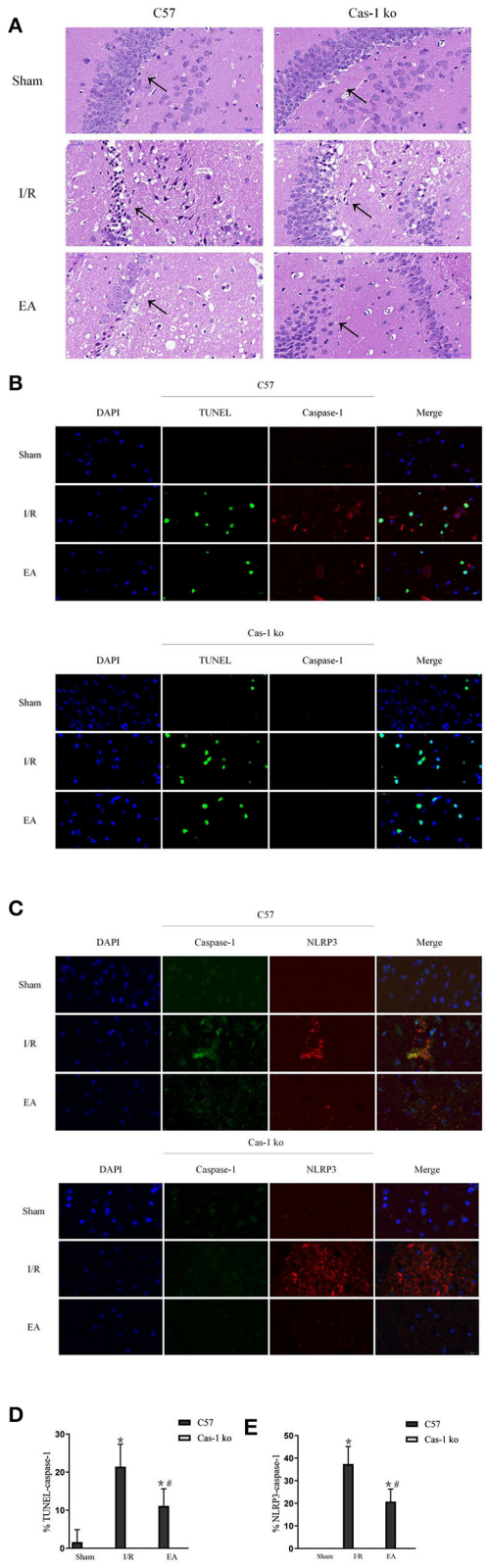

FIGURE 3 | Morphological observation of neuronal injury in hippocampus after I/R injury. **(A)** Pathological HandE staining of neurons in hippocampus. **(B,D)** TUNEL (green)/caspase-1 (red) double-labeled staining of neurons in

(Continued)

FIGURE 3 | hippocampus and quantitative analysis of double-labeled cells. **(C,E)** Double immunofluorescent labeling with caspase-1 (green)/NLRP3 (red) and quantitative analysis of colocalization percentage. Comparison within the same genotype: $^{*}p < 0.05$ vs. Sham group; $^{\#}p < 0.05$ vs. I/R group. Comparison within the I/R group: $\blacktriangle p < 0.05$ vs. C57 mice. Comparison within the EA group: $\Delta p < 0.05$ vs. C57 mice. Data are representative of four independent experiments [**(A–E)** mean ± SD are representative of values from four independent experiments in **(D,E)**].

injury (Chavarría-Smith and Vance, 2015). The results of our Western blot verified this conclusion. In the I/R group, the NLRP3 level of C57 and Cas-1 ko mice was highly expressed, which was significantly different from that of the Sham group. Knockout of caspase-1 gene had no effect on the expression of NLRP3. Cas-1 ko mice expressed NLRP3 at the same level as C57 mice in the I/R group. Studies have shown that activated caspase-1 cleaves gsdmd protein and activates IL-18 and IL-1β precursors at the same time. The cleaved gsdmd protein binds to the inner lobules of the plasma membrane and oligomerizes, resulting in the formation of 10–20 nm pores in the cell membrane, and the release of mature IL-18, IL-1β, and other cell contents outside the cell, thus activating a strong inflammatory cascade (He et al., 2015; Wang et al., 2018). In this study, the expression of pro-caspase-1, cleaved caspase-1 p20, pro-IL-1β, cleaved IL-1β, and GSDMD in C57 mice after cerebral ischemia/reperfusion was significantly higher than those in Cas-1 ko mice in the same treatment group, suggesting that blocking the activation of caspase-1 can effectively inhibit the inflammatory response after cerebral ischemia/reperfusion. After EA intervention, the expression of NLRP3, pro-caspase-1, cleaved caspase-1 p20, pro-IL-1β, cleaved IL-1β, and GSDMD in C57 mice decreased significantly, and the expressions of NLRP3 in Cas-1 ko mice decreased significantly, indicating that EA could inhibit the expression of NLRP3, pro-caspase-1, cleaved caspase-1 p20, pro-IL-1β, cleaved IL-1β, and GSDMD in hippocampus after cerebral ischemia/reperfusion. IL-1β plays an important role in promoting inflammation. Under the pathological conditions of ischemia and hypoxia, it becomes active IL-1β after being cut by caspase-1, induces the activation and adhesion of inflammatory cells, leads to microvascular obstruction, and intensifies the inflammatory response (Davis et al., 2011; Man and Kanneganti, 2015). Therefore, the above results suggest that the neuroprotective effect of EA on cerebral ischemia/reperfusion injury reduces the pyroptosis of nerve cells by inhibiting the expression of NLRP3 and caspase-1, thereby reducing the release of inflammatory factors, such as IL-1β, so as to reduce the inflammatory response.

Studies by Man et al. (2017) described that having a deletion of caspase-1 leads to deletion of caspase-11. Cas-1 ko mice used in this study are C57BL/6N background. Theoretically, caspase-11 is normally expressed and the results of Western blot also confirmed the same. In addition, we also noticed that in the results of cerebral infarction volume measurement and TUNEL staining, there were differences between C57 mice and Cas-1 ko mice in the EA group, and the only factor causing these

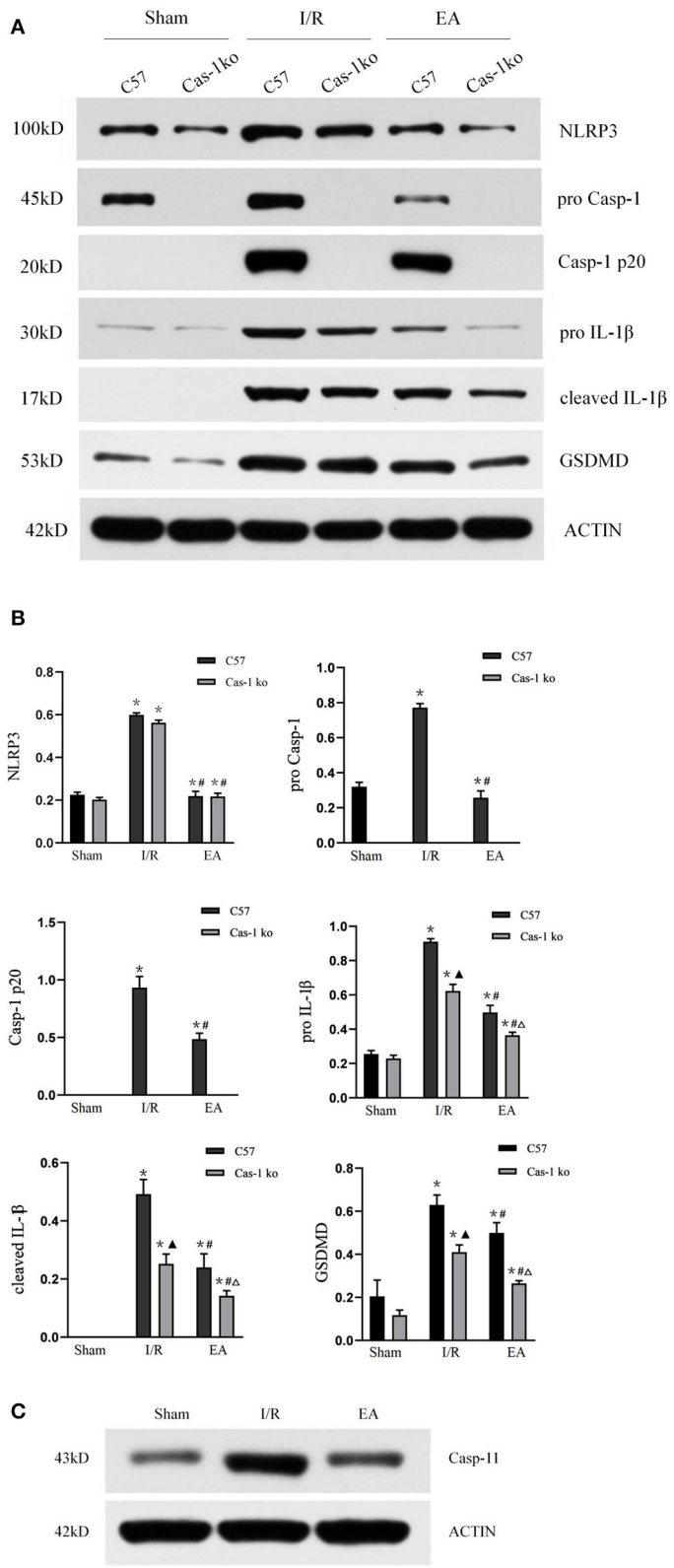

FIGURE 4 | Protein expression of pyroptosis-related proteins. **(A,B)** Western blotting analysis of NLRP3, pro-Casp-1, Casp-1 p20, IL-1β, cleaved IL-1β, and GSDMD in different treatment groups and quantitative analysis of bands. **(C)** Western blotting analysis of casp-11 in Cas-1 ko mice. Comparison within the same genotype: $^{*}p < 0.05$ vs. Sham group; $^{\#}p < 0.05$ vs. I/R group. Comparison within the I/R group: $\blacktriangle p < 0.05$ vs. C57 mice. Comparison within the EA group: $\Delta p < 0.05$ vs. C57 mice. Data are representative of two **(C)** or four independent experiments [**(A,B)** mean ± SD are representative of values from four independent experiments in **(B)**].

differences was caspase-1 knockout. Combined with the protein electrophoresis data of C57 mice, EA can inhibit the expression of caspase-1, but it cannot completely block the gene as Cas-1 ko mice. Interestingly, there was no significant difference between the neurological function score and the staining results of different genotypes in the EA group. We speculated that EA could not only inhibit the occurrence of pyroptosis, but also play a neuroprotective role in other ways. Our previous studies have confirmed that EA can upregulate the p-ERK protective pathway and inhibit p38MAPK apoptosis pathway after cerebral ischemia–reperfusion in mice (Wu et al., 2015, 2018; Lan et al., 2017). These mechanisms can be used as an evidence of our above hypothesis, that is, EA can resist cerebral ischemia–reperfusion injury in a variety of ways.

In conclusion, EA at points "LU5," "LI4," "ST36," and "SP6" can significantly improve the symptoms of nerve injury and morphological changes of brain cells in mice with cerebral ischemia/reperfusion injury, reduce the infarct area, and protect brain tissue from ischemic injury. This treatment reduced the expression of NLRP3, caspase-1, and IL-1β, and the occurrence of cell pyroptosis and inflammatory response, suggesting that the protective effect of EA on cerebral ischemia/reperfusion injury may be played by inhibiting the pyroptosis pathway dependent on caspase-1.

DATA AVAILABILITY STATEMENT

The original contributions presented in the study are included in the article/supplementary materials, further inquiries can be directed to the corresponding author/s.

ETHICS STATEMENT

The animal study was reviewed and approved by Animal Ethics and Welfare Committee of Southern Medical University of China.

AUTHOR CONTRIBUTIONS

G-PZ obtained funding and participated in study concept and design, and paper authorization. X-HX and ML purchased animals and material instruments. Z-YY analyzed data. LC wrote the paper. M-MD operated the acupuncture. LY ensured the integrity of the data. All authors approved the final version of the article.

FUNDING

This study was supported by the National Natural Science Foundation of China, (No. 81674048). The funding body played no role in the study design, in the collection, analysis, and interpretation of data, in the writing of the report, or in the decision to submit the article for publication.

ACKNOWLEDGMENTS

The authors are very grateful to all staff from the Experimental Animal Center of the Southern Medical University of China and thank all the researchers involved in animal experiments.

REFERENCES

Bergsbaken, T., and Fink, S. L. (2009). Pyroptosis: host cell death and inflammation. *Nat. Rev. Microbiol.* 7, 99–109. doi: 10.1038/nrmicro2070

Chavarría-Smith, J., and Vance, R. E. (2015). The NLRP1 inflammasomes. *Immunol. Rev.* 265, 22-34. doi: 10.1111/imr.12283

Dabrowska-Bender, M., Milewska, M., Gołabek, A., and Duda-Zalewska, A. (2017). The impact of ischemic cerebral stroke on the quality of life of patients based on clinical, social, and psychoemotional factors. *J. Stroke Cerebrovasc. Dis.* 26, 101–107. doi: 10.1016/j.jstrokecerebrovasdis.2016.08.036

Davis, B. K., Wen, H., and Ting, J. P. (2011). The inflammasome NLRs in immunity, inflammation, and associated diseases. *Annu. Rev. Immunol.* 29, 707-35. doi: 10.1146/annurev-immunol-031210-101405

Doitsh, G., Galloway, N. L., Geng, X., Yang, Z., Monroe, K. M., and Zepeda, O. (2014). Cell death by pyroptosis drives CD4 T-cell depletion in HIV-1 infection. *Nature* 505, 509–514. doi: 10.1038/nature12940

Fann, D., Lee, Y. W., Manzanero, S. Y., Tang, S., Gelderblom, S. C., and Chunduri, M. P., et al. (2013). Intravenous immunoglobulin suppresses NLRP1 and NLRP3 inflammasome-mediated neuronal death in ischemic stroke. *Cell Death Dis.* 4, e790–e790. doi: 10.1038/cddis.2013.326

Fink, S. L., and Cookson, B. T. (2005). Apoptosis, pyroptosis, and necrosis: mechanistic description of dead and dying eukaryotic cells. *Infect. Immun.* 73, 1907–1916. doi: 10.1128/IAI.73.4.1907-1916.2005

He, Q. I., Li, Z., Wang, Y., Hou, Y., and Li, L. (2017). Resveratrol alleviates cerebral ischemia/reperfusion injury in rats by inhibiting NLRP3 inflammasome activation through Sirt1-dependent autophagy induction. *Int. Immunopharmacol.* 50, 208–215. doi: 10.1016/j.intimp.2017.06.029

He, W. T., Wan, H., Hu, L., Chen, P., Wang, X., Huang, Z., et al. (2015). Gasdermin D is an executor of pyroptosis and required for interleukin-1β secretion. *Cell Res.* 25, 1285–1298. doi: 10.1038/cr.2015.139

Jin, C. (2010). Molecular mechanism of NLRP3 inflammasome activation. *J. Clin. Immunol.* 30, 628-631. doi: 10.1007/s10875-010-9440-3

Jittiwat, J. (2019). Baihui point laser acupuncture ameliorates cognitive impairment, motor deficit, and neuronal loss partly via antioxidant and anti-inflammatory effects in an animal model of focal ischemic stroke. *Evid Based Complement Alternat Med.* 2019, 1–9. doi: 10.1155/2019/1204709

Jorgensen, I. (2015). Pyroptotic cell death defends against intracellular pathogens. *Immunol. Rev.* 265, 130–142. doi: 10.1111/imr.12287

Kawaguchi, M., Takahashi, M., Hata, T., Kashima, Y., Usui, F., and Morimoto, H. (2011). Inflammasome activation of cardiac fibroblasts is essential for myocardial ischemia/reperfusion injury. *Circulation* 123, 594–604. doi: 10.1161/CIRCULATIONAHA.110.982777

Kim, J. H., Choi, K. H., Jang, Y. J., Bae, S. S., Shin, B. C., Choi, B. T., et al. (2013a). Electroacupuncture acutely improves cerebral blood flow and attenuates moderate ischemic injury via an endothelial mechanism in mice. *PLoS ONE.* 8, e56736. doi: 10.1371/journal.pone.0056736

Kim, Y. R., Kim, H. N., Jang, J. Y., Park, C., Lee, J. H., and Shin, H. K. (2013b). Effects of electroacupuncture on apoptotic pathways in a rat model of focal cerebral ischemia. *Int. J. Mol. Med.* 32, 1303–1310. doi: 10.3892/ijmm.2013.1511

Lan, X., Zhang, X., Zhou, G. P., Wu, C. X., and Li, C. (2017). Electroacupuncture reduces apoptotic index and inhibits p38 mitogen-activated protein kinase signaling pathway in the hippocampus of rats with cerebral ischemia/reperfusion injury. *Neural Regener. Res.* 12, 409–416. doi: 10.4103/1673-5374.202944

Li, Z. R. (2007). *Experimental Acupuncture Science*. Beijing: China Press of Traditional Chinese Medicine.

Liang, Y., Song, P., Chen, W., Xie, X., Luo, R., Su, J., et al. (2021). Inhibition of caspase-1 ameliorates ischemia-associated blood-brain barrier dysfunction and integrity by suppressing pyroptosis activation. *Front. Cell Neurosci*. 14, 540669. doi: 10.3389/fncel.2020.540669

Liu, W., Chen, Y., Meng, J., Wu, M., Chang, B. i. F., and Li, C. H and Zhang L. (2018). Ablation of caspase-1 protects against TBI-induced pyroptosis in vitro and in vivo. *J Neuroinflammation*. 15, 48. doi: 10.1186/s12974-018-1083-y

Liu, X., Zhang, M., Liu, H., Zhu, R., He, H., and Zhou, Y. (2021). Bone marrow mesenchymal stem cell-derived exosomes attenuate cerebral ischemia-reperfusion injury-induced neuroinflammation and pyroptosis by modulating microglia M1/M2 phenotypes. *Exp. Neurol.* 341, 113700. doi: 10.1016/j.expneurol.2021.113700

Longa, E. Z., Weinstein, P. R., and Carlson, S. (1989). Reversible middle cerebral artery occlusion without craniectomy in rats. *Stroke* 20, 84–91. doi: 10.1161/01.STR.20.1.84

Lv, B., Jiang, X. M., Wang, D. W., Chen, J., and Han, D. F. (2020). Protective effects and mechanisms of action of ulinastatin against cerebral ischemia-reperfusion injury. *Curr. Pharm. Des.* 26, 3332–3340. doi: 10.2174/1381612826666200303114955

Man, S. M., and Kanneganti, T. D. (2015). Regulation of inflammasome activation. *Immunol. Rev*. 265, 6–21. doi: 10.1111/imr.12296

Man, S. M., Karki, R., Briard, B., Burton, A., Gingras, S., Pelletier, S., et al. (2017). Differential roles of caspase-1 and caspase-11 in infection and inflammation. *Sci. Rep*. 7, 45126. doi: 10.1038/srep45126

Mirzayans, R., and Murray, D. (2020). Do TUNEL and other apoptosis assays detect cell death in preclinical studies? *Int. J. Mol. Sci*. 21, 9090. doi: 10.3390/ijms21239090

Nierhaus, T., Chang, Y., Liu, B., Shi, X., Yi, M., Witt, C. M., et al. (2019). Somatosensory stimulation with XNKQ acupuncture modulates functional connectivity of motor areas. *Front. Neurosci*. 13, 147. doi: 10.3389/fnins.2019.00147

Rathinam, V. A. (2016). Inflammasome complexes: emerging mechanisms and effector functions. *Cell* 165, 792–800. doi: 10.1016/j.cell.2016.03.046

Ren, L., Wang, Y. K., Fang, Y. N., Zhang, A. W., and Li, X. L. (2010). Effect of electroacupuncture therapy on the expression of Na(v)1.1 and Na(v)1.6 in rat after acute cerebral ischemia. *Neurol Res.* 32, 1110–1116. doi: 10.1179/016164110X12700393823453

Sun, Y. B., Zhao, H., Mu, D. L., Zhang, W., Cui, J., Wu, L., et al. (2019). Dexmedetomidine inhibits astrocyte pyroptosis and subsequently protects the brain in in vitro and in vivo models of sepsis. *Cell Death Dis*. 10, 167. doi: 10.1038/s41419-019-1416-5

Walsh, J. G., and Muruve, D. A. (2014). Inflammasomes in the CNS. *Nat. Rev. Neurosci.* 15, 84–97. doi: 10.1038/nrn3638

Wang, J., Sahoo, M., Lantier, L., Warawa, J., Cordero, H., Deobald, K., et al. (2018). Caspase-11-dependent pyroptosis of lung epithelial cells protects from melioidosis while caspase-1 mediates macrophage pyroptosis and production of IL-18. *PLoS Pathog.* 14, e1007105. doi: 10.1371/journal.ppat.1007105

Wang, T., Liu, C. Z., Jiang, Y. u. J. C., and Han, W. JX. (2008). Acupuncture protected cerebral multi-infarction rats from memory impairment by regulating the expression of apoptosis related genes Bcl-2 and Bax in hippocampus. *Physiol. Behav*. 96, 155–161. doi: 10.1016/j.physbeh.2008.09.024

Wang, Y., Shen, Y., Lin, H. P., Li, Z., and Chen, Y. Y. (2016). Large-conductance Ca2+-activated K+ channel involvement in suppression of cerebral ischemia/reperfusion injury after electroacupuncture at Shuigou (GV26) acupoint in rats. *Neural Regener. Res.* 11, 957–962. doi: 10.4103/1673-5374.184495

Wellington, M., Koselny, K., and Sutterwala, F. S. (2014). Candida albicans triggers NLRP3-mediated pyroptosis in macrophages. *Eukar. Cell* 13, 329–340. doi: 10.1128/EC.00336-13

Wu, C., Wang, J., Li, C., Zhou, G., Xu, X., and Zhang, X. (2015). Effect of electroacupuncture on cell apoptosis and ERK signal pathway in the hippocampus of adult rats with cerebral ischemia-reperfusion. *Evid. Based Complement. Alternat. Med*. 2015, 1–10. doi: 10.1155/2015/414965

Wu, C., Zhou, L. C., Yang, G., Jiang, L., Chen, G., Li, J., et al. X. (2017). Effects of electroacupuncture on the cortical extracellular signal regulated kinase pathway in rats with cerebral ischaemia/reperfusion. *Acupunct Med*. 35, 430–436. doi: 10.1136/acupmed-2016-011121

Wu, C. X., Feng, Y. H., Yang, L., Zhan, Z. L., Xu, X. H., and Hu, X. Y. (2018). Electroacupuncture exerts neuroprotective effects on ischemia/reperfusion injury in JNK knockout mice: the underlying mechanism. *Neural Regener. Res.* 13, 1594–1601. doi: 10.4103/1673-5374.235294

Xue, X., You, Y., Tao, J., Ye, X., Huang, J., Yang, S., et al. (2014). Electro-acupuncture at points of Zusanli and Quchi exerts anti-apoptotic effect through the modulation of PI3K/Akt signaling pathway. *Neurosci. Lett*. 558, 14–19. doi: 10.1016/j.neulet.2013.10.029

Yang, Z. X., Xie, J. H., Liu, Y. P., Miao, G. X., Wang, Y. H., and Wu, S. M. (2015). Systematic review of long-term Xingnao Kaiqiao needling effcacy in ischemic stroke treatment. *Neural Regener. Res.* 10, 583–588. doi: 10.4103/1673-5374.155431

Zhang, G. C., Fu, W. B., Xu, N. G., Liu, J. H., Zhu, X. P., and Liang, Z. H. (2012). Meta analysis of the curative effect of acupuncture on post-stroke depression. *J. Tradition. Chin. Med.* 32, 6–11. doi: 10.1016/S0254-6272(12)60024-7

Zhou, M., Wang, H., Zeng, X., Yin, P., Zhu, J., and Chen, W. (2019). Mortality, morbidity, and risk factors in China and its provinces, 1990–2017: a systematic analysis for the Global Burden of Disease Study 2017. *Lancet* 394, 1145–1158. doi: 10.1016/S0140-6736(19)30427-1

Zhu, W., Ye, Y., Liu, Y., Wang, X. R., Shi, G. X., and Zhang, S. (2017). Mechanisms of acupuncture therapy for cerebral ischemia: an evidence-based review of clinical and animal studies on cerebral ischemia. *J. Neuroimmune Pharmacol.* 12, 575–592. doi: 10.1007/s11481-017-9747-4

Conflict of Interest: The authors declare that the research was conducted in the absence of any commercial or financial relationships that could be construed as a potential conflict of interest.

Publisher's Note: All claims expressed in this article are solely those of the authors and do not necessarily represent those of their affiliated organizations, or those of the publisher, the editors and the reviewers. Any product that may be evaluated in this article, or claim that may be made by its manufacturer, is not guaranteed or endorsed by the publisher.

frontiers | Frontiers in Molecular Neuroscience

ORIGINAL RESEARCH
published: 10 May 2022
doi: 10.3389/fnmol.2022.852882

Efficacy and Mechanism of Moxibustion Treatment on Mild Cognitive Impairment Patients: An fMRI Study Using ALFF

Ziyan Lai[1†], Qingping Zhang[1†], Lingyan Liang[1†], Yichen Wei[1†], Gaoxiong Duan[1], Wei Mai[2], Lihua Zhao[2], Peng Liu[3] and Demao Deng[1]*

[1]*Department of Radiology, The People's Hospital of Guangxi Zhuang Autonomous Region, Guangxi Academy of Medical Sciences, Nanning, China,* [2]*Department of Acupuncture, The First Affiliated Hospital, Guangxi University of Chinese Medicine, Nanning, China,* [3]*Life Science Research Center, School of Life Science and Technology, Xidian University, Xi'an, China*

OPEN ACCESS

Edited by:
Jiao Liu,
Fujian University of Traditional Chinese Medicine, China

Reviewed by:
Yiheng Tu,
Institute of Psychology (CAS), China
Ling Zhao,
Chengdu University of Traditional Chinese Medicine, China
Huangan Wu,
Shanghai University of Traditional Chinese Medicine, China
Yi-Hung Chen,
China Medical University (Taiwan), Taiwan

***Correspondence:**
Demao Deng
demaodeng@163.com

†These authors have contributed equally to this work and share first authorship

Specialty section:
This article was submitted to Neuroplasticity and Development, a section of the journal Frontiers in Molecular Neuroscience

Received: *11 January 2022*
Accepted: *19 April 2022*
Published: *10 May 2022*

Citation:
Lai Z, Zhang Q, Liang L, Wei Y, Duan G, Mai W, Zhao L, Liu P and Deng D (2022) Efficacy and Mechanism of Moxibustion Treatment on Mild Cognitive Impairment Patients: An fMRI Study Using ALFF. Front. Mol. Neurosci. 15:852882. doi: 10.3389/fnmol.2022.852882

Background: Mild Cognitive Impairment (MCI), as a high risk of Alzheimer's disease (AD), represents a state of cognitive function between normal aging and dementia. Moxibustion may effectively delay the progression of AD, while there is a lack of studies on the treatments in MCI. This study aimed to evaluate the effect of moxibustion treatment revealed by the amplitude of low-frequency fluctuation (ALFF) in MCI.

Method: We enrolled 30 MCI patients and 30 matched healthy controls (HCs) in this study. We used ALFF to compare the difference between MCI and HCs at baseline and the regulation of spontaneous neural activity in MCI patients by moxibustion. The Mini-Mental State Examination and Montreal Cognitive Assessment scores were used to evaluate cognitive function.

Results: Compared with HCs, the ALFF values significantly decreased in the right temporal poles: middle temporal gyrus (TPOmid), right inferior temporal gyrus, left middle cingulate gyrus, and increased in the left hippocampus, left middle temporal gyrus, right lingual gyrus, and right middle occipital gyrus in MCI patients. After moxibustion treatment, the ALFF values notably increased in the left precuneus, left thalamus, right temporal poles: middle temporal gyrus, right middle frontal gyrus, right inferior temporal gyrus, right putamen, right hippocampus, and right fusiform gyrus, while decreased in the bilateral lingual gyrus in MCI patients. The Mini-Mental State Examination and Montreal Cognitive Assessment scores increased after moxibustion treatment, and the increase in Mini-Mental State Examination score was positively correlated with the increase of ALFF value in the right TPOmid, the right insula, and the left superior temporal gyrus.

Conclusion: Moxibustion treatment might improve the cognitive function of MCI patients by modulating the brain activities within the default mode network, visual network, and subcortical network with a trend of increased ALFF values and functional asymmetry of the hippocampus. These results indicate that moxibustion holds great potential in the treatment of MCI.

Keywords: mild cognitive impairment, dementia, functional magnetic resonance imaging, neurological function, amplitude of low frequency fluctuation

INTRODUCTION

Mild Cognitive Impairment (MCI) has evolved over the past two decades to represent a pathological state between normal cognitive aging and dementia (Petersen, 2016). It increases the risk of developing Alzheimer's disease (AD) or other dementia (Alzheimer's Disease International M. U., 2021). The prevalence of amyloid pathology, which serves as an essential biomarker of AD, increased from 27% to 71% among MCI patients (Jansen et al., 2015), and the annual incidence rate of individuals with MCI progressing to AD is about 10%–12% (Langa and Levine, 2014). Early and timely effective treatment for individuals in this state may prevent or delay the progression to AD, even revert to normal cognitive function. Unfortunately, there are no approved treatment approaches for MCI.

Moxibustion is a treatment that uses the heat generated by burning moxa sticks to stimulate acupoints, producing a central nervous system regulation similar to acupuncture (Bao et al., 2016). It is a commonly accepted treatment approach for cognitive impairment in East Asia (Aum et al., 2021), with the advantages of painlessness, ease of operation, and fewer adverse events. A systematic review showed that moxibustion could participate in inhibiting oxidative stress and cell apoptosis, adjusting inflammation and Aβ genesis activation of vascular endothelial growth factor, and regulating the metabolic products in the tricarboxylic acid cycle and fatty acid metabolism (Aum et al., 2021). In addition, moxibustion could alleviate the depression-like behavior and adjust tryptophan transport and 5-HT generation (Li et al., 2019). Ha et al. (2020) found that the effect of moxibustion on the cognition of aging mice is associated with the genes and proteins involved in the APP metabolic pathway. Through these mechanisms, moxibustion has good potential in treating cognitive impairment diseases, especially in restraining AD-related Aβ genesis. Recently a review provided credible support for moxibustion in the treatment of AD (A et al., 2021). In the study of vascular dementia rats, it has also been confirmed that moxibustion improves cognitive function, and its mechanism may be related to the inhibition of hippocampal neuronal apoptosis (Yang et al., 2021). The effect of moxibustion on the central nervous system is mainly reflected in the brain function regulation of the default mode network (DMN) including the medial prefrontal cortex and posterior cingulate cortex (Bao et al., 2016). DMN is involved in the process of advanced cognition and is the most susceptible brain network in AD patients (Krajcovicova et al., 2014). Some studies showed that moxibustion could regulate symptoms of MCI (Liu et al., 2020; Zhang et al., 2020), but the efficacy has not been fully validated, and the mechanism remains unclear.

Rest-state functional magnetic resonance imaging (rs-fMRI) has good sensitivity for detecting neuronal activity and functional abnormalities in neurodegenerative diseases. The amplitude of the cerebral blood oxygen level-dependent (BOLD) signals detected by rs-fMRI reflects the energy expenditure and intensity of neuronal activity (Tomasi et al., 2013). The amplitude of low-frequency fluctuation (ALFF) is a data-driven rs-fMRI analysis method that measures the total power of the BOLD signals in the low-frequency range of 0.01 Hz to 0.1 Hz, reflecting abnormal spontaneous neural activity in the brain region (Fox and Raichle, 2007; Zang et al., 2007; Zou et al., 2008). ALFF was able to reflect trends in altered neural activity in AD spectrum disorders and identify differences in healthy people, MCI, and AD (Yang et al., 2018). It was observed to characterize the spontaneous brain activity in MCI or AD patients reliably (Cha et al., 2015). Therefore, we chose ALFF to analyze the abnormal brain function in MCI patients and explore the central mechanism of moxibustion on MCI.

MATERIALS AND METHODS

Participants

A total of 30 MCI patients were recruited through posting advertisements in the local elderly activity center and communities, and 30 normal subjects were recruited as healthy controls (HCs).

The inclusion criteria for MCI patients: (1) between 55 and 75 years old; (2) no dementia; (3) memory impairment was the chief complaint and confirmed by the informant; (4) the ability of daily living was not affected; (5) general cognitive function is basically normal or slightly impaired; (6) without diseases that can lead to the decline of brain function; (7) the clinical dementia rating score: 0.5 points, and the Global deterioration Scale score: 2–3 points.

The exclusion criteria for MCI patients: (1) history of mental illness, such as major depressive disorder; (2) history of neurological diseases that could cause cognitive abnormalities, including encephalitis, brain tumors, and epilepsy; (3) history of other systemic diseases that could cause cognitive abnormalities, including thyroid dysfunction, severe anemia, and syphilis; (4) communication and language impairments, including severe hearing or vision disorders; (5) history of vascular diseases, such as cerebral infarction; (6) taking drugs that could induce cognitive changes or vital organs failure, such as brain, kidneys, and heart; (7) contraindications to MRI; (8) left-handed or two-handed people, or old people with no hands.

Moxibustion Treatment

According to previous studies on the treatment of cognitive disorders with moxibustion (Aum et al., 2021), we selected six acupoints including Guanyuan, Baihui, bilateral Xuanzhong, and bilateral Zusanli in the MCI group. All MCI patients were treated with moxibustion by the same acupuncturist. Because scarring moxibustion may cause suppuration and leave a scar, our research used non-scarring moxibustion which was similar to other researchers and more acceptable (Pacific WHOROftW, 2007; Bao et al., 2016). When treated with moxibustion, vaseline was applied on the acupoints to protect the subjects' skin and facilitate the fixing of the moxa-cones. A moxa-cone had a diameter of 1.5 cm, height of 3 cm, and a weight of 5 g. Each acupoint was placed with a moxa-cone, and each moxa-cone was burned for about 3–4 min. The moxa-cone was replaced when the length of the burning moxa-cone was close to the patient's skin and the patient felt the burning and uncomfortable. Three moxa-cones were used each time in one acupoint. At the end of each duration, the acupuncture points were gently massaged

with cotton swabs. The MCI group was treated every other day, with a total of two courses of treatment, 15 times as a course of treatment, and a 3-day rest interval between the two courses.

Clinical Measurements

The main desired therapeutic effect in the present study is the improvement of cognitive function, which needs to be measured by practical evaluation tools. Currently recognized tools for evaluating cognitive function include the Mini-Mental State Examination (MMSE) and Montreal Cognitive Assessment (MoCA). The higher the MMSE and MoCA scores, the better cognitive function. In our study, MCI patients and HCs were evaluated at baseline, respectively, and then MCI patients were re-evaluated after two months of moxibustion treatment.

MRI Data Acquisition

All MRI data were collected by a 3.0 T Siemens Magnetom Verio MRI System (Siemens Medical, Erlangen, Germany). A 6-min rs-MRI data was collected at HCs without any intervention. However, MCI patients need to collect MRI data twice totally in without intervention and after a moxibustion treatment. To reduce movement, each subject's head was immobilized by foam pads in a standard head coil. The 6-min rs-fMRI data were acquired with a single-shot gradient-recalled echo-planar imaging (EPI) sequence with the following parameters: repetition time (TR) = 2,000 ms; echo time (TE) = 30 ms; flip angle (FA) = 90°; field of view (FOV) = 240 mm × 240 mm; matrix size: 64 × 64; slice thickness = 5 mm (no-gap); 31 slices and 180 volumes. High resolution T1-weighted images were then obtained with a magnetization-prepared rapid acquisition gradient-echo sequences (3D MPRAGE) with the following parameters: TR = 1,900 ms; TE = 2.22 ms; FOV = 250 mm × 250 mm; matrix size: 256 × 256; FA = 9°; slice thickness = 1 mm and 176 slices.

Data Preprocessing

The rs-fMRI data were analyzed by the Data Processing and Analysis for Brain Imaging (DPABI[1]) with Statistical Parametric Mapping, version 12 (SPM12[2]) running under MATLAB platform. The preprocessing steps are as follows: the first five-time points were removed; slice timing correction; head motion correction; normalizing the corrected images spatial to the Montreal Neurological Institute (MNI) space (EPI template with 3 × 3 × 3 mm^3 voxel size); nuisance signal removal (including head motion parameters, global signal, white matter, cerebrospinal fluid as covariates); linear detrended removal and temporal bandpass filtering (0.01–0.1 Hz). If the translation or rotation of head movement was >2.5 mm or >2.5° in any direction, we excluded subjects' data from further analysis.

ALFF Analysis

Each subject used the DPABI program described above for ALFF analysis. The ALFF reflects the intensity of regional spontaneous neural activity and is more sensitive to distinguishing the differences between groups (Fox and Raichle, 2007; Zang et al., 2007; Zou et al., 2008). Fast Fourier transform (FFT) was used to convert the filtered time series to the frequency domain and calculated the square root of the power at each frequency to obtain the amplitude value. ALFF was computed as the sum of the amplitudes of the low low-frequency power range from 0.01 to 0.1 Hz. In order to reduce the overall effect of variability among different participants, each subject used the mean value of within-brain ALFF to standardize ALFF. In addition, the calculation of ALFF was spatially smoothed using a Gaussian kernel with a full width at half maximum of 6 × 6 × 6 mm^3.

Statistical Analysis

Demographic and neuropsychological data of the MCI and HCs groups were calculated by SPSS software (version 22.0; IBM, Armonk, New York). Normal distribution continuous variables were tested by two independent samples t-test, and non-normally distributed variables were tested by Mann-Whitney *U*-test. Pearson's Chi-square test compared categorical variables. In all comparisons, the statistical significance threshold was set at $p < 0.05$.

We used a two-sample t-test to investigate the differences in the normalized ALFF values between MCI patients and HCs (gender, age, and educational level were considered insignificant covariates). Using paired t-tests to quantitatively compare the differences of ALFF values between pre- and post-moxibustion treatment within a gray matter mask using statistical parametric mapping. All statistical graphs are calibrated using the false discovery rate (FDR) correction method, and the significance of the voxel level was set at a $p < 0.05$.

To investigate relationships between changed ALFF of the whole brain and changed clinical symptoms (after treatment − before treatment), and to avoid any unintentional bias induced by region-specific prior hypotheses, a regression analysis was conducted to evaluate the relationships of ALFF values with MMSE in MCI patients. The significance level was set at $p < 0.05$ (FDR correction).

RESULTS

Demographic and Clinical Neuropsychological Data

This study included 60 subjects, including 30 MCI patients and matched HCs. There were no statistically significant differences between the two groups regarding age, gender ratio, and educational level. Compared with HCs, the MoCA and MMSE scores were significantly lower ($p < 0.0001$) in MCI patients. Their demographic data and cognitive scores are summarized in **Table 1**. After moxibustion treatment, the MoCA and the MMSE scores significantly increased in MCI patients ($p < 0.0001$; **Table 2**).

ALFF Contrasts

We first compared MCI patients and HCs to find the regions showing altered ALFF values in MCI patients (**Figure 1**; **Table 3**). Compared with HCs, MCI patients showed significantly decreased ALFF values in the right temporal poles: middle

[1]http://rfmri.org/dpabi
[2]http://www.fil.ion.ucl.ac.uk/spm

TABLE 1 | Demographic data and cognitive scores in MCI patients and HCs.

Characteristic	MCI (n = 30) (mean±SD)	HCs (n = 30) (mean±SD)	p value
Age (years)	64.30 ± 6.05	66.07 ± 5.91	0.257[a]
Gender (M/F)	10/20	13/17	0.425[b]
Education (years)	11 (11–14)[d]	14 (8–15)[d]	0.129[c]
Pre-MMSE	26 (25–27)[d]	29 (28–30)[d]	0.000[c]
Pre-MoCA	21.83 ± 2.60	25.57 ± 2.06	0.000[a]

[a]*p-values were calculated with a two-sample t-test.* [b]*p-values were calculated with a chi-square test.* [c]*p-values were calculated with Mann-Whitney U-test.* [d]*Median (interquartile range).*

TABLE 2 | Cognitive scores of MCI patients pre- and post-moxibustion treatment.

Characteristic	MCI_POST (n = 30)	MCI_PRE (n = 30)	p value
MMSE change	29.5 (28–30)[d]	26 (25–27)[d]	0.000[e]
MoCA change	27 (25–28.25)[d]	21 (20.75–23.25)[d]	0.000[e]

MoCA change: post-treatment MoCA score minus pre-treatment MoCA score. MMSE change: post-treatment MMSE score minus pre-treatment MMSE score. [d]*Median (interquartile range).* [e]*P-values were calculated with Wilcoxon Signed Ranks Test.*

temporal gyrus (TPOmid), right inferior temporal gyrus (ITG), left middle cingulate gyrus (MCC). As well, the ALFF values in the left hippocampus (HIPP), left middle temporal gyrus (MTG), right lingual gyrus (LING), and right middle occipital gyrus (MOG) increased.

Then, we performed comparisons in pre- and post-moxibustion treatment to explore the effects of moxibustion in MCI (**Figure 2**; **Table 4**). After moxibustion treatment, the ALFF values in the left precuneus (PCUN), left thalamus (THA), right TPOmid, right middle frontal gyrus (MFG), right ITG, right putamen (PUT), right HIPP, and right fusiform gyrus (FFG) significantly increased. However, the ALFF values in the bilateral LING decreased.

The Association Between ALFF Values and Clinical Changes

After moxibustion treatment, the increase of MMSE score was significantly positively correlated with the increase of ALFF value in the right TPOmid, the right insula, and the left superior temporal gyrus (**Figure 3**). There was no significant negative correlation between any ALFF value in brain regions in brain regions and MMSE scores in MCI patients.

DISCUSSION

Our study applied the ALFF approach to fMRI data to investigate the alterations of spontaneous neural activity and the central mechanism of moxibustion in MCI patients. We found that MCI patients showed altered ALFF in a set of brain regions, mainly including the DMN and visual network (VIN). Moxibustion improved the cognitive function by regulating the spontaneous

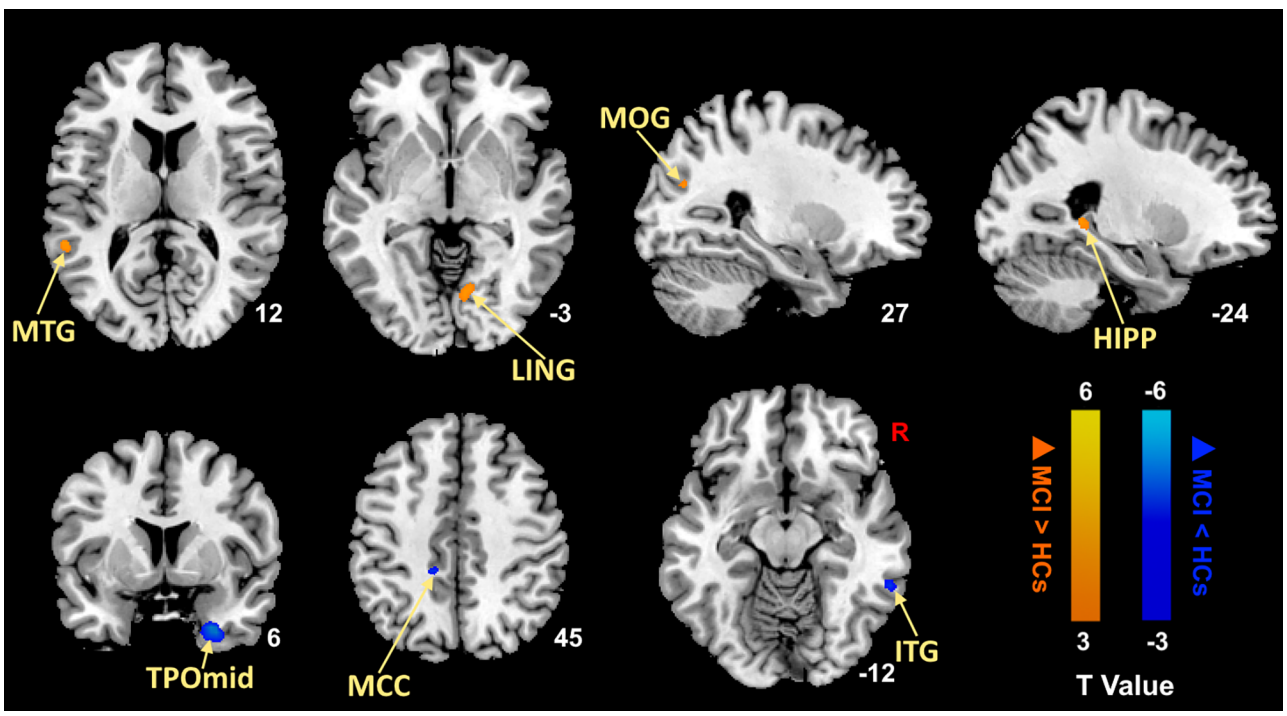

FIGURE 1 | Brain regions with significantly different ALFF values of MCI patients compared with HCs ($p < 0.05$, FDR correction). Warm color represents an increase and cool color represents a decrease respectively. ALFF, amplitude of low-frequency fluctuation; FDR, false discovery rate; MTG, middle temporal gyrus; LING, lingual gyrus; MOG, middle occipital gyrus; HIPP, hippocampus; TPOmid, temporal poles: middle temporal gyrus; MCC, middle cingulate gyrus; ITG, inferior temporal gyrus; MCI, mild cognitive impairment; HCs, healthy controls.

TABLE 3 | Brain regions with different ALFF values between MCI patients and HCs in the resting state.

	Brain regions	Brodmann area	Peak MNI coordinates			Cluster size	T-value
			x	y	z		
decreased in MCI	R_TPOmid	36	27	5	−36	78	−4.49
	R_ITG	20	60	−45	−12	107	−3.68
	L_MCC	0	−12	−36	45	102	−3.21
increased in MCI	L_HIPP	37	−24	−39	3	84	3.06
	L_MTG	22	−54	−45	12	86	3.22
	R_LING	18	9	−69	−3	96	3.32
	R_MOG	19	27	−72	24	88	3.02

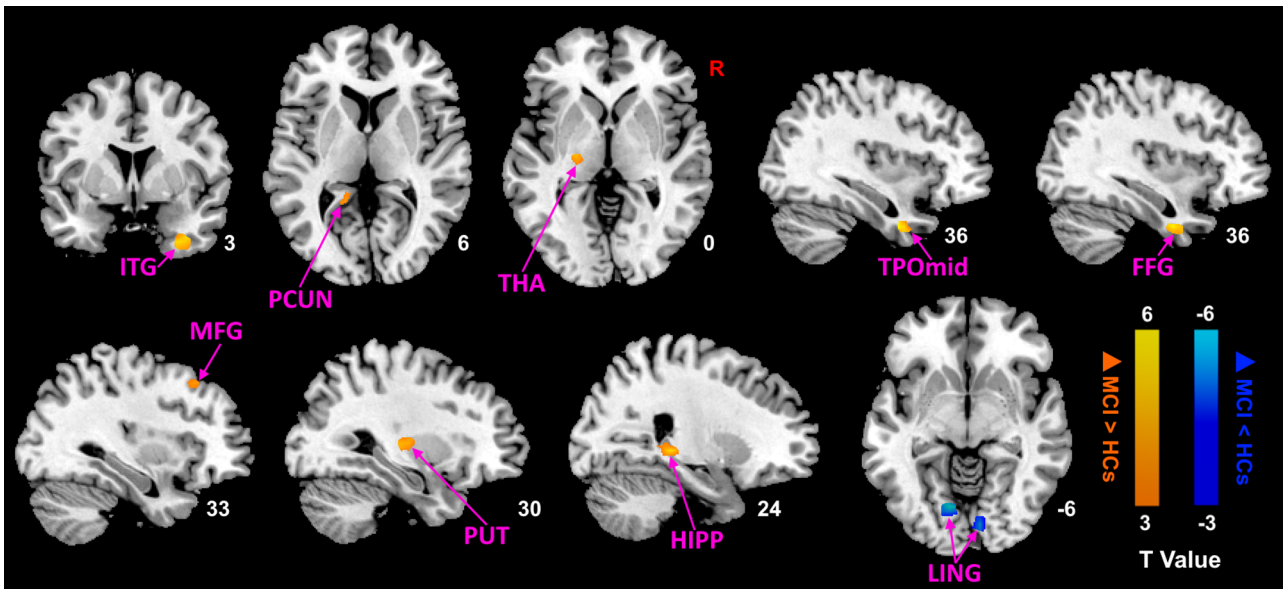

FIGURE 2 | ALFF analysis of MCI patients after moxibustion treatment ($p < 0.05$, FDR correction). Warm color represents an increase and cool color represents a decrease respectively. ALFF, amplitude of low-frequency fluctuation; FDR, false discovery rate; ITG, inferior temporal gyrus; PCUN, precuneus; THA, thalamus; TPOmid, temporal poles: middle temporal gyrus; FFG, fusiform gyrus; MFG, middle frontal gyrus; PUT, putamen; HIPP, hippocampus; LING, lingual gyrus; MCI, mild cognitive impairment; HCs, healthy controls.

TABLE 4 | Brain regions demonstrating altered ALFF values of MCI patients after moxibustion.

	Brain regions	Brodmann area	Peak MNI coordinates			Cluster size	T-value
			x	y	z		
increased after moxibustion	L_PCUN	27	−15	−42	6	105	3.03
	L_THA	0	−21	−18	0	108	3.93
	R_TPOmid	36	36	3	−36	86	5.08
	R_MFG	9	33	24	48	75	3.38
	R_ITG	36	36	3	−39	88	4.8
	R_PUT	48	30	−18	6	108	4.16
	R_HIPP	37	24	−33	0	55	5.26
	R_FFG	36	36	−3	−36	80	6.55
decreased after moxibustion	L_LING	18	−12	−72	−6	88	−5.13
	R_LING	18	9	−84	−6	100	−4.62

neuronal activity in the DMN, VIN, and subcortical network (SCN) with an increasing trend of the ALFF values. The increase in MMSE score was positively correlated with the increase of ALFF value in the right TPOmid, the right insula, and the left superior temporal gyrus.

Altered Spontaneous Brain Activity Occurred in MCI Patients

Compared with HCs, the altered ALFF values of MCI patients mainly included in the DMN (the left HIPP, left MTG, and right TPOmid) and the VIN (the right LING, right MOG, right ITG,

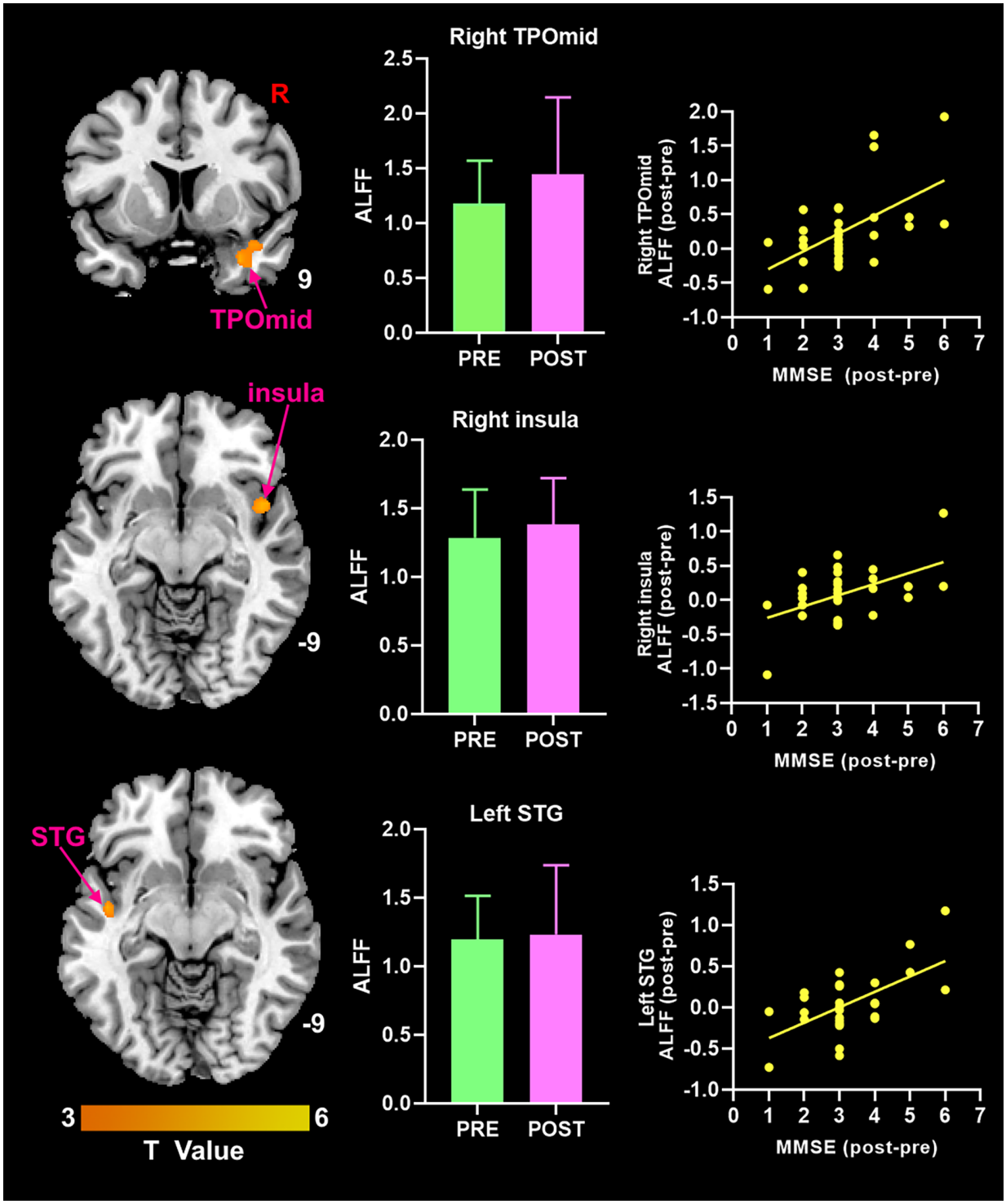

FIGURE 3 | The increase of MMSE score was positively correlated with the increase of ALFF value in brain regions ($p < 0.05$, FDR correction). ALFF, amplitude of low-frequency fluctuation; MMSE, Mini-Mental State Examination; TPOmid, temporal poles: middle temporal gyrus; STG, superior temporal gyrus.

and left MCC), which were consistent with the results of the previous meta-analysis revealing altered ALFF values in brain regions mainly involving DMN, salience network and VIN (Li et al., 2015; Pan et al., 2017).

The DMN, as the most extensively studied brain network among AD patients and high-risk subjects, is related to advanced cognitive functions (Krajcovicova et al., 2014). This network is believed to involve self-referencing processes, intuitive thinking,

memory processes, and perhaps information integration and preservation (Beason-Held et al., 2017). The cortical regions of DMN distribution widely overlapped with areas of early Aβ plaque deposition (Hoenig et al., 2018; Zott et al., 2018). Huijbers et al. (2015) mentioned that amyloid-β positive patients with MCI showed increased hippocampal activation and Clinical Dementia Rating score. Yang et al. (2018) observed increased ALFF value in the left HIPP, and spontaneous activity of neurons in this region enhanced to maintain cognitive ability. Some of the increased connectivity of DMN can compensate for interruptions in other areas of the network (Beason-Held et al., 2017). It suggests that the brain region with a reduced ALFF value represents an impaired function, while the increased region may represent a functional impairment or a compensatory mechanism. In other words, we could call it the perturbed activity pattern of the DMN. The abnormality of DMN may be an important feature of the neuroimaging model of MCI patients, which can provide an auxiliary MRI basis for the clinical diagnosis of MCI.

In addition to the DMN, the brain regions of Tau pathological accumulation and the VIN distribution also have a high overlap (Hoenig et al., 2018). The occipital gyrus and LING are steady in the visual system network (Yang et al., 2015). Metabolomics and transcriptomics studies confirmed that the metabolite changes of ITG are related to the severity of AD pathology (Mahajan et al., 2020). Visual processing difficulties are often present in AD and MCI (Krajcovicova et al., 2017). In the Parkinson's study, the stability of the VIN and DMN are associated with the severity of visual hallucinations symptoms (Dujardin et al., 2020). It may be inferred that visual hallucinations also occur in MCI patients with the same altered VIN spontaneous neural activity. Meanwhile, inefficient VIN activation might interfere with higher cognitive processing in AD patients (Li et al., 2015). Consistent with the previous conclusions, we conclude that VIN also has a functional impairment and a compensation mechanism. Furthermore, there may be some correlation in terms of vision between VIN and DMN wait for verification.

Moxibustion Modulates the Brain Region of MCI Patients

Our study found extensive changes in ALFF values in the brain region mainly involving the DMN, VIN, and SCN after moxibustion in MCI patients, and the ALFF values primarily increased. Meanwhile, the MMSE and MoCA scores increased after moxibustion, indicating the improvement of cognitive function. The perturbed activity pattern of DMN is a crucial feature of abnormal central nervous activity in MCI and AD. Our study revealed that the target brain regions of moxibustion are mainly located in DMN, VIN, and SCN. Moreover, the ALFF value in the right TPOmid of MCI patients was decreased but increased after moxibustion and was positively correlated with the MMSE score. Our results indicate that DMN is a vital target region of moxibustion's central nervous regulation mechanism, consistent with the previous study (Bao et al., 2016). In particular, the changed ALFF values in the right ITG, right TPOmid, and the right LING were reversed, from decreasing to increasing, and the abnormalities of the HIPP happened on the contralateral side. These results provide evidence that moxibustion can regulate central nervous spontaneous activity and improve cognitive function in MCI patients.

The role of DMN and VIN in AD-related diseases has been discussed earlier in this article. In addition, this study also increased ALFF values in SCN, including THA and PUT. They are part of the corticobasal ganglia–thalamic circuits that are critical for a variety of cognitive functions, like working memory and perceptual decision-making (Wei and Wang, 2016). In comparison between dementia-related processes and aging, authors found that HIPP and amygdala demonstrated high disease-related effects, while the THA, PUT and white matter revealed weakly related to cognitive decline but a strong association with aging (Wachinger et al., 2016). Functional neuroimaging and pathological studies found that the THA and PUT activated in the process of reading and speaking (Seghier and Price, 2010). The THA is associated with the transmission and integration of cognitive information; its medial part includes the Papez circuit, which is involved in memory and learning processes (Beh et al., 2013). A previous study presented that with cognitive decline in AD, the integrity of thalamic connections is gradually compromised (Zhu et al., 2015). The PUT is traditionally associated with reinforcement learning and motor control, including speech articulation (Viñas-Guasch and Wu, 2017). The ALFF values in the right PUT were significantly related to the memory decline over time and more severe AD pathology (Ren et al., 2016), and the hypoactivation of PUT was found in task-based fMRI studies in MCI (Li et al., 2015). In the present study, altered ALFF values in the THA and PUT were only found after treatment, and we speculate that they may be related to normal aging and affected by the abnormal activities of other brain regions before treatment.

HIPP is a crucial part of DMN and plays a vital role in the brain's ability for memory storage and retrieval (particularly episodic memories in humans; Knierim, 2015) and social behavior adaptation (Montagrin et al., 2018). Hippocampal atrophy is one of the most readily available and effective biomarkers of AD (de Flores et al., 2015), and the structural asymmetry of HIPP, amygdala, caudate, and cortex may be a sensitive biomarker to predict the progression from MCI to AD (Wachinger et al., 2016). Furthermore, the functional asymmetry of the HIPP is critical for cognitive processes, and it is found to increase in dementia (Muntsant and Giménez-Llort, 2020). The study of neurofunctional topography of the human HIPP segmented the left HIPP into emotional processing, cognitive operations, and post perceptual cluster, while the segmentation of the right HIPP required further confirmation (Robinson et al., 2015). Neurodegeneration associated with aging and disease may preferentially affect the left hemisphere, which innervates speech and movement (Minkova et al., 2017). In AD spectrum disease, the asymmetric pattern of HIPP was found a gradual trend of HC-SCD-MCI. A meta-analysis showed increased ALFFs in the left HIPP in amnestic MCI (Pan et al., 2017). Our results of increased ALFF values in the left HIPP in MCI compared with HCs were in line with the literature. After moxibustion, the spontaneous brain functional activity

in right HIPP increased compared with baseline status. In the research of spatial navigation and episodic memory, the activation of the right HIPP prompts the heterocentric spatial model (Iglói et al., 2010). Disruption of the right hippocampal structure has been found in the subcortical vascular MCI (Lyu et al., 2019), and the increased susceptibility of iron deposition in the right HIPP of subcortical vascular MCI patients is related to memory and language functional tests scores (Sun et al., 2017). More importantly, abnormalities in the right HIPP are associated with MMSE and MoCA scores in SCD which is proposed as a high-risk state of AD (Yue et al., 2018). Although the ALFF value of the right HIPP was not statistically correlated with the cognitive scores of the patients, the cognitive scores and function of MCI patients significantly improved after moxibustion. Thus, moxibustion might improve cognitive function by modulating the functional activity of the right HIPP. Previous studies have also shown that moxibustion improves cognitive function, and its mechanism may be related to the inhibition of hippocampal neuron apoptosis and Aβ deposition which might be the mechanism of inducing AD (Aum et al., 2021; Yang et al., 2021). It is concluded that moxibustion might be of great potential in the treatment of MCI.

It is worth noting that the present study showed a gender imbalance in the random sample of MCI among women as twice compared to men, which is consistent with the recent comprehensive study on the prevalence, risk factors, and management of dementia and MCI in China (Jia et al., 2020). Although gender differences in the incidence of AD are controversial across studies, most results also support a higher prevalence in women (Mielke et al., 2014; Fiest et al., 2016; Nebel et al., 2018). The possible mechanisms of gender differences in MCI and AD mainly include differences in genes, sex hormones, brain structure, glial cells, and immunity (Fisher et al., 2018; Honarpisheh and McCullough, 2019), while MRI has confirmed gender differences in brain structure. Studies using longitudinal MRI data from AD to MCI also confirmed different patterns of gray matter atrophy in different genders, especially in bilateral anterior cuneus nucleus, caudate nucleus, THA, and MTG (Skup et al., 2011). In addition, women with MCI lose more volume in the HIPP than men (Sundermann et al., 2017). Current studies on precision medicine suggest the need to pay attention to gender in the clinical manifestations, pathophysiological mechanisms, and treatment of patients with MCI or AD (Nebel et al., 2018). It may be of interest to have a sex-disaggregated study of brain fMRI in MCI patients in the future with a large sample size.

In conclusion, there existed changes in ALFF values of brain regions related to cognition in MCI, mainly involved in the DMN and VIN. Moxibustion might improve the cognitive function of MCI patients by modulating the brain activities in regions involving the cognitive processes with a trend of increased ALFF values, as well as the functional asymmetry of the HIPP. In particular, DMN is a vital target region of moxibustion's central nervous regulation mechanism.

This study used the ALFF method to study the abnormal brain activity of MCI patients and the regulation of moxibustion on the brain activity of MCI patients, but this study had limitations. First of all, our samples used a cross-sectional design, and a longitudinal study needs further exploration. Second, we only used ALFF as the analytical method instead of more research methods to verify together, such as regional homogeneity and functional connectivity. The role of moxibustion in the regulation of MCI patients needs the exploration of multimodal brain imaging technology. Third, physiological noise during scanning, such as breathing movement, might affect the stability of fMRI signals. Much spurious information might be arisen due to the low-frequency spontaneous fluctuation of BOLD signals and the physiological noise such as cardiac and respiratory cycles (Li et al., 2014). Fourth, our study's relatively small sample size may have influenced the results, and future studies with a larger sample size will help provide the credibility of our results. Finally, as the entire course of moxibustion lasted for two months, challenges were presented for healthy controls. Therefore, we did not use moxibustion to intervene HCs.

DATA AVAILABILITY STATEMENT

The raw data supporting the conclusions of this article will be made available by the authors, without undue reservation.

ETHICS STATEMENT

The studies involving human participants were reviewed and approved by The Medicine Ethics Committee of First Affiliated Hospital, Guangxi University of Chinese Medicine. The patients/participants provided their written informed consent to participate in this study.

AUTHOR CONTRIBUTIONS

DD contributed design of the study and revised the final version of the manuscript. ZL, QZ, and YW conducted data collection, researched and drafted manuscripts. PL, LL, and GD were involved in manuscript editing. PL, WM, and LZ contributed to MRI processing and data analysis. All authors contributed to the article and approved the submitted version.

FUNDING

This research was funded by the National Natural Science Foundation of China (grant no. 82060315, 81760886, and 82102032) and the Scientific Research and Technology Development Program of Guangxi (grant no. 14124004-1-27).

ACKNOWLEDGMENTS

We thank all study participants, researchers, and clinicians who contributed to this study.

REFERENCES

A, R., Yue, R., Chen, B., and Huang, X. (2021). Moxibustion for the treatment of Alzheimer's disease: a protocol for a systematic reviews and meta-analysis. *Medicine (Baltimore)* 100:e24657. doi: 10.1097/MD.0000000000024657

Alzheimer's Disease International M. U. (2021). World Alzheimer Report 2021. Available online at: www.alz.co.uk. Accessed September 21, 2021.

Aum, S., Choe, S., Cai, M., Jerng, U. M., and Lee, J. H. (2021). Moxibustion for cognitive impairment: a systematic review and meta-analysis of animal studies. *Integr. Med. Res.* 10:100680. doi: 10.1016/j.imr.2020.100680

Bao, C., Liu, P., Liu, H., Jin, X., Calhoun, V. D., Wu, L., et al. (2016). Different brain responses to electro-acupuncture and moxibustion treatment in patients with Crohn's disease. *Sci. Rep.* 6:36636. doi: 10.1038/srep36636

Beason-Held, L. L., Hohman, T. J., Venkatraman, V., An, Y., and Resnick, S. M. (2017). Brain network changes and memory decline in aging. *Brain Imaging Behav.* 11, 859–873. doi: 10.1007/s11682-016-9560-3

Beh, S. C., Frohman, T. C., and Frohman, E. M. (2013). Isolated mammillary body involvement on MRI in Wernicke's encephalopathy. *J. Neurol. Sci.* 334, 172–175. doi: 10.1016/j.jns.2013.07.2516

Cha, J., Hwang, J. M., Jo, H. J., Seo, S. W., Na, D. L., and Lee, J. M. (2015). Assessment of functional characteristics of amnestic mild cognitive impairment and Alzheimer's disease using various methods of resting-state FMRI analysis. *Biomed. Res. Int.* 2015:907464. doi: 10.1155/2015/907464

de Flores, R., La Joie, R., and Chételat, G. (2015). Structural imaging of hippocampal subfields in healthy aging and Alzheimer's disease. *Neuroscience* 309, 29–50. doi: 10.1016/j.neuroscience.2015.08.033

Dujardin, K., Roman, D., Baille, G., Pins, D., Lefebvre, S., Delmaire, C., et al. (2020). What can we learn from fMRI capture of visual hallucinations in Parkinson's disease? *Brain Imaging Behav.* 14, 329–335. doi: 10.1007/s11682-019-00185-6

Fiest, K. M., Roberts, J. I., Maxwell, C. J., Hogan, D. B., Smith, E. E., Frolkis, A., et al. (2016). The prevalence and incidence of dementia due to Alzheimer's disease: a systematic review and meta-analysis. *Can. J. Neurol. Sci.* 43, S51–82. doi: 10.1017/cjn.2016.36

Fisher, D. W., Bennett, D. A., and Dong, H. (2018). Sexual dimorphism in predisposition to Alzheimer's disease. *Neurobiol. Aging* 70, 308–324. doi: 10.1016/j.neurobiolaging.2018.04.004

Fox, M. D., and Raichle, M. E. (2007). Spontaneous fluctuations in brain activity observed with functional magnetic resonance imaging. *Nat. Rev. Neurosci.* 8, 700–711. doi: 10.1038/nrn2201

Ha, L., Yang, B., Wang, S., An, Y., Wang, H., and Cui, Y. (2020). Effect of moxibustion on behavioral changes and expression of APP and BACE1 in hippocampus of SAMP8 mice. *Evid. Based Complement. Alternat. Med.* 2020:3598930. doi: 10.1155/2020/3598930

Hoenig, M. C., Bischof, G. N., Seemiller, J., Hammes, J., Kukolja, J., Onur Ö, A., et al. (2018). Networks of tau distribution in Alzheimer's disease. *Brain* 141, 568–581. doi: 10.1093/brain/awx353

Honarpisheh, P., and McCullough, L. D. (2019). Sex as a biological variable in the pathology and pharmacology of neurodegenerative and neurovascular diseases. *Br. J. Pharmacol.* 176, 4173–4192. doi: 10.1111/bph.14675

Huijbers, W., Mormino, E. C., Schultz, A. P., Wigman, S., Ward, A. M., Larvie, M., et al. (2015). Amyloid-β deposition in mild cognitive impairment is associated with increased hippocampal activity, atrophy and clinical progression. *Brain* 138, 1023–1035. doi: 10.1093/brain/awv007

Iglói, K., Doeller, C. F., Berthoz, A., Rondi-Reig, L., and Burgess, N. (2010). Lateralized human hippocampal activity predicts navigation based on sequence or place memory. *Proc. Natl. Acad. Sci. U S A* 107, 14466–14471. doi: 10.1073/pnas.1004243107

Jansen, W. J., Ossenkoppele, R., Knol, D. L., Tijms, B. M., Scheltens, P., Verhey, F. R., et al. (2015). Prevalence of cerebral amyloid pathology in persons without dementia: a meta-analysis. *JAMA* 313, 1924–1938. doi: 10.1001/jama.2015.4668

Jia, L., Du, Y., Chu, L., Zhang, Z., Li, F., Lyu, D., et al. (2020). Prevalence, risk factors and management of dementia and mild cognitive impairment in adults aged 60 years or older in China: a cross-sectional study. *Lancet Public Health* 5, e661–e671. doi: 10.1016/S2468-2667(20)30185-7

Knierim, J. J. (2015). The hippocampus. *Curr. Biol.* 25, R1116–1121. doi: 10.1016/j.cub.2015.10.049

Krajcovicova, L., Barton, M., Elfmarkova-Nemcova, N., Mikl, M., Marecek, R., and Rektorova, I. (2017). Changes in connectivity of the posterior default network node during visual processing in mild cognitive impairment: staged decline between normal aging and Alzheimer's disease. *J. Neural Transm. (Vienna)* 124, 1607–1619. doi: 10.1007/s00702-017-1789-5

Krajcovicova, L., Marecek, R., Mikl, M., and Rektorova, I. (2014). Disruption of resting functional connectivity in Alzheimer's patients and at-risk subjects. *Curr. Neurol. Neurosci. Rep.* 14:491. doi: 10.1007/s11910-014-0491-3

Langa, K. M., and Levine, D. A. (2014). The diagnosis and management of mild cognitive impairment: a clinical review. *JAMA* 312, 2551–2561. doi: 10.1001/jama.2014.13806

Li, H. J., Hou, X. H., Liu, H. H., Yue, C. L., He, Y., and Zuo, X. N. (2015). Toward systems neuroscience in mild cognitive impairment and Alzheimer's disease: a meta-analysis of 75 fMRI studies. *Hum. Brain Mapp.* 36, 1217–1232. doi: 10.1002/hbm.22689

Li, H., Sang, L., Xia, X., Zhao, R., Wang, M., Hou, X., et al. (2019). Therapeutic duration and extent affect the effect of moxibustion on depression-like behaviour in rats *via* regulating the brain tryptophan transport and metabolism. *Evid. Based Complement. Alternat. Med.* 2019:7592124. doi: 10.1155/2019/7592124

Li, Y., Wee, C. Y., Jie, B., Peng, Z., and Shen, D. (2014). Sparse multivariate autoregressive modeling for mild cognitive impairment classification. *Neuroinformatics* 12, 455–469. doi: 10.1007/s12021-014-9221-x

Liu, Q. Q., Chen, S. J., Shen, G. M., Jia, X. Y., Qiao, X. D., and Wu, G. L. (2020). [Effect of electronic moxibustion on memory function in patients with amnestic mild cognitive impairment]. *Zhongguo Zhen Jiu* 40, 352–356. doi: 10.13703/j.0255-2930.20190608-k0002

Lyu, H., Wang, J., Xu, J., Zheng, H., Yang, X., Lin, S., et al. (2019). Structural and functional disruptions in subcortical vascular mild cognitive impairment with and without depressive symptoms. *Front. Aging Neurosci.* 11:241. doi: 10.3389/fnagi.2019.00241

Mahajan, U. V., Varma, V. R., Griswold, M. E., Blackshear, C. T., An, Y., Oommen, A. M., et al. (2020). Dysregulation of multiple metabolic networks related to brain transmethylation and polyamine pathways in Alzheimer disease: a targeted metabolomic and transcriptomic study. *PLoS Med.* 17:e1003012. doi: 10.1371/journal.pmed.1003012

Mielke, M. M., Vemuri, P., and Rocca, W. A. (2014). Clinical epidemiology of Alzheimer's disease: assessing sex and gender differences. *Clin. Epidemiol.* 6, 37–48. doi: 10.2147/CLEP.S37929

Minkova, L., Habich, A., Peter, J., Kaller, C. P., Eickhoff, S. B., and Klöppel, S. (2017). Gray matter asymmetries in aging and neurodegeneration: a review and meta-analysis. *Hum. Brain Mapp.* 38, 5890–5904. doi: 10.1002/hbm.23772

Montagrin, A., Saiote, C., and Schiller, D. (2018). The social hippocampus. *Hippocampus* 28, 672–679. doi: 10.1002/hipo.22797

Muntsant, A., and Giménez-Llort, L. (2020). Impact of social isolation on the behavioral, functional profiles and hippocampal atrophy asymmetry in dementia in times of Coronavirus pandemic (COVID-19): a translational neuroscience approach. *Front. Psychiatry* 11:572583. doi: 10.3389/fpsyt.2020.572583

Nebel, R. A., Aggarwal, N. T., Barnes, L. L., Gallagher, A., Goldstein, J. M., Kantarci, K., et al. (2018). Understanding the impact of sex and gender in Alzheimer's disease: a call to action. *Alzheimers Dement.* 14, 1171–1183. doi: 10.1016/j.jalz.2018.04.008

Pacific WHOROftW. (2007). *WHO International Standard Terminologies on Traditional Medicine in the Western Pacific Region*. Manila: World Health Organization, Western Pacific Region.

Pan, P., Zhu, L., Yu, T., Shi, H., Zhang, B., Qin, R., et al. (2017). Aberrant spontaneous low-frequency brain activity in amnestic mild cognitive impairment: a meta-analysis of resting-state fMRI studies. *Ageing Res. Rev.* 35, 12–21. doi: 10.1016/j.arr.2016.12.001

Petersen, R. C. (2016). Mild cognitive impairment. *Continuum (Minneapolis Minn)* 22, 404–418. doi: 10.1212/CON.0000000000000313

Ren, P., Lo, R. Y., Chapman, B. P., Mapstone, M., Porsteinsson, A., and Lin, F. (2016). Longitudinal alteration of intrinsic brain activity in the striatum in mild cognitive impairment. *J. Alzheimers Dis.* 54, 69–78. doi: 10.3233/JAD-160368

Robinson, J. L., Barron, D. S., Kirby, L. A., Bottenhorn, K. L., Hill, A. C., Murphy, J. E., et al. (2015). Neurofunctional topography of the human

hippocampus. *Hum. Brain Mapp.* 36, 5018–5037. doi: 10.1002/hbm.22987

Seghier, M. L., and Price, C. J. (2010). Reading aloud boosts connectivity through the putamen. *Cereb. Cortex* 20, 570–582. doi: 10.1093/cercor/bhp123

Skup, M., Zhu, H., Wang, Y., Giovanello, K. S., Lin, J. A., Shen, D., et al. (2011). Sex differences in grey matter atrophy patterns among AD and aMCI patients: results from ADNI. *Neuroimage* 56, 890–906. doi: 10.1016/j.neuroimage.2011.02.060

Sun, Y., Ge, X., Han, X., Cao, W., Wang, Y., Ding, W., et al. (2017). Characterizing brain iron deposition in patients with subcortical vascular mild cognitive impairment using quantitative susceptibility mapping: a potential biomarker. *Front. Aging Neurosci.* 9:81. doi: 10.3389/fnagi.2017.00081

Sundermann, E. E., Biegon, A., Rubin, L. H., Lipton, R. B., Landau, S., and Maki, P. M. (2017). Does the female advantage in verbal memory contribute to underestimating Alzheimer's disease pathology in women versus men? *J. Alzheimers Dis.* 56, 947–957. doi: 10.3233/JAD-160716

Tomasi, D., Wang, G. J., and Volkow, N. D. (2013). Energetic cost of brain functional connectivity. *Proc. Natl. Acad. Sci. U S A* 110, 13642–13647. doi: 10.1073/pnas.1303346110

Viñas-Guasch, N., and Wu, Y. J. (2017). The role of the putamen in language: a meta-analytic connectivity modeling study. *Brain Struct. Funct.* 222, 3991–4004. doi: 10.1007/s00429-017-1450-y

Wachinger, C., Salat, D. H., Weiner, M., and Reuter, M. (2016). Whole-brain analysis reveals increased neuroanatomical asymmetries in dementia for hippocampus and amygdala. *Brain* 139, 3253–3266. doi: 10.1093/brain/aww243

Wei, W., and Wang, X. J. (2016). inhibitory control in the cortico-basal ganglia-thalamocortical loop: complex regulation and interplay with memory and decision processes. *Neuron* 92, 1093–1105. doi: 10.1016/j.neuron.2016.10.031

Yang, Y. L., Deng, H. X., Xing, G. Y., Xia, X. L., and Li, H. F. (2015). Brain functional network connectivity based on a visual task: visual information processing-related brain regions are significantly activated in the task state. *Neural Regen. Res.* 10, 298–307. doi: 10.4103/1673-5374.152386

Yang, K., Song, X. G., Ruan, J. R., Cai, S. C., Zhu, C. F., Qin, X. F., et al. (2021). [Effect of moxibustion on cognitive function and proteins related with apoptosis of hippocampal neurons in rats with vascular dementia]. *Zhongguo Zhen Jiu* 41, 1371–1378. doi: 10.13703/j.0255-2930.20210124-k0006

Yang, L., Yan, Y., Wang, Y., Hu, X., Lu, J., Chan, P., et al. (2018). Gradual disturbances of the amplitude of low-frequency fluctuations (ALFF) and fractional ALFF in Alzheimer spectrum. *Front. Neurosci.* 12:975. doi: 10.3389/fnins.2018.00975

Yue, L., Wang, T., Wang, J., Li, G., Wang, J., Li, X., et al. (2018). Asymmetry of hippocampus and amygdala defect in subjective cognitive decline among the community dwelling chinese. *Front. Psychiatry* 9:226. doi: 10.3389/fpsyt.2018.00226

Zang, Y. F., He, Y., Zhu, C. Z., Cao, Q. J., Sui, M. Q., Liang, M., et al. (2007). Altered baseline brain activity in children with ADHD revealed by resting-state functional MRI. *Brain Dev.* 29, 83–91. doi: 10.1016/j.braindev.2006.07.002

Zhang, T., Wang, L. P., Wang, G. L., Sun, J. Q., Mao, X. W., Jiang, H. L., et al. (2020). Effects of moxibustion on symptoms of mild cognitive impairment: protocol of a systematic review and meta-analysis. *BMJ Open* 10:e033910. doi: 10.1136/bmjopen-2019-033910

Zhu, Q. Y., Bi, S. W., Yao, X. T., Ni, Z. Y., Li, Y., Chen, B. Y., et al. (2015). Disruption of thalamic connectivity in Alzheimer's disease: a diffusion tensor imaging study. *Metab. Brain Dis.* 30, 1295–1308. doi: 10.1007/s11011-015-9708-7

Zott, B., Busche, M. A., Sperling, R. A., and Konnerth, A. (2018). What happens with the circuit in Alzheimer's disease in mice and humans? *Annu. Rev. Neurosci.* 41, 277–297. doi: 10.1146/annurev-neuro-080317-061725

Zou, Q. H., Zhu, C. Z., Yang, Y., Zuo, X. N., Long, X. Y., Cao, Q. J., et al. (2008). An improved approach to detection of amplitude of low-frequency fluctuation (ALFF) for resting-state fMRI: fractional ALFF. *J. Neurosci. Methods* 172, 137–141. doi: 10.1016/j.jneumeth.2008.04.012

Conflict of Interest: The authors declare that the research was conducted in the absence of any commercial or financial relationships that could be construed as a potential conflict of interest.

Publisher's Note: All claims expressed in this article are solely those of the authors and do not necessarily represent those of their affiliated organizations, or those of the publisher, the editors and the reviewers. Any product that may be evaluated in this article, or claim that may be made by its manufacturer, is not guaranteed or endorsed by the publisher.

frontiers | Frontiers in Molecular Neuroscience

REVIEW
published: 26 May 2022
doi: 10.3389/fnmol.2022.888716

Non-invasive Brain Stimulation for Chronic Pain: State of the Art and Future Directions

Huan-Yu Xiong[1], Jie-Jiao Zheng[2] and Xue-Qiang Wang[1,3]**

[1] Department of Sport Rehabilitation, Shanghai University of Sport, Shanghai, China, [2] Huadong Hospital, Shanghai, China, [3] Department of Rehabilitation Medicine, Shanghai Shangti Orthopaedic Hospital, Shanghai, China

As a technique that can guide brain plasticity, non-invasive brain stimulation (NIBS) has the potential to improve the treatment of chronic pain (CP) because it can interfere with ongoing brain neural activity to regulate specific neural networks related to pain management. Treatments of CP with various forms of NIBS, such as repetitive transcranial magnetic stimulation (rTMS) and transcranial direct current stimulation (tDCS), using new parameters of stimulation have achieved encouraging results. Evidence of moderate quality indicates that high-frequency rTMS of the primary motor cortex has a clear effect on neuropathic pain (NP) and fibromyalgia. However, evidence on its effectiveness regarding pain relief in other CP conditions is conflicting. Concerning tDCS, evidence of low quality supports its benefit for CP treatment. However, evidence suggesting that it exerts a small treatment effect on NP and headaches is also conflicting. In this paper, we describe the underlying principles behind these commonly used stimulation techniques; and summarize the results of randomized controlled trials, systematic reviews, and meta-analyses. Future research should focus on a better evaluation of the short-term and long-term effectiveness of all NIBS techniques and whether they decrease healthcare use, as well as on the refinement of selection criteria.

Keywords: non-invasive brain stimulation, chronic pain, neuromodulation, tDCS, rTMS

OPEN ACCESS

Edited by:
Siyi Yu,
Chengdu University of Traditional Chinese Medicine, China

Reviewed by:
Xi Chen,
Wenzhou Medical University, China
Min Su,
Soochow University, China

****Correspondence:***
Jie-Jiao Zheng
zjjcss@163.com
Xue-Qiang Wang
wangxueqiang@sus.edu.cn

Specialty section:
This article was submitted to Neuroplasticity and Development, a section of the journal Frontiers in Molecular Neuroscience

Received: *03 March 2022*
Accepted: *27 April 2022*
Published: *26 May 2022*

Citation:
Xiong H-Y, Zheng J-J and Wang X-Q (2022) Non-invasive Brain Stimulation for Chronic Pain: State of the Art and Future Directions. Front. Mol. Neurosci. 15:888716. doi: 10.3389/fnmol.2022.888716

INTRODUCTION

Conceptually, chronic pain (CP) is a process of neuroplasticity disorder caused by excitatory and inhibitory imbalances in pain processing pathways (Peyron and Fauchon, 2019). According to the United States Centers for Disease Control and Prevention, the prevalence of CP in the general population in 2018 is between 11 and 40%, and it costs the economy between $560 billion and $635 billion annually in the United States alone (Steglitz et al., 2012; Dahlhamer et al., 2018). A systematic review of 19 studies conducted in the United Kingdom showed that the mean prevalence of CP is 43.5% (Fayaz et al., 2016). Approximately 40% of patients with CP report difficulty in pain control, and over 60% reveal inadequate pain relief from medications (Breivik et al., 2006).

CP is the dynamic result of a range of biological, psychological, and social factors, and the most common medications no longer provide sufficient analgesia for most patients. Therefore, specific, predictable, and effective modalities of CP management must be explored and developed.

USING BASIC SCIENTIFIC KNOWLEDGE TO DEVELOP AN EFFECTIVE, NEURAL CIRCUIT-BASED TREATMENT FOR CHRONIC PAIN

Non-invasive brain stimulation (NIBS) has the potential to improve the treatment of CP because it can regulate specific neural networks related to pain processing in the brain, such as the anterior cingulate cortex (ACC) and the thalamus, and promote a downward pain suppression mechanism to relieve pain (Peyron et al., 2007; **Figure 1**). Imaging studies in humans have suggested that CP is the result of changes in neural networks and central pain mechanisms, including perception, sensitization, and pain regulation pathways (Perocheau et al., 2014). Moreover, pain is a personal experience that requires different brain circuits to process. Therefore, NIBS technique may be effective in relieving pain by exciting or inhibiting specific neural networks associated with pain processing.

As an alternative intervention to invasive brain stimulation, NIBS can remarkably reduce the incidence of invasive stimulation. Over the past 20 years, the number of studies that used NIBS techniques for pain treatment has exponentially grown, a trend that possibly reflects the importance of this field (**Figure 2** and **Table 1**). Thus far, NIBS has been applied to manage various CP conditions, including fibromyalgia (Forogh et al., 2021), neuropathic pain (NP) (Galhardoni et al., 2019), and migraine (Schading et al., 2021). Although the neural mechanisms underlying the analgesic effects of NIBS are not yet fully understood, the mechanisms behind the functional effects of each NIBS technique are different (Leocani et al., 2019). Moreover, the analgesic effects of NIBS seem to be highly correlated with the stimulated brain regions. Therefore, we hypothesize that patients with different types of CP may benefit from stimulation of different target brain regions through different NIBS techniques. At the cellular level, stimulation can change the electrical state of individual neurons; at the neurohumoral signal level, stimulation can cause neurotransmitter activity; at the network level, stimulation can change neuronal circuits; at the behavioral level, stimulation can cause changes in pain and function (Knotkova et al., 2021).

Given that most NIBS techniques modulate neural activity in a frequency- or polar-dependent manner, most applications of CP research have involved excitatory NIBS, such as high-frequency transcranial magnetic stimulation (TMS) or anodal transcranial direct current stimulation (tDCS) (**Figure 3**). In this review, we outline the possibilities and limitations of the NIBS approach in CP research, with particular emphasis on best practices and selected developments.

REPETITIVE TRANSCRANIAL MAGNETIC STIMULATION

Underlying Neurophysiological Mechanisms of Repetitive Transcranial Magnetic Stimulation in Chronic Pain Treatment

Transcranial magnetic stimulation uses dynamic magnetic fields to generate induced currents to regulate individual neurons and neuron groups in the cortex and the neural networks connected to them (Young et al., 2014). Strong effects can sufficiently depolarize neurons to trigger action potentials (Young et al., 2014). If TMS pulse stimulation is repeatedly given, it is called repetitive TMS (rTMS).

Regulating the Excitability of the Pain Loop

In general, the stimulatory effect of rTMS depends on the frequency: high-frequency stimulation ($\geq$5 Hz) increases cortical excitability, whereas low-frequency stimulation ($\leq$1 Hz) decreases it (Hoogendam et al., 2010). The excitability induced by high-frequency rTMS (HF-rTMS) may be the result of the weakened intracortical inhibition mediated by the gamma-aminobutyric acid (GABA) rather than directly caused by increased excitability (Ziemann, 2004). By contrast, low-frequency rTMS (LF-rTMS) may enhance GABA-mediated intracortical inhibition, thereby reducing cortical excitability.

The rationale for applying rTMS to treat pain is that it can modulate neural activity in cortical and subcortical brain structures associated with pain processing, such as the thalamus, in both local and remote brain regions. Compared with electrical stimulation, magnetic stimulation allows the study of local nerve tissue activation, where the signal is not hindered by other tissues and is minimally invasive to humans. In turn, the activation of the cortical structure transmits the action potential to neural circuits related to pain processing, such as the cingulate cortex and the thalamus, regardless if it is forward or reverse (Strafella et al., 2001; Perocheau et al., 2014). Previous studies have confirmed that rTMS can also directly excite the thalamus through the cortical–thalamic projection system, thereby inhibiting the transmission of injury information through the spinothalamic pathway (Bestmann et al., 2004; Martin et al., 2013). In other words, when HF-rTMS is used, the pain information transmitted through the spinothalamic tract and the ipsilateral thalamic nucleus may be suppressed. By contrast, when LF-rTMS is utilized, pain transmission may be unsuppressed.

Synaptic Plasticity

Another mechanism by which TMS alleviates pain is by changing the plasticity of the nervous system, whereas long-term changes in neuron excitability are associated with long-term changes in synaptic effects, especially long-term potentiation (LTP) and long-term depression (LTD). Similar to basic synaptic physiology, enhancing the synaptic strength is often referred to as LTP, whereas reducing the synaptic strength is referred to as LTD (**Figure 4**).

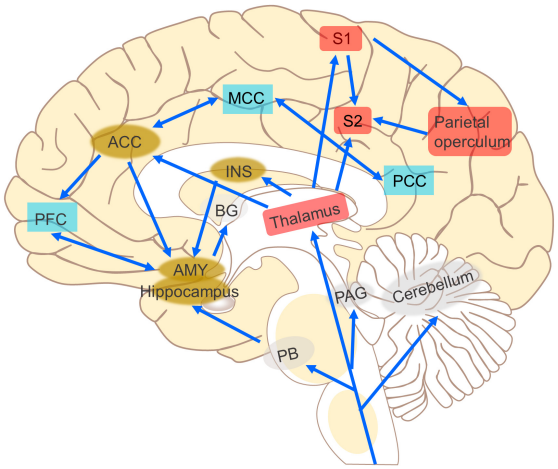

FIGURE 1 | Neural networks related to pain. The primary cortical pain matrix (thalamus, S1, S2, posterior insula, and parietal operculum) contributes to pain perception and location. The secondary (ACC, INS, AMY, and hippocampus) represent common structures identified in the affective motivational pain pathway, such as empathy for pain. The third (PFC, MCC, and PCC) represents one component of the cognitive evaluative pain system. The arrows represent multiple cortical connections between regions and systems indicating the complex interconnectedness of brain regions involved with pain. ACC, anterior cingulate cortex; PFC, prefrontal cortex; AMY, amygdala; PAG, periaqueductal gray; RVM, rostroventral medulla; DH, dorsal horn; INS, insula; S1, primary somatosensory cortex; S2, secondary somatosensory cortex; MCC, medial cingulate cortex; PCC, posterior cingulate cortex; PB, parabrachial nucleus.

Repetitive transcranial magnetic stimulation exerts an accumulation effect through repeated, continuous, and regular stimulation that can excite more neurons. More importantly, rTMS can affect the brain functions of local and remote areas and realize the reconstruction of cortical functions (Moisset et al., 2016). Pridmore et al. (2005) reported that a single session of LF-rTMS reduced the excitability of the primary motor cortex (M1) region for about 15–30 min. However, after multiple and continuous sessions of LF-rTMS, the excitability of the M1 region decreased, which lasted for 30 min on the first day and extended to 2 h on the second day. Therefore, rTMS can probably cause cumulative plasticity changes in brain neural tissues. A few words should be added regarding the mechanisms of analgesic action of rTMS delivered to M1. A previous study highlighted a significant release of endogenous opioids within a bihemispheric brain network involved in the perception and modulation of pain, which was produced by a single session of 10 Hz rTMS of M1 in a positron emission tomography (PET) study based on 10 healthy subjects (Lamusuo et al., 2017). This was consistent with previous observations made in CP patients treated with invasive epidural motor cortex stimulation (Maarrawi et al., 2007, 2013). However, the mechanisms of action of M1 stimulation in pain are surely more complex and multiple, involving various pain modulatory systems concerned with emotion, attention, and/or sensory discrimination processing, related to various neural pathways connecting different brain regions, thalamic nuclei, and/or the spine, and with various neurotransmitter systems beyond endogenous opioids, such as glutamate, GABA, and/or dopamine for example (Nguyen et al., 2011; Lefaucheur, 2016; Moisset and Lefaucheur, 2019). All of these factors can contribute to the development of long-term synaptic plasticity that provides significant pain relief beyond the time of stimulation.

Optimizing Neurotransmitter Levels

Many studies have proved that the analgesic mechanism of rTMS is not only due to the induction of LTP or LTD in the process of neuron depolarization and hyperpolarization, either of which leads to changes in nerve excitability and synaptic connections, but also due to secondary changes in neurotransmitter secretion related to pain. Studies have reported that the release of endogenous opioids in the ACC and periaqueductal gray (PAG) matter is related to the noxious effects of rTMS (de Andrade et al., 2011). rTMS can optimize neurotransmitter levels, promote

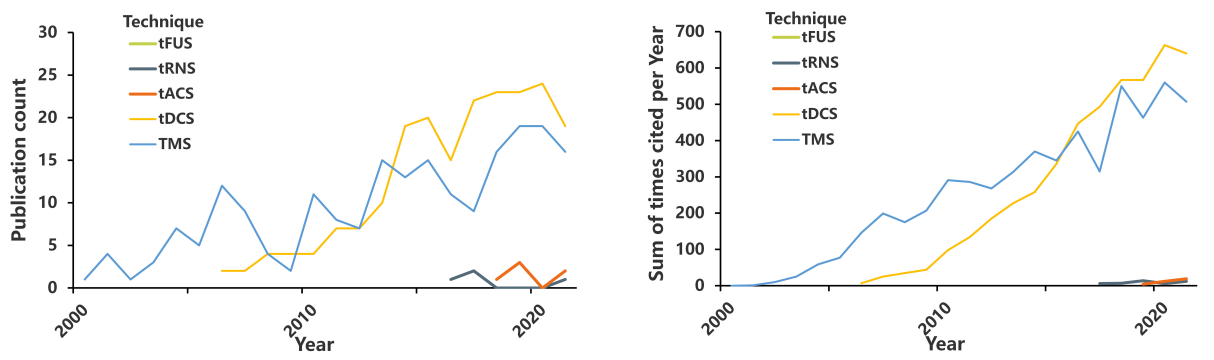

FIGURE 2 | The number of annual publications and annual citations on TMS, tDCS, tACS, tRNS, tFUS, and pain. https://www.webofscience.com/wos/alldb/basic-search; search dates from 2000 to 2021.

TABLE 1 | Systematic and evidence-based reviews of non-invasive brain stimulation techniques for chronic pain.

	Sample size	Disease	Intervention	Duration of the trial period	Follow-up	Primary outcomes	Main results	AMSTAR-2 rating
rTMS								
Zhang et al., 2021	29 studies (24 for rTMS) 826 participants (736 for rTMS)	Neuropathic pain	Intervention: rTMS Control: sham stimulation	1 session (minimum)–15 sessions (maximum)	NA	Pain level (VAS and NRS)	rTMS successfully relieved the pain symptoms of 715 (97.1%) NP patients. The stimulation parameters of rTMS that best induce an analgesic effect are a target cortex of M1, a stimulation frequency of 10–20 Hz, 1000–2000 pulses, and 5–10 sessions.	Low
Jin et al., 2015	32 studies 589 participants	Neuropathic pain	Intervention: HF-rTMS (>1 Hz) over the M1 Control: sham stimulation, parallel-group, and crossover designs	1 session–10 sessions	1 month (minimum)–2 months (maximum)	Pain level (VAS and NRS)	All 3 HF-rTMS treatments (5, 10, and 20 Hz) produced pain reduction, while there were no differences between them, with the maximal pain reduction found after 1 and 5 sessions of rTMS. This significant analgesic effect remained for 1 month after 5 sessions of rTMS treatment.	Moderate
Saltychev and Laimi, 2017	7 RCTs 210 participants	Fibromyalgia	Intervention: rTMS Control: sham stimulation, other treatment, or no control treatment	8 sessions–24 sessions	1 week–3 months	Pain level (VAS and NRS)	Both pooled results of pain severity (−1.2 for NRS and −0.7 for VAS) were below the minimal clinically important difference of 1.5 points. There is moderate evidence that rTMS is not more effective than sham in reducing the severity of pain in fibromyalgia patients.	Moderate
Knijnik et al., 2016	5 RCTs 143 participants	Fibromyalgia	Intervention: rTMS Control: sham stimulation	10 sessions–14 sessions	NA	Pain intensity (VAS and BPI) Depression (HDRS and BDI) QoL (FIQ)	In comparison with sham stimulation, rTMS demonstrated a superior effect on the QoL of patients with FM 1 month after starting therapy. rTMS showed a trend toward reducing pain intensity but did not change depressive symptoms.	Moderate
Stilling et al., 2019	34 studies (6 for TMS, 16 for rTMS) 631 participants	Headache (19/22 studies for migraine)	Intervention: TMS and rTMS Control: sham stimulation or alternative standard of care (i.e., botulinum toxin, headache drug)	1 session–23 sessions	4 weeks–20 weeks	Headache frequency, duration, intensity, use of abortive medications, depression, anxiety, and QoL.	There is moderate evidence for rTMS contributes to reductions in headache frequency, duration, intensity, abortive medication use, depression, and functional impairment. However, only a few studies reported changes greater than sham treatment.	Low
Lan et al., 2017	5 RCTs 313 participants	Migraine	Intervention: rTMS Control: sham stimulation	1 session–23 sessions	NA	Pain intensity	Single-pulse transcranial magnetic stimulation is effective for the acute treatment of migraine with aura after the first attack ($p = 0.02$). The efficacy of TMS on chronic migraine was not significant ($p = 0.14$).	High

(Continued)

TABLE 1 | (Continued)

	Sample size	Disease	Intervention	Duration of the trial period	Follow-up	Primary outcomes	Main results	AMSTAR-2 rating
tDCS								
Zhang et al., 2021	29 studies (5 for tDCS) 826 participants (95 for tDCS)	Neuropathic pain	Intervention: tDCS Control: sham stimulation	1 session–10 sessions	NA	Pain level (VAS and NRS)	Five studies involving 95 NP patients (76.0%) showed that tDCS successfully relieved NP. The most effective parameters of tDCS are a current intensity of 2 mA, a session duration of 20–30 min, and 5–10 sessions.	Low
David et al., 2018	8 studies 127 participants	Neuropathic pain	Intervention: tDCS Control: sham stimulation	1 session–20 sessions	90 min–6 months	Pain level (VAS and NRS)	All of the studies showed significant effects of tDCS on NP (spinal cord injury, stroke, and amputation) when compared to the control group, except for one with SCI and another related to radiculopathy. Positive effects in the follow-up studies lasted up to 7 days.	Low
Mehta et al., 2015	5 studies 83 participants	Neuropathic pain after spinal cord injury	Intervention: tDCS Control: sham stimulation	1 session–10 sessions	NA	Pain level (VAS and NRS)	The pooled analysis found a significant effect of tDCS on reducing neuropathic pain after SCI post-treatment ($p = 0.012$); however, this effect was not maintained at follow-up ($p = 0.194$).	Moderate
Lloyd et al., 2020	14 studies 452 participants	Fibromyalgia	Intervention: tDCS Control: sham stimulation	1 session–10 sessions	NA	Pain level (VAS and NRS)	Meta-analysis of data from 8 controlled trials provides tentative evidence of pain reduction when active tDCS is delivered compared to sham.	
Zhu et al., 2017	6 studies 192 participants	Fibromyalgia	Intervention: tDCS Control: sham stimulation alone or sham stimulation combined with other interventions for fibromyalgia	1 session–10 sessions	NA	Pain level (VAS and NRS)	Significant improvement in pain and general fibromyalgia related function was seen with anodal transcranial direct current stimulation over the primary motor cortex ($p < 0.05$). However, the pressure pain threshold did not improve ($p > 0.05$).	High
Stilling et al., 2019	34 studies (12 for tDCS) 413 participants	Headache (8/12 studies for migraine)	Intervention: tDCS Control: sham stimulation or alternative standard of care (i.e., botulinum toxin, headache drug)	5 session–20 sessions	NA	Headache frequency, duration, intensity, use of abortive medications, depression, anxiety, and QoL.	There is moderate evidence for tDCS in the treatment of headaches concerning reduction in headache frequency, intensity, abortive medication use, depression, and anxiety.	Low
Feng et al., 2019	9 studies (4 for tDCS) 276 participants (115 for tDCS)	Migraine	Intervention: tDCS Control: sham stimulation or no control treatment	10 session–20 sessions	1 month–12 weeks	Pain level (VAS and NRS)	tDCS over the M1 or the DLPFC showed significant effects on reducing headache intensity in patients with migraine.	Moderate
Alwardat et al., 2020	9 studies 411 participants	Chronic low back pain	Intervention: tDCS Control: sham stimulation	1 session–15 sessions	3 weeks–6 months	Pain level (VAS and NRS)	The meta-analysis showed non-significant effect of multiple sessions of tDCS over M1 on pain reduction ($p = 0.249$) and disability ($p = 0.434$) post-treatment, respectively.	Low

Reviews selected to avoid redundancy with text and other reviews. AMSTAR-2 ratings represent a grading system for systematic reviews, with confidence in findings rated as high, moderate, low, or critically low based on 16 items (13 for reviews without meta-analyses). AMSTAR, A Measurement Tool to Assess Systematic Reviews; NIBS, non-invasive brain stimulation; RCTs, randomized controlled trials; TMS, transcranial magnetic stimulation; sTMS, single-pulse TMS; dTMS, deep transcranial magnetic stimulation; rTMS, repetitive transcranial magnetic stimulation; HF-rTMS, high frequency transcranial magnetic stimulation; tDCS, transcranial direct current stimulation; VAS, Visual Analog Scale; QoL, quality of life; NP, neuropathic pain; SCI, spinal cord injury; RMT, resting motor threshold; BPI, brief pain inventory; HDRS, Hamilton Depression Rating Scale; BDI, beck depression inventory; NRS, Numeric Rating Scale; MPQ, McGill Pain Questionnaire.

the release of endogenous opioids and the secretion of brain-derived neurotrophic factors, and increase the concentration of GABA, thereby improving pain (Dall'Agnol et al., 2014). Lefaucheur et al. (2006) found that HF-rTMS of M1 can reduce pain and enhance cortical inhibition, and the degree of pain reduction is positively correlated with intracortical inhibition. They speculated that rTMS may regulate the balance between inhibitory neurotransmitters and excitatory glutamate neurotransmitters in the cerebral cortex, thus achieving an analgesic effect.

Improving Regional Cerebral Blood Flow and Metabolism in the Brain

Notably, changes in regional cerebral blood flow (rCBF) and metabolism after rTMS treatment may be correlated with the decrease in pain score. Tamura et al. (2004) found that after LF-rTMS treatment, the rCBF of the medial prefrontal cortex was remarkably reduced, and the rCBF of the tail of the ACC and the contralateral premotor area was considerably increased. Meanwhile, the subjects' pain was substantially reduced. In addition, the degree of pain relief was positively correlated with the decrease in rCBF in the medial prefrontal cortex, suggesting that the analgesic effect caused by rTMS is related to changes in rCBF (Tamura et al., 2004).

Repetitive Transcranial Magnetic Stimulation for Neuropathic Pain

The pathophysiological mechanism of NP may be related to changes in the structural or functional plasticity of the central nervous system (Leung et al., 2009). The maintenance of NP mainly depends on central sensitization. Central sensitization refers to the abnormal increase in excitability or synaptic transmission of central pain-related neurons, including the increase in spontaneous discharge activity of neurons, the expansion of sensory domains, and the reduction of the threshold value to external stimuli, thus amplifying the transmission of pain signals (Nickel et al., 2012). rTMS acts on the cerebral cortex and adjacent structures under the cortex through high-level regulation of the central nervous system, and it exerts various effects on the pain process, thereby exerting an analgesic effect. Yang et al. (2018) suggested that HF-rTMS may reduce central sensitization and relieve NP by downregulating the overexpression of neuronal nitric oxide synthase in ipsilateral dorsal root ganglions and inhibiting the activity and proliferation of astrocytes in the L4–L6 spinal dorsal horns ipsilateral to NP.

A meta-analysis of 25 studies (589 long-term follow-up patients) evaluated the efficacy of HF-rTMS for the treatment of NP (Jin et al., 2015). Pooled analgesic results showed a statistically significant effect size of -0.86 ($p < 0.05$), indicating that rTMS can effectively reduce the pain intensity of NP from different sources. The result indicated that a single rTMS treatment can remarkably reduce the pain intensity of patients with NP. When the number of sessions was increased from 2 to 10, the subjects also produced considerable pain relief, especially among patients with pain after suffering from central stroke. After 1–2 months of follow-up (161 participants), the analgesic effects of multiple rTMS treatments ($\geq$5 sessions) were observed to last at least 1 month but not more than 2 months, indicating that the different analgesic effects of rTMS may depend on the neuroanatomical source of the pathophysia of NP, that is, the more effective source of the therapeutic effects of rTMS on NP is the "top" (supraspinal, cranial, or spinal) rather than the "bottom" (nerve roots or peripheral nerves). Similarly, Zhang et al. (2021) systematically reviewed 29 studies (24 for rTMS, 736 participants), and found that rTMS successfully improved the pain symptoms of 97.1% of patients with NP (715 participants). The analgesic effect of rTMS was maintained for 2 weeks after the last session, but this beneficial effect usually lasted for less than 1 month. In addition, the M1 region was targeted in almost all patients (82.5%, 607 participants).

As recent reviews have concluded, the application of HF-rTMS of M1 may alleviate various types of NP. Some of the NP conditions with the greatest response to rTMS include post-stroke central pain and trigeminal neuralgia, whereas NP conditions with more peripheral anatomical origins, such as post-traumatic peripheral NP, are less reactive to rTMS (Lefaucheur, 2016; Leung et al., 2020). Although a few studies suggest this conclusion, we think it is premature to present this type of assertion which is not based on published data on large series. It is unclear whether any particular type of NP would be considered a better indication for rTMS treatment.

Repetitive Transcranial Magnetic Stimulation for Fibromyalgia

Fibromyalgia is usually insensitive to conventional treatment. Previous studies indicated that rTMS may work by modulating pain pathways (Bestmann et al., 2004; Yoo et al., 2008), such as the descending inhibitory pathway, and by modulating social–affective areas of the brain, such as the right temporal lobe (Boyer et al., 2014). A meta-analysis (7 studies, 210 patients) evaluated the efficacy of HF-rTMS of M1 in the treatment of fibromyalgia (Saltychev and Laimi, 2017). Based on the patients' scores on a 0–10 numerical rating scale, their pain intensity before and after the last rTMS session decreased by 1.2 points. Moreover, the pain intensity before the last stimulation and 1 week to 1 month after the last stimulation decreased by 0.7 points. Both pooled results were statistically significant but below the cut-off point of a minimum clinically significant difference of 1.5 points. In a narrative review that analyzed 12 studies on fibromyalgia, 9 studies concluded that rTMS of M1 was effective in relieving pain in patients with this condition (Yang and Chang, 2020). By contrast, the remaining three randomized controlled trials (RCTs) denied that patients with fibromyalgia benefited from rTMS.

Although the results of some studies were negative, the fact that fibromyalgia is difficult to manage suggests that rTMS is a potential analgesic method for managing fibromyalgia.

Repetitive Transcranial Magnetic Stimulation for Migraine

Recent studies suggested that the mechanism of migraine may be linked to neurological causes, such as cerebral cell hyperexcitability and altered cortical excitability

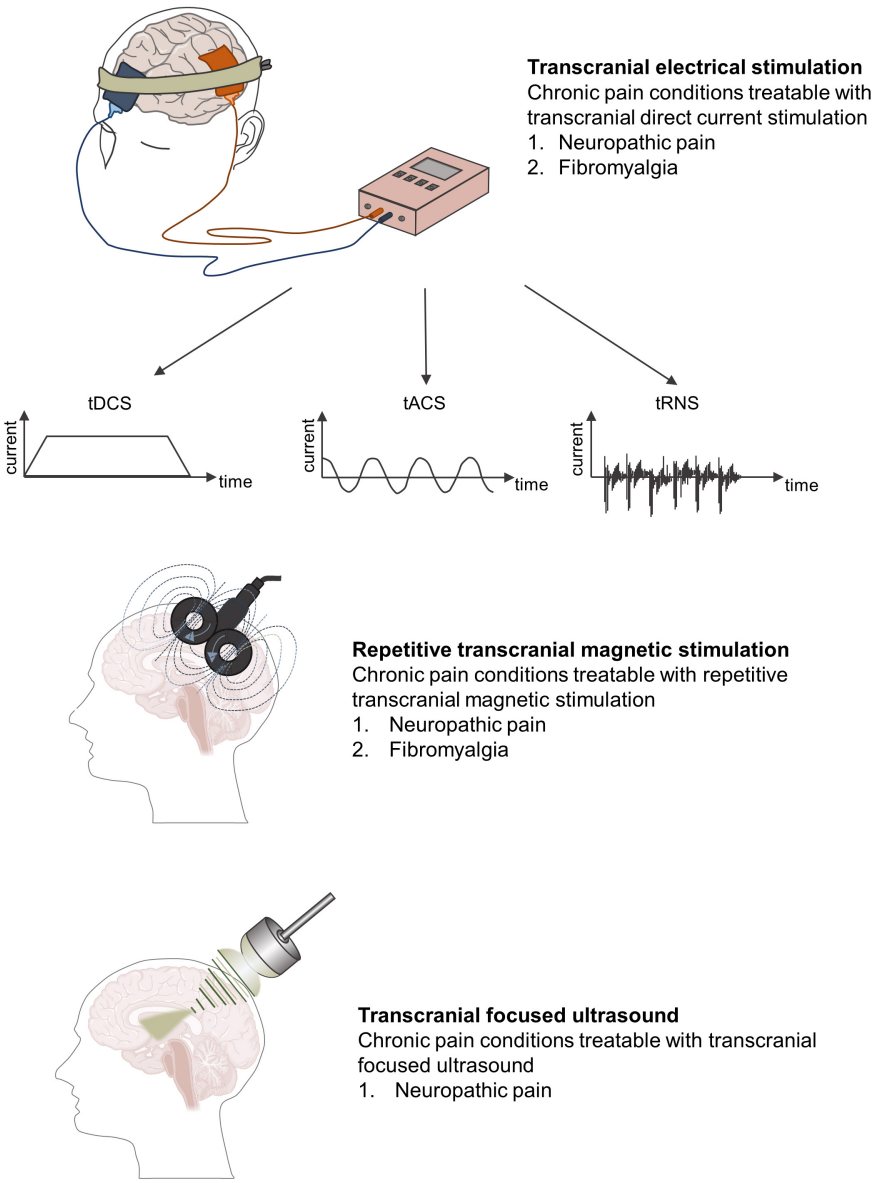

FIGURE 3 | Different forms of non-invasive brain stimulation techniques and chronic pain conditions most amenable to treatment.

(Cosentino et al., 2014; Lan et al., 2017). On the one hand, rTMS can regulate the excitability of cortical structures involved in pain control, such as inhibiting cortical spreading depression (Chervyakov et al., 2015). Therefore, rTMS may contribute to the prevention and relief of headache symptoms during migraine attacks. On the other hand, rTMS can promote the release of endogenous analgesic substances, such as dopamine and endogenous opioid peptides, thereby relieving headaches.

Currently, in the United States, acute migraine with aura is the only FDA-approved indication for single-pulse TMS45. A meta-analysis also reported that single-pulse TMS was effective in the acute treatment of aura migraine after the first attack ($p = 0.02$), but not in chronic migraine ($p = 0.14$) (Lan et al., 2017). However, another systematic review found that TMS and rTMS contributed to reductions in headache frequency, duration, intensity, abortive medication use, depression, and dysfunction in both chronic primary and secondary headaches (Stilling et al., 2019). In addition, consistent with the findings of Lan et al. (2017), only a few studies reported greater changes than sham stimulation (Stilling et al., 2019). Similarly, another systematic review found that, compared with sham stimulation, the outcome indicators of patients suffering from migraine who received HF-rTMS treatment substantially improved, including headache frequency, pain intensity, headache duration, and dosage (Yang and Chang, 2020). However, two studies showed that the results after rTMS were not superior to those after sham stimulation, and both showed a strong placebo response. Despite conflicting

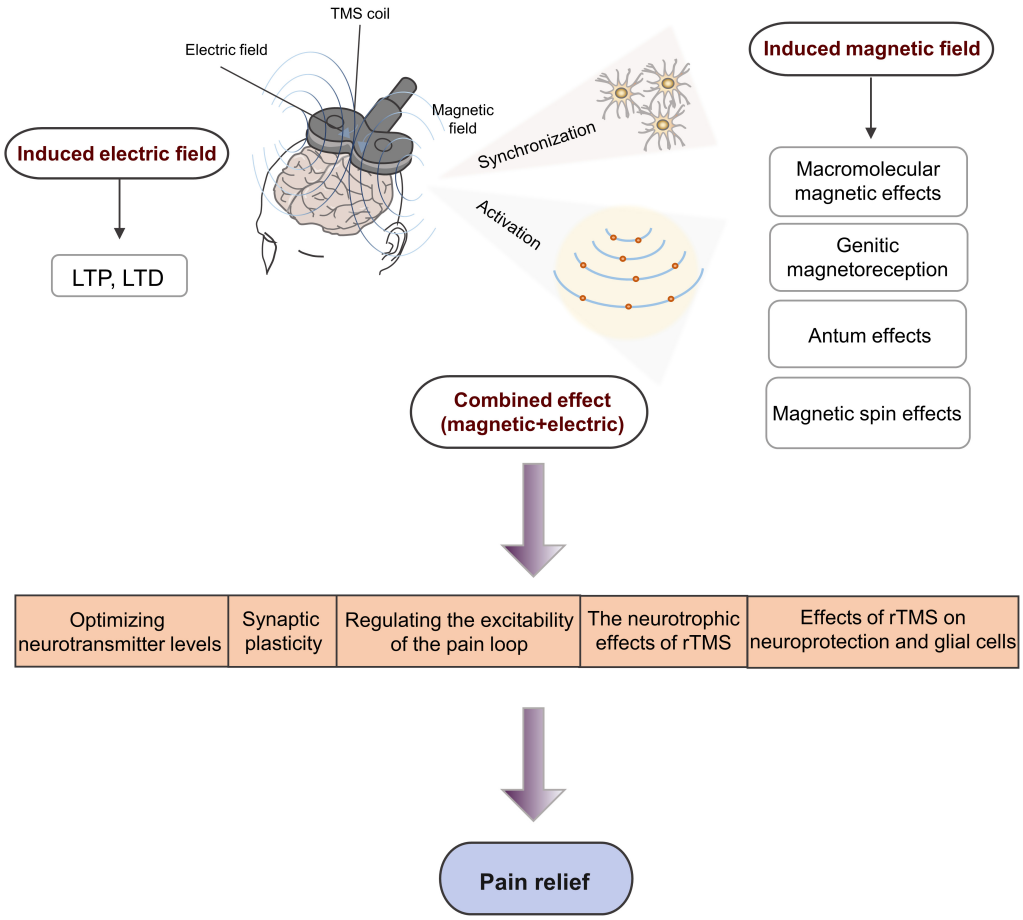

FIGURE 4 | Schematic diagram demonstrating the underlying neurophysiological mechanism of rTMS involved in pain management. LTP, long-term potentiation; LTD, long-term depression.

evidence on its efficacy, rTMS may still be a potential option for patients with migraine.

Repetitive Transcranial Magnetic Stimulation for Chronic Low Back Pain

Previous studies have demonstrated that abnormal postural control of trunk muscles may lead to the occurrence of chronic low back pain (CLBP) (Deliagina et al., 2006). Furthermore, the M1 region is believed to play a key role in postural control regulation (Ambriz-Tututi et al., 2016). Ambriz-Tututi et al. (2016) evaluated the long-term effects of rTMS on CLBP and compared them with those of physical therapy and sham stimulation. Results showed that the patients who received HF-rTMS of M1 had a remarkable decrease in pain intensity after 1 week of treatment. After 3 weeks of continuous treatment, their pain intensity was reduced by nearly 80% compared with the baseline and was substantially lower than that of the group that received sham stimulation or physical therapy. In addition, a previous study reported that, compared with sham stimulation, 1 session of HF-rTMS can significantly lessen the pain intensity felt by patients with CLBP ($p < 0.001$) (Johnson et al., 2006). Compared with those on fibromyalgia and headache, there is less evidence to suggest the efficacy of rTMS on CLBP.

Summary of Repetitive Transcranial Magnetic Stimulation

In Canada, Australia, Japan, the European Union, and Israel, TMS devices have been approved for depression, schizophrenia, and NP (Marangell et al., 2007). However, in the United States, the application of TMS to pain management is only considered investigational.

Thus far, most high-quality RCTs and systematic reviews have shown that rTMS applied to the dorsolateral prefrontal cortex (DLPFC), the supplementary motor area (SMA), or the primary somatosensory cortex (S1) lacks analgesic effects, while stimulation of M1 provides pain relief (Marangell et al., 2007; Lefaucheur et al., 2020). In 2020, the guidelines for the use of rTMS developed by an expert panel in Europe stated that HF-rTMS of M1 has a clear effect on NP and fibromyalgia (level A evidence) (Lefaucheur et al., 2020). The selection of stimulation targets and stimulation parameters is the most basic and important issue that determines the analgesic effect of

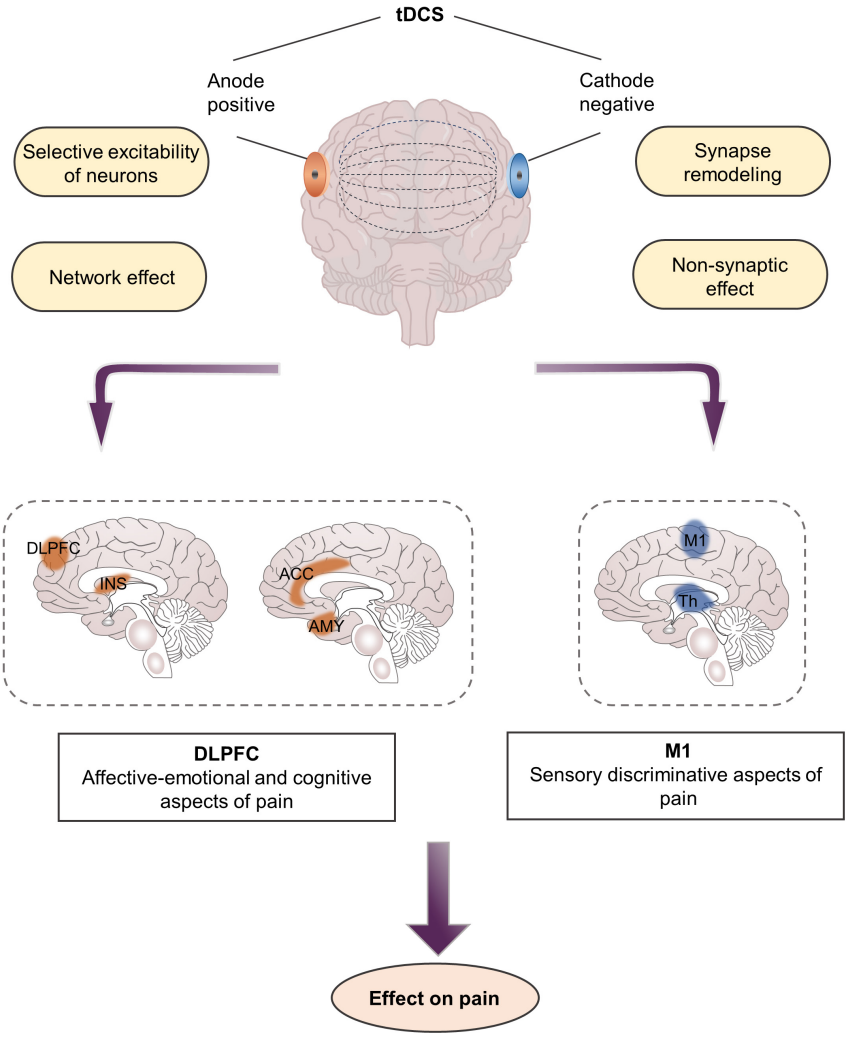

FIGURE 5 | Mechanisms and targets of transcranial direct current stimulation in pain management. DLPFC, dorsolateral prefrontal cortex; M1, primary motor cortex; INS, Insula; Th, thalamus.

rTMS. Some of the current issues in stimulating targets are as follows: (1) whether different types of CP conditions require specific stimulation targets; (2) whether combined treatment with different stimulation targets will enhance their analgesic effect; (3) lack of evidence from studies that compared the analgesic effects of different stimulation targets; and (4) few use image-guided navigation to improve the accuracy and repeatability of targeting. Another potential concern with rTMS is the duration effect. The number of sessions in most TMS studies ranged from 1 to 10 sessions. Some studies have reported that the analgesic effects of rTMS are cumulative and require multiple sessions to achieve clinically significant effects (Brighina et al., 2009). A single rTMS session may not be sufficient to induce changes in cortical excitability, and multiple sessions are required to induce changes in neuroplasticity. However, prolonged use of rTMS to increase stimulation intensity may also lead to a reduction or even reversal of the stimulatory effect of motor cortical excitability, making the treatment counterproductive. Therefore, the number of sessions with rTMS should be investigated to provide best practice for the analgesic effects of rTMS.

TRANSCRANIAL DIRECT CURRENT STIMULATION

Underlying Neurophysiological Mechanisms by Which Transcranial Direct Current Stimulation Relieves Chronic Pain

Transcranial direct current stimulation works by using two or more electrodes to apply a low-amplitude direct current (typically from 0.5 to 2 mA) to specific brain regions to modulate their excitability, thereby relieving pain (Nitsche and Paulus, 2000). Traditional tDCS usually uses two sponge electrodes, one as

the anode and the other as the cathode. HD tDCS utilizes a set of smaller electrodes, such as 4 × 1, to provide more focused stimulation.

Selective Excitability of Neurons

Unlike TMS, tDCS employs a weak current and generally does not cause an action potential but only changes the resting membrane potential of nerve cells, thereby regulating the excitability of nerve cells (Nitsche et al., 2008). The change in membrane potential is the physiological basis of the immediate regulatory effect of tDCS. The effect of tDCS on cortical excitability depends on polarity: anodal stimulation leads to depolarization of the nerve membrane, thereby increasing excitability, whereas cathodal stimulation results in hyperpolarization of the nerve membrane, which in turn inhibits excitability (Lefaucheur et al., 2017; Lefaucheur and Wendling, 2019; **Figure 5**). However, changes in cell membrane potential do not explain the subsequent effects of cessation of tDCS, such as the persistence of analgesic effects several weeks after stimulation.

Notably, the cortical excitation effect of tDCS is related to the direction and intensity of the current, but it is not a linear relationship, that is, the greater the current intensity, the better the stimulus effect (Utz et al., 2010). Sometimes this effect will be reversed with the increase in current intensity. The immediate to long-term effects of tDCS vary depending on the selected stimulation parameters (Shekhawat et al., 2016). Studies have reported that the analgesic effect of tDCS is cumulative, requiring multiple sessions to achieve clinically significant results (Lefaucheur et al., 2017). In general, a stimulation lasting for at least 5 min is needed to produce biological effects. Changes in neural activity occur not only during tDCS but also several hours after stimulation has ended.

Network Effect

Aside from regulating local activity at the stimulus site, tDCS also exerts network effects that alter structural and functional connections between different brain regions (Cummiford et al., 2016; Lin et al., 2017). A PET study of patients with CP showed that motor cortex stimulation acts as a "gate" that triggers the activity in the stimulated and distant brain tissues, including the thalamus, anterior insula, and PAG (Garcia-Larrea and Peyron, 2007). Specifically, anodal stimulation of the M1 region alleviates pain by activating various neural circuits in the precentral gyrus, which may be afferent or efferent to structures connected to the sensory or emotional components of pain processing, such as the thalamus or ACC (Lefaucheur, 2006; Nguyen et al., 2011). Cummiford et al. (2016) found that, compared with sham stimulation, applying 20 min of anodal tDCS over left M1 five times can reduce functional connectivity among the left ventrolateral thalamus and the medial prefrontal lobe, and the left auxiliary motor area, as well as functional connectivity among the right ventrolateral thalamus and the cerebellum and the left auxiliary motor area in patients with fibromyalgia. These brain regions are the components of the pain matrix involved in the processing and regulation of pain, especially the emotional components of pain (**Figure 1**).

Synapse Remodeling

Aside from changing the polarity of membrane potential, tDCS also regulates the synaptic microenvironment and modulates neuronal function at the synaptic level. tDCS interacts with several neurotransmitters, including serotonin, dopamine, and acetylcholine, and affects various neuronal membrane channels, such as sodium and calcium ions (Lefaucheur et al., 2017). In general, direct current stimulates cortical neurons to regulate the expression of NMDA receptors and the release of GABA, resulting in LTP or LTD, both of which cause synaptic remodeling (Stagg and Nitsche, 2011). Previous studies have argued that calcium-dependent synaptic plasticity in glutamate neurons plays a key role in the mechanism of long-lasting neuroplasticity in tDCS because blocking NMDA receptors attenuates the after-effects of tDCS. In addition, tDCS can alleviate pain by modulating the thalamic inhibitory network and interfering with the cortex–cortical and cortex–subcortical synaptic connections related to pain formation (Liebetanz et al., 2002; Batsikadze et al., 2013).

Non-synaptic Effect

Although tDCS regulates resting membrane potentials at the synaptic level, it more commonly regulates resting membrane potentials along the entire axon, which may lead to non-synaptic effects (Ardolino et al., 2005). These non-synaptic mechanisms of tDCS are probably due to conformational and functional changes in various axon molecules. When exposed to a direct current electric field, various phenomena, such as transmembrane ion conductance, membrane structure changes, cytoskeleton changes, or axon transmission, will occur around axons (Jefferys, 1995). In addition, Zheng et al. (2011) found that the effect of tDCS is related to changes in cerebral blood flow. After they administered cathodal tDCS, the blood flow substantially decreased and lasted for a period of time. This condition may also be the key mechanism underlying the analgesic effect of tDCS.

Transcranial Direct Current Stimulation for Neuropathic Pain

In addition to network effects and changes in central nervous excitability, tDCS may also alleviate NP by regulating the central nervous immune system and inhibiting glial cell activation. Cioato et al. (2016) investigated the effects of tDCS on nociceptive responses and measured IL-1 β, IL-10, and TNF-α levels in the central nervous system structure of NP rats. After tDCS, the levels of IL-1β and TNF-α decreased, whereas those of IL-10 increased, suggesting that tDCS may modulate the immune system to alleviate NP. Recent studies have established that microglia and astrocytes in the nervous system play key roles in the initiation and maintenance of NP, respectively (Gritsch et al., 2016). As a common method for regulating cortical excitability in superficial pain-related areas, tDCS can inhibit neuronal sensitivity after peripheral nerve injury and downregulate the expression of the P2 × 4 receptor, thereby inhibiting microglia activity, ultimately leading to NP remission (Zhang et al., 2020).

A systematic review (8 studies, 127 participants) suggested that, compared with sham stimulation, tDCS could notably

reduce pain intensity in patients with NP associated with spinal cord injury (SCI), stroke, and amputation, and its analgesic effect lasted for 1 week after the end of the intervention (David et al., 2018). However, no significant differences between the groups were observed in patients with radiculopathy. Similarly, a meta-analysis reported a moderate effect of tDCS in reducing NP in patients with SCI; however, the effect was not maintained at follow-up (Mehta et al., 2015). A mean pooled decrease of 1.33 units on a 10-item scale was found post treatment. In another systematic review (6 studies, 125 patients with NP), 5 studies found that, compared with sham stimulation, anodal tDCS remarkably alleviated NP (Zhang et al., 2021). Overall, many studies have confirmed that tDCS has a moderate effect on pain relief among individuals with chronic NP, but this effect is not maintained during follow-up.

Transcranial Direct Current Stimulation for Fibromyalgia

The pathogenesis of fibromyalgia may be related to the dysfunction of the central nervous system (Cook et al., 2007; Brown et al., 2014). As a neuromodulation technique that targets the central nervous system, tDCS may theoretically help relieve pain. A meta-analysis of 6 studies (192 patients with fibromyalgia) reported that, compared with sham stimulation, anodal tDCS of M1 was more likely to relieve pain and improve fibromyalgia-related function, whereas cathodal tDCS of M1 and anodal tDCS of left DLPFC did not produce notable analgesic effects (Zhu et al., 2017). Although this meta-analysis was unable to calculate the overall effect of tDCS on fibromyalgia during the follow-up period, some of the studies it included concluded that 10 sessions of anodal tDCS over M1 was more likely to control pain than 5 sessions, and this effect might last up to 2 months. Similarly, Lloyd et al. (2020) also reported that active tDCS applied at an intensity of 2 mA to left M1 for 20 min/days for 10 sessions appears to be able to lower pain intensity in fibromyalgia. Hou et al. (2016) reviewed 16 studies (5 for tDCS, 11 for rTMS; 572 patients with fibromyalgia), found that aside from improving cognitive function, both tDCS and rTMS had similar positive effects on pain symptoms, sleep disturbances, and tender spots. However, rTMS produced a greater analgesic effect than tDCS. Therefore, excitatory rTMS/tDCS should be considered in the treatment of patients with fibromyalgia, especially for those with painful symptoms that are not responding to other therapies or for whom the continuation of such therapies is not possible due to their adverse side effects (as is commonly the case with FDA-approved drugs).

Transcranial Direct Current Stimulation for Migraine

A systematic review of 12 studies on chronic headache (8 for migraine, 413 participants) found that, compared with baseline, tDCS substantially reduced headache frequency in 7 studies (Stilling et al., 2019). However, only one study showed that, compared with sham stimulation, tDCS considerably decreased headache frequency. Six studies reported that tDCS shortened headache duration, but only one study was statistically different from the control group. Seven studies found that tDCS reduced pain intensity, but only two studies showed significant differences between groups. Similarly, Feng et al. (2019) reviewed 9 studies (4 for tDCS, 115 participants), and found that anodal tDCS of M1 markedly reduced the frequency and intensity of headaches in patients suffering from migraine. Moreover, tDCS over DLPFC substantially reduced pain intensity in these patients, but it had no notable effect on attack frequency. In addition, compared with sham stimulation, cathodal tDCS applied to the vertex or visual cortex did not remarkably change the frequency and intensity of headaches in these patients. Compared with those on fibromyalgia and NP, there is less evidence to suggest the efficacy of tDCS on migraine.

Transcranial Direct Current Stimulation for Chronic Low Back Pain

Unlike acute low back pain, non-specific CLBP usually has no peripheral cause (Latremoliere and Woolf, 2009). Central mechanisms have been hypothesized to explain the development and maintenance of pain. Great functional connectivity between the dorsal medial PFC–amygdala–accumbens circuit in patients with subacute low back pain contributes to the risk of CP (Vachon-Presseau et al., 2016). Therefore, brain network disturbance is considered one of the possible causes of CLBP. A recent systematic analysis (eight studies) revealed that, compared with sham stimulation, 1 session of tDCS treatment resulted in substantial pain relief (Patricio et al., 2021). By contrast, multiple sessions of tDCS treatment did not improve short-term and medium-term pain. In 2019, based on two studies on tDCS, an expert panel proposed a level A recommendation against the use of tDCS of M1 for the treatment of CLBP (Baptista et al., 2019).

Recent systematic analyses did not support the use of tDCS for CLBP treatment, and evidence of low quality suggests that tDCS negatively affects CLBP. A possible explanation for these negative findings is that the pathogenesis of CLBP is affected by multiple factors. Therefore, the participants enrolled in these reviews might have had other mechanical diseases or complications, such as cervical spondylosis or small joint disorders. In addition, visceral pain involving the lower back can be a misleading condition, leading doctors to misdiagnose or miss a diagnosis.

Summary of Transcranial Direct Current Stimulation

In the United States, tDCS has not been approved for any clinical indications but is only used as a research technique for pain management. The guidelines for neurostimulation therapy of CP issued by the European Academy of Neurology gave "weak recommendations" for the use of tDCS for the treatment of peripheral NP and "uncertain recommendations" for the treatment of fibromyalgia (Cruccu et al., 2016; Knotkova et al., 2021). In the United States, tDCS has not been approved for any clinical indications but is only used as a research technique for pain management. The effectiveness of tDCS in relieving CP may vary according to pain subtype, including spontaneous,

paroxysmal, and persistent pain (Soler et al., 2010). Thus far, many high-quality RCTs and systematic reviews have shown that the application of tDCS to DLPFC, SMA, or S1 lacks analgesic effects, whereas stimulation of the M1 region provides pain relief (Lefaucheur et al., 2017). It is worth noting that tDCS is non-local with a network effect, and cortices adjacent to the stimulation target may also be affected. As a result, it is essential to combine tDCS with neuroimaging and functional connectivity analysis so that we can attribute specific efficacy to neuromodulation of M1 only, but unfortunately, the majority of tDCS studies lack the corresponding neuroimaging evaluation. In addition, the current level of evidence supporting the positive effect of the application of tDCS over M1 on pain relief is considerably lower than that of rTMS. Compared with that of rTMS, the after-effect of tDCS is also less obvious (Ngernyam et al., 2013).

TRANSCRANIAL ALTERNATING CURRENT STIMULATION

Transcranial alternating current stimulation (tACS) changes the nerve oscillation signal by applying a sinusoidal alternating current stimulation with a fixed amplitude and frequency to the brain, thereby regulating pain intensity (Antal and Herrmann, 2016; Tavakoli and Yun, 2017; Arendsen et al., 2018). Previous studies have confirmed that the neural oscillation signals in the alpha and gamma bands before pain stimulation can regulate the individual's perception of pain stimulation (Tu et al., 2016). Given that the neural synchronization effect is related to endogenous neural oscillation signals, the stimulation frequency selected in analgesia studies is the frequency corresponding to the neural oscillation signals closely related to pain processing, such as the alpha and gamma neural oscillation signals (Tu et al., 2016). After the pain stimulation, the neural oscillation signals in the alpha band are weakened, whereas the nerve oscillation signals in the gamma band are strengthened. The neural oscillation signal in the gamma band is not affected by the saliency of the stimulus but reflects the individual's perception of pain intensity, and it can encode intra- and interindividual pain sensitivity (Zhang et al., 2012; Hu and Iannetti, 2019). Thus, the use of tACS in regulating pain perception has a theoretical basis.

So far, only one study has investigated the analgesic effect of tACS on fibromyalgia. An RCT of 15 patients with fibromyalgia found that tACS combined with physical therapy administered 5 days per week for 2 weeks effectively reduced pain Visual Analog Scale (VAS) scores immediately after the intervention (Bernardi et al., 2021). However, this positive analgesic effect was no longer present 4 weeks after the end of the intervention. Similarly, only one study has investigated the effectiveness of tACS for CLBP treatment. Ahn et al. (2019) found that applying tACS with an amplitude of 1 mA and a frequency of 10 Hz to the F3 and F4 electrodes of EEG electrode caps for 40 min can reduce the pain intensity of patients with CLBP. Moreover, tACS enhances the alpha oscillation signal intensity of the electrode near the somatosensory area, and this increase in the alpha oscillation signal is also strongly related to the decrease in pain intensity.

Despite its appeal, tACS seems to be rarely used in the field of CP research. Apart from somatosensory areas, few studies have evaluated the analgesic effect of tACS on CP in other brain areas (Ahn et al., 2019; Bernardi et al., 2021). Although previous studies have demonstrated that the application of alpha tACS over S1 can enhance alpha oscillations and thus induce pain relief, the quality of evidence is extremely low.

TRANSCRANIAL RANDOM NOISE STIMULATION

As an innovative form of electrical stimulation, transcranial random noise stimulation (tRNS) is based on the principle of stochastic resonance that uses alternating current with a frequency randomly varying between 0 and 640 Hz to increase the excitability of the cortex regardless of the orientation of the current (Paulus, 2011). Studies have shown that weak tRNS of M1 led to enhanced motor cortical excitability, where high-frequency subdivision of the whole tRNS spectrum between 100 and 640 Hz was functionally responsible for inducing excitability enhancement (Terney et al., 2008; Paulus, 2011; Moret et al., 2019). In addition, 10 min of tRNS stimulation was reported to induce a consistent excitability increase lasting over 1 h after stimulation (Terney et al., 2008). This effect could be attributed to the repeated opening of sodium channels or to the increased sensitivity of neuronal networks to field modulation (Terney et al., 2008; Paulus, 2011). These evidence raise the possibility that tRNS may prove as an effective and reliable means to relieve pain perception.

Curatolo et al. (2017) applied 10 sessions of tRNS of M1 to 20 women with fibromyalgia. The results showed that, compared with placebo, active tRNS remarkably reduced pain and fibromyalgia impact questionnaire scores. By contrast, Palm et al. (2016) reported that, immediately after tRNS, no notable intergroup differences in mean pain VAS score, attention performance, and mood scale were observed between the tRNS and placebo groups.

Evidence supporting the effects of tRNS as a single intervention for CP treatment is limited. Moreover, drawing conclusions on whether tRNS is useful in this situation is difficult. Therefore, large multicenter RCTs are warranted to evaluate the better potential of tRNS for pain management.

TRANSCRANIAL FOCUSED ULTRASOUND

As a NIBS method that can focus on deep brain structures, transcranial focused ultrasound (tFUS) can stimulate deep brain targets with a high level of spatial resolution and generate superimposed ultrasonic pulses deep in the brain by using transducers containing piezoelectric elements (Aubry and Tanter, 2016; Folloni et al., 2019). Through this feature, tFUS can target almost any part of the peripheral or central nervous system (Xiao and Zhang, 2018). Previous studies have demonstrated that adjusting ultrasound parameters can

produce different physiological effects on the nervous system, ranging from reversible activation or suppression of neural activity (low intensity, low-frequency ultrasound) to irreversible tissue ablation (high intensity focused ultrasound) (di Biase et al., 2019). tFUS can produce an analgesic effect through various mechanisms, such as by increasing blood–brain barrier permeability, improving the concentration of central acting analgesics in the central nervous system, or modulating gene expression in pain perception (di Biase et al., 2019). If the neuromodulation of tFUS can act on specific neural networks related to pain processing, it may be developed for pain management. Currently, tFUS has been approved only for thalamotomy in chronic NP and for ablation of specific tumors (di Biase et al., 2021).

In a cross-controlled study of 19 healthy adults, Badran et al. (2020) found that tFUS targeting the right anterior thalamus could modulate the antinociceptive effects of the pain processing network. Compared with sham stimulation, a 20-min tFUS treatment significantly increased the heat pain threshold; but tFUS did not remarkably alter the heat pain tolerance threshold. Their findings suggested that tFUS could modulate pain sensitivity through its interaction with the thalamus and by affecting the afferent sensory-discriminative component of pain. Compared with other NIBS techniques focusing on CP, there is less evidence to suggest the efficacy of tFUS on CP.

FUTURE DIRECTIONS

New insights into the neuromodulation mechanisms underlying CP have opened new perspectives on new treatments. Over the past 20 years, NIBS techniques have emerged as one of the most promising tools for treating pain. NIBS may be an effective treatment for alleviating CP as indicated by many Cochrane meta-analyses of CP syndromes. However, in most cases, the corresponding analgesic effects are weak and variable. Except for rTMS, which has been proved effective in the treatment of major depression, no NIBS protocol has been certified as a routinely used CP management tool.

Given that the brain is an advanced center for pain control, CP treatment based on neural network systems may be the future trend of transcranial modulation of brain activities. On the one hand, researchers must value multi-site approaches to target various networks or sites of networks. On the other hand, researchers must study further the functions of pain-related nuclei in the brain and control CP through precise regulation of pain-related nuclei in the brain. Progress in NIBS research requires a deeper understanding of the relationship between the underlying neurophysiological effects and functional outcomes of pain, as well as better identification of clinical and non-clinical factors that influence pain reactivity.

AUTHOR CONTRIBUTIONS

H-YX collected the data, elaborated the design of the study, and wrote the manuscript. X-QW and J-JZ organized the research project and corrected the manuscript. All authors read and approved the manuscript.

FUNDING

This work was supported by Fok Ying-Tong Education Foundation of China (161092); the Scientific and Technological Research Program of the Shanghai Science and Technology Committee (Fund Number: 19080503100); the Shanghai Key Lab of Human Performance (Shanghai University of Sport) (11DZ2261100); Shanghai Frontiers Science Research Base of Exercise and Metabolic Health; Talent Development Fund of Shanghai Municipal (2021081); and Shanghai Clinical Research Center for Rehabilitation Medicine (21MC1930200).

REFERENCES

Ahn, S., Prim, J. H., Alexander, M. L., McCulloch, K. L., and Frohlich, F. (2019). Identifying and Engaging Neuronal Oscillations by Transcranial Alternating Current Stimulation in Patients With Chronic Low Back Pain: A Randomized, Crossover, Double-Blind, Sham-Controlled Pilot Study. *J. Pain* 20, e271–e277. doi: 10.1016/j.jpain.2018.09.004

Alwardat, M., Pisani, A., Etoom, M., Carpenedo, R., Chiné, E., Dauri, M., et al. (2020). Is transcranial direct current stimulation (tDCS) effective for chronic low back pain? a systematic review and meta-analysis. *J. Neural. Transm. (Vienna)*, 127, 1257–1270. doi: 10.1007/s00702-020-02223-w

Ambriz-Tututi, M., Alvarado-Reynoso, B., and Drucker-Colin, R. (2016). Analgesic effect of repetitive transcranial magnetic stimulation (rTMS) in patients with chronic low back pain. *Bioelectromagnetics* 37, 527–535. doi: 10.1002/bem.22001

Antal, A., and Herrmann, C. S. (2016). Transcranial Alternating Current and Random Noise Stimulation: possible Mechanisms. *Neural Plast.* 2016:3616807. doi: 10.1155/2016/3616807

Ardolino, G., Bossi, B., Barbieri, S., and Priori, A. (2005). Non-synaptic mechanisms underlie the after-effects of cathodal transcutaneous direct current stimulation of the human brain. *J. Physiol.* 568(Pt 2), 653–663. doi: 10.1113/jphysiol.2005.088310

Arendsen, L. J., Hugh-Jones, S., and Lloyd, D. M. (2018). Transcranial Alternating Current Stimulation at Alpha Frequency Reduces Pain When the Intensity of Pain is Uncertain. *J. Pain* 19, 807–818. doi: 10.1016/j.jpain.2018.02.014

Aubry, J. F., and Tanter, M. (2016). MR-Guided Transcranial Focused Ultrasound. *Adv. Exp. Med. Biol.* 880, 97–111. doi: 10.1007/978-3-319-22536-4_6

Badran, B. W., Caulfield, K. A., Stomberg-Firestein, S., Summers, P. M., Dowdle, L. T., Savoca, M., et al. (2020). Sonication of the anterior thalamus with MRI-Guided transcranial focused ultrasound (tFUS) alters pain thresholds in healthy adults: A double-blind, sham-controlled study. *Brain Stimul.* 13, 1805–1812. doi: 10.1016/j.brs.2020.10.007

Baptista, A. F., Fernandes, A., Sa, K. N., Okano, A. H., Brunoni, A. R., Lara-Solares, A., et al. (2019). Latin American and Caribbean consensus on noninvasive central nervous system neuromodulation for chronic pain management (LAC2-NIN-CP). *Pain Rep.* 4:e692. doi: 10.1097/PR9.0000000000000692

Batsikadze, G., Moliadze, V., Paulus, W., Kuo, M. F., and Nitsche, M. A. (2013). Partially non-linear stimulation intensity-dependent effects of direct current stimulation on motor cortex excitability in humans. *J. Physiol.* 591, 1987–2000. doi: 10.1113/jphysiol.2012.249730

Bernardi, L., Bertuccelli, M., Formaggio, E., Rubega, M., Bosco, G., Tenconi, E., et al. (2021). Beyond physiotherapy and pharmacological treatment for fibromyalgia syndrome: tailored tACS as a new therapeutic tool. *Eur. Arch. Psychiatry Clin. Neurosci.* 271, 199–210. doi: 10.1007/s00406-020-01214-y

Bestmann, S., Baudewig, J., Siebner, H. R., Rothwell, J. C., and Frahm, J. (2004). Functional MRI of the immediate impact of transcranial magnetic stimulation on cortical and subcortical motor circuits. *Eur. J. Neurosci.* 19, 1950–1962. doi: 10.1111/j.1460-9568.2004.03277.x

Boyer, L., Dousset, A., Roussel, P., Dossetto, N., Cammilleri, S., Piano, V., et al. (2014). rTMS in fibromyalgia: a randomized trial evaluating QoL and its brain metabolic substrate. *Neurology* 82, 1231–1238. doi: 10.1212/WNL.0000000000000280

Breivik, H., Collett, B., Ventafridda, V., Cohen, R., and Gallacher, D. (2006). Survey of chronic pain in Europe: prevalence, impact on daily life, and treatment. *Eur. J. Pain* 10, 287–333. doi: 10.1016/j.ejpain.2005.06.009

Brighina, F., Palermo, A., and Fierro, B. (2009). Cortical inhibition and habituation to evoked potentials: relevance for pathophysiology of migraine. *J. Headache Pain* 10, 77–84. doi: 10.1007/s10194-008-0095-x

Brown, C. A., El-Deredy, W., and Jones, A. K. (2014). When the brain expects pain: common neural responses to pain anticipation are related to clinical pain and distress in fibromyalgia and osteoarthritis. *Eur. J. Neurosci.* 39, 663–672. doi: 10.1111/ejn.12420

Chervyakov, A. V., Chernyavsky, A. Y., Sinitsyn, D. O., and Piradov, M. A. (2015). Possible Mechanisms Underlying the Therapeutic Effects of Transcranial Magnetic Stimulation. *Front. Hum. Neurosci.* 9:303. doi: 10.3389/fnhum.2015.00303

Cioato, S. G., Medeiros, L. F., Marques Filho, P. R., Vercelino, R., de Souza, A., Scarabelot, V. L., et al. (2016). Long-Lasting Effect of Transcranial Direct Current Stimulation in the Reversal of Hyperalgesia and Cytokine Alterations Induced by the Neuropathic Pain Model. *Brain Stimul.* 9, 209–217. doi: 10.1016/j.brs.2015.12.001

Cook, D. B., Stegner, A. J., and McLoughlin, M. J. (2007). Imaging pain of fibromyalgia. *Curr. Pain Headache Rep.* 11, 190–200. doi: 10.1007/s11916-007-0190-8

Cosentino, G., Fierro, B., Vigneri, S., Talamanca, S., Paladino, P., Baschi, R., et al. (2014). Cyclical changes of cortical excitability and metaplasticity in migraine: evidence from a repetitive transcranial magnetic stimulation study. *Pain* 155, 1070–1078. doi: 10.1016/j.pain.2014.02.024

Cruccu, G., Garcia-Larrea, L., Hansson, P., Keindl, M., Lefaucheur, J. P., Paulus, W., et al. (2016). EAN guidelines on central neurostimulation therapy in chronic pain conditions. *Eur. J. Neurol.* 23, 1489–1499. doi: 10.1111/ene.13103

Cummiford, C. M., Nascimento, T. D., Foerster, B. R., Clauw, D. J., Zubieta, J. K., Harris, R. E., et al. (2016). Changes in resting state functional connectivity after repetitive transcranial direct current stimulation applied to motor cortex in fibromyalgia patients. *Arthritis Res. Ther.* 18:40. doi: 10.1186/s13075-016-0934-0

Curatolo, M., La Bianca, G., Cosentino, G., Baschi, R., Salemi, G., Talotta, R., et al. (2017). Motor cortex tRNS improves pain, affective and cognitive impairment in patients with fibromyalgia: preliminary results of a randomised sham-controlled trial. *Clin. Exp. Rheumatol.* 105, 100–105.

Dahlhamer, J., Lucas, J., Zelaya, C., Nahin, R., Mackey, S., DeBar, L., et al. (2018). Prevalence of Chronic Pain and High-Impact Chronic Pain Among Adults - United States, 2016. *MMWR Morb. Mortal Wkly. Rep.* 67, 1001–1006. doi: 10.15585/mmwr.mm6736a2

Dall'Agnol, L., Medeiros, L. F., Torres, I. L., Deitos, A., Brietzke, A., Laste, G., et al. (2014). Repetitive transcranial magnetic stimulation increases the corticospinal inhibition and the brain-derived neurotrophic factor in chronic myofascial pain syndrome: an explanatory double-blinded, randomized, sham-controlled trial. *J. Pain* 15, 845–855. doi: 10.1016/j.jpain.2014.05.001

David, M., Moraes, A. A., Costa, M. L. D., and Franco, C. I. F. (2018). Transcranial direct current stimulation in the modulation of neuropathic pain: a systematic review. *Neurol. Res.* 40, 555–563. doi: 10.1080/01616412.2018.1453190

de Andrade, D. C., Mhalla, A., Adam, F., Texeira, M. J., and Bouhassira, D. (2011). Neuropharmacological basis of rTMS-induced analgesia: the role of endogenous opioids. *Pain* 152, 320–326. doi: 10.1016/j.pain.2010.10.032

Deliagina, T. G., Orlovsky, G. N., Zelenin, P. V., and Beloozerova, I. N. (2006). Neural bases of postural control. *Physiology* 21, 216–225. doi: 10.1152/physiol.00001.2006

di Biase, L., Falato, E., Caminiti, M. L., Pecoraro, P. M., Narducci, F., and Di Lazzaro, V. (2021). Focused Ultrasound (FUS) for Chronic Pain Management: approved and Potential Applications. *Neurol. Res. Int.* 2021:8438498. doi: 10.1155/2021/8438498

di Biase, L., Falato, E., and Di Lazzaro, V. (2019). Transcranial Focused Ultrasound (tFUS) and Transcranial Unfocused Ultrasound (tUS) Neuromodulation: from Theoretical Principles to Stimulation Practices. *Front. Neurol.* 10:549. doi: 10.3389/fneur.2019.00549

Fayaz, A., Croft, P., Langford, R. M., Donaldson, L. J., and Jones, G. T. (2016). Prevalence of chronic pain in the UK: a systematic review and meta-analysis of population studies. *BMJ Open* 6:e010364. doi: 10.1136/bmjopen-2015-010364

Feng, Y., Zhang, B., Zhang, J., and Yin, Y. (2019). Effects of Non-invasive Brain Stimulation on Headache Intensity and Frequency of Headache Attacks in Patients With Migraine: A Systematic Review and Meta-Analysis. *Headache* 59, 1436–1447. doi: 10.1111/head.13645

Folloni, D., Verhagen, L., Mars, R. B., Fouragnan, E., Constans, C., Aubry, J. F., et al. (2019). Manipulation of Subcortical and Deep Cortical Activity in the Primate Brain Using Transcranial Focused Ultrasound Stimulation. *Neuron* 101, 1109–1116.e5. doi: 10.1016/j.neuron.2019.01.019

Forogh, B., Haqiqatshenas, H., Ahadi, T., Ebadi, S., Alishahi, V., and Sajadi, S. (2021). Repetitive transcranial magnetic stimulation (rTMS) versus transcranial direct current stimulation (tDCS) in the management of patients with fibromyalgia: A randomized controlled trial. *Neurophysiol. Clin.* 51, 339–347. doi: 10.1016/j.neucli.2021.03.002

Galhardoni, R., Aparecida da Silva, V., Garcia-Larrea, L., Dale, C., Baptista, A. F., Barbosa, L. M., et al. (2019). Insular and anterior cingulate cortex deep stimulation for central neuropathic pain: disassembling the percept of pain. *Neurology* 92, e2165–e2175. doi: 10.1212/WNL.0000000000007396

Garcia-Larrea, L., and Peyron, R. (2007). Motor cortex stimulation for neuropathic pain: from phenomenology to mechanisms. *Neuroimage* 37(Suppl. 1), S71–S79. doi: 10.1016/j.neuroimage.2007.05.062

Gritsch, S., Bali, K. K., Kuner, R., and Vardeh, D. (2016). Functional characterization of a mouse model for central post-stroke pain. *Mol. Pain* 12:1744806916629049. doi: 10.1177/1744806916629049

Hoogendam, J. M., Ramakers, G. M., and Di Lazzaro, V. (2010). Physiology of repetitive transcranial magnetic stimulation of the human brain. *Brain Stimul.* 3, 95–118. doi: 10.1016/j.brs.2009.10.005

Hou, W. H., Wang, T. Y., and Kang, J. H. (2016). The effects of add-on non-invasive brain stimulation in fibromyalgia: a meta-analysis and meta-regression of randomized controlled trials. *Rheumatology* 55, 1507–1517. doi: 10.1093/rheumatology/kew205

Hu, L., and Iannetti, G. D. (2019). Neural indicators of perceptual variability of pain across species. *Proc. Natl. Acad. Sci. U.S.A.* 116, 1782–1791. doi: 10.1073/pnas.1812499116

Jefferys, J. G. (1995). Nonsynaptic modulation of neuronal activity in the brain: electric currents and extracellular ions. *Physiol. Rev.* 75, 689–723. doi: 10.1152/physrev.1995.75.4.689

Jin, Y., Xing, G., Li, G., Wang, A., Feng, S., Tang, Q., et al. (2015). High Frequency Repetitive Transcranial Magnetic Stimulation Therapy For Chronic Neuropathic Pain: A Meta-analysis. *Pain Physician* 18, E1029–E1046.

Johnson, S., Summers, J., and Pridmore, S. (2006). Changes to somatosensory detection and pain thresholds following high frequency repetitive TMS of the motor cortex in individuals suffering from chronic pain. *Pain* 123, 187–192. doi: 10.1016/j.pain.2006.02.030

Knijnik, L. M., Dussán-Sarria, J. A., Rozisky, J. R., Torres, I. L., Brunoni, A. R., Fregni, F., et al. (2016). Repetitive transcranial magnetic stimulation for fibromyalgia: systematic review and meta-analysis. *Pain Pract.* 16, 294–304. doi: 10.1111/papr.12276

Knotkova, H., Hamani, C., Sivanesan, E., Le Beuffe, M. F. E., Moon, J. Y., Cohen, S. P., et al. (2021). Neuromodulation for chronic pain. *Lancet* 397, 2111–2124. doi: 10.1016/S0140-6736(21)00794-7

Lamusuo, S., Hirvonen, J., Lindholm, P., Martikainen, I. K., Hagelberg, N., Parkkola, R., et al. (2017). Neurotransmitters behind pain relief with transcranial magnetic stimulation - positron emission tomography evidence for release of endogenous opioids. *Eur. J. Pain.* 21, 1505–1515. doi: 10.1002/ejp.1052

Lan, L., Zhang, X., Li, X., Rong, X., and Peng, Y. (2017). The efficacy of transcranial magnetic stimulation on migraine: a meta-analysis of randomized controlled trails. *J. Headache Pain* 18:86. doi: 10.1186/s10194-017-0792-4

Latremoliere, A., and Woolf, C. J. (2009). Central sensitization: a generator of pain hypersensitivity by central neural plasticity. *J. Pain* 10, 895–926. doi: 10.1016/j.jpain.2009.06.012

Lefaucheur, J. P. (2006). The use of repetitive transcranial magnetic stimulation (rTMS) in chronic neuropathic pain. *Neurophysiol. Clin.* 36, 117–124. doi: 10.1016/j.neucli.2006.08.002

Lefaucheur, J. P. (2016). Cortical neurostimulation for neuropathic pain: state of the art and perspectives. *Pain* 157(Suppl. 1), S81–S89. doi: 10.1097/j.pain.0000000000000401

Lefaucheur, J. P., Aleman, A., Baeken, C., Benninger, D. H., Brunelin, J., Di Lazzaro, V., et al. (2020). Evidence-based guidelines on the therapeutic use of repetitive transcranial magnetic stimulation (rTMS): an update (2014-2018). *Clin. Neurophysiol.* 131, 474–528. doi: 10.1016/j.clinph.2019.11.002

Lefaucheur, J. P., Antal, A., Ayache, S. S., Benninger, D. H., Brunelin, J., Cogiamanian, F., et al. (2017). Evidence-based guidelines on the therapeutic use of transcranial direct current stimulation (tDCS). *Clin. Neurophysiol.* 128, 56–92. doi: 10.1016/j.clinph.2016.10.087

Lefaucheur, J. P., Drouot, X., Menard-Lefaucheur, I., Keravel, Y., and Nguyen, J. P. (2006). Motor cortex rTMS restores defective intracortical inhibition in chronic neuropathic pain. *Neurology* 67, 1568–1574. doi: 10.1212/01.wnl.0000242731.10074.3c

Lefaucheur, J. P., and Wendling, F. (2019). Mechanisms of action of tDCS: A brief and practical overview. *Neurophysiol. Clin.* 49, 269–275. doi: 10.1016/j.neucli.2019.07.013

Leocani, L., Chieffo, R., Gentile, A., and Centonze, D. (2019). Beyond rehabilitation in MS: insights from non-invasive brain stimulation. *Mult. Scler.* 25, 1363–1371. doi: 10.1177/1352458519865734

Leung, A., Donohue, M., Xu, R., Lee, R., Lefaucheur, J. P., Khedr, E. M., et al. (2009). rTMS for suppressing neuropathic pain: a meta-analysis. *J. Pain* 10, 1205–1216. doi: 10.1016/j.jpain.2009.03.010

Leung, A., Shirvalkar, P., Chen, R., Kuluva, J., Vaninetti, M., Bermudes, R., et al. (2020). Transcranial Magnetic Stimulation for Pain, Headache, and Comorbid Depression: INS-NANS Expert Consensus Panel Review and Recommendation. *Neuromodulation* 23, 267–290. doi: 10.1111/ner.13094

Liebetanz, D., Nitsche, M. A., Tergau, F., and Paulus, W. (2002). Pharmacological approach to the mechanisms of transcranial DC-stimulation-induced after-effects of human motor cortex excitability. *Brain* 125(Pt 10), 2238–2247. doi: 10.1093/brain/awf238

Lin, R. L., Douaud, G., Filippini, N., Okell, T. W., Stagg, C. J., and Tracey, I. (2017). Structural Connectivity Variances Underlie Functional and Behavioral Changes During Pain Relief Induced by Neuromodulation. *Sci. Rep.* 7:41603. doi: 10.1038/srep41603

Lloyd, D. M., Wittkopf, P. G., Arendsen, L. J., and Jones, A. K. P. (2020). Is Transcranial Direct Current Stimulation (tDCS) Effective for the Treatment of Pain in Fibromyalgia? A Systematic Review and Meta-Analysis. *J. Pain* 21, 1085–1100. doi: 10.1016/j.jpain.2020.01.003

Maarrawi, J., Peyron, R., Mertens, P., Costes, N., Magnin, M., Sindou, M., et al. (2007). Motor cortex stimulation for pain control induces changes in the endogenous opioid system. *Neurology* 69, 827–834. doi: 10.1212/01.wnl.0000269783.86997.37

Maarrawi, J., Peyron, R., Mertens, P., Costes, N., Magnin, M., Sindou, M., et al. (2013). Brain opioid receptor density predicts motor cortex stimulation efficacy for chronic pain. *Pain* 154, 2563–2568. doi: 10.1016/j.pain.2013.07.042

Marangell, L. B., Martinez, M., Jurdi, R. A., and Zboyan, H. (2007). Neurostimulation therapies in depression: a review of new modalities. *Acta Psychiatr. Scand.* 116, 174–181. doi: 10.1111/j.1600-0447.2007.01033.x

Martin, L., Borckardt, J. J., Reeves, S. T., Frohman, H., Beam, W., Nahas, Z., et al. (2013). A pilot functional MRI study of the effects of prefrontal rTMS on pain perception. *Pain Med.* 14, 999–1009. doi: 10.1111/pme.12129

Mehta, S., McIntyre, A., Guy, S., Teasell, R. W., and Loh, E. (2015). Effectiveness of transcranial direct current stimulation for the management of neuropathic pain after spinal cord injury: a meta-analysis. *Spinal Cord* 53, 780–785. doi: 10.1038/sc.2015.118

Moisset, X., de Andrade, D. C., and Bouhassira, D. (2016). From pulses to pain relief: an update on the mechanisms of rTMS-induced analgesic effects. *Eur. J. Pain* 20, 689–700. doi: 10.1002/ejp.811

Moisset, X., and Lefaucheur, J. P. (2019). Non pharmacological treatment for neuropathic pain: invasive and non-invasive cortical stimulation. *Rev. Neurol.* 175, 51–58. doi: 10.1016/j.neurol.2018.09.014

Moret, B., Donato, R., Nucci, M., Cona, G., and Campana, G. (2019). Transcranial random noise stimulation (tRNS): a wide range of frequencies is needed for increasing cortical excitability. *Sci. Rep.* 9:15150. doi: 10.1038/s41598-019-51553-7

Ngernyam, N., Jensen, M. P., Auvichayapat, N., Punjaruk, W., and Auvichayapat, P. (2013). Transcranial Direct Current Stimulation in Neuropathic Pain. *J. Pain Relief* Suppl 3:001. doi: 10.4172/2167-0846.S3-001

Nguyen, J. P., Nizard, J., Keravel, Y., and Lefaucheur, J. P. (2011). Invasive brain stimulation for the treatment of neuropathic pain. *Nat. Rev. Neurol.* 7, 699–709. doi: 10.1038/nrneurol.2011.138

Nickel, F. T., Seifert, F., Lanz, S., and Maihofner, C. (2012). Mechanisms of neuropathic pain. *Eur. Neuropsychopharmacol.* 22, 81–91. doi: 10.1016/j.euroneuro.2011.05.005

Nitsche, M. A., Cohen, L. G., Wassermann, E. M., Priori, A., Lang, N., Antal, A., et al. (2008). Transcranial direct current stimulation: state of the art 2008. *Brain Stimul.* 1, 206–223. doi: 10.1016/j.brs.2008.06.004

Nitsche, M. A., and Paulus, W. (2000). Excitability changes induced in the human motor cortex by weak transcranial direct current stimulation. *J. Physiol.* 527(Pt 3), 633–639. doi: 10.1111/j.1469-7793.2000.t01-1-00633.x

Palm, U., Chalah, M. A., Padberg, F., Al-Ani, T., Abdellaoui, M., Sorel, M., et al. (2016). Effects of transcranial random noise stimulation (tRNS) on affect, pain and attention in multiple sclerosis. *Restor. Neurol. Neurosci.* 34, 189–199. doi: 10.3233/RNN-150557

Patricio, P., Roy, J. S., Rohel, A., Gariepy, C., Emond, C., Hamel, E., et al. (2021). The Effect of Non-invasive Brain Stimulation to Reduce Non-specific Low Back Pain: A Systematic Review and Meta-analysis. *Clin. J. Pain* [Epub ahead of print]. doi: 10.1097/AJP.0000000000000934

Paulus, W. (2011). Transcranial electrical stimulation (tES - tDCS; tRNS, tACS) methods. *Neuropsychol. Rehabil.* 21, 602–617. doi: 10.1080/09602011.2011.557292

Perocheau, D., Laroche, F., and Perrot, S. (2014). Relieving pain in rheumatology patients: repetitive transcranial magnetic stimulation (rTMS), a developing approach. *Joint Bone Spine* 81, 22–26. doi: 10.1016/j.jbspin.2013.04.015

Peyron, R., Faillenot, I., Mertens, P., Laurent, B., and Garcia-Larrea, L. (2007). Motor cortex stimulation in neuropathic pain. Correlations between analgesic effect and hemodynamic changes in the brain. A PET study. *Neuroimage* 34, 310–321. doi: 10.1016/j.neuroimage.2006.08.037

Peyron, R., and Fauchon, C. (2019). Functional imaging of pain. *Rev. Neurol.* 175, 38–45. doi: 10.1016/j.neurol.2018.08.006

Pridmore, S., Oberoi, G., Marcolin, M., and George, M. (2005). Transcranial magnetic stimulation and chronic pain: current status. *Australas. Psychiatry* 13, 258–265. doi: 10.1080/j.1440-1665.2005.02197.x

Saltychev, M., and Laimi, K. (2017). Effectiveness of repetitive transcranial magnetic stimulation in patients with fibromyalgia: a meta-analysis. *Inter. J. Rehabilit. Res.* 40, 11–18. doi: 10.1097/MRR.0000000000000207

Schading, S., Pohl, H., Gantenbein, A., Luechinger, R., Sandor, P., Riederer, F., et al. (2021). Tracking tDCS induced grey matter changes in episodic migraine: a randomized controlled trial. *J. Headache Pain* 22, 139. doi: 10.1186/s10194-021-01347-y

Shekhawat, G. S., Sundram, F., Bikson, M., Truong, D., De Ridder, D., Stinear, C. M., et al. (2016). Intensity, Duration, and Location of High-Definition Transcranial Direct Current Stimulation for Tinnitus Relief. *Neurorehabil. Neural Repair* 30, 349–359. doi: 10.1177/1545968315595286

Soler, M. D., Kumru, H., Pelayo, R., Vidal, J., Tormos, J. M., Fregni, F., et al. (2010). Effectiveness of transcranial direct current stimulation and visual illusion on neuropathic pain in spinal cord injury. *Brain* 133, 2565–2577. doi: 10.1093/brain/awq184

Stagg, C. J., and Nitsche, M. A. (2011). Physiological basis of transcranial direct current stimulation. *Neuroscientist* 17, 37–53. doi: 10.1177/1073858410386614

Steglitz, J., Buscemi, J., and Ferguson, M. J. (2012). The future of pain research, education, and treatment: a summary of the IOM report "Relieving pain in America: a blueprint for transforming prevention, care, education, and research". *Transl. Behav. Med.* 2, 6–8. doi: 10.1007/s13142-012-0110-2

Stilling, J. M., Monchi, O., Amoozegar, F., and Debert, C. T. (2019). Transcranial Magnetic and Direct Current Stimulation (TMS/tDCS) for the Treatment of

Headache: A Systematic Review. *Headache* 59, 339–357. doi: 10.1111/head.13479

Strafella, A. P., Paus, T., Barrett, J., and Dagher, A. (2001). Repetitive transcranial magnetic stimulation of the human prefrontal cortex induces dopamine release in the caudate nucleus. *J. Neurosci.* 21:RC157. doi: 10.1523/JNEUROSCI.21-15-j0003.2001

Tamura, Y., Okabe, S., Ohnishi, T. D., N Saito, D., Arai, N., and Mochio, S., et al. (2004). Effects of 1-Hz repetitive transcranial magnetic stimulation on acute pain induced by capsaicin. *Pain* 107, 107–115. doi: 10.1016/j.pain.2003.10.011

Tavakoli, A. V., and Yun, K. (2017). Transcranial Alternating Current Stimulation (tACS) Mechanisms and Protocols. *Front. Cell. Neurosci.* 11:214. doi: 10.3389/fncel.2017.00214

Terney, D., Chaieb, L., Moliadze, V., Antal, A., and Paulus, W. (2008). Increasing human brain excitability by transcranial high-frequency random noise stimulation. *J. Neurosci.* 28, 14147–14155. doi: 10.1523/JNEUROSCI.4248-08.2008

Tu, Y., Zhang, Z., Tan, A., Peng, W., Hung, Y. S., Moayedi, M., et al. (2016). Alpha and gamma oscillation amplitudes synergistically predict the perception of forthcoming nociceptive stimuli. *Hum. Brain Mapp.* 37, 501–514. doi: 10.1002/hbm.23048

Utz, K. S., Dimova, V., Oppenlander, K., and Kerkhoff, G. (2010). Electrified minds: transcranial direct current stimulation (tDCS) and galvanic vestibular stimulation (GVS) as methods of non-invasive brain stimulation in neuropsychology–a review of current data and future implications. *Neuropsychologia* 48, 2789–2810. doi: 10.1016/j.neuropsychologia.2010.06.002

Vachon-Presseau, E., Tetreault, P., Petre, B., Huang, L., Berger, S. E., Torbey, S., et al. (2016). Corticolimbic anatomical characteristics predetermine risk for chronic pain. *Brain* 139(Pt 7), 1958–1970. doi: 10.1093/brain/aww100

Xiao, X., and Zhang, Y. Q. (2018). A new perspective on the anterior cingulate cortex and affective pain. *Neurosci. Biobehav. Rev.* 90, 200–211. doi: 10.1016/j.neubiorev.2018.03.022

Yang, L., Wang, S. H., Hu, Y., Sui, Y. F., Peng, T., and Guo, T. C. (2018). Effects of Repetitive Transcranial Magnetic Stimulation on Astrocytes Proliferation and nNOS Expression in Neuropathic Pain Rats. *Curr. Med. Sci.* 38, 482–490. doi: 10.1007/s11596-018-1904-3

Yang, S., and Chang, M. C. (2020). Effect of Repetitive Transcranial Magnetic Stimulation on Pain Management: A Systematic Narrative Review. *Front. Neurol.* 11:114. doi: 10.3389/fneur.2020.00114

Yoo, W. K., You, S. H., Ko, M. H., Tae Kim, S., Park, C. H., Park, J. W., et al. (2008). High frequency rTMS modulation of the sensorimotor networks: behavioral changes and fMRI correlates. *Neuroimage* 39, 1886–1895. doi: 10.1016/j.neuroimage.2007.10.035

Young, N. A., Sharma, M., and Deogaonkar, M. (2014). Transcranial magnetic stimulation for chronic pain. *Neurosurg. Clin. N. Am.* 25, 819–832. doi: 10.1016/j.nec.2014.07.007

Zhang, K. L., Yuan, H., Wu, F. F., Pu, X. Y., Liu, B. Z., Li, Z., et al. (2021). Analgesic Effect of Noninvasive Brain Stimulation for Neuropathic Pain Patients: A Systematic Review. *Pain Ther.* 10, 315–332. doi: 10.1007/s40122-021-00252-1

Zhang, K. Y., Rui, G., Zhang, J. P., Guo, L., An, G. Z., Lin, J. J., et al. (2020). Cathodal tDCS exerts neuroprotective effect in rat brain after acute ischemic stroke. *BMC Neurosci.* 21:21. doi: 10.1186/s12868-020-00570-8

Zhang, Z. G., Hu, L., Hung, Y. S., Mouraux, A., and Iannetti, G. D. (2012). Gamma-band oscillations in the primary somatosensory cortex–a direct and obligatory correlate of subjective pain intensity. *J. Neurosci.* 32, 7429–7438. doi: 10.1523/JNEUROSCI.5877-11.2012

Zheng, X., Alsop, D. C., and Schlaug, G. (2011). Effects of transcranial direct current stimulation (tDCS) on human regional cerebral blood flow. *Neuroimage* 58, 26–33. doi: 10.1016/j.neuroimage.2011.06.018

Zhu, C. E., Yu, B., Zhang, W., Chen, W. H., Qi, Q., and Miao, Y. (2017). Effiectiveness and safety of transcranial direct current stimulation in fibromyalgia: A systematic review and meta-analysis. *J. Rehabil. Med.* 49, 2–9. doi: 10.2340/16501977-2179

Ziemann, U. (2004). TMS induced plasticity in human cortex. *Rev. Neurosci.* 15, 253–266. doi: 10.1515/revneuro.2004.15.4.253

Conflict of Interest: The authors declare that the research was conducted in the absence of any commercial or financial relationships that could be construed as a potential conflict of interest.

Publisher's Note: All claims expressed in this article are solely those of the authors and do not necessarily represent those of their affiliated organizations, or those of the publisher, the editors and the reviewers. Any product that may be evaluated in this article, or claim that may be made by its manufacturer, is not guaranteed or endorsed by the publisher.

frontiers | Frontiers in Molecular Neuroscience

TYPE Review
PUBLISHED 03 November 2022
DOI 10.3389/fnmol.2022.817738

OPEN ACCESS

EDITED BY
Siyi Yu,
Chengdu University of Traditional Chinese Medicine, China

REVIEWED BY
Sang Hoon Lee,
University of Cincinnati, United States
Cyril Rivat,
Université de Montpellier, France

*CORRESPONDENCE
Rui Chen
unioncr@163.com
Feng-xia Liang
fxliang5@hotmail.com

†These authors have contributed equally to this work

SPECIALTY SECTION
This article was submitted to Neuroplasticity and Development, a section of the journal Frontiers in Molecular Neuroscience

RECEIVED 18 November 2021
ACCEPTED 25 January 2022
PUBLISHED 03 November 2022

CITATION
Luo D, Liu L, Zhang H-m, Zhou Y-d, Zhou M-f, Li J-x, Yu Z-m, Chen R and Liang F-x (2022) Relationship between acupuncture and transient receptor potential vanilloid: Current and future directions. *Front. Mol. Neurosci.* 15:817738. doi: 10.3389/fnmol.2022.817738

Relationship between acupuncture and transient receptor potential vanilloid: Current and future directions

Dan Luo[1,2†], Li Liu[3†], Hai-ming Zhang[1,4†], Yu-dian Zhou[1], Min-feng Zhou[5], Jin-xiao Li[5], Zhao-min Yu[6], Rui Chen[5*] and Feng-xia Liang[1*]

[1]Department of Acupuncture and Moxibustion, Hubei University of Traditional Chinese Medicine, Wuhan, China, [2]Department of Respiratory, Wuhan No. 1 Hospital, Wuhan, China, [3]Department of Pathology, Wuhan No. 1 Hospital, Wuhan, China, [4]Department of Oncology, Integrated Traditional Chinese and Western Medicine, The Central Hospital of Wuhan, Tongji Medical College, Huazhong University of Science and Technology, Wuhan, China, [5]Department of Integrated Traditional Chinese and Western Medicine, Union Hospital, Tongji Medical College, Huazhong University of Science and Technology, Wuhan, China, [6]Department of Oncology, Hubei Province Hospital of Integrated Traditional Chinese and Western Medicine, Wuhan, China

Acupuncture is a common complementary and alternative therapy around the world, but its mechanism remains still unclear. In the past decade, some studies indicated that transient receptor potential vanilloid (TRPV) channels play a great role in the response of acupuncture stimulation. In this article, we discussed the relationship between acupuncture and TRPV channels. Different from inhibitors and agonists, the regulation of acupuncture on TRPV channels is multi-targeted and biphasic control. Acupuncture stimulation shows significant modulation on TRPV1 and TRPV4 at the autonomic nervous system (ANS) including central and peripheral nervous systems. On the contrary, the abundant expression and functional participation of TRPV1 and TRPV4 were specific to acupuncture stimulation at acupoints. The enhancement or inhibition of TRPV channels at different anatomical levels will affect the therapeutic effect of acupuncture. In conclusion, TRPV channels help to understand the principle of acupuncture stimulation, and acupuncture also provides a potential approach to TRPV-related trials.

KEYWORDS

acupuncture, TRPV channels, autonomic nervous system, central nervous system, peripheral sensory nervous

Abbreviations: TRPV, transient receptor potential vanilloid; ANS, autonomic nervous system; CNS, central nervous system; PNS, peripheral nervous system; MA, manual acupuncture; EA, electroacupuncture; MCAO, middle cerebral artery occlusion; DRG, dorsal root ganglion; SCDH, spinal cord dorsal horn; ATP, adenosine triphosphate; DRG, dorsal root ganglion; Perk, phosphoactivation of extracellular signal-regulated kinase; pPKA, phosphorylated protein kinase A; pCREB, cAMP-response-element-binding protein; NTS, nucleus tractus solitarius; nNOS, neuronal nitric oxide synthase; TLR4, toll-like receptor 4; MyD88, myeloid differentiation primary response 88.

Introduction

Acupuncture originated in China over 3,000 years ago. In acupuncture theory, stimulation at certain areas, also known as acupoints, with needles could dynamically harmonize Yin-Yang and Qi to cure diseases (Kaptchuk, 2002). Nowadays, acupuncture is confined as an important complementary and alternative therapy all over the world (Rubin, 2019; Slomski, 2019). Some systematic reviews and meta-analysis have confirmed that acupuncture has encouraging effects on pain (He et al., 2020) and obesity (Kim et al., 2018).

Neurobiological mechanisms underlying acupuncture's effectiveness have been widely discussed in modern research. Acupuncture is effective on the endocannabinoid system (Hu et al., 2017), purinergic signaling (Tang et al., 2016), and neuro-immune microenvironment (Gong et al., 2020). Current studies have shown that acupuncture plays a great role in the autonomic nervous system (ANS) (Shu et al., 2016). Liu et al. (2021) performed studies on acupuncture relieving inflammation, which showed that both vagal-adrenal axis and NPY-expressing sympathetic pathway (Liu et al., 2020) could be regulated by acupuncture stimulation at certain acupoints through specific autonomic pathways. It is worth mentioning that either anti-inflammatory or pro-inflammatory effects of acupuncture depend on the state of diseases. Although several biological correlates in ANS may explain the principle of acupuncture (Lim et al., 2016), the biological basis of stimulation at acupoints affecting physiology and pathology of internal organs remains unknown.

Since transient receptor potential vanilloid (TRPV) 1, which is sensitive to both heat and capsaicin, was first found in neurons in 1997 (Caterina et al., 1997), other five TRPV family members including TRPV2-6 have been identified in the next few years (Smith et al., 2002; Patapoutian et al., 2003; van de Graaf et al., 2003). Recent studies showed that TRPV channels are widely expressed in various excitable and non-excitable cell types in the human body. TRPV channels not only respond to thermosensation (Paricio-Montesinos et al., 2020) but also play a great role in the physiological or pathological processes of pain, inflammation, immunity, diabetes, and obesity (Jordt and Ehrlich, 2007; Samanta et al., 2018).

Physical stimulation such as pressure, vibration, pain, and temperature can be felt by sensory receptors at the peripheral nervous system, and the signal will be further passed to the central nervous system (CNS) through dorsal root ganglia (DRG). The operation of acupuncture produces pain, pressure, and vibration at the acupoints for neurobiological regulations. Hence, it is reasonable to assume that there is a specific relationship between acupuncture and TRPV channels. To the best of our knowledge, some studies have shown that acupuncture is closely associated with TRPV1 and TRPV4, which is elaborated in this review.

Transient receptor potential vanilloid channels

As sensory receptors, TRPV channels are sensitive to various tissue-damaging signals and have a strong link with signaling pathways such as phosphorylation of protein kinase A (PKA) and protein kinase C (PKC) (Por et al., 2013). Hence, TRPV channels are also considered as nociceptors (Satheesh et al., 2016). TRPV channels in the CNS play a great role not only in pain but also in neuropsychiatric disorders, such as depression, stress, and anxiety (Singh et al., 2019). It was found that all kinds of tissues and organs with TRPV channels expression contribute to a plethora of physiological or pathophysiological effects (Seebohm and Schreiber, 2021).

TRPV1 has been the most widely studied TRPV channel in the past decade. TRPV1 expresses in both neuronal cells, such as peripheral sensory neurons (C- and Aδ-fibers), DRG, trigeminal ganglia, and vagal ganglia (Cao et al., 2013), and non-neuronal cells, such as skin and muscles (Cavanaugh et al., 2011). After TRPV1 was knocked out, mice exhibited no vanilloid-evoked pain behavior and impaired nociception shown in inflammation pain mice models (Caterina et al., 2000). But it should be noted that TRPV1 agonists are also effective on neuropathic pain. Agonists could over-activate TRPV1 channels and lead to internalization and subsequent desensitization of afferent nerve endings or degeneration of neurons by Ca^{2+}-induced neurotoxicity (Fischer et al., 2020).

Capsaicin, an important component in spiciness with a spicy sensation, could selectively block pain signals at primary afferent neurons targeting TRPV1 (Szolcsanyi, 2008). Besides capsaicin, TRPV1 could be activated by many physical and chemical stimuli, and activation pathways exist for specific stimuli (Yang and Zheng, 2017). The extracellular pore domain and transmembrane domains of TRPV1 could respond to different stimulation from physical and chemical inputs (Zheng, 2013). Many small molecules as potential analgesics aimed to inhibit TRPV1, but most of them failed in clinical trials due to severe side effects (Carnevale and Rohacs, 2016). Until now, only 8% capsaicin patch was approved by the European Union and the US Food and Drug Administration (FDA) for the treatment of postherpetic neuralgia, namely, peripheral neuropathic pain (Basith et al., 2016).

Similar to TRPV1, TRPV4 channels are broadly expressed in organs and tissues to participate in many physiological and pathophysiological processes. The therapeutic effect of TRPV4 antagonism on pain, gastrointestinal disorders, and respiratory diseases has been suggested through animal studies (Grace et al., 2017). GSK2798745, a potent and selective TRPV4 inhibitor, has been investigated in early phase clinical trials for heart failure (Brooks et al., 2019). To date, TRPV4 agonists could lead to unpredictable toxicity during systemic activation of TRPV4 and only suggested local delivery (Lawhorn et al., 2020).

TABLE 1 Acupuncture affects TRPV channels.

Models	Acupuncture delivery	Acupoints	Target organs	Main results	References
Mice, Inflammatory pain models	MA	ST36	Muscle at ST36	TRPV1 and TRPV4 channels were abundantly expressed	Wu et al., 2014
			epimysium at ST36		
			Subcutaneous loose connective tissue at ST36		
			Neural tissue at ST36		
Mice, Inflammatory pain models	EA, 2 Hz 1 mA	ST36	DRG	TRPV1 channel overexpression was decreased	Liao et al., 2017
			SCDH		
Mice, Inflammatory pain models	EA, 2 Hz 1 mA	ST36	DRG	TRPV1 channel overexpression was decreased	Yang et al., 2017
			Spinal cord		
Mice, Inflammatory pain models	EA, 2 Hz 1 mA	LI4	Prefrontal cortex	TRPV1 channel overexpression was decreased	Yen et al., 2019
			Hypothalamus		
			Periaqueductal gray	TRPV1 channel suppression was reversed	
Mice, Inflammatory pain models	EA, 2 Hz 1 mA	ST36	Cerebellum lobules V, VIa and VII	TRPV1 channel overexpression was decreased	Inprasit and Lin, 2020
Mice, Chronic pain and depression models	EA, 2 Hz 1 mA	ST36	Cerebellum lobules VI, VII, VIII	TRPV1 channel inhibition was revised	Lottering and Lin, 2021
Rats, Inflammatory pain models	EA, 2 Hz, 100 Hz, 2/100 Hz 0.5-1.0-1.5 mA	ST36	L4-6 DRG neurons	TRPV1 channel overexpression was decreased high-frequency EA was more effective	Fang et al., 2018
Mice, Fibromyalgia models	EA, 2 Hz 1 mA	ST36	DRG neurons	TRPV1 channel overexpression was decreased	Lin et al., 2015
			Spinal cord		
				TRPV4 channel overexpression was decreased	
Mice, Fibromyalgia models	EA, 2 Hz 1 mA	ST35	Thalamus	TRPV1 channel overexpression was decreased	Hsu et al., 2020
			Amygdala		
			Somatosensory cortex		
Rats, carcinoma cell inoculation to cancer pain models	EA, 2 Hz 1 mA	ST36	DRG neurons	TRPV1 channel overexpression was decreased	Zhang Z. et al., 2012
Mice, cold stress-induced nociception and depression models	EA, 2 Hz 1 mA	ST36	Medial prefrontal cortex	TRPV1 channel suppression was reversed	Lin et al., 2020
			Hippocampus	TRPV1 channel overexpression was decreased	
			Periaqueductal gray		
			Amygdala		
Rats, high fat diet-induced obese models	EA, 10 Hz 1 mA	ST36	Medulla regions	TRPV1 channel suppression was reversed	Ji et al., 2013
			Skin at ST36		
Rats, paclitaxel-induced peripheral neuropathy models	EA, 2 Hz 0.5–1.5 mA	ST36 and BL60	L4-6 DRG neurons	TRPV1 channel overexpression was decreased	Li et al., 2019
Rats, MCAo models	EA, 2 Hz 2 mA	GV20	Hippocampal CA1 areas	TRPV1 channel overexpression was decreased	Lin and Hsieh, 2010

(Continued)

TABLE 1 (Continued)

Models	Acupuncture delivery	Acupoints	Target organs	Main results	References
Rats, MCAo models	EA, 2/100 Hz 2 mA	GV20, BL23 and, SP6	Hippocampal	TRPV1 channel overexpression was decreased	Long et al., 2019
Mice	EA, 2 Hz 1 mA	ST36	DRG neurons	TRPV1 channel was upregulated	Choowanthanapakorn et al., 2015
			Spinal cord		
Mice, motion sickness models	EA, 2 Hz 1 mA	PC6	Thalamus	TRPV1 channel overexpression was decreased	Inprasit et al., 2018
			Hypothalamic		
			Brain stem		
Rats	EA, 1 mA	BL40	Subepidermal nerve fibers at BL40	TRPV1 channel was upregulated	Abraham et al., 2011
Mice	MA	ST36	Peripheral DRG neurons	Components of the TRPV1-related signaling pathway was upregulated	Chen et al., 2018
	EA 2, 15, 50 Hz and 1 mA		Somatosensory cortex		
Rats	EA 2, 15 Hz and 1 mA	ST36	Splenic CD4 + T cells	TRPV1 channel was upregulated	Chen et al., 2017
Rats, gastric distension to cardiovascular reflexes models	MA	P5 and P6	C7-8 DRG neurons	TRPV1 channel was upregulated	Guo et al., 2018
	EA, 2 Hz 0.3–0.5 mA				

MA, manual acupuncture; EA, electroacupuncture; MCAo, middle cerebral artery occlusion; DRG, dorsal root ganglion; SCDH, spinal cord dorsal horn.

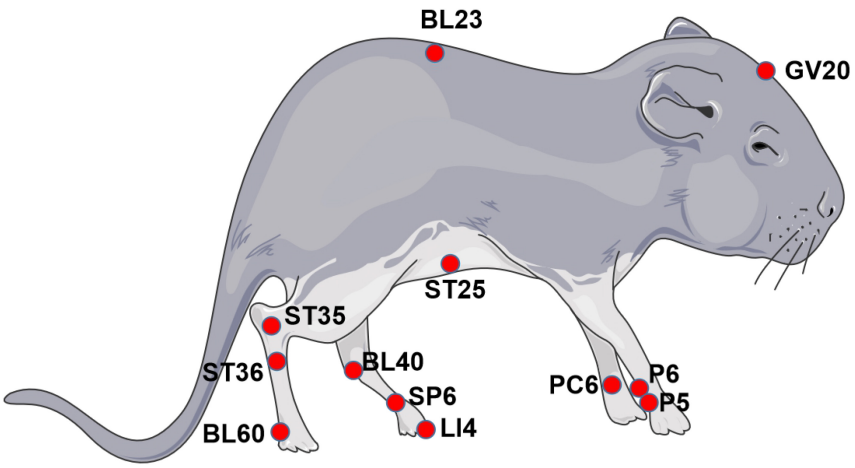

FIGURE 1
Acupoints in murine. Acupuncture delivery is through the insertion of needles into the muscle at acupoints with 1–3 mm depth and triggering of a local reaction by means of manual manipulation or electrical stimulation. Sham acupuncture is usually performed in the tissue adjacent to the targeted acupoint without manual operation or electrode connection.

Acupuncture stimulation

Acupuncture is a treatment that involves inserting needles at specific acupoints in the body. In traditional Chinese medicine theory, the key to the curative effect of acupuncture treatment lies in the human body's response to acupuncture stimulation, including heaviness, numbness, soreness, and distension, which is also called "De Qi" (Mao et al., 2007). It is believed that acupuncture stimulation could activate mechanically sensitive pain fibers and various types of lesser-known deep tissue receptors (Zhao, 2008).

The analgesic effect of acupuncture has been studied for a long time. Brain imaging shows that acupuncture could alter activation patterns in brain areas against pain processing (Huang et al., 2012). Endorphins (Han, 2004), serotonin (Zhang Y. et al., 2012), and various neuromodulators and neurotransmitters in CNS and/or peripheral nervous system (PNS) can be regulated by acupuncture stimulation. A systematic review based on quantitative sensory testing (QST) has found that acupuncture significantly changed the sensory threshold and activated neuromodulation (Baeumler et al., 2014). A large number of preclinical trials have shown that the analgesic effect of electroacupuncture is optimistic, and the peripheral, spinal, and supraspinal mechanisms related to the activation of a variety of bioactive chemicals show more difference in health than that in pain conditions (Zhang et al., 2014).

Acupuncture affects transient receptor potential vanilloid channels

A total of 24 animal studies were included in this article, and acupuncture/electroacupuncture showed significantly beneficial effects. The regulation of acupuncture/electroacupuncture to TRPV channels differs in models (**Table 1**). To help readers understand the implementation methods of acupuncture, we listed the acupoints of the animal related to this article in **Figure 1** (Jin et al., 2018).

The relationship between acupuncture and TRPV channels involves the whole PNS, including sensory receptors and afferent nerves. Acupuncture could significantly increase the subepidermal nerve fibers with high expression of TRPV1 (Abraham et al., 2011). DRG neurons are believed to act as the bridge for acupuncture stimulation projecting to CNS. However, the effect of acupuncture on TRPV channels at DRG may be completely opposite in different models. In studies focused on diseases related to pain, the overexpression of TRPV1 channel in DRG neurons by drugs or surgery, which causes pain, would be reversed by acupuncture (Zhang Z. et al., 2012; Lin et al., 2015; Liao et al., 2017; Yang et al., 2017). But in other studies based on normal animals or obese models, acupuncture enhanced the expression of TRPV1 channels in DRG neurons (Ji et al., 2013; Choowanthanapakorn et al., 2015; Chen et al., 2018). Acupuncture at different acupoints would lead to TRPV channel changes in different DRG neurons. Stimulation at ST36 and BL40 is likely passed to L4-6 DRG neurons (Li et al., 2019), while acupuncture at P5 and P6 targets at C7-8 DRG neurons (Guo et al., 2018). Meanwhile, the effect of electroacupuncture on regulating TRPV channels is positively correlated with frequency (Fang et al., 2018).

It is noticed that acupuncture stimulation could modulate TRPV channels in the brain and spinal cord (Liao et al., 2017; Yang et al., 2017; Inprasit et al., 2018). Similar to PNS, the regulation of acupuncture on CNS is also bidirectional. Acupuncture significantly inhibits the trend of TRPV channels' overexpression in pain-related models but promotes TRPV channels' expression in obesity (Ji et al., 2013) or normal condition (Choowanthanapakorn et al., 2015). Meanwhile, stimulation at acupoints could lead to a multi-targeted effect on the central nervous system. For example, after stimulation at ST36, the changes of TRPV channels in the spinal cord (Yang et al., 2017); cerebellum lobules V, VIa, VI, VII, and VIII (Inprasit and Lin, 2020; Lottering and Lin, 2021); hippocampus; periaqueductal gray; and medial prefrontal cortex (Lin et al., 2020) could be observed.

In addition to nerves, acupuncture stimulation could also directly regulate the expression of TRPV1 and TRPV4 channels in different anatomical layers of skin at acupoints including muscles, epimysium, and subcutaneous loose connective tissue (Ji et al., 2013; Wu et al., 2014). It is noticed that electroacupuncture at ST36 enhances immune cytokines by promoting the TRPV1 channels in splenic $CD4^+$ T cells (Chen et al., 2017). Mast cells could also be activated by acupuncture through TRPV2 channels to release histamine (Huang et al., 2018).

Transient receptor potential vanilloid channels influence the effect of acupuncture

The use of TRPV gene knockout, agonist, and antagonism provides us with an opportunity to understand the relationship between acupuncture and TRPV from another perspective (**Table 2**). When acupuncture enhances TRPV expression in wild models, the effect of acupuncture could be significantly inhibited after TRPV gene knockout (Yu et al., 2016; Huang et al., 2018). If TRPV over-expression is related to the progress of disease such as hyperpathia, the TRPV gene knockout mimics the analgesic effect of acupuncture (Liao et al., 2017; Yang et al., 2017). Delivery of TRPV agonist or antagonist on different areas of PNS could lead to different effects of acupuncture. The injection of TRPV1 antagonist into ST36 could mimic the acupuncture-like analgesic effect, but it was not replicated through the injection of TRPV4 agonist (Wu et al., 2014). The injection of TRPV1 antagonist into P5 and P6 could inhibit the modulation of sympathoexcitatory responses in manual acupuncture but not in electroacupuncture (Guo et al., 2018). A study performed by Fang et al. (2018) found that the injection of capsaicin into the dorsum of the foot could exhibit an analgesic effect similar to acupuncture. But Li et al. (2019) found that the injection of capsaicin into the dorsum of the foot reversed the effect of acupuncture and TRPV1 antagonist showed a contrary result.

TABLE 2 TRPV channels could influence the effect of acupuncture.

Models	Intervention on TRPV	Methods	Main results	References
Mice inflammatory pain models	TRPV1 agonist	Capsaicin injected into ST36	Replicated the acupuncture-like analgesic effect	Wu et al., 2014
	TRPV4 agonist	GSK1016790A injected into ST36	Did not induce an analgesic effect	
Mice inflammatory pain models	TRPV1 antagonist	TRPV1 gene knockout	Replicated the acupuncture-like analgesic effect	Liao et al., 2017
Mice inflammatory pain models	TRPV1 antagonist	TRPV1 gene knockout	Replicated the acupuncture-like analgesic effect	Yang et al., 2017
Mice inflammatory pain models	TRPV1 antagonist	TRPV1 gene knockout	Replicated the acupuncture-like analgesic effect	Yen et al., 2019
Mice, chronic pain and depression models	TRPV1 antagonist	TRPV1 gene knockout	There is no significant difference with the model group	Lottering and Lin, 2021
Mice inflammatory pain models	TRPV1 agonist	Capsaicin injected into the dorsum of the foot	Replicated the acupuncture-like analgesic effect	Fang et al., 2018
Mice, fibromyalgia models	TRPV1 antagonist	TRPV1 gene knockout	Replicated the acupuncture-like analgesic effect	Lin et al., 2015
Mice, cold stress-induced nociception and depression models	TRPV1 antagonist	TRPV1 gene knockout	Replicated the acupuncture-like analgesic effect	Lin et al., 2020
Rats, paclitaxel-induced peripheral neuropathy models	TRPV1 agonist	Capsaicin injected into dorsal part of the ipsilateral hind paw	Inhibited the analgesic effect of acupuncture	Li et al., 2019
	TRPV1 antagonist	AMG9810 injected into dorsal part of the ipsilateral hind paw	Replicated the analgesic effect of acupuncture	
Rats, MCAo models	TRPV1 agonist	Capsaicin, subcutaneous injection	Inhibited the analgesic effect of acupuncture	Long et al., 2019
	TRPV1 antagonist	AMG-517, intraperitoneal injection	Replicated the analgesic effect of acupuncture	
Mice	TRPV1 antagonist	TRPV1 gene knockout	Inhibited the weight-loss effect of acupuncture	Choowanthanapakorn et al., 2015
Mice, motion sickness models	TRPV1 antagonist	TRPV1 gene knockout	Replicated the acupuncture-like relieving motion sickness symptoms effect	Inprasit et al., 2018
Mice	TRPV1 antagonist	TRPV1 gene knockout	Inhibited the phosphorylated effect of acupuncture	Chen et al., 2018
Rats	TRPV1 antagonist	TRPV1 gene knockout	Inhibited the CD4 + T cells active effect of acupuncture	Chen et al., 2017
Rats, gastric distension to cardiovascular reflexes models	TRPV1 antagonist	SiRNA, injected into C7-8 DRG neurons	Inhibited the inhibition of reflex increases in blood pressure by MA but not in EA	Guo et al., 2018
		Iodoresiniferatoxin, injected into P5 and P6	Inhibited the modulation of sympathoexcitatory responses by MA but not in EA	
Mice	TRPV1 antagonist	TRPV1 gene knockout	Inhibited the analgesic effect of EA and significant in higher intensity	Xin et al., 2016
Rats, acute adjuvant arthritis models	TRPV2 antagonist	TRPV2 gene knockout	Inhibited the acupuncture activation effect of mast cells and analgesic effect	Huang et al., 2018
Rats	TRPV1 antagonist	TRPV1 gene knockout	Inhibited the effect of acupuncture in suppressing the motor activity of the jejunum in an intensity-dependent manner	Yu et al., 2016

Acupuncture and transient receptor potential vanilloid channels participate in complex molecular networks

No matter how acupuncture regulates TRPV channels or how TRPV channels influence the effect of acupuncture as described above, TRPV channels mediate the communication between acupuncture and body tissues (**Table 3**). Through TRPV channels, acupuncture could regulate complex molecular networks, including adenosine triphosphate (ATP), extracellular signal-regulated kinase (ERK), toll-like receptor 4 (TLR4), and others. Phosphorylation of downstream molecules was widely found after acupuncture-regulated TRPV channels (Inprasit et al., 2018). Inprasit and Lin (2020) and

TABLE 3 Acupuncture and TRPV channels play a great role in related molecules and pathways.

Models	Acupuncture delivery	Acupoints	TRPV	Targets	Related molecules or pathways	References
Mice inflammatory pain models	MA	ST36	TRPV1 and TRPV4	Cell membrane at muscle, epimysium, and neuron	Promote ATP signaling	Wu et al., 2014
Mice inflammatory pain models	EA, 2 Hz 1 mA	ST36	TRPV1	DRG and SCDH	Inhibit PI3K, AKT, CREB, NF-κB, Nav1.7, and Nav1.8	Liao et al., 2017
Mice inflammatory pain models	EA, 2 Hz 1 mA	ST36	TRPV1	DRG and Spinal cord	Inhibit pPKA, pPI3K, pPKC, pERK, pp38, pJNK, pCREB, pNF-κB, Nav1.7, Nav1.8, GFAP, S100B, and RAGE	Yang et al., 2017
Mice inflammatory pain models	EA, 2 Hz 1 mA	LI4	TRPV1	Brain	Inhibit pPKA, pPI3K, pPKC, pERK, pp38, pJNK, pCREB, pNF-κB, Nav1.7, Nav1.8	Yen et al., 2019
Mice inflammatory pain models	EA, 2 Hz 1 mA	ST36	TRPV1	Cerebellum lobules V, VIa and VII	Inhibit pPI3K, pmTOR, pAkT, pERK, pPKCε, pPKAIIα, pNFkB, pCREB, and S100B	Inprasit and Lin, 2020
Mice, chronic pain and depression models	EA, 2 Hz 1 mA	ST36	TRPV1	Cerebellum lobules VI, VII, VIII	Promote pmTOR, pPI3K, NMDAR1, pPKCε, pAkt, TrkB, pNFκB, GABAAα1, pPKAIIα, pCREB, and Perk	Lottering and Lin, 2021
Mice fibromyalgia models	EA, 2 Hz 1 mA	ST36	TRPV1 and TRPV4	L5 DRG neurons	Inhibit pERK signaling	Lin et al., 2015
Mice fibromyalgia models	EA, 2 Hz 1 mA	ST35	TRPV1	Brain	inhibit pERK signaling	Hsu et al., 2020
Mice, cold stress-induced nociception and depression models	EA, 2 Hz 1 mA	ST36	TRPV1	Medial prefrontal cortex, hippocampus and periaqueductal gray	Promote pPKA, pPI3K, pPKC, pAKT, pmTOR, pERK, pp38, pJNK, pCREB, and pNFκB	Lin et al., 2020
Rats, high fat diet-induced obese models	EA, 10 Hz 1 mA	ST36	TRPV1	Nucleus tractus solitarius/gracile nucleus regions	Promote nNOS	Ji et al., 2013
				Skin at ST36		
Rats, paclitaxel-induced peripheral neuropathy models	EA, 2 Hz 0.5 to 1.5 mA	ST36 and BL60	TRPV1	L4-6 DRG neurons	Inhibit TLR4 and MyD88 signaling	Li et al., 2019
Rats, MCAo models	EA, 2/100 Hz 2 mA	GV20, BL23 and, SP6	TRPV1	Hippocampal	Inhibit pp38	Long et al., 2019
Mice	EA, 2 Hz 1 mA	ST36	TRPV1	DRG and spinal cord	Promote pPKA, pPKC, and pERK signaling	Choowanthanapakorn et al., 2015
Mice, motion sickness models	EA, 2 Hz 1 mA	PC6	TRPV1	Thalamus	Inhibit pPI3K, pAKT, pmTOR, pERK, pp38, npJNK, pCREB, and pNFκB	Inprasit et al., 2018
Rats	EA, 1 mA	BL40	TRPV1	Subepidermal nerve fibers, C-fibers and A-δ fibers	Promote nNOS	Abraham et al., 2011
Mice	MA and EA 2, 15, 50 Hz and 1 mA	ST36	TRPV1	DRG and somatosensory cortex	Promote ppPKA, pPI3K, pPKC-pERK, pAKT and pNR1-pCaMKII pathway,	Chen et al., 2018
Rats	EA 2, 15 Hz and 1 mA	ST36	TRPV1	Splenic CD4 + T cells	Promote Ca2 + signaling	Chen et al., 2017
Rats, gastric distension to cardiovascular reflexes models	MA	P5 and P6	TRPV1	C7-8 DRG neurons	Promote pERK signaling	Guo et al., 2018
	EA, 2 Hz 0.3-0.5 mA			Group III and IV bimodal sensory afferent nerves		
Rats acute adjuvant arthritis models	MA	ST36	TRPV2	Mast cells	Active histamine H1 and adenosine A1 receptor	Huang et al., 2018
Rats	EA, 2 to 15 Hz	ST25	TRPV1	-	Promote sympathetic pathway	Yu et al., 2016

ATP, adenosine triphosphate; DRG, dorsal root ganglion; pERK, phosphoactivation of extracellular signal-regulated kinase; pPKA, phosphorylated protein kinase A; pCREB, cAMP-response-element-binding protein; NTS, nucleus tractus solitarius; nNOS, neuronal nitric oxide synthase; TLR4, toll-like receptor 4; MyD88, myeloid differentiation primary response 88.

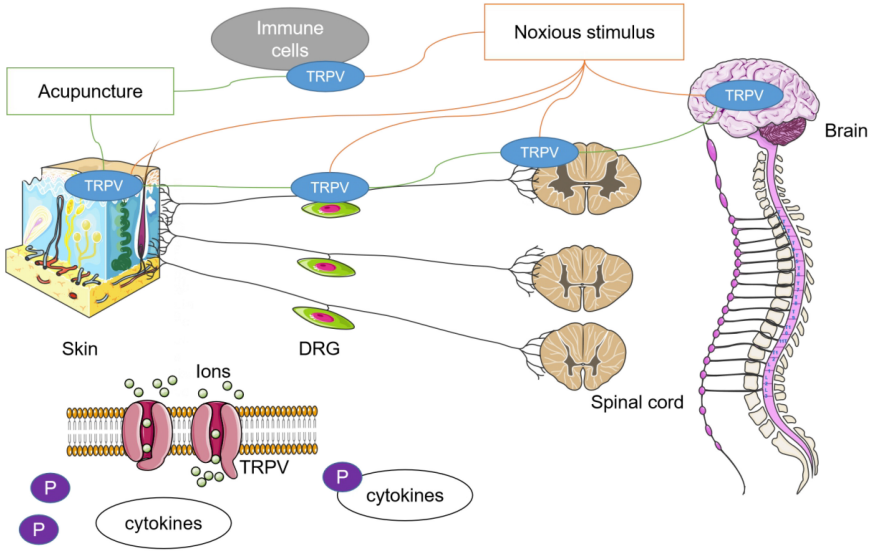

FIGURE 2
Relationship between acupuncture and TRPV channels. Noxious stimulus could lead to the imbalance of TRPV channel in multiple tissues. In many studies, it has been found that the therapeutic effect of acupuncture may be related to the agitation or antagonism of TRPV1 and TRPV4. The role of acupuncture in achieving systemic conditions through stimulation of specific acupoints may be closely dependent on the autonomic nervous system. Phosphorylation is an important mechanism in which acupuncture regulates downstream cytokines through TRPV channels.

Lottering and Lin (2021) performed a series of studies to clarify the role of acupuncture and TRPV in the cerebellum lobules. Both complete Freund's adjuvant (CFA) and acid saline (AS) could lead to chronic pain, but the expression of TRPV1 in the cerebellum lobules is completely opposite. Although it is observed that the analgesic effect of acupuncture at ST36 is obvious in both studies, the regulation of TRPV1 and phosphorylation of molecules in MAPK pathways by acupuncture are quite different. Behavioral results indicate that the mechanism of TRPV1 and related inflammatory factors in pain is not single and decisive in different models. The AS model restores the general concept of hyperalgesia caused by the pathological overexpression of TRPV and inflammation, and the influence of TRPV1 and inflammatory factors on pain sensation was not significant in the CFA model. In addition, the low expression of TRPV1 and inflammatory factors also leads to the formation of depression in mice after the injection of CFA.

Conclusion and future directions

Current studies have identified that there is a special relationship between acupuncture and TRPV channels including TRPV1 and TRPV4. First, stimulation at local acupoints can lead to systemic changes in TRPV channels, and the regulation of acupuncture to TRPV varies in different diseases or noxious stimuli. Second, the abundant expression and functional participation of TRPV1 and TRPV4 were specific to acupoints, and the enhancement or inhibition of TRPV channels at different anatomical levels will affect the therapeutic effect of acupuncture. Third, acupuncture and TRPV channels participate in complex molecular networks and that may explain the mechanism of acupuncture. All of the concepts are presented in Figure 2.

The regulation of acupuncture to TRPV channels is significantly different from that of TRPV agonist or antagonist. Similar to the balance of Yin and Yang pursued in acupuncture theory, acupuncture exhibits a bidirectional regulation to TRPV channels in multiple targets and contributes to an overall improvement of clinical symptoms and physiological functions in different diseases or stages of illness. In the past decades, TRPV1-targeted drugs have been long studied for human pain conditions (Iftinca et al., 2021). Many drugs attempting to block TRPV1 may lead to mixed results (Basso and Altier, 2017). Only the efficacy of topical use of TRPV agonists such as capsaicin patches has been recognized, but the systemic administration was not suggested because of the adverse effects on blood pressure, breathing, and other reflex pathways (Lu et al., 2020). The regulation of acupuncture to the p38 signaling pathway *via* TRPV in several nervous system diseases has been discussed by Wei and Hsieh (2020). Similar to this article, the role of acupuncture to p38 signal pathways is bidirectional, but it can improve the symptoms of a disease.

TRPV channels may also help us understand the principle of acupuncture. TRPV channels tend to be highly expressed at acupoints after acupuncture stimulation. Compared with sham

acupuncture, only acupuncture stimulation at acupoints could cause TRPV response. The expression of TRPV and the effect of using TRPV agonist or antagonist were also different from various acupuncture methods. For example, TRPV is sensitive to the intensity and duration of electroacupuncture, which suggests that there might be a more precise adjustment between acupuncture and TRPV channels.

There are still some limitations. All studies in this review were based on animal models. Therefore, the results in humans are inconclusive. In a single study, the regulatory relationship between acupuncture and TRPV was clear, but these effects became complex after consideration of similar studies. This prevents us from simply defining acupuncture as an agonist or inhibitor, as capsaicin does. At the same time, only a few articles compared the changes of acupuncture efficacy after local use of TRPV-related drugs, making it difficult to evaluate acupuncture and existing TRPV agonists or antagonist. As described earlier, activation of TRPV is structurally specific and selective. However, there are no studies on the changes of TRPV structure after acupuncture intervention. With the cryo-EM resolution revolution, the structural insights into the gating mechanisms of TRPV channels developed rapidly (Pumroy et al., 2020), and the role of TRPV channels in the endoplasmic reticulum has also been noticed (Haustrate et al., 2020). Compared with the current TRPV-related drugs, the effectiveness and safety of acupuncture in pain have been widely discussed (Cherkin et al., 2003; Manheimer et al., 2005). In conclusion, acupuncture has a strong relationship with TPPV1 and TRPV4. Acupuncture may provide a viable intervention target to TRPV channels. TRPV channels also help us understand how acupuncture works, especially for pain-related diseases. But the mechanism is unclear between acupuncture and TRPV channels, and further study is still needed.

Author contributions

DL: conceptualization. DL, LL, H-mZ, Y-dZ, M-fZ, J-xL, and Z-mY: data curation. DL, LL, and H-mZ: writing—original draft preparation. F-xL and RC: writing—review and editing. All authors read and agreed to the published version of the manuscript and contributed to the article and approved the submitted version.

Funding

This study was supported by the National Natural Science Foundation of China (Nos. 81774420, 81774401, 82105009, and 82274634), the Traditional Chinese Medicine Scientific Research Project of Hubei Provincial Health Commission (No. ZY2021Q031), and the Wuhan Medical Research Project (Nos. WX19Y18 and WZ22Q32).

Conflict of interest

The authors declare that the research was conducted in the absence of any commercial or financial relationships that could be construed as a potential conflict of interest.

Publisher's note

References

Abraham, T. S., Chen, M. L., and Ma, S. X. (2011). TRPV1 expression in acupuncture points: Response to electroacupuncture stimulation. *J. Chem. Neuroanat.* 41, 129–136. doi: 10.1016/j.jchemneu.2011.01.001

Baeumler, P. I., Fleckenstein, J., Takayama, S., Simang, M., Seki, T., Irnich, D., et al. (2014). Effects of acupuncture on sensory perception: A systematic review and meta-analysis. *PLoS One* 9:e113731. doi: 10.1371/journal.pone.0113731

Basith, S., Cui, M., Hong, S., and Choi, S. (2016). Harnessing the therapeutic potential of capsaicin and its analogues in pain and other diseases. *Molecules* 21:966. doi: 10.3390/molecules21080966

Basso, L., and Altier, C. (2017). Transient Receptor Potential Channels in neuropathic pain. *Curr. Opin. Pharmacol.* 32, 9–15. doi: 10.1016/j.coph.2016.10.002

Brooks, C. A., Barton, L. S., Behm, D. J., Eidam, H. S., Fox, R. M., Hammond, M., et al. (2019). Discovery of GSK2798745: A clinical candidate for inhibition of transient receptor potential vanilloid 4 (TRPV4). *ACS Med. Chem. Lett.* 10, 1228–1233. doi: 10.1021/acsmedchemlett.9b00274

Cao, E., Cordero-Morales, J. F., Liu, B., Qin, F., and Julius, D. (2013). TRPV1 channels are intrinsically heat sensitive and negatively regulated by phosphoinositide lipids. *Neuron* 77, 667–679. doi: 10.1016/j.neuron.2012.12.016

Carnevale, V., and Rohacs, T. (2016). TRPV1: A target for rational drug design. *Pharmaceuticals* 99:52. doi: 10.3390/ph9030052

Caterina, M. J., Leffler, A., Malmberg, A. B., Martin, W. J., Trafton, J., Petersen-Zeitz, K. R., et al. (2000). Impaired nociception and pain sensation in mice lacking the capsaicin receptor. *Science* 288, 306–313. doi: 10.1126/science.288.5464.306

Caterina, M. J., Schumacher, M. A., Tominaga, M., Rosen, T. A., Levine, J. D., Julius, D., et al. (1997). The capsaicin receptor: A heat-activated ion channel in the pain pathway. *Nature* 389, 816–824. doi: 10.1038/39807

Cavanaugh, D. J., Chesler, A. T., Jackson, A. C., Sigal, Y. M., Yamanaka, H., Grant, R., et al. (2011). Trpv1 reporter mice reveal highly restricted brain distribution and functional expression in arteriolar smooth muscle cells. *J. Neurosci.* 31, 5067–5077. doi: 10.1523/JNEUROSCI.6451-10.2011

Chen, H. C., Chen, M. Y., Hsieh, C. L., Wu, S. Y., Hsu, H. C., Lin, Y. W., et al. (2018). TRPV1 is a responding channel for acupuncture manipulation in mice peripheral and central nerve system. *Cell Physiol. Biochem.* 49, 1813–1824. doi: 10.1159/000493627

Chen, L., Xu, A., Yin, N., Zhao, M., Wang, Z., Chen, T., et al. (2017). Enhancement of immune cytokines and splenic CD4+ T cells by electroacupuncture at ST36 acupoint of SD rats. *PLoS One* 12:e175568. doi: 10.1371/journal.pone.0175568

Cherkin, D. C., Sherman, K. J., Deyo, R. A., and Shekelle, P. G. (2003). A review of the evidence for the effectiveness, safety, and cost of acupuncture, massage therapy, and spinal manipulation for back pain. *Ann. Intern. Med.* 138, 898–906. doi: 10.7326/0003-4819-138-11-200306030-00011

Choowanthanapakorn, M., Lu, K. W., Yang, J., Hsieh, C. L., and Lin, Y. W. (2015). Targeting TRPV1 for body weight control using TRPV1(-/-) mice and electroacupuncture. *Sci. Rep.* 5:17366. doi: 10.1038/srep17366

Fang, J. Q., Du, J. Y., Fang, J. F., Xiao, T., Le, X. Q., Pan, N. F., et al. (2018). Parameter-specific analgesic effects of electroacupuncture mediated by degree of regulation TRPV1 and P2X3 in inflammatory pain in rats. *Life Sci.* 200, 69–80. doi: 10.1016/j.lfs.2018.03.028

Fischer, M., Ciotu, C. I., and Szallasi, A. (2020). The mysteries of Capsaicin-Sensitive afferents. *Front. Physiol.* 11:554195. doi: 10.3389/fphys.2020.554195

Gong, Y., Li, N., Lv, Z., Zhang, K., Zhang, Y., Yang, T., et al. (2020). The neuro-immune microenvironment of acupoints-initiation of acupuncture effectiveness. *J. Leukoc. Biol.* 108, 189–198. doi: 10.1002/JLB.3AB0420-361RR

Grace, M. S., Bonvini, S. J., Belvisi, M. G., and McIntyre, P. (2017). Modulation of the TRPV4 ion channel as a therapeutic target for disease. *Pharmacol. Ther.* 177, 9–22. doi: 10.1016/j.pharmthera.2017.02.019

Guo, Z. L., Fu, L. W., Su, H. F., Tjen-A-Looi, S. C., and Longhurst, J. C. (2018). Role of TRPV1 in acupuncture modulation of reflex excitatory cardiovascular responses. *Am J. Physiol. Regul. Integr. Comp. Physiol.* 314, R655–R666. doi: 10.1152/ajpregu.00405.2017

Han, J. S. (2004). Acupuncture and endorphins. *Neurosci. Lett.* 361, 258–261. doi: 10.1016/j.neulet.2003.12.019

Haustrate, A., Prevarskaya, N., and Lehen'Kyi, V. (2020). Role of the TRPV channels in the endoplasmic reticulum calcium homeostasis. *Cells* 9:317. doi: 10.3390/cells9020317

He, Y., Guo, X., May, B. H., Zhang, A. L., Liu, Y., Lu, C., et al. (2020). Clinical evidence for association of acupuncture and acupressure with improved cancer pain: A systematic review and Meta-Analysis. *JAMA Oncol.* 6, 271–278. doi: 10.1001/jamaoncol.2019.5233

Hsu, H. C., Hsieh, C. L., Lee, K. T., and Lin, Y. W. (2020). Electroacupuncture reduces fibromyalgia pain by downregulating the TRPV1-pERK signalling pathway in the mouse brain. *Acupunct. Med.* 38, 101–108. doi: 10.1136/acupmed-2017-011395

Hu, B., Bai, F., Xiong, L., and Wang, Q. (2017). The endocannabinoid system, a novel and key participant in acupuncture's multiple beneficial effects. *Neurosci. Biobehav. Rev.* 77, 340–357. doi: 10.1016/j.neubiorev.2017.04.006

Huang, M., Wang, X., Xing, B., Yang, H., Sa, Z., Zhang, D., et al. (2018). Critical roles of TRPV2 channels, histamine H1 and adenosine A1 receptors in the initiation of acupoint signals for acupuncture analgesia. *Sci. Rep.* 8:6523. doi: 10.1038/s41598-018-24654-y

Huang, W., Pach, D., Napadow, V., Park, K., Long, X., Neumann, J., et al. (2012). Characterizing acupuncture stimuli using brain imaging with FMRI–a systematic review and meta-analysis of the literature. *PLoS One* 7:e32960. doi: 10.1371/journal.pone.0032960

Iftinca, M., Defaye, M., and Altier, C. (2021). TRPV1-Targeted drugs in development for human pain conditions. *Drugs* 81, 7–27. doi: 10.1007/s40265-020-01429-2

Inprasit, C., and Lin, Y. W. (2020). TRPV1 responses in the cerebellum lobules v, VIa and VII using electroacupuncture treatment for inflammatory hyperalgesia in murine model. *Int. J. Mol. Sci.* 21:3312. doi: 10.3390/ijms21093312

Inprasit, C., Lin, Y. W., Huang, C. P., Wu, S. Y., and Hsieh, C. L. (2018). Targeting TRPV1 to relieve motion sickness symptoms in mice by electroacupuncture and gene deletion. *Sci. Rep.* 8:10365. doi: 10.1038/s41598-018-23793-6

Ji, B., Hu, J., and Ma, S. (2013). Effects of electroacupuncture Zusanli (ST36) on food intake and expression of POMC and TRPV1 through afferents-medulla pathway in obese prone rats. *Peptides* 40, 188–194. doi: 10.1016/j.peptides.2012.10.009

Jin, C., Lu, Y., Lu, M., Cai, H., and Zhang, J. (2018). [Discussion on the cognition and development process of experimental animal acupoints]. *Zhongguo Zhen Jiu* 38, 963–966. doi: 10.13703/j.0255-2930.2018.09.015

Jordt, S. E., and Ehrlich, B. E. (2007). TRP channels in disease. *Subcell. Biochem.* 45, 253–271. doi: 10.1007/978-1-4020-6191-2_9

Kaptchuk, T. J. (2002). Acupuncture: Theory, efficacy, and practice. *Ann. Intern. Med.* 136, 374–383. doi: 10.7326/0003-4819-136-5-200203050-00010

Kim, S. Y., Shin, I. S., and Park, Y. J. (2018). Effect of acupuncture and intervention types on weight loss: A systematic review and meta-analysis. *Obes. Rev.* 19, 1585–1596. doi: 10.1111/obr.12747

Lawhorn, B. G., Brnardic, E. J., and Behm, D. J. (2020). Recent advances in TRPV4 agonists and antagonists. *Bioorg. Med. Chem. Lett.* 30:127022. doi: 10.1016/j.bmcl.2020.127022

Li, Y., Yin, C., Li, X., Liu, B., Wang, J., Zheng, X., et al. (2019). Electroacupuncture alleviates Paclitaxel-Induced peripheral neuropathic pain in rats via suppressing TLR4 signaling and TRPV1 upregulation in sensory neurons. *Int. J. Mol. Sci.* 20:5917. doi: 10.3390/ijms20235917

Liao, H. Y., Hsieh, C. L., Huang, C. P., and Lin, Y. W. (2017). Electroacupuncture Attenuates CFA-induced Inflammatory Pain by suppressing Nav1.8 through S100B, TRPV1, Opioid, and Adenosine Pathways in Mice. *Sci. Rep.* 7:42531. doi: 10.1038/srep42531

Lim, H. D., Kim, M. H., Lee, C. Y., and Namgung, U. (2016). Anti-Inflammatory Effects of Acupuncture Stimulation via the Vagus Nerve. *PLoS One* 11:e151882. doi: 10.1371/journal.pone.0151882

Lin, J. G., Hsieh, C. L., and Lin, Y. W. (2015). Analgesic effect of electroacupuncture in a mouse fibromyalgia model: Roles of TRPV1. TRPV4, and pERK. *PLoS One* 10:e128037. doi: 10.1371/journal.pone.0128037

Lin, Y. W., Chou, A., Su, H., and Su, K. P. (2020). Transient receptor potential V1 (TRPV1) modulates the therapeutic effects for comorbidity of pain and depression: The common molecular implication for electroacupuncture and omega-3 polyunsaturated fatty acids. *Brain Behav. Immun.* 89, 604–614. doi: 10.1016/j.bbi.2020.06.033

Lin, Y. W., and Hsieh, C. L. (2010). Electroacupuncture at Baihui acupoint (GV20) reverses behavior deficit and long-term potentiation through N-methyl-d-aspartate and transient receptor potential vanilloid subtype 1 receptors in middle cerebral artery occlusion rats. *J. Integr. Neurosci.* 9, 269–282. doi: 10.1142/s0219635210002433

Liu, S., Wang, Z., Su, Y., Qi, L., Yang, W., Fu, M., et al. (2021). A neuroanatomical basis for electroacupuncture to drive the vagal-adrenal axis. *Nature* 598, 641–645. doi: 10.1038/s41586-021-04001-4

Liu, S., Wang, Z. F., Su, Y. S., Ray, R. S., Jing, X. H., Wang, Y. Q., et al. (2020). Somatotopic organization and intensity dependence in driving distinct NPY-Expressing sympathetic pathways by electroacupuncture. *Neuron* 108, 436–450. doi: 10.1016/j.neuron.2020.07.015

Long, M., Wang, Z., Zheng, D., Chen, J., Tao, W., Wang, L., et al. (2019). Electroacupuncture pretreatment elicits neuroprotection against cerebral Ischemia-Reperfusion injury in rats associated with transient receptor potential vanilloid 1-Mediated Anti-Oxidant stress and Anti-Inflammation. *Inflammation* 42, 1777–1787. doi: 10.1007/s10753-019-01040-y

Lottering, B., and Lin, Y. W. (2021). TRPV1 responses in the cerebellum lobules VI, VII, VIII using electroacupuncture treatment for chronic pain and depression comorbidity in a murine model. *Int. J. Mol. Sci.* 22:5028. doi: 10.3390/ijms22095028

Lu, M., Chen, C., Lan, Y., Xiao, J., Li, R., Huang, J., et al. (2020). Capsaicin-the major bioactive ingredient of chili peppers: Bio-efficacy and delivery systems. *Food Funct.* 11, 2848–2860. doi: 10.1039/d0fo00351d

Manheimer, E., White, A., Berman, B., Forys, K., and Ernst, E. (2005). Meta-analysis: Acupuncture for low back pain. *Ann. Intern. Med.* 142, 651–663. doi: 10.7326/0003-4819-142-8-200504190-00014

Mao, J. J., Farrar, J. T., Armstrong, K., Donahue, A., Ngo, J., Bowman, M. A., et al. (2007). De qi: Chinese acupuncture patients' experiences and beliefs regarding acupuncture needling sensation–an exploratory survey. *Acupunct. Med.* 25, 158–165. doi: 10.1136/aim.25.4.158

Paricio-Montesinos, R., Schwaller, F., Udhayachandran, A., Rau, F., Walcher, J., Evangelista, R. A., et al. (2020). The sensory coding of warm perception. *Neuron* 106, 830–841. doi: 10.1016/j.neuron.2020.02.035

Patapoutian, A., Peier, A. M., Story, G. M., and Viswanath, V. (2003). ThermoTRP channels and beyond: Mechanisms of temperature sensation. *Nat. Rev. Neurosci.* 4, 529–539. doi: 10.1038/nrn1141

Por, E. D., Gomez, R., Akopian, A. N., and Jeske, N. A. (2013). Phosphorylation regulates TRPV1 association with beta-arrestin-2. *Biochem. J.* 451, 101–109. doi: 10.1042/BJ20121637

Pumroy, R. A., Fluck, E. R., Ahmed, T., and Moiseenkova-Bell, V. Y. (2020). Structural insights into the gating mechanisms of TRPV channels. *Cell Calcium* 87:102168. doi: 10.1016/j.ceca.2020.102168

Rubin, R. (2019). Medicare proposes coverage of acupuncture for lower back pain. *JAMA* 322:716. doi: 10.1001/jama.2019.11573

Samanta, A., Hughes, T., and Moiseenkova-Bell, V. Y. (2018). Transient receptor potential (TRP) channels. *Subcell. Biochem.* 87, 141–165. doi: 10.1007/978-981-10-7757-9_6

Satheesh, N. J., Uehara, Y., Fedotova, J., Pohanka, M., Busselberg, D., Kruzliak, P., et al. (2016). TRPV currents and their role in the nociception and neuroplasticity. *Neuropeptides* 57, 1–8. doi: 10.1016/j.npep.2016.01.003

Seebohm, G., and Schreiber, J. A. (2021). Beyond hot and spicy: TRPV channels and their pharmacological modulation. *Cell Physiol. Biochem.* 55, 108–130. doi: 10.33594/000000358

Shu, Q., Wang, H., Litscher, D., Wu, S., Chen, L., Gaischek, I., et al. (2016). Acupuncture and Moxibustion have Different Effects on Fatigue by Regulating the Autonomic Nervous System: A Pilot Controlled Clinical Trial. *Sci. Rep.* 6:37846. doi: 10.1038/srep37846

Singh, R., Bansal, Y., Parhar, I., Kuhad, A., and Soga, T. (2019). Neuropsychiatric implications of transient receptor potential vanilloid (TRPV) channels in the reward system. *Neurochem. Int.* 131:104545. doi: 10.1016/j.neuint.2019.104545

Slomski, A. (2019). Acupuncture may reduce menopausal symptoms. *JAMA* 321:1558. doi: 10.1001/jama.2019.4593

Smith, G. D., Gunthorpe, M. J., Kelsell, R. E., Hayes, P. D., Reilly, P., Facer, P., et al. (2002). TRPV3 is a temperature-sensitive vanilloid receptor-like protein. *Nature* 418, 186–190. doi: 10.1038/nature00894

Szolcsanyi, J. (2008). Hot target on nociceptors: Perspectives, caveats and unique features. *Br. J. Pharmacol.* 155, 1142–1144. doi: 10.1038/bjp.2008.374

Tang, Y., Yin, H. Y., Rubini, P., and Illes, P. (2016). Acupuncture-Induced analgesia: A neurobiological basis in purinergic signaling. *Neuroscientist* 22, 563–578. doi: 10.1177/1073858416654453

van de Graaf, S. F., Hoenderop, J. G., Gkika, D., Lamers, D., Prenen, J., Rescher, U., et al. (2003). Functional expression of the epithelial Ca(2+) channels (TRPV5 and TRPV6) requires association of the S100A10-annexin 2 complex. *Embo. J.* 22, 1478–1487. doi: 10.1093/emboj/cdg162

Wei, T. H., and Hsieh, C. L. (2020). Effect of Acupuncture on the p38 Signaling Pathway in Several Nervous System Diseases: A Systematic Review. *Int. J. Mol. Sci.* 21:4693. doi: 10.3390/ijms21134693

Wu, S. Y., Chen, W. H., Hsieh, C. L., and Lin, Y. W. (2014). Abundant expression and functional participation of TRPV1 at Zusanli acupoint (ST36) in mice: Mechanosensitive TRPV1 as an "acupuncture-responding channel". *BMC Complement. Altern. Med.* 14:96. doi: 10.1186/1472-6882-14-96

Xin, J., Su, Y., Yang, Z., He, W., Shi, H., Wang, X., et al. (2016). Distinct roles of ASIC3 and TRPV1 receptors in electroacupuncture-induced segmental and systemic analgesia. *Front. Med.* 10, 465–472. doi: 10.1007/s11684-016-0482-7

Yang, F., and Zheng, J. (2017). Understand spiciness: Mechanism of TRPV1 channel activation by capsaicin. *Protein Cell* 8, 169–177. doi: 10.1007/s13238-016-0353-7

Yang, J., Hsieh, C. L., and Lin, Y. W. (2017). Role of Transient Receptor Potential Vanilloid 1 in Electroacupuncture Analgesia on Chronic Inflammatory Pain in Mice. *Biomed. Res. Int.* 2017:5068347. doi: 10.1155/2017/5068347

Yen, C. M., Wu, T. C., Hsieh, C. L., Huang, Y. W., and Lin, Y. W. (2019). Distal electroacupuncture at the LI4 acupoint reduces CFA-Induced inflammatory pain via the brain TRPV1 signaling pathway. *Int. J. Mol. Sci.* 20:4471. doi: 10.3390/ijms20184471

Yu, Z., Zhang, N., Lu, C. X., Pang, T. T., Wang, K. Y., Jiang, J. F., et al. (2016). Electroacupuncture at ST25 inhibits jejunal motility: Role of sympathetic pathways and TRPV1. *World J. Gastroenterol.* 22, 1834–1843. doi: 10.3748/wjg.v22.i5.1834

Zhang, R., Lao, L., Ren, K., and Berman, B. M. (2014). Mechanisms of acupuncture-electroacupuncture on persistent pain. *Anesthesiology* 120, 482–503. doi: 10.1097/ALN.0000000000000101

Zhang, Y., Zhang, R. X., Zhang, M., Shen, X. Y., Li, A., Xin, J., et al. (2012). Electroacupuncture inhibition of hyperalgesia in an inflammatory pain rat model: Involvement of distinct spinal serotonin and norepinephrine receptor subtypes. *Br. J. Anaesth.* 109, 245–252. doi: 10.1093/bja/aes136

Zhang, Z., Wang, C., Gu, G., Li, H., Zhao, H., Wang, K., et al. (2012). The effects of electroacupuncture at the ST36 (Zusanli) acupoint on cancer pain and transient receptor potential vanilloid subfamily 1 expression in Walker 256 tumor-bearing rats. *Anesth. Analg.* 114, 879–885. doi: 10.1213/ANE.0b013e318246536d

Zhao, Z. Q. (2008). Neural mechanism underlying acupuncture analgesia. *Prog. Neurobiol.* 85, 355–375. doi: 10.1016/j.pneurobio.2008.05.004

Zheng, J. (2013). Molecular mechanism of TRP channels. *Compr. Physiol.* 3, 221–242. doi: 10.1002/cphy.c120001

frontiers | Frontiers in Cellular Neuroscience

TYPE Review
PUBLISHED 10 November 2022
DOI 10.3389/fncel.2022.817732

OPEN ACCESS

EDITED BY
Binlong Zhang,
Guang'anmen Hospital, China
Academy of Chinese Medical Sciences, China

REVIEWED BY
Elizabeth Hernández-Echeagaray, National Autonomous University of Mexico, Mexico
Abdelrahman Fouda, University of Arkansas for Medical Sciences, United States

*CORRESPONDENCE
Zhifang Xu
xuzhifangmsn@hotmail.com
Yang Guo
guoguo_guoyang@hotmail.com

†These authors have contributed equally to this work and share first authorship

SPECIALTY SECTION
This article was submitted to Cellular Neuropathology, a section of the journal Frontiers in Cellular Neuroscience

RECEIVED 18 November 2021
ACCEPTED 24 October 2022
PUBLISHED 10 November 2022

CITATION
Qin S, Zhang Z, Zhao Y, Liu J, Qiu J, Gong Y, Fan W, Guo Y, Guo Y, Xu Z and Guo Y (2022) The impact of acupuncture on neuroplasticity after ischemic stroke: a literature review and perspectives.
Front. Cell. Neurosci. 16:817732.
doi: 10.3389/fncel.2022.817732

The impact of acupuncture on neuroplasticity after ischemic stroke: a literature review and perspectives

Siru Qin[1†], Zichen Zhang[1†], Yadan Zhao[1], Jingyi Liu[1], Jiwen Qiu[1,2,3], Yinan Gong[1,2], Wen Fan[4], Yongming Guo[1,2,3], Yi Guo[1,3,5], Zhifang Xu[1,2,3]* and Yang Guo[3,6]*

[1]Research Center of Experimental Acupuncture Science, Tianjin University of Traditional Chinese Medicine, Tianjin, China, [2]School of Acupuncture & Moxibustion and Tuina, Tianjin University of Traditional Chinese Medicine, Tianjin, China, [3]National Clinical Research Center for Chinese Medicine Acupuncture and Moxibustion, Tianjin, China, [4]Department of Rehabilitation Physical Therapy Course, Faculty of Health Science, Suzuka University of Medical Science, Suzuka, Japan, [5]School of Traditional Chinese Medicine, Tianjin University of Traditional Chinese Medicine, Tianjin, China, [6]Acupuncture Department, First Teaching Hospital of Tianjin University of Traditional Chinese Medicine, Tianjin, China

Ischemic stroke is common in the elderly, and is one of the main causes of long-term disability worldwide. After ischemic stroke, spontaneous recovery and functional reconstruction take place. These processes are possible thanks to neuroplasticity, which involves neurogenesis, synaptogenesis, and angiogenesis. However, the repair of ischemic damage is not complete, and neurological deficits develop eventually. The WHO recommends acupuncture as an alternative and complementary method for the treatment of stroke. Moreover, clinical and experimental evidence has documented the potential of acupuncture to ameliorate ischemic stroke-induced neurological deficits, particularly sequelae such as dyskinesia, spasticity, cognitive impairment, and dysphagia. These effects are related to the ability of acupuncture to promote spontaneous neuroplasticity after ischemic stroke. Specifically, acupuncture can stimulate neurogenesis, activate axonal regeneration and sprouting, and improve the structure and function of synapses. These processes modify the neural network and function of the damaged brain area, producing the improvement of various skills and adaptability. Astrocytes and microglia may be involved in the regulation of neuroplasticity by acupuncture, such as by the production and release of a variety of neurotrophic factors, including brain-derived neurotrophic factor (BDNF) and nerve growth factor (NGF). Moreover, the evidence presented indicates that acupuncture promotes neuroplasticity by modulating the functional reconstruction of the whole brain after ischemia. Therefore, the promotion of neuroplasticity is expected to become a new target for acupuncture in the treatment of neurological deficits after ischemic stroke, and research into the mechanisms responsible for these actions will be of significant clinical value.

KEYWORDS

acupuncture, ischemic stroke, neuroplasticity, neurogenesis, axon regeneration, synapse, neurotrophic factors, glia

Introduction

Ischemic stroke is common in the elderly, and its incidence increases with age. It is one of the leading causes of long-term disability worldwide (Go et al., 2014). The primary cause of ischemic stroke is the interruption of blood flow by cerebral vascular occlusion. Acutely and sub-acutely lack of blood supply produces metabolic acidosis, excitotoxicity, inflammation, oxidative stress, and cytotoxic edema, resulting in necrosis or apoptosis of neurons. However, spontaneous recovery appears in the brain damaged by an ischemic stroke. For instance, in the subacute stage of stroke, neurotrophic factors (NTFs) and associated signaling pathways, such as protein-serine-threonine kinase (Akt) pathway, trigger the neuroprotective effect. In the chronic phase, neurogenesis, angiogenesis, and synaptogenesis are the main processes of spontaneous neuroplasticity, but the repair is often incomplete due to the limited regenerative capacity of neurons (Chavez et al., 2017). Therefore, understanding the mechanisms of promoting spontaneous and therapeutic neuroplasticity-mediated structural reconstruction and functional recovery is of great significance for the treatment and prognosis of ischemic stroke (Cassidy and Cramer, 2017).

Brain neuroplasticity refers to the ability of the brain to modify its morphological structure and functional activity in response to internal or external stimuli (Carey et al., 2019). It occurs throughout the entire lifespan, and the structural and functional plasticity may be enhanced after brain injury. Brain neuroplasticity can be observed at different levels, such as changes in the structure and function of synapses, cells, and regions, subsequent modifications in the communication and networks among cells and regions, and, ultimately, changes in neurologic behavior and function, such as sensory perception, motor behavior, and cognition (Murphy and Corbett, 2009; Pekna et al., 2012). Since the brain has a remarkable capacity for plasticity and reorganization, it would be useful to exploit these properties to improve the clinical efficacy of ischemic stroke therapy.

Acupuncture, a process of inserting fine needles into the skin or deep tissues of specific parts (acupoints) of the body, is an essential component of Traditional Chinese Medicine. Acupuncture can be applied by hand, electric stimulation, or heating (Li and Wang, 2013), and is characterized by a safe, efficient, economical, and simple operation. Lines of clinical and experimental evidence have demonstrated that acupuncture can improve ischemic stroke-induced neurological deficits, especially for the sequelae of stroke (World Health Organization, 2002; Li et al., 2021; Shao et al., 2021). The effect of acupuncture starts from the stimulation of the acupoints, i.e., excitable complexes of muscle and skin nerves with a high density of nerve endings (Li et al., 2004). After converting physical or chemical information to electrical activity in acupoints, the signal is sent along afferent fibers to the spinal cord and brain (Zhao, 2008). There is evidence that acupuncture can modulate neuroplasticity in central nervous system (CNS) by modifying neural structure and function (Chavez et al., 2017). However, the detailed mechanisms of the effect of acupuncture on brain neuroplasticity in ischemic stroke have not been systematically reviewed.

This review analyzes neuroplasticity as the basis for the discussion of the effects of acupuncture on ischemic stroke and their potential mechanisms. The understanding of how acupuncture promotes and modulates neurogenesis, axonal regeneration and sprouting, synaptic plasticity, neuroglial crosstalk, and functional reconstruction reviewed in this work provides novel insights into the therapeutic mechanism of this procedure on ischemic stroke. It is hoped that the information provided will promote the clinical application of acupuncture for the functional recovery of ischemic stroke worldwide.

Methods

Search strategy

We searched the PubMed database for studies published between January 2010 and April 2021 using the MeSH terms "Acupuncture," "Ischemic Stroke" and relevant entry terms. The search identified 211 relevant articles.

Study selection

We developed the following study inclusion criteria to study the treatment of ischemic stroke by acupoint stimulation *via* regulating neuroplasticity: stimulation methods included manual acupuncture, electroacupuncture, and moxibustion, and the research topics were related to neuroplasticity, specifically, neurogenesis, axon sprouting, axon regeneration, synaptic plasticity, and functional reorganization of the brain regions. Following the identification of 211 articles by the search engine, we performed a manual search of the reference lists of articles to identify further relevant articles that met the inclusion criteria based on the titles and abstracts. We excluded 62 articles due to duplication, the lack of an abstract or lack of relevance to ischemic stroke before conducting full-text assessments. This left 149 articles, including 66 basic research articles, 54 clinical research articles, and 29 review articles or meta-analyses. The full texts of the 66 basic research and 54 clinical research articles were obtained and evaluated carefully. Of the 66 basic research articles, 35 were selected and 31 were excluded as they did not focus on neuroplasticity. Of the 54 clinical studies, 12 were selected and 42 were excluded as they described single case reports, editorials, incomplete or uncontrolled trials, or were irrelevant to neuroplasticity. Thus, a total of 47 articles were

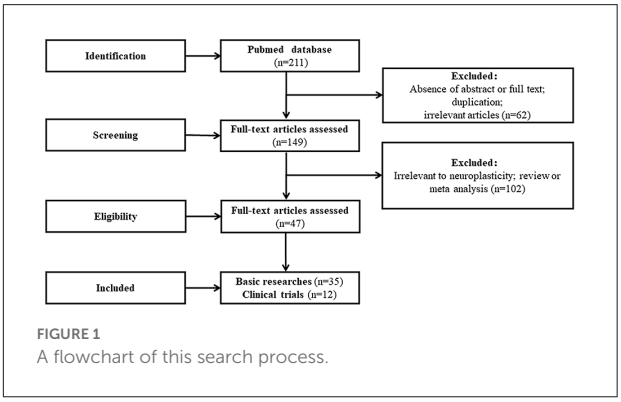

FIGURE 1
A flowchart of this search process.

included in our review. A flowchart of this search process is illustrated in **Figure 1**.

Data extraction

Two authors independently evaluated the titles and abstracts of the retrieved articles and assessed the full texts of the articles. All of the 47 articles were finally included in the review, from which the data were extracted and listed according to the prespecified criteria, to analyze the mechanisms of acupuncture in regulating neuroplasticity in the treatment of ischemic stroke. Any disagreement was resolved by discussion between the authors.

Clinical effect of acupuncture on ischemic stroke

Neurological deficits after ischemic stroke can be self-repaired to varying degrees, which may be due to the plasticity of the remaining brain tissue. Despite this, damage to the functional areas of the brain may persist in areas responsible for motion, cognition, sensation, vision, and language (Rathore et al., 2002). Therefore, a wide range of rehabilitation treatments for stroke recovery has been developed, including the use of drugs, stem cells, behavioral therapy, robotics, and acupuncture (Cramer, 2008). Of these types of therapy, many systematic reviews have indicated that acupuncture can improve the neurological function of patients with ischemic stroke (Liu et al., 2015; Yang et al., 2016; Hung et al., 2019). A Cochrane review included 31 trials with a total of 2,257 participants in the subacute or chronic stages of stroke, and found that compared with no acupuncture, acupuncture was beneficial for the improvement of dependency, global neurological deficiency, and specific neurological impairments including motor, cognitive, and swallowing functions, as well as depression and pain (Yang et al., 2016). Four trials in this systematic review and other randomized controlled trials (RCTs) used the Fugl-Meyer Assessment scale (FMI) to evaluate the impact of acupuncture therapy after an ischemic stroke on the motor function of the upper and lower limbs. The results showed greater improvement in motor function in the acupuncture group compared with the non-acupuncture group (Li et al., 2015; Yang et al., 2016; Wu J. et al., 2017). The results of 11 trials in this review and other following RCTs found that the dependence measured by continuous scales [Barthel Index (BI), Modified Barthel Index and Activity of Daily Living Scale] in the acupuncture group was significantly improved compared with the control group (Yang et al., 2016; Wu J. et al., 2017; Wu et al., 2018). Furthermore, in this review, 13 trials were conducted to evaluate the improvement of cognitive function by acupuncture, using the Mini-Mental State Examination, Montreal Cognitive Assessment Scale, and Revised Hasegawa Dementia Scale. The results showed that acupuncture was superior to non-acupuncture in the improvement of cognitive function in convalescent stroke patients. The authors also concluded that acupuncture is most beneficial in the first 3 months with reduced benefit after 6 months. However, in terms of long-term follow-up, including mortality and quality of life, there is a lack of data from RCTs on the clinical outcomes of acupuncture in the treatment of stroke (Yang et al., 2016). The analysis of the recurrence of ischemic stroke treated with or without acupuncture has shown that patients treated with both medications and acupuncture had a lower rate of recurrence than patients treated only pharmaceutically (Shih et al., 2015). However, we still need more reliable evidence of major outcomes from more stringent RCTs, including the setting of grouping concealment, to draw conclusions about the efficacy of acupuncture on stroke.

RCTs focused on the use of acupuncture for the treatment of stroke have shown satisfactory results when acupuncture is applied at acupoints to treat various stroke sequelae, such as hemiplegia, dysphagia, and cognitive impairment. For hemiplegia, the most commonly used acupoints include *Baihui* (GV20), *Yintang* (EX-HN3), and the anterior oblique line of vertex-temporal of the head, *Jianyu* (LI15), *Quchi* (LI11), *Shousanli* (LI10), *Waiguan* (TB5), *Hegu* (LI4) of upper limbs, *Liangqiu* (ST34), *Zusanli* (ST36), *Yanglingquan* (GB34), *Sanyinjiao* (SP6), *Fenglong* (ST40), *Jiexi* (ST41), and *Taichong* (LR3) of lower limbs. These acupoints are important to inhibit muscle spasm, restore the coordination function of extensors and flexors, and inhibit their synergic movement, improving in this manner the limb function in hemiplegia (Chen J. et al., 2014; Wang et al., 2017). For aphasia, No. 1, 2, and 3 language sections of the head are selected according to the type of aphasia, in which language section No. 1 is for motor aphasia, No. 2 is for anomic aphasia, No. 3 is for sensory aphasia, and No. 1 combined with No. 2 is for mixed aphasia. In addition, *Fengchi* (GB20), *Yamen* (GV15), *Jinjin* (EX-HN12), *Yuye* (EX-HN13), *Tongli* (HT5), and *Lianquan* (CV23) acupoints are used, which are located near

the tongue and above the Heart Meridian of Hand-shaoyin associated with the tongue (Sun et al., 2012). For a mild cognitive impairment, GV20, *Shenting* (GV24), *Benshen* (GB13), *Taiyang* (EX-HN5), *Touwei* (ST8), *Sishencong* (EX-HN1) are employed. Among them, EX-HN5, ST8, and EX-HN1 acupoints are located in the anterior and medial sides of the temporal lobe and adjacent areas, which control memory function and mental activity (Chen J. et al., 2014; Kalaria et al., 2016). Although acupuncture protocols differ according to the different impaired functions, they all conform to the principle of the of integral-local combined selection, i.e., matching the acupoints of brain functional areas with those of specific lesion areas.

Acupuncture modulates neuroplasticity

Recovery of lost functions after ischemic stroke is thought to depend on neuroplasticity, that is, the ability of the brain to restructure and reconstruct in response to endogenous and exogenous stress and injuries (Murphy, 2015; Dąbrowski et al., 2019). Neuroplasticity manifests in short-term functional changes and long-term structural changes. Short-term functional changes consist of modifications of synaptic efficiency, while the long-term structural changes reflect adaptations of neural connections. The core components of neuroplasticity are neurogenesis, axon sprouting, axon regeneration, and synaptic plasticity (Hickmott and Ethell, 2006; Lillard and Erisir, 2011). These processes and the potential mechanisms by which acupuncture can affect them are reviewed below and summarized in **Table 1**.

Acupuncture promotes endogenous neurogenesis

The neurogenesis of the adult mammalian brain continues throughout the lifespan of an organism. The main neurogenic niches are located in the subventricular zone (SVZ) of the lateral ventricle and the subgranular zone (SGZ) of the dentate gyrus in the hippocampus. Neural stem cells (NSCs) and neural precursor cells (NPCs) from SVZ migrate to the olfactory bulb through the rostral migratory stream and are thought to be responsible for the maintenance and reorganization of the interneuron system within the olfactory bulb. The cells from the SGZ migrate to the granule cell layer and differentiate into granulosa cells that form synapses with existing neurons and have an important function in neuroplasticity (Merson and Bourne, 2014; Xiao et al., 2018). Increasing evidence suggests that adult neurogenesis also occurs in several other regions of the CNS, including the spinal cord, striatum, neocortex, cerebellum, substantia nigra, amygdala, and hypothalamus, particularly following a CNS injury (Martino et al., 2011; Sandvig et al., 2018).

Cell death occurs immediately in the ischemic core of the cerebral infarction, followed by the spread of injury to the ischemic penumbra. Therefore, enhancing the survival, proliferation, and migration of endogenous NSCs to the injured region by upregulating local secretion of NTFs facilitates the formation of new synapses and circuits and the restoration of the structure and function of the brain. NSCs can differentiate into neurons, astrocytes, oligodendrocytes, and other neural cells, which gradually migrate to target areas (Yamashita et al., 2006; Brouns and De Deyn, 2009). Since the number of endogenous NSCs and NPCs is too small to sustain the recovery of neurologic functions after ischemic stroke, strategies aiming at the promotion of their proliferation and directional differentiation into neurons with normal functions are the focus of intense research. At the same time, the transformation of astrocytes into neurons to assume neuronal functions after brain injury is also a new research hotspot (Magnusson et al., 2014).

Many studies have suggested that acupuncture can promote the proliferation, migration, and differentiation of NSCs, protecting the brain from ischemic damage and improving neurological deficits. For instance, the study conducted by Luo et al. (2014) demonstrated that middle cerebral artery occlusion (MCAO) in rats produced a large number of cells positive for nestin (a specific marker of NSCs), 5-bromo-2'-dexoyuridine (BrdU, a marker of cell proliferation), and cells double-positive for both markers in the brain, while cells positive for these markers were absent in control non-MCAO mice, and acupuncture at *Shuigou* (GV26) further increased the number of nestin/BrdU positive regenerative cells in MCAO mice. These results indicated that a certain extent of "self-healing" takes place after brain damage induced by focal cerebral ischemia, and acupuncture treatment promotes the proliferation of NSCs. This study also demonstrated that the expression of nestin mRNA in the cortex in the acupuncture group was much higher than in the non-MCAO and non-acupuncture groups. Moreover, with acupuncture, nestin expression increased slightly in the hippocampus and decreased in the striatum, indicating that acupuncture at GV26 promoted more extensive proliferation and/or migration of new neurons to the cortex than to the hippocampus and striatum (Luo et al., 2014). In another study, electroacupuncture (EA) was applied to the acupoints ST36 and LI11 at 1/20 Hz to treat MCAO rats. At 7 and 14 days after the induction of ischemia, the number of BrdU/glial fibrillary acidic protein (GFAP, a marker of astrocyte activation) double-positive cells in SVZ and BrdU/NeuN (a marker of mature neurons) and double-positive cells in the striatum was higher in EA-treated rats (Tao et al., 2010). Liao et al. (2017) also obtained similar results by applying 2 Hz EA in ST36 and ST37 for cerebral infarction rats with ischemia reperfusion injury. These results suggest that EA therapy can induce cell proliferation and differentiation into astrocytes and mature neurons.

Acupuncture mediates the upregulation of neurogenesis-related factors and the activation of related cell signaling

TABLE 1 The mechanisms of acupuncture on regulating neuroplasticity in the treatment of ischemic stroke.

Study	Model/Objects	Intervention	Acupoints	Comparison	Acupuncture parameters	Effect measurements	Biochemical measurements
Luo et al. (2014)	MCAO rats	MA	GV26	Non-MA	Thrust/lifted at 3 times per second, 1 min, 3 days after MCAO immediately	Zausinger' 6-point scale neural deficit scores↑; cerebral blood flow↑	Cortex and hippocampus: $BrdU^+$ cells↑, $nestin^+$ cells↑, $BrdU^+$ /$nestin^+$ cells↑, nestin mRNA↑; Cortex, hippocampus, and ST: GSK-3β↑, PP2A↓, GSK-3β/PP2A↑
Tao et al. (2010)	MCAO rats	EA	ST36, LI11	Non-EA	1/20 Hz, 20 min, 4/7/14/21 days from 24 h after MCAO	Neurological deficit scores↓	SVZ: $BrdU^+$ cells↑, $BrdU^+$ /$GFAP^+$ cells↑, $BrdU^+$ /$NeuN^+$ cells↑
Liao et al. (2017)	MCAO rats	EA	ST36, ST37	Non-EA	EA1: 2 Hz EA2: 15 Hz	mNSS↓; rotarod test: latency time↑; I/H ratio (EA1)↑	Penumbra area: $Ki67^+$ cells (EA1)↑, $GFAP^+$ cells (EA1)↑, $nestin^+$ cells↑; ischemic core area: $nestin^+$ cells↑
Tan et al. (2018)	MCAO rats	EA	GV14, GV20	Non-EA	5/20 Hz, 2-4 mA, 30 min	mNSS↓	CA1 region: viable neuron percentage↑; DG zone: $BrdU^+$ /$nestin^+$ cells↑, $BrdU^+$ /DCX^+ cells↑; brain: PRG5↑, RhoA↓, LPA↓, NogoA↓
Kim et al. (2014)	MCAO mice	EA	GV14, GV20	Non-EA	2 Hz, 20 min, 10 days from 5 d after MCAO	Rotarod test: latency time↑; MWM test: mean time to find platform↓	Ipsilateral and contralateral hemisphere: $BrdU^+$ cells↑; whole brain: $BrdU^+$ /DCX^+ cells↑, $BrdU^+$ /$NeuN^+$ cells↑; ipsilateral hippocampus, SVZ and cortex: $BrdU^+$ cells↑; ipsilateral hippocampus and SVZ: $BrdU^+$ /DCX^+ cells↑, $BrdU^+$ /$NeuN^+$ ↑, $BrdU^+$ /$GFAP^+$ cells↑; ipsilateral hemisphere: BDNF and VEGF mRNA↑; ipsilateral hippocampus: mBDNF↑; ipsilateral hippocampus and cortex: VEGF↑; ipsilateral hippocampus and SVZ: $mBDNF^+$ cells↑; hippocampus and ipsilateral SVZ: $VEGF^+$ cells↑; ipsilateral and contralateral hippocampus, SVZ and cortex: $pPI3K^+$ /$BrdU^+$ cells↑
		EA	GV14, GV20	Non-EA	2 Hz, 20 min, 12 days from 5 d after MCAO	Corner test: number of turns↓; cylinder test: held on cylinder wall with both paws↓; passive avoidance test: entry latency↑	ST: atrophic changes↑; ST and SVZ: $BrdU^+$ cells↑, $Ki67^+$ /$Sox2^+$ cells↑, $mBDNF^+$ /$NeuN^+$ cells↑, pTrkB↑, pCREB↑; ST, SVZ and hippocampus: $Ki67^+$ cells↑; ST, SVZ and hippocampus: mBDNF↑; hippocampus: NT4↑, $NT4^+$ /$NeuN^+$ cells↑
Kim et al. (2018)	MCAO mice	EA+mBMSC	GV14, GV20	mBMSC	2 Hz, 20 min, 12 days from 5 d after MCAO	Corner test: number of turns↓; cylinder test: held on cylinder wall with both paws↑; passive avoidance test: entry latency↑	ST and SVZ: $BrdU^+$ cells↑, $BrdU^+$ /DCX^+ cells↑, $Ki67^+$ /PSA-$NCAM^+$ cells↑, $NT4^+$ /$NeuN^+$ cells↑, pCREB↑, $pCREB^+$ /DCX^+ cells↑; ST, SVZ and hippocampus: $Ki67^+$ cells↑, $Ki67^+$ /$Sox2^+$ cells↑, mBDNF↑, NT4↑; hippocampus: $mBDNF^+$ /$NeuN^+$ cells↑

(*Continued*)

10.3389/fncel.2022.817732

TABLE 1 (Continued)

Study	Model/Objects	Intervention	Acupoints	Comparison	Acupuncture parameters	Effect measurements	Biochemical measurements
Chen et al. (2015)	MCAO-induced focal I/R injury rats	EA	ST36, LI11	Non-EA	1/20 Hz, 30 min, 3 days from 24 h after MCAO	Neurological deficits scores↓; infarct volume↓	Cortical peri-infarct area: $GFAP^+$ reactive astrocytes↑, $nestin^+$ cells↑, $nestin^+$ /$GFAP^+$ cells↑, Wnt1 and β-catenin↑, transcription of GSK3↓
Zhao et al. (2013)	MCAO rats	EA	GV20, GV26	Non-EA	4/20 Hz, 1-2 mA, 15 min, 3/7/14/21 days from 3 d after MCAO	Total mNSS↓, movement score of mNSS↓; MWM test: escape latency↓	DG zone: $BrdU^+$ /$GFAP^+$ cells↑, $BrdU^+$ /$NeuN^+$ cells↑, Notch1 and Hes1↑
Hong et al. (2013)	tMCAO rats	EA	ST36, LI11	Non-EA	5/20 Hz, 2-4 mA, 20 min, 4 weeks	Infarct volume↓; time spent walking, rearing and grooming↑; time spent feeding↓	Raldh1 and Raldh2 mRNA↑
		EA	TE5, ST36	Non-EA	20 Hz, 1 mA, 30 min, 7 days from 24 h after MCAO	mNSS↓; infarct volume↓	Ischemic cortical region: histological changes↓; SVZ and hippocampal: apoptotic cells↓, miR-223↑, PTEN mRNA↓, nestin mRNA↑, Notch1 protein and the NOTCH1 gene↑
Sha et al. (2019)	MCAO-induced focal I/R injury rats	EA+AntagomiR-223-3p	TE5, ST36	EA	20 Hz, 1 mA, 30 min, 7 days from 24 h after MCAO	mNSS↑	Ischemic cortical region: histological changes↑; SVZ and hippocampal: apoptotic cells↑, miR-223↓, PTEN mRNA↑, nestin mRNA↓
Zhang et al. (2020)	MCAO rats	EA	ST36, LI11	Non-EA	1/20 Hz, 1 mA, 30 min, 21 days	mNSS↓	Peri-ischemic ST: CD81 and TSG101↑, exosomal miR-146b↑, miR-146b↑; peri-ischemic ST and SVZ of the ischemic hemisphere: $NeuN^+$ /$Brdu^+$ cells↑; SVZ of the ischemic hemisphere: NeuroD1↑, $NeuroD1^+$ /DCX^+ cells↑
		EA+miR-146b inhibitors	ST36, LI11	EA	1/20 Hz, 1 mA, 30 min, 21 days	-	Peri-ischemic ST and SVZ of the ischemic hemisphere: $NeuN^+$ /$Brdu^+$ cells↓; SVZ of the ischemic hemisphere: NeuroD1↓, $NeuroD1^+$ /DCX^+ cells↓
Zhou et al. (2011)	MCAO rats	EA	ST36, PC6	Non-EA	4/20 Hz, 0.5 mA, 20 min, 1/7/14 days from 12 h after MCAO	Bederson neurologic deficits scores↓	ST and cortical peri-infarct area: $GAP\text{-}43^+$ cells↑
Xu et al. (2017)	Heat-coagulation MCAO rats	MA+RT	GV26, PC6	Non-MA+non-RT	GV26: thrust/lifted like sparrow pecking for 10 times, PC6: thrust/lifted and turned, 1 min. 7/14/21 days from 3 d after MCAO	Zea-Longa 5-point assessment: neurological deficits scores↓; balance beam test scores↓; rotarod test scores↓	Cortical peri-infarct area: $GAP\text{-}43^+$ cells↑
Qing et al. (2016)	MCAO rats	Group1: bilateral EA+RT, group2: unilateral EA+RT	ST36, GV20, LI11	Non-EA+non-RT	5/10 Hz, 2 mA, 30 min, 6 days/week, 2 weeks from 24 h after MCAO	Neurological deficits scores↓	Ischemic frontal cortex: the arrangement of nerve cells in slightly disordered, some nuclei were pyknotic, the damage of cells↓; hippocampal CA3 region: GAP-43↑, SYP↑

(*Continued*)

10.3389/fncel.2022.817732

TABLE 1 (Continued)

Study	Model/Objects	Intervention	Acupoints	Comparison	Acupuncture parameters	Effect measurements	Biochemical measurements
Chen S. Q. et al. (2020)	MCAO-induced transient cerebral I/R injury model	EA	GV20	Non-EA	2 Hz, 1 mA, 30 min, 7 days after reperfusion	Infarct size↓; Garcia JH neurological score↑	Ischemic penumbra cortex: OMgp↓, NogoA↓, NgR↓, NgR mRNA↓, ROCK2↓, MYPT1↓, MLC1↓, RhoA↓, ROCK mRNA↓, MLC mRNA↓, GAP43↑, BDNF↑, GAP43 mRNA↑, BDNF mRNA↑
		EA	GV20	Non-EA	2/10 Hz, 1-2mA, 30 min, 5 days from 24 h after MCAO	Infarct volumes↓; Garcia JH neurological score↑; time on rotarod↑; limb placement test scores↑; left/total body swing numbers↓; unsuccessful contralateral forelimb placing↓	Ischemic penumbra: miR-132↑, SOX2↓
Zhao et al. (2018)	MCAO-induced focal I/R injury rats	EA+miR-132 inhibitor	GV20	EA	2/10 Hz, 1-2 mA, 30 min, 5 days from 24 h after MCAO	Infarct volumes↑; Garcia JH neurological score↓; time on rotarod↓; limb placement test scores↓; left/total body swing numbers↑; unsuccessful contralateral forelimb placing↑	Ischemic penumbra: SOX2↑, miR-132↓
		EA	GV20	Non-EA	2/10 Hz, 1-2 mA, 30 min, 5 days/week, 4 weeks	mNSS↓; time on rotarod↑; grip strength test: newtons↑	Middle and left sides of the spinal cord gray matter (C3-5): BDA^+ CST axons amounts↑; injection ipsilateral site: fiber numbers↑; ischemic penumbra: NF-200↑, RhoA↓, GAP43 protein↑, pirb mRNA↓, PirB protein↓, $PirB^+$ neurons↓, miR-181b↑
Deng et al. (2016)	MCAO rats	EA+miR-181b inhibitor	GV20	EA	2/10 Hz, 1-2 mA, 30 min, 5 days/week, 4 weeks	mNSS↑; time on rotarod↓; grip strength test: newtons↓	Ischemic penumbra: pirb mRNA↓, PirB protein↓
Yi et al. (2006)	Heat-coagulation MCAO rats	EA1: 2 weeks after ischemia, EA2: 5 weeks after ischemia	GV14, GV20	Non-EA	EA1: 5/10 Hz, 30 min, 2 weeks EA2: 5/10 Hz, 30 min, 5 weeks	-	Ischemic cortex: Nv↓, Sv↑, Vv↓, the curvature of synaptic interface (EA2)↓, PSD (EA2)↑, synaptic cleft width↑; cortical periâĂŚinfarct area: COD of P38 (EA2)↑, COD of GAP-43↑, NGF^+ cells↑, $BDNF^+$ cells↑
Xia et al. (2017)	MCAO rats	MA	KI3, LR3	Non-EA	Perpendicularly needled 2–3 mm in depth, 30 min, 7 days/course, 2 courses	mNSS↓; MWM test: escape latency↓	Hippocampal regions: BDNF, SYN, PSD and synaptic curvatures↑, synapse cleft width↓
Xie et al. (2019)	MCAO-induced I/R injury rats	EA	GV20, GV24	Non-EA	1/20 Hz, 0.2 mA, 30 min, 14 days from 24 h after MCAO/R	Zea-Longa 5-point assessment: neurological deficits scores↓; step-down passive avoidance test: the step-down latency time↑	Hippocampal CA1 region: $PSD\text{-}95^+$ and SYN^+ cells↑, synapses numbers↑, fusion of synaptic space↓, loss of synaptic vesicles↓, incomplete synaptic structure↓, swelling of the presynaptic terminal↓, p-JAK2 and p-STAT3↓
Lin et al. (2016)	MCAO-induced I/R injury rats	EA	GV20, GV24	Non-EA	1-20 Hz, 30 min, 6 days from 24 h after reperfusion	Infarct volumes↓; MWM test: escape latency↓, swim distance↓, frequency of crossing the platform↑	Hippocampus: density of dendritic spines↑; hippocampus of the left brain: Cdc42, Rac1 and F-actin↑, RhoA protein↓

(*Continued*)

10.3389/fncel.2022.817732

TABLE 1 (Continued)

Study	Model/Objects	Intervention	Acupoints	Comparison	Acupuncture parameters	Effect measurements	Biochemical measurements
Liu et al. (2017)	MCAO-induced cognitive deficit model	EA	GV20, GV24	Non-EA	1-20 Hz, 0.2 mA, 30 min, 14 days from 24 h after MCAO	MWM test: escape latency↓, probe time↑, time spent in target quadrant↑	Left cortex, hippocampus, corpus ST, and thalamus: lesions volumes↓; hippocampal CA1: density of dendritic spines↑, number synapses↑, total LIMK1 level and p-LIMK1↑, miR-134 expression↓
Yang et al. (2017)	Stroke patients (n = 10)	MA	LI11, LI10, TB5, LI4, ST36, GB34, SP6, EX-UE9	Self-control	Thrust/lifted at 120 times per min, rotated at 180 degrees, 120 circle per min, conducted until *Deqi*	-	Left FDI: MEPs↓; right FDI: MEPs↑; the percentage of MEP amplitudes from TS at CS intensity 100%, 130% and 150%↑; inhibition from the right M1 (contralateral to acupuncture side) to the left M1 (ipsilateral to acupuncture side)↓
He et al. (2019)	Stroke patients (n = 18)	MA	LI11, TB5	Sham acupuncture	Thrust/lifted until *Deqi*	-	Contralateral hemisphere of the acupuncture sites: the cortex excitability (when 12–20min with the needle *in situ*)↓, the MEP amplitudes (when 8–10 min with the needle removed)↑; ipsilateral hemisphere of the acupuncture sites: the MEP amplitudes (when 4–10 min with the needle *in situ*)↑, the cortex excitability (when 1–5 min with the needle removed)↑; contralateral cortical of the acupuncture sites: MEP amplitudes induced by acupoint needling↓, MEP amplitudes after needle removal↑; ipsilateral cortical of the acupuncture sites: MEP amplitudes induced by acupoint needling↓, MEP amplitudes after needle removal↑
		MA+PAS	LI11, TB5	Self-control	Thrust/lifted until *Deqi*	-	Contralateral cortical of the acupuncture sites: MEP amplitudes after PAS intervention and needle removal↑, MEP amplitudes induced by needle *in situ*↓; ipsilateral cortical of the acupuncture sites: MEP amplitudes after PAS intervention with the needle *in situ* and removal↑
		MA+MP	LI11, TB5	Self-control	Thrust/lifted until *Deqi*	-	Contralateral cortical of the acupuncture sites: MEP amplitude after MP and pretreatment with acupuncture↓, MEP amplitudes after the combined treatment with acupuncture and MP↓, MEP amplitudes after needle removal↑, FDI muscle MEP amplitude after acupuncture and acupuncture + MP↑
Lin and Hsieh (2010)	MCAO rats	EA	GV20	Non-EA	2 Hz, 2 mA, 20 min, 10 min after MCAO	Neurological scores↓	Hippocampal CA1: LTP↑, NR1↓, TRPV1↓

(*Continued*)

10.3389/fncel.2022.817732

TABLE 1 (Continued)

Study	Model/Objects	Intervention	Acupoints	Comparison	Acupuncture parameters	Effect measurements	Biochemical measurements
Ye et al. (2017)	2VO-induced Vascular dementia rats	MA	Group1: ST36, GV20; Group2: GV20, GV24; Group3: ST36, SP10	-	Twirling reinforcing manipulation, 6 days a week, 2 weeks from 3 days after 2VO	MWM test: escape latency↑, swimming distance↑, time in the target quadrant↑ (group1 was superior over other groups)	-
		MA	ST36, GV20	Non-MA	Twirling reinforcing manipulation, 6 days a week, 2 weeks from 3 days after 2VO	-	Hippocampus: LTP at the PP-DG synapse↑, Dopamine, HVA and epinephrine↑; hippocampal DG region: D1R and D5R↑
		MA+D1/D5Rs Antagonists SCH23390	ST36, GV20	MA	Twirling reinforcing manipulation, 6 days a week, 2 weeks from 3 days after 2VO	MWM test: escape latency↓, swimming distance↓, time in the target quadrant↓	PP-DG synapse: LTP↓

Notes: ↑, upregulated by acupuncture; ↓, downregulated by acupuncture. Abbreviation: MCAO, middle cerebral artery occlusion; MA, manual acupuncture; GV26, Shuigou; GSK-3β, glycogen synthase kinase 3Îš; PP2A, Protein phosphatase 2A; EA, electroacupuncture; ST36, Zusanli; LI11, Quchi; GFAP, glial fibrillary acidic protein; SVZ, subventricular zone; ST37, Shangjuxu; mNSS, modified Neurological Severity Score; I/H ratio, ratio of the ischemic area to the ipsilateral hemisphere area; GV14, Dazhui; GV20, Baihui; DCX, doublecortin; DG, dentate gyrus; PRG5, plasticity-related gene 5; RhoA, Ras homolog family member A; LPA, Lysophosphatidic acid; NogoA, neurite outgrowth inhibitor protein A; BDNF, brain-derived neurotrophic factor; VEGF, vascular endothelial growth factor; mBDNF, mature BDNF; ST, striatum; pPI3K, phosphorylated phosphatidylinositol 3-kinase; pTrkB, phosphorylated tyrosine receptor kinase B; pCREB, phosphorylated cyclic adenylate monophosphate response element-binding protein; MSCs, mesenchymal stem cells; PSA-NCAM, polysialylated form of the neural cell adhesion molecule; NT4, Neurotrophin 4; I/R, ischemia/reperfusion; tMCAO, transient middle cerebral artery occlusion; Raldh1, retinaldehyde hydroxylase 1; Raldh2, retinaldehyde dehydrogenase 2; TE5, Waiguan; PC6, Neiguan; GAP-43, growth-associated protein 43; RT, rehabilitation training; SYP, synaptophysin; OMgp, oligodendrocyte-myelin glycoprotein; NgR, Nogo receptor; MYPT1, myosin phosphatase target subunit-1; BDA, biotionylated dextran amine; CST, corticospinal tract; PirB, Paired immunoglobulin-like receptor B; Nv, numerical density; Sv, surface density; Vv, volume density; COD, corneal optical density; P38, synaptophysin; KI3, Taixi; LR3, Taichong; SYN, synaptophysin; PSD, post-synaptic density; GV24, Shenting; Cdc42, cell division cycle 42; Rac1, Ras-related C3 botulinum toxin substrate 1; LIMK1, LIM domain kinase; MEPs, motor-evoked potentials; FDI, first dorsal interosseous; TS, testing stimulus; CS, conditioning stimulus; M1, primary motor cortex; PAS, paired-associative stimulation; MP, motor practice; LTP, long-term potentiation; NR1, N-methyl-d-aspartate receptor subtype 1; TRPV1, transient receptor potential vanilloid subtype 1; 2VO, permanent bilateral common carotid artery occlusion; SP10, Xuehai; PP, perforant pathway; HVA, homovanillic acid; D1R, dopamine D1 receptor; D5R, dopamine D5 receptor.

10.3389/fncel.2022.817732

pathways that promote the proliferation, migration, and differentiation of NSCs. Tan et al. (2018) found that stimulation at GV20 and *Dazhui* (GV14) by 5/20 Hz EA induced the proliferation and differentiation of endogenous NSCs in MCAO rats, together with upregulating the expression of plasticity-related gene 5 (PRG5, a key factor of neurogenesis) and downregulating the expression of three neurogenesis inhibitors, including the neurite outgrowth inhibitor NogoA, lysophosphatidic acid, and Ras homolog family member A (RhoA), indicating that EA may promote the proliferation and differentiation of endogenous NSCs by regulating PRG5/RhoA signaling. Stimulation with 2 Hz EA at the same acupoints led to the promotion of NSC proliferation and differentiation by brain-derived neurotrophic factor (BDNF), together with vascular endothelial growth factor (VEGF)-mediated angiogenesis of downstream phosphatidylinositol 3-kinase (PI3K) signaling. Specifically, EA increased both proliferation and differentiation in the hippocampus and SVZ and the mRNA and protein levels of BDNF and VEGF in the ipsilateral hippocampus and SVZ, as well as enhancing the levels of phosphorylated PI3K in the newly formed neuroblasts. In addition, the levels of various neurogenesis-related factors were up-regulated, including forkhead box protein G1 (FOXG1), nuclear receptor subfamily 4, group A, member 3 (NR4R3) protein, and zinc finger protein 423 (ZNF423; Wang et al., 2012; Kim et al., 2014). Kim et al. (2018) transplanted bone marrow mesenchymal stem cells (MSCs) into the striata of MCAO mice and stimulated them with 2 Hz EA at GV20 and GV14. The treatment reduced the atrophy of the striatum and promoted the proliferation of NPCs in the SVZ and peristriatal area. Increased numbers of BDNF and neurotrophin-4 (NT-4)-positive neurons were detected in the peristriatal area and the hippocampus. These results indicated that the combined treatment of MSCs and EA could promote neurogenesis in the ischemic brain by upregulating the expression of neurotrophic factors such as BDNF and NT-4, thus improving the motor function of MCAO mice (Kim et al., 2018). Another study in MCAO rats showed that after 1/20 Hz EA at ST36 and LI11 in the affected limb, the number of nestin/GFAP-positive cells was increased in the cortex, as well as the gene and protein levels of Wnt1 and β-catenin, while the transcription of glycogen synthase kinase 3 (GSK3) was inhibited, which suggested that EA may promote the proliferation of nerve stem/progenitor cells in the area around the cortical infarction after stroke through the Wnt/β-catenin pathway, thereby reducing the infarct volume and improving the neurological impairment (Chen et al., 2015). It was also observed that EA significantly enhanced the activity of the neurogenic locus notch homolog protein 1 (Notch1) signaling pathway and its downstream transcription target Hes1, leading to increased NSC proliferation and differentiation (Zhao et al., 2015). Studies have shown that Retinoic Acid (RA) is a key factor in regulating the proliferation of adult hippocampal nerve stem/progenitor cells (Mishra et al., 2018). Hong et al. (2013) found that 5/20 Hz EA at ST36 and LI11 may reduce the infarct volume and promote the recovery of neurological function by regulating the RA pathway in the ischemic brain.

MicroRNAs (miRNAs, miRs) are involved in the post-transcriptional modification of gene expression. In cerebral ischemia/reperfusion injury, acupuncture can promote the regeneration and repair of damaged nerves by regulating miRNAs. Sha et al. found that in rats with cerebral ischemia/reperfusion injury, stimulation with 20 Hz EA at *Waiguan* (TE5) and ST36 on the affected limb increased the expression of miR-223 and reduced the expression of phosphatase and tensin homolog deleted on chromosome ten (PTEN) in the SVZ and hippocampus by activating the Notch1 signaling pathway, thereby increasing the numbers of NSCs (Sha et al., 2019). Another study, *in vivo* and *in vitro*, revealed that EA regulated endogenous neurogenesis through the action of exosomal miRNAs. Specifically, 1/20 Hz EA at ST36 and LI11 on the affected limb induced the differentiation of endogenous NSCs into neurons in the ischemic striatum and SVZ by promoting the release of exosomes containing miR-146b in the ischemic striatum, thereby improving neurological impairment in MCAO rats (Zhang et al., 2020).

Therefore, acupuncture can indeed activate endogenous neurogenesis by stimulating proliferation and differentiation of NSCs in the SVZ and SGZ through activation of related cell-signaling pathways and upregulation of neurogenesis-related factors. It is also worth exploring which acupoints and stimulation parameters are optimal for the induction of neurogenesis. Furthermore, the number of endogenous NSCs is limited and not adequate to generate a sufficient number of differentiated functional neurons, and resolving this obstacle needs further innovative research.

Acupuncture promotes axonal regeneration and sprouting

Ischemic stroke is characterized acutely by a massive and rapid loss of axons, and recovery depends on axonal regeneration and sprouting, which constitute the compensatory mechanism to establish the new functional connections and strengthen the communication between neurons (Hinman, 2014). Axonal regeneration involves the regrowth of injured axons that is initiated by the formation of the growth cone at the broken ends, while axonal sprouting is the process of collateral sprouting and elongation of uninjured axons (Darian-Smith, 2009). Therefore, promoting axonal regeneration and the development of sprouting in the right direction contributes to the recovery of ischemic stroke patients.

Growth-associated protein-43 (GAP-43) is a growth cone-associated protein that promotes neurite outgrowth by regulating cytoskeletal organization *via* protein kinase C

signaling. The expression of GAP-43 decreases with nerve development, but when the brain is damaged, the neurons adjacent to the injured area compensate for the loss of cells by collateral sprouting and reactive axon regeneration. Under these conditions, the local expression of GAP-43 is again upregulated. Therefore, GAP-43 is considered to represent a molecular marker of axonal growth and plasticity (Felling and Song, 2015). It has been documented that EA at ST36 and *Neiguan* (PC6), performed daily for 20 min, can improve the neurological function in rats with cerebral infarction. The mechanism may be related to the statistically significant upregulation of GAP-43 in the ischemic region, from the 7th day after the injury (Zhou et al., 2011). A similar effect was also obtained by applying acupuncture on both sides of PC6 and GV26 for 7 days (Xu et al., 2017). A study performed in rats showed that bilateral EA at LI11 and ST36 (5 Hz/10 Hz, 2 mA) improved the neurobehavioral score after ischemic stroke more than a unilateral EA, and the expression level of GAP-43 was increased in the CA3 of the hippocampus by EA (Qing et al., 2016). These findings may be explained by the structural organization of the innervation of the limbs. The cerebral cortex innervates the activity of bilateral limbs because 80% of the nerve fibers from the anterior central gyrus innervate the movement of the contralateral limbs, and a small fraction of them, which are not crossed, descend directly to form the anterior corticospinal tract and innervate the movement of the ipsilateral limbs. The secondary fibers of some posterior root fibers are combined with the ascending fibers of the ipsilateral spinothalamic tract, and the bilateral projection effect of the upper and lower fibers of the brain stem network determine the effect of acupuncture signals on the bilateral cerebral cortex. Thus, the cerebral cortex acts as the master center that dominates the movement and sensation of the bilateral limbs (Qing et al., 2016). In addition, another study revealed that 2 Hz EA stimulation of GV20 can not only promote nerve regeneration by upregulating GAP-43 and BDNF after cerebral ischemia but can also reduce inhibition of axon regeneration by downregulation of myelin-associated inhibitors and the RhoA/Rho-associated coiled-coil-containing protein kinase (ROCK) signaling pathway after cerebral ischemia, thus reducing the size of the cerebral infarction and improving neuronal function and hippocampal ultrastructural damage (Chen S. Q. et al., 2020).

MiRNAs are also involved in acupuncture-promoted axonal regeneration. Zhao et al. (2018) have shown that the expression of miR-132 was downregulated after MCAO, and that EA inhibited the transcription of SRY-box transcription factor 2 (SOX2) by upregulating miR-132. These changes resulted in the promotion of axonal sprouting and alleviation of neurological deficits, suggesting that neurobehavioral functional recovery after ischemic injury depends on axonal sprouting enabled by the inhibition of SOX2 translation *via* miR-132 (Zhao et al., 2018). Moreover, it was found that within 28 days after reperfusion in MCAO rats, after 2/10 Hz EA stimulation of GV20, the expressions of paired immunoglobulin-like receptor B (PirB), RhoA, and GAP-43 were regulated by modulating miR-181b directly targeting Pirb mRNA in the penumbra, promoting axon regeneration and new projections of corticospinal tracts after oxygen-glucose deprivation injury, which improved the neurological deficits (Deng et al., 2016).

Acupuncture modulates synaptic plasticity

Synapse is not only the specific site of intercellular information transmission but also a sensitive site of neuroplasticity. Synaptic plasticity mostly refers to morphological and functional modifications of synaptic connections, including long-term changes in synaptic structure and number, as well as the short-term changes in the strength and efficiency of neurotransmission (Neves et al., 2008).

Plasticity of synaptic structure

The plasticity of the synapsis depends on the modification of its ultrastructure, which includes the following aspects: (1) contact area (total number of synapses, number density of synapses, area density of synapses, average area of single synapse; Mundy et al., 2008); (2) content of active substances, such as synaptophysin (SYN), in synaptic contact area (Kwon and Chapman, 2011); (3) synapse-related subcellular structure, such as the postsynaptic density (PSD)-95 (Xie et al., 2019); and (4) synaptic gap width and interface curvature (Xiao et al., 2018).

Acupuncture has been demonstrated to modify the synaptic structure and promote the synaptic plasticity in rodent models of stroke by upregulating SYN and increasing PSD (Xia et al., 2017; Xiao et al., 2018). After 5 weeks of EA with a 5/10 Hz wave at GV20 and GV14, the thickness of synaptic PSD, and the number and surface densities of synapses were increased in MCAO rats, without significant changes in other indices of synaptic ultrastructure, such as volume density and synaptic curvature. These modifications were accompanied by the upregulation of P38, GAP-43, nerve growth factor (NGF), and BDNF in the ischemic cerebral cortex, indicating that EA could protect synaptic ultrastructure by increasing the level of these proteins (Yi et al., 2006). However, another study found that after 2 weeks of acupuncture in *Taixi* (KI3) and LR3, motor and cognitive deficits were noticeably improved compared with the untreated group at the 7th and 14th day after ischemic stroke. The improvement was accompanied by an increase in BDNF, SYN, PSD, and synaptic curvatures, and a smaller width of the synapse cleft. These results suggested the possibility that the inconsistency in the modifications of the

synaptic structure might be caused by differences in acupoints, parameters, target brain areas, and observation points (Xia et al., 2017). Xie et al. (2019) demonstrated that the MCAO injury reduced the number of PSD-95/SYN double-positive cells in the hippocampal CA1 area, and 14 days of EA stimulation of GV20 and GV24 points reversed this trend, thus affecting synaptic plasticity. Activation of the Janus-activated kinase 2 (JAK2)/signal transducer and activator of transcription 3 (STAT3) signaling has been proved to induce spatial learning and memory impairment by inhibiting synaptic plasticity in the hippocampal CA1 region. EA treatment decreased the levels of phosphorylation of JAK2 and STAT3 in the CA1, indicating that the intervention at GV20 and GV24 improved synaptic plasticity by inhibiting the JAK2/STAT3 signaling pathway (Xie et al., 2019). In addition, after 1/20 Hz EA at the same acupoints, it was found that the density of dendritic spines was increased and the cognitive function of MCAO rats was improved. It was suggested that the mechanism may be related to the upregulation of Cdc42, RAS-related C3 botulinus toxin substrate 1 (Rac1), and Filamentous actin (F-actin) in the hippocampus, as well as down-regulation of RhoA expression (Lin et al., 2016).

Plasticity of synaptic function

It has been proposed that the plasticity of synaptic function is dependent on its structural plasticity. Functional plasticity is mostly related to the strength of synaptic transmission efficiency in the form of long-term potentiation (LTP) and long-term depression (LTD), which are prevalent paradigms of micro-neuroplasticity (Matsuzaki et al., 2004). LTP facilitates synaptic transmission, amplifies presynaptic signals, and enhances the persistence of postsynaptic potentials, thereby appearing more relevant to synaptic remodeling than LTD (Kim E. et al., 2012; Stewart and Dringenberg, 2016). Cognitive impairment often occurs after ischemic stroke and leads to difficulties in memory, learning, analysis, organization, interpretation, and concentration, decreasing the quality of life (Liu F. et al., 2014), which is the main cause of persistent sequelae of ischemic stroke. In these processes, LTP can enhance long-term memory through acquisition, consolidation, and storage of information, while LTD can verify the memory content and regulate LTP (Neves et al., 2008; Xiao et al., 2018).

Dendritic spines contribute to the spread of information *via* deformation and control synaptic efficacy by modulating LTP and LTD that are related to learning and memory (Schacher and Hu, 2014; Park et al., 2015). It has been reported that LIM domain kinase 1 (LIMK1) regulates LTP and long-term memory by activating cyclic adenylate monophosphate response element-binding protein (CREB), and LIMK1 knockout mice suffer from the severe damage of dendritic spines and LTP in the hippocampus. MiRNAs, which play important roles in learning and memory formation, can regulate LIMK1 expression to induce synaptic-dendritic plasticity. Therefore, the modulation of miRNA-LIMK1 represents a potential target for the treatment of cognitive deficit. Liu et al. (2017) demonstrated by T2-weighted imaging that EA at GV20 and GV24 alleviated cognitive impairment and reduced the volume of multiple brain lesions. Importantly, synaptic-dendritic loss in hippocampal CA1 pyramidal cells could be rescued by EA. This effect was associated with the suppression of the increase in the expression of miR-134 and LIMK1, indicating that these molecules might mediate the induction of hippocampal synaptic plasticity by EA, which contributed to the improvement of learning and memory during the recovery from ischemic stroke (Liu et al., 2017). In addition, acupuncture could lead to lasting changes in cortical excitability by affecting the activity of neurosynapses (Yang et al., 2017). For instance, a study in which 18 healthy subjects were subjected to acupuncture at the LI11 and TB5 acupoints showed an increased muscle excitability that lasted for 20 min after the needle was pulled out, proving the existence of a time-dependent effect of acupuncture on the excitability of bilateral primary motor cortex, which can induce LTP-like plasticity and increase motor learning (He et al., 2019).

Numerous studies have demonstrated that acupuncture enhances LTP in rats subjected to MCAO. For example, EA at GV20 for 6 days can reverse the MCAO-induced impairment of memory and decrease in hippocampal LTP, and inhibit the overexpression of N-methyl-d-aspartate receptor subtype 1 (NR1) and transient receptor potential vanilloid subtype 1 (TRPV1) receptors in the CA1 area of the hippocampus, indicating that NR1 and TRPV1 may mediate the effect of EA on MCAO-induced behavioral defects and LTP damage (Lin and Hsieh, 2010). Ye et al. (2017) have documented that acupuncture at GV20 and ST36 restored cognitive dysfunction in the rat two-vessel occlusion (2VO) model. The primary mechanism underlying this acupuncture effect was the improvement of decreased LTP by promoting the release of dopamine and its main metabolites and reversing the decline in dopamine D1/D5 receptors (Ye et al., 2017).

This section summarized the evidence that acupuncture regulates structural plasticity after stroke, that is, acupuncture can stimulate neurogenesis, axonal regeneration and sprouting, improve the structure and function of the synapse, to provide a theoretical basis for the improvement of the neurological deficits of ischemic stroke by acupuncture.

Glial cells play a key role in the regulation of neuroplasticity by acupuncture

Glial cells, including astrocytes, oligodendrocytes, and microglia, play a key role in acupuncture's regulation of

neuroplasticity. By interacting with neurons, they regulate the formation and remodeling of synapses and neural circuits, thus contributing to the reconstruction of the functional brain (Stogsdill and Eroglu, 2017). Acupuncture can regulate neuroplasticity through glial cells, and the evidence is shown in **Table 2**.

Glial cells regulate neuroplasticity by secreting NTFs

It is well documented that NTFs are required for neurogenesis, axonal regeneration, synaptic activity and plasticity, and other neuroplasticity processes in CNS diseases, and can improve neurological deficits. NGF, BDNF, neurotrophin-3, and NT-4 are four members of the mammalian neurotrophin family (Gibon and Barker, 2017).

BDNF

The role of BDNF in neuroplasticity makes it an excellent candidate for stroke treatment (Mang et al., 2013). Additionally, BDNF acts on NSCs, promoting their survival, proliferation, and differentiation by interacting with TrkB and initiating downstream pathways, such as mitogen-activated protein kinase (MAPK)/extracellular signal-regulated kinase (ERK) and PI3K/Akt cascades. MAPK/ERK and PI3K/Akt signaling can reduce neuronal death induced by excitotoxicity in the ischemic penumbra (Tejeda et al., 2019). BDNF can also increase the formation of dendrite branches and connections between dendrites and promote the development and maturation of the CNS (Song et al., 2017). BDNF is directly involved in angiotensin-1 receptor blocker-mediated functional recovery, angiogenesis, and synaptic formation (Fouda et al., 2017). Finally, BDNF can provide local anti-inflammatory effect by downregulating the expression of tumor necrosis factor alpha (TNF-α) and upregulating the expression of interleukin-10 (IL-10), to promote nerve repair. BDNF increases the number of activated and phagocytic microglia *via* the increase in intracellular Ca^{2+}. Once activated, microglia can further secrete BDNF and other NTFs, generating a positive feedback loop (Jiang et al., 2010).

In animal models of MCAO, acupuncture utilizing different parameters, such as acupoints, frequency, and intervention time, produces distinct effects on BDNF in the brain. The EA treatment at the GV20 and *Qubin* (GB7) acupoints for 14 days after MCAO, utilizing a bipolar waveform current of 3 Hz applied for bursts of 5 s and 2 s intervals, increased the levels of BDNF in the ischemic lobe and improved functional and motor recovery (Kim M. W. et al., 2012). Similarly, EA at GV20 and GV14 for two times with 5 Hz/10 Hz enhanced the expression of BDNF in the ischemic area (Cheng et al., 2014; Chavez et al., 2017). In MCAO mice, the expression of BDNF mRNA in the hippocampus was upregulated by EA applied for seven consecutive days at the *Shenshu* (BL23), *Geshu* (BL17), and GV20 acupoints (Zhao et al., 2013). Furthermore, EA at the GV20 once a day for 2 weeks improved motor function, elevated BDNF in the ischemic hemisphere, and increased the number of BDNF-positive cells and the expression of TrkB (Kim M. W. et al., 2012). Thus, acupuncture may play a neuroprotective role in ischemic stroke by modulating the expression of BDNF, but the functional verification of this possibility remains to be obtained.

NGF

NGF is the first NTF identified by Rita Levi-Montalcini and Viktor Hamburger in mouse sarcoma *in vitro* in the 1950s. Subsequent studies have established that NGF binds to the tropomyosin-related kinase A (TrkA) and p75NTR receptors to activate downstream signaling cascades, such as MAPK/ERK and PI3K/Akt. The stimulation of these pathways modulates the transcription of neurite outgrowth inhibition protein A, Nogo receptor, Rho family small GTPases A, Rho-associated kinase 2, thus promoting the differentiation and survival of neurons and growth of axon growths (Chang et al., 2016; Keefe et al., 2017). Furthermore, NGF exhibits neuroprotective activity by reducing intracellular calcium overload and antagonizing the excitotoxicity of amino acids after cerebral ischemia (Keefe et al., 2017).

Yi et al. (2006) demonstrated that EA at the GV20 and GV14 points increased the expression of NGF after ischemic brain injury. A higher level of NGF was essential to protect neurons by promoting synaptic plasticity and axonal regeneration, reflected by the increase of numerical density, surface density, volume density, and gap width of cortical synapses, as well as PSD and GAP-43 expression in the ischemic area. The results also documented an increase in expression of NGF from 2 to 5 weeks after EA intervention, indicating that acupuncture can not only increase NGF but also maintain its expression at a high level for a prolonged time, achieving a long-lasting protective effect (Yi et al., 2006).

Other NTFs, such as glial cell line-derived neurotrophic factor (GDNF; Manni et al., 2011), VEGF, insulin-like growth factor (IGF; Liu S. J. et al., 2014), stromal cell-derived factor-1a, and ciliary neurotrophic factor (Kim et al., 2013), have also been demonstrated to mediate the regulatory effects of acupuncture on neuroplasticity. Therefore, the ability of acupuncture to enhance neuroplasticity and improve neural function defects appears to be dependent on the NTFs family of growth factors (Manni et al., 2010; Xiao et al., 2018). In addition to the secretion of neurotrophic factors, other mechanisms by which astrocytes and microglia influence neuroplasticity are also worthy of attention.

TABLE 2 The mechanisms of glial cells in the regulation of neuroplasticity by acupuncture in the treatment of ischemic stroke.

Study	Model/Objects	Intervention	Acupoints	Comparison	Acupuncture parameters	Effect measurements	Biochemical measurements
Kim E. et al. (2012)	MCAO rats	EA	GV20, GB7	Non-EA	3 Hz, 5 min, 2/7/14 days	Garcia scale scores↑	BDNF↑
Cheng et al. (2014)	MCAO rats	EA	GV20, GV14	Non-EA	5 Hz, 2.7–3.0 mA, 25 min, 6 days from 24 h after reperfusion	Cerebral infarct area↓; neurological deficit scores↓	Penumbra area: $GFAP^+$ cells↓, $S100B^+$ cells↓, NF-κB $(p50)^+$ cells↓, TNF-α^+ cells↓, $iNOS^+$ cells↓, nuclear NF-κB (p50)↓, GFAP/S100B immunoreactivity↓, S100B/nitrotyrosine immunoreactivity↓, $TUNEL^+$ cells↓, cytosolic GFAP↓, p-p38 MAPK↓, cytosolic TRADD↓, FADD↓, cleaved caspase-8↓, cleaved caspase-3↓
Zhao et al. (2013)	MCAO rats	EA	BL23, BL17, GV20	Non-EA	1/7 days	-	Hippocampus: BDNF mRNA↑
Yi et al. (2006)	MCAO rats	EA1: 2 weeks after ischemia, EA2: 5 weeks after ischemia	GV14, GV20	Non-EA	5-10 Hz, 30 min, 2/5 weeks from MCAO immediately	-	Synaptic numerical density (EA2)↑, synaptic surface density↑, PSD(EA2)↑, synaptic cleft width↑, P38(EA2)↑, NGF↑, BDNF↑
Tao et al. (2016)	MCAO rats	EA	LI11, ST36	Non-EA	1/20 Hz, 30 min, 3 days from 24 h after MCAO	Neurological deficit scores↓; cerebral infarct volumes↓; average speed of catwalk↑; mean duration on the rotarod↓	Peri-infarct cortex and ST: $GFAP^+$ /$Vimentin^+$ cells↑, $GFAP^+$ /$Nestin^+$ cells↑, $GFAP^+$ /$BrdU^+$ cells↑, Cyclin D1↑, CDK4↑, p-Rb↑, BDNF↑
Huang et al. (2017)	MCAO rats	EA	GV20, GV24	Non-EA	2/20 Hz, 0.2 mA, 30 min, 7 days from the 12 h after MCAO	Neurological deficit scores↓; mNSS↓; escape latency↓; swimming speed↓; target crossing↑; cerebral infarct volumes↓	Peri-infarct hippocampal CA1 and sensorimotor cortex: $ED1^+$ cells↓, $GFAP^+$ cells↓, IL-1β↓, IL-10↑, $P2X7R^+$ /$ED1^+$ cells↓, $P2X7^+$ /$GFAP^+$ cells↓, $P2Y1R^+$ /$ED1^+$ cells↓, $P2Y1R^+$ /$GFAP^+$ cells↓

Notes: ↑, upregulated by acupuncture; ↓, downregulated by acupuncture. Abbreviation: GB20, Fengchi; GB39, Xuanzhong; LI11, Quchi; LI4, Hegu; ST36, Zusanli; SP6, Sanyinjiao; GV20, Baihui; FMA, Fugl-Meyer Assessment; GV24, Shenting; MICD, middle cerebral artery occlusion induced cognitive deficit; MWM test, Morris water maze test; GB33, Xiyangguan; ReHo, regional homogeneity; BA, Brodmann Area; NDS, nervous functional deficiency scale; MBI, modified Barthel index; MCAO, middle cerebral artery occlusion; CPu, Caudate putamen; MCTX, motor cortex; SCTX, somatosensory cortex; FC, functional connectivity; LPs, superior parietal lobule; SMA, Supplementary Motor Area; TE5, Waiguan; GB7, Qubin; M1, Primary motor area; PMC, premotor cortex; RSC, retrosplenial cortex; GMV, Grey Matter Volume; ISSA, International Standard Scalp Acupuncture; PG, parahippocampal gyrus.

10.3389/fncel.2022.817732

TABLE 3 The mechanisms of acupuncture on regulating functional reorganization in the treatment of ischemic stroke.

Study	Model/Objects	Intervention	Acupoints	Comparison	Acupuncture parameters	Effect measurements	Biochemical measurements
Li et al. (2015)	Stroke patients with unimanual motor deficits (n = 14)	Acupuncture + conventional treatment	GB20, GB39, LI11, LI4, ST36, SP6, (bilateral), GV20	Conventional treatment	30 min, 5 days, 4 weeks	FMA↑	Diffusion indices values were changed in the corpus callosum and bilateral corticospinal tracts, the inferior longitudinal fasciculus, the inferior frontooccipital fasciculus, the superior longitudinal fasciculus, the forceps minor, the cingulum gyrus, and the thalamic radiation.
Wen et al. (2018)	MICD rats	EA	GV20, GV24	Non-EA	1/20 Hz, 6 V, 2 mA, 30 min, 14 days from 24 h from MICD	MWM test: the time to find the platform↓, the number of times the platform crossed↑	The activation of hippocampus, retrosplenial cortex, cingulate gyrus, prelimbic cortex, and sensory cortex↑
Wu P. et al. (2017)	Ischemic stroke patients (n = 21)	Acupuncture + conventional treatment	GV20, GB20, LI11, LI4, ST36, GB33, GB39, SP6	Conventional treatment	30 min, 5 days, 4 weeks	NDS↓, FMA↑, MBI↑	ReHo in the frontal lobe (BA6, BA46), supra-marginal gyrus (BA40), middle temporal gyrus (BA21), cerebellum, and insula↑
Wu et al. (2018)	MCAO rats	EA	LI11, ST36	Non-EA	2/20 Hz, 30 min, 7 days from 24 h after reperfusion	Neurological deficits↓; the infarct volumes↓; catwalk gait and rotarod test: the motor function↑	The neural activity of CPu, MCTX, SCTX regions↑
Liang et al. (2017)	MCAO rats	EA	ST36, LI11	Non-EA	1/20 Hz, 6 V, 2 mA, 30 min, 7 days from 24 h after MCAO	Neurologic deficits↓; the cerebral infarctions↓	The neural activity of motor cortex, dorsal thalamus, and ST↑
Li et al. (2021)	MCAO rats	EA	ST36, LI11	Non-EA	2/20 Hz, 30 min, 14 days from 24 h after MCAO	Infarct volumes↓; mNSS↑; motor functional performances↑	The FC between the left motor cortex and the motor function-related brain regions, including the motor cortex, sensory cortex and ST↑
Chen S. et al. (2020)	Patients with ischemic stroke in the left hemiplegia (n = 10)	MA	ST36, LI11	Self-control	Twisting for ± 180°, 60 circles per min, 15 min	-	ReHo values at the right precentral gyrus and superior frontal gyrus↑, ReHo values at right LPs, left fusiform gyrus and left SMA↓
Chen J. et al. (2014)	Patients with ischemic stroke in the left basal ganglia (n = 24)	Acupuncture	TE5	Sham acupuncture, non-acupoint acupuncture	Twisted for ± 180°, 60 circles, 6 min and 30 s	-	The sensorimotor network of the ipsilesional hemisphere is regulated, the contralesional sensorimotor network is stimulated, the cooperation of bilateral sensorimotor networks is increased, and the synchronization between the cerebellum and cerebrum is changed.
Huang et al. (2013)	Patients with ischemic stroke in the left hemisphere (n = 10)	MA	Right TE5	Tactile stimulation	30-s twist and 30-s rest, six times, 60 circles per min	-	The activation of the postcentral gyrus (BA2, BA3), precentral gyrus (BA4, BA6), medial frontal gyrus (BA6)↑, the postcentral (BA3), precentral gyrus (BA6)↓

(*Continued*)

10.3389/fncel.2022.817732

TABLE 3 (Continued)

Study	Model/Objects	Intervention	Acupoints	Comparison	Acupuncture parameters	Effect measurements	Biochemical measurements
Huang et al. (2012)	Patients with ischemic stroke in the left internal capsule ($n = 43$)	MA	Right TE5	Sham needling, Non-needling	Twirling the needling 180°, 60 times, 3 min	-	The activation of BA30↑ (Compared with the non-needling group), BA13, 19, and 47↑ (Compared with sham needling at TE5), BA9↓ (Compared with needling at the sham point)
Fang et al. (2012)	Patients with ischemic stroke in the right basal ganglion region ($n = 6$)	EA	GV20, right GB7	Self-control	2 Hz, 20 min	-	First EA treatment: the activation of M1, PMC, LPs bilaterally, SMA↑ on the unaffected right hemisphere 3 weeks of EA treatments: Bilateral M1 and LPs significantly↑, insula, putamen, and cerebellum↑
Zhang et al. (2021)	MICD rats	EA	GV20, GV24	Non-EA	1/20 Hz, 6 V, 0.2 mA, 30 min, 14 days from 24 h after MICD	MWM test: escape latency times↓, the number of times the platform crossed↑	FC between the RSC and hippocampus, cingulate gyrus and midbrain↑
Wu et al. (2018)	Ischemic stroke patients	Acupuncture + conventional treatment	GV20, GB20, LI11, LI4, GB33, ST36, SP6, GB39	Conventional treatment	30 min, 5 days/week, 4 weeks	MBI scores↑	The GMV of left frontal lobe, precentral gyrus, superior parietal gyrus, anterior cingulate cortex, middle temporal gyrus↑, the right frontal gyrus, inferior parietal gyrus, middle cingulate cortex ↓
Chen et al. (2013)	Patients with ischemic stroke in the left hemisphere ($n = 10$) and six healthy controls ($n = 6$)	EA	Right TE5	Self-control	Twirling the needle ± 180°, 60 times, 6 min	-	The activation of left BA5, 6, 7, 18, 19, 24, 32, hypothalamus, the ventral posterolateral nucleus, the right BA4, 6, 7, 18, 19, 32↑, left BA13, the hypothalamus, posterior lobe of the tonsil of cerebellum, the culmen of the anterior lobe of hypophysis, right BA13↓; the deactivation of the left BA6, 11, 20, 22, 37, 47, the culmen of the anterior lobe of hypophysis, alae lingulae cerebella, the posterior lobe of the tonsil of cerebellum, right BA8, 37, 45, 47, the culmen of the anterior lobe of hypophysis, nodule of the anterior lobe of hypophysis, inferior border of the lentiform nucleus, lateral globus pallidus, the parahippocampal gyrus↑, BA7↓
Liu et al. (2020)	Patients with acute infarction in the middle cerebral artery supply area in the dominant hemisphere ($n = 30$)	MA + conventional treatment	ISSA, needling at the parietal midline (MS5) and left anterior/posterior parietal-temporal oblique lines (MS6 and MS7)	Conventional treatment	Twisting at 200 turns, 30 min, two times a day, six days	NIHSS scores↑; motor function scores↑	Centered to the seed region of the left SMA, FC at the left middle cerebellar peduncle, left cerebellum posterior lobe (uvula and declive), vermis, fusiform gyrus, lingual gyrus, inferior occipital gyrus, calcarine, cuneus, precuneus, BA7, BA18, and BA19, etc↑; Centered to the seed region of the left PG, FC at the left precuneus, inside-paracingulate, inferior parietal gyrus, paracentral lobule, BA5, BA6, BA7, and BA40, right median cingulate, precuneus, BA19, BA23, and BA31, etc↑.

Notes: ↑, upregulated by acupuncture; ↓, downregulated by acupuncture. Abbreviation: MCAO, middle cerebral artery occlusion; EA, electroacupuncture; GV20, Baihui; GB7, Qubin; BDNF, brain-derived neurotrophic factor; GV14, Dazhui; GFAP, glial fibrillary acidic protein; NF-κB, Nuclear Factor kappa B; TNF-α, Tumour Necrosis Factor alpha; iNOS, Inducible nitric oxide synthase; MAPK, mitogen-activated protein kinases; TRADD, TNFR1-associated death domain protein; FADD, Fas-associated protein with death domain; BL23, Shenshu; BL17, Geshu; PSD, post-synaptic density; NGF, Nerve growth factor; LI11, Quchi; ST36, Zusanli; BrdU, 5-bromo-2'-dexoyuridine; CDK4, cyclin-dependent kinase 4; p-Rb, phosphorylated retinoblastoma protein; IL-1β, interleukin-1beta; IL-10, interleukin-10; P2X7R, P2X7 receptor; P2Y1R, P2Y1 receptor.

10.3389/fncel.2022.817732

Mechanisms of astrocyte regulation of neuroplasticity

Astrocytes have an important effect on neuroplasticity. In addition to secreting NTFs, astrocytes can also secrete or express specific mediators that regulate the number, morphology, and function of synapses, such as Maverick (a member of TGF-β superfamily), Hevin/Sparcl1, and thrombospondin. Cholesterol synthesized by astrocytes can significantly enhance the transmission efficiency of synapses, which is also promoted by glutamic acid and homocysteine released by astrocytes. D-serine plays an essential role in the induction of LTP without apparent effects on normal synaptic transmission (Allen and Eroglu, 2017). On the other hand, reactive astrocytes subsets residing within hundreds of microns from the infarcted area are involved in the formation of glial scar separating the infarct from the surrounding intact brain tissue. However, the overgrowth of astrocytes is detrimental because the upregulation of extracellular matrix proteins and other inhibitors of cell growth can prevent the effective regeneration of axons (Silver and Miller, 2004). For example, the deposition of chondroitin sulfate proteoglycans released by astrocytes *via* RhoA/ROCK-mediated pathways restricts neuroplasticity in the proximity of the glial scar, permitting the reconstruction of the neural circuit only distal sites (Carmichael et al., 2005; Sims and Yew, 2017).

The number of cells double-positive for GFAP/BrdU, GFAP/vimentin (expressed in radial neuroglia cells and neural and glial precursors), and GFAP/nestin in the cortex and striatum of MCAO rats was further increased 3 days after the EA of LI11 and ST36, indicating that EA can promote the proliferation of astrocytes in the cortex and striatum. At the same time, increased expression of cyclins, including cyclin Dl, cyclin-dependent kinase 4 (CDK4), and phospho-Rb, in the cortex and striatum regulates the activation of the G1-to-S transition, suggesting reactive astrocyte proliferation. In addition, EA enhanced the local expression of BDNF in the cortex and striatum. Together, these results indicated that EA plays a neuroprotective role by stimulating the proliferation of GFAP/vimentin/nestin-positive reactive astrocytes, which, in turn, secrete BDNF (Tao et al., 2016). It may be reflected in improving the structural characteristics of the synaptic interface, including numerical density, surface density, volume density, and gap width of the cortical synapse, enhancing the transmission function of the synapse, and modifying its structure and function, thus stimulating the regeneration of nerves and repair of the injury (Allen and Eroglu, 2017). At a later stage, acupuncture can increase the formation of new neurons and inhibit the excessive proliferation and differentiation of astrocytes, preventing the inhibition of axon regeneration by the excess of harmful substances (Jiang et al., 2016). It has been demonstrated that in the traumatic brain injury model not in cerebral infarction model, the number of BrdU/GFAP double-positive cells in the rats after acupuncture at GV20, GV26, *Fengfu* (GV16), GV15, and bilateral LI4 acupoints was significantly higher than that in the untreated group, which decreased to the same level as that in the untreated group at 7 days, reaching the same value as that of the sham-operated rats at 14 days, while the level remained higher in the injured animals not treated with acupuncture. These investigations demonstrated that acupuncture is conducive to the moderate proliferation and differentiation of astrocytes.

Mechanisms of microglia regulating neuroplasticity

Resident microglia perform a variety of functions in response to the pathological changes associated with the ischemic injury. They can rapidly change their morphology and migrate to the site of injury, affecting the integrity of neurons, changing synaptic input and activity, and activating neurogenesis. All these processes are beneficial to the recovery and reconstruction of neural function (Pocock and Kettenmann, 2007; Morrison and Filosa, 2013). Activated microglia complement receptor 3 can trigger LTD of peripheral neurons by regulating nicotinamide adenine dinucleotide phosphate oxidase, one of the main mediators of stroke neurotoxicity (Zhang et al., 2014). Another study showed that after cerebral ischemia, the activity-dependent connection between microglia and synapses was significantly prolonged for approximately 1 h, while the connection in the intact brain was maintained for approximately 5 min, suggesting that microglia can regulate LTP. This ability of microglia is critical for the reconstruction of the neural circuit after cerebral ischemic injury (Wake et al., 2009). Stimulation of microglia with low levels of interferon-gamma (IFN-γ) promotes early neurogenesis after stroke (Butovsky et al., 2006). In the chronic stage of ischemia, 16 weeks, the expression of IGF-1, GDNF, and BDNF in the M2 microglia in the ipsilateral SVZ (Ekdahl et al., 2009), generates conditions conducive to the continuous neurogenesis and recovery of function (Neumann et al., 2006; Nakajima et al., 2008). Additionally, microglia secrete chemokines, such as stromal cell-derived factor-1 α, which can bind to its receptor C-X-C chemokine receptor 4 (CXCR4) that is highly expressed in neural progenitor cells, promoting the migration of NSCs to the infarcted area.

At present, most of the research on the action of acupuncture on the neurological deficits of ischemic stroke has been from the perspective of reducing neuroinflammation, represented by reducing microglial activation and the release of proinflammatory mediators and neurotoxic substances. For example, Huang et al. (2017) performed EA on GV20 and GV24 for 7 days, and the results showed that EA could improve the neurological deficits and motor function of MCAO rats, as well as playing an anti-inflammatory role by reducing

the secretion of interleukin-1beta (IL-1β) and promoting the release of IL-10 (Huang et al., 2017). However, there is little clinical and experimental evidence of the role of microglia in the acupuncture-mediated modulation of neuroplasticity after ischemic stroke, and this should be addressed in future research.

In conclusion, the role of glial cells in neuroplasticity has become an important research topic. These cells not only secrete NTFs and other factors but also transmit signals through their interaction with neurons. However, much is still not understood, specifically, the involvement of glial-neuronal interactions on the regulation of neuroplasticity by acupuncture.

Acupuncture promotes the functional reorganization of different brain regions

The functional reorganization of different brain regions after cerebral ischemic injury depends on the plasticity of both individual neurons and the functional networks of the brain, including contralateral transfer, ipsilateral functional compensation, and the activation of latent pathways. Experimental models of stroke in mice, rats, and monkeys allowed the identification of new connections formed in the ipsilateral cerebral hemisphere between the motor, somatosensory, and premotor areas of the cerebral cortex adjacent to the stroke. Stroke can also induce new connections between frontal motor regions and parts of the brainstem or spinal cord that have lost their projections from the stroke region in the contralateral hemisphere (Carmichael et al., 2017). At the same time, increased cerebral blood flow and excitability in the contralateral cortex contribute to recovery from stroke. There is simultaneous compensation within the ipsilateral and contralateral hemispheres, although this is dependent on the dominant hemisphere. For example, when a cortical lesion is large, the compensatory effect of the ipsilateral residual cortex is weakened, while the contralateral compensatory effect is enhanced (Fang et al., 2012). The functional compensation of both the tissue surrounding the lesion and the contralateral hemisphere may be explained by the activation of latent pathways or dormant synapses (Xiao et al., 2017). Acupuncture has been suggested to be complementary to mainstream rehabilitation after stroke, promoting the improvement of motor, sensory, cognitive, and other impairments, and is closely related to the activation of the corresponding brain areas (Li et al., 2015; Wu J. et al., 2017; Wen et al., 2018). This section explains the underlying functional plasticity mechanism activated by acupuncture during the regulation of neurological deficits after stroke, as shown in **Table 3**.

Numerous imaging studies have revealed that acupuncture can induce changes in bilateral brain regions or functional connections between brain regions by stimulating unilateral limbs, thus improving sensorimotor disorders after ischemic stroke. Animal experiments showed that after EA treatment at the LI11 and ST36 acupoints of the affected limbs, the infarct volume of MCAO rats was significantly reduced and motor function was recovered. It has been suggested that the possible reason for this is that neural activity and functional connections among brain regions related to motor function were stimulated by EA, including the caudate putamen, motor cortex, somatosensory cortex, dorsal thalamus, and striatum (Liang et al., 2017; Wu P. et al., 2017; Li et al., 2021). Using regional homogeneity (ReHo) analysis in a resting state in patients, it was found that the ReHo values of the right precentral gyrus and superior frontal gyrus were increased, and the ReHo values of the right superior parietal lobule, left fusiform gyrus, and left supplementary motor area were decreased after needling LI11 and ST36 of the right (healthy) limb, indicating that needling one side could stimulate changes in neuronal activity in bilateral brain regions (Chen S. et al., 2020). Acupuncture at the TE5 acupoint can regulate the sensorimotor network of the ipsilateral hemisphere, stimulate the contralateral sensorimotor network, enhance the synergy of the bilateral sensorimotor network, and alter the synchronicity between the cerebellum and the brain (Chen L. et al., 2014). The application of acupuncture together with twisting manipulation affected broad areas of the brain, influencing the contralateral intact hemisphere in patients with unilateral cerebral apoplexy of the primary sensorimotor area and the medial frontal cortex, which suggested that the effects of acupuncture are redistributed throughout the cortex, including the unaffected hemisphere, thereby enhancing the effect of the compensatory process (Huang et al., 2013). For example, the brain region responsible for motor execution and the limbic system of the affected hemisphere were activated by acupuncture at TE5, as well as the brain region related to motor execution and the cerebellum of the unaffected hemisphere. At the same time, improving glucose metabolism in the affected hemisphere also contributes to brain compensation (Huang et al., 2012). EA at GV20 and right GB7 resulted in immediate changes in glucose metabolism in both hemispheres in response to excitatory changes in various brain regions, including bilateral effects in the primary motor area (M1), premotor cortex, and superior parietal lobule (LPs), as well as the supplementary motor area in the unaffected hemisphere. The effect was still apparent 3 weeks after the acupuncture treatment with significant changes observed in glucose metabolism in bilateral M1 and LPs, as well as in other sites such as the insula, putamen, and cerebellum (Fang et al., 2012). These studies show that acupuncture activated bilateral motor areas of the brain, as well as neural tissues related to motor activity, to promote motor function after ischemic stroke. There is, thus, functional reorganization of multiple affected and unaffected areas of the cerebral cortex, and activation of potential functional areas to enhance compensation, especially in the unaffected hemisphere.

EA at GV20 and GV24 can improve cognitive dysfunction in rats after ischemic stroke, and its protective effect may be related to the activation of cognition-related brain regions, such as the hippocampus, retrosplenial cortex, cingulate gyrus, prelimbic cortex, and sensory cortex (Wen et al., 2018), as well as increasing the functional connectivity of these regions (Zhang et al., 2021). Other studies have reported that acupuncture can cause the structural restructuring of the network of the frontal lobe and default mode network (Wu et al., 2018). These brain regions may be the potential therapeutic targets and mechanisms for acupuncture to promote motor and cognitive recovery. In addition to movement, sensation, and cognition, acupuncture can also regulate brain regions related to visual function. For example, acupuncture at TE5 resulted in modulation of brain regions such as BA18 and BA19 (Chen et al., 2013). The International Standard Scalp Acupuncture, namely, acupuncture of the parietal midline (MS5) and left anterior/posterior parietal-temporal oblique lines (MS6 and MS7), can regulate functional brain connections in the dominant hemisphere of patients with acute middle cerebral artery infarction, and specifically strengthen the connections among vision-related brain regions such as BA18 and BA19, and the calcarine, fusiform, and lingual gyri (Liu et al., 2020). At present, most of the imaging studies on the use of acupuncture in the treatment of ischemic stroke have focused on improving the relationships between motor, sensory, and cognitive impairment, and functional compensation in bilateral brain regions, while the neurophysiological mechanism underlying the functional integration of the various CNS components after ischemic stroke remains to be investigated.

Discussion and conclusion

The selection of acupoints is critical to the acupuncture process. Clinical investigations have emphasized specific treatments and have aimed to verify the effectiveness of acupuncture for the different sequelae of ischemic stroke, such as hemiplegia, dysphagia, and cognitive impairment. Although acupuncture treatments may vary according to the different types of functional impairment, they all comply with the principle of integral-local combination, that is, the acupoints in the functional areas of the brain are matched with those in specific lesion areas. These acupoints are located on yang meridians, especially Yangming and Shaoyang meridians, which have been verified by Dr. Zhang et al. (2018) through data mining technology (Zhang et al., 2018). Basic research solves a specific scientific question and emphasizes standardized acupuncture techniques and repeatability, resulting in differences between the treatment protocols in clinical and basic research. The selection of acupoints in basic research partially follows the clinical principle of integral-local combination, and many studies use head or body acupoints alone. Single or no more than five acupoints are generally used in basic research, with most of the selected acupoints used being acupoints that have been found to be effective in clinical practice, such as GV24, GV20, ST36, LI11, and TE5.

The neuroprotective effect was influenced by the different frequencies and waveforms of EA. Through the analysis of the data, we found that density-sparse waves were the most used, such as 1/20 Hz and 2/10 Hz. Previous studies have shown that the neuroprotective effect generated by density-sparse waves is the most marked, followed by intermittent waves, with continuous waves performing the worst. The reason may be that the density-sparse wave can activate different signaling pathways through conversion between low-, medium-, and high-frequency stimuli, to stimulate the release of different types of neurochemicals, leading to the neuroprotective effect, while the continuous wave can induce tolerance to electrical stimulation (Li and Wang, 2013). In addition, the acupuncture period is also one of the important factors affecting the curative effect of acupuncture. We observed that EA for 5 and 30 min has a superior effect in reducing the sizes of the ischemic cerebral infarction and neurological deficits, consistent with the conclusions of previous studies (Zhou et al., 2013).

The intervention time window of acupuncture is of great significance to the prognosis of ischemic stroke. In this review, most of the acupuncture intervention time point in the included basic studies was 24 h following the induction of MCAO, but a few studies carried out acupuncture intervention at 3 and 5 days after modeling. The duration of acupuncture ranged from 3 to 21 days. In terms of clinical research, a systematic review and network meta-analysis on the efficacy and safety of dissimilar acupuncture intervention time-points in treating stroke found that the faster the acupuncture intervention, the more effective it is in improving FMA score and BI. The optimal time point for acupuncture intervention is within 48 h after stroke, and the significant validity period lasts until 15 days after onset (Zhuo et al., 2021). Therefore, both clinical and basic studies suggest that acupuncture treatment within 24 and 48 h after cerebral infarction is more beneficial. The period of acupuncture treatment was less than 3 weeks due to greater self-recovery ability in animal models of cerebral infarction. Comparatively speaking, the clinical stroke patients have a longer course of disease, so in addition to giving acupuncture as early as possible, longer acupuncture period can be implemented to promote neuroplasticity and improve the sequelae of ischemic stroke.

In conclusion, spontaneous recovery takes place in the damaged brain due to neuroplasticity after ischemic stroke. However, the recovery is often incomplete, eventually leading to neurological deficit. Several lines of clinical evidence have shown that acupuncture can improve neurological deficits induced by ischemic stroke, particularly dyskinesia, spasticity, cognitive impairment, and dysphagia. Acupuncture plays a key role in regulating neuroplasticity, as shown in **Figure 2**. Specifically, acupuncture promotes the replacement of functional cells that

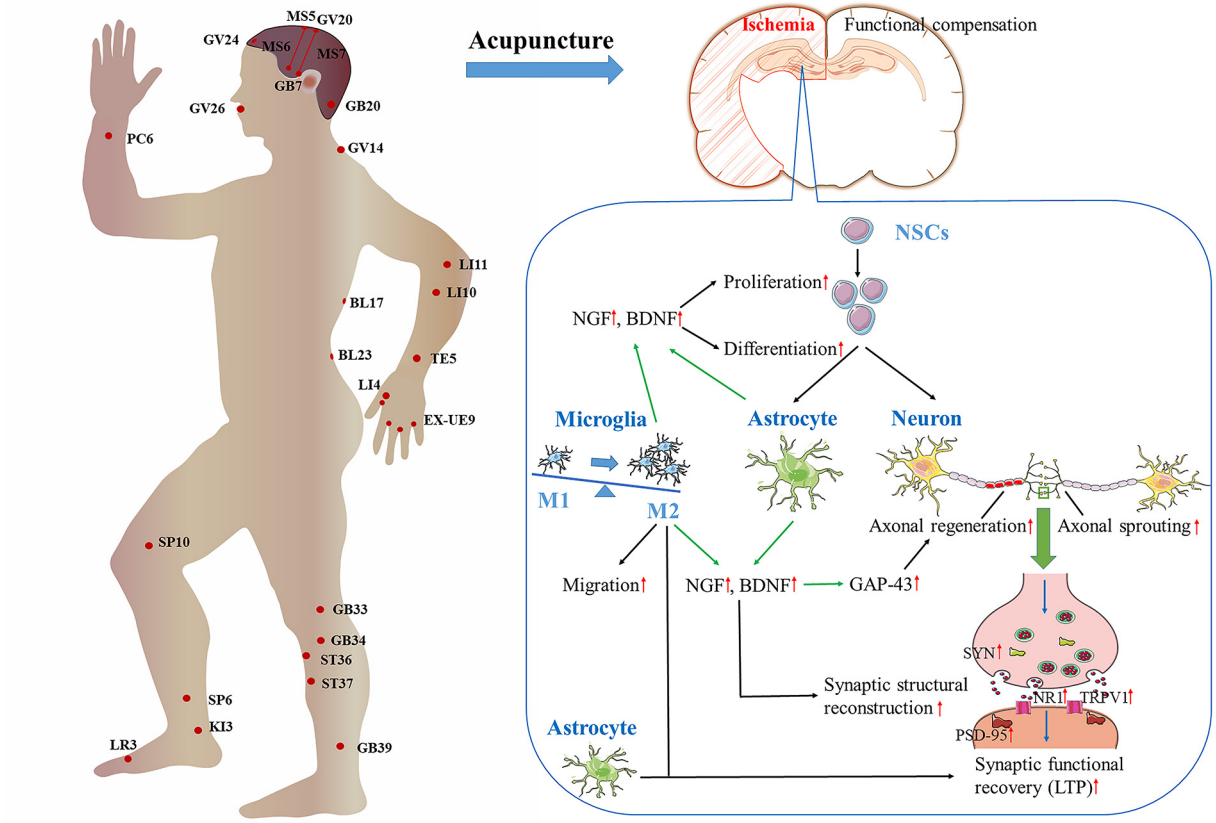

FIGURE 2
Schematic representation showing the modulation of neuroplasticity by acupuncture after ischemic stroke by the promotion of functional compensation and structural plasticity. The data of acupoint selection and mechanism are derived from the mechanistic studies by using human and rodents. PC6, *Neiguan*; GV26, *Shuigou*; GV24, *Shenting*; GV20, *Baihui*; GB7, *Qubin*; GB20, *Fengchi*; GV14, *Dazhui*; LI11, *Quchi*; LI10, *Shousanli*; TE5, *Waiguan*; LI4, *Hegu*; GB33, *Xiyangguan*; GB34, *Yanglingquan*; ST36, *Zusanli*; ST37, *Shangjuxu*; GB39, *Xuanzhong*; LR3, *Taichong*; KI3, *Taixi*; SP6, *Sanyinjiao*; SP10, *Xuehai*; EX-UE9, *Baxie*; NSCs, neural stem cells; NGF, nerve growth factor; BDNF, brain-derived neurotrophic factor; GAP-43, growth associated protein-43; SYN, synaptophysin; NR1, N-methyl-d-aspartate receptor subtype 1; TRPV1, transient receptor potential vanilloid subtype 1; PSD-95, postsynaptic density-95; LTP, long-term potentiation.

have died after stroke by stimulating nerve cell regeneration, laying the structural foundation for the establishment of contacts and synapses between the cells by promoting the growth of new nerve processes or the regeneration of damaged axons, and thus ultimately promoting information transfer by enhancing structural connections and transmission by individual synapses, neural networks, and brain regions, leading to neuroplasticity-mediated structural reconstruction and functional recovery. Glial cells represented by astrocytes and microglia, as well as the NTFs secreted by them, such as BDNF and NGF, play important roles in supporting and promoting the neuroplasticity regulated by acupuncture. However, many factors have not been discussed in depth in this review due to the lack of direct evidence, for example, there are few studies on the role of M2 microglia in acupuncture-regulated post-stroke neural plasticity, which will be the focus of future research. In addition, high-quality clinical trials and systematic investigation of relevant mechanisms are needed to obtain more conclusive evidence. For example, while it has been found in clinical studies that many nuclei are activated after acupuncture, the conduction paths of the neural circuits require confirmation by systematic basic research. In addition, the compatibility of acupoints, dose-effect relationships, time windows of intervention, and other parameters, require in-depth investigation to promote a greater clinical application of acupuncture in the treatment of ischemic stroke.

Author contributions

ZX and YaG: conceptualization. SQ and ZZ: methodology, data collection, and manuscript writing. YZ and JL: data collection and analysis. YGo and WF: preparation of the figures and the graphical abstract. YoG, YiG, JQ, ZX, and YaG: review and editing. All authors contributed to the article and approved the submitted version.

Funding

This study was financially supported by the National Natural Science Foundation of China (NSFC) No. 82004464, 81904295, and 81873369; The Natural Science Foundation of Tianjin No. 20JCQNJC00920.

Conflict of interest

The authors declare that the research was conducted in the absence of any commercial or financial relationships that could be construed as a potential conflict of interest.

Publisher's note

All claims expressed in this article are solely those of the authors and do not necessarily represent those of their affiliated organizations, or those of the publisher, the editors and the reviewers. Any product that may be evaluated in this article, or claim that may be made by its manufacturer, is not guaranteed or endorsed by the publisher.

References

Allen, N. J., and Eroglu, C. (2017). Cell biology of astrocyte-synapse interactions. *Neuron* 96, 697–708. doi: 10.1016/j.neuron.2017.09.056

Brouns, R., and De Deyn, P. P. (2009). The complexity of neurobiological processes in acute ischemic stroke. *Clin. Neurol. Neurosurg.* 111, 483–495. doi: 10.1016/j.clineuro.2009.04.001

Butovsky, O., Ziv, Y., Schwartz, A., Landa, G., Talpalar, A. E., Pluchino, S., et al. (2006). Microglia activated by IL-4 or IFN-gamma differentially induce neurogenesis and oligodendrogenesis from adult stem/progenitor cells. *Mol. Cell. Neurosci.* 31, 149–160. doi: 10.1016/j.mcn.2005.10.006

Carey, L., Walsh, A., Adikari, A., Goodin, P., Alahakoon, D., Silva, D. De., et al. (2019). Finding the intersection of neuroplasticity, stroke recovery and learning: scope and contributions to stroke rehabilitation. *Neural Plast.* 2019:5232374. doi: 10.1155/2019/5232374

Carmichael, S. T., Archibeque, I., Luke, L., Nolan, T., Momiy, J., Li, S., et al. (2005). Growth-associated gene expression after stroke: evidence for a growth-promoting region in peri-infarct cortex. *Exp. Neurol.* 193, 291–311. doi: 10.1016/j.expneurol.2005.01.004

Carmichael, S. T., Kathirvelu, B., Schweppe, C. A., and Nie, E. H. (2017). Molecular, cellular and functional events in axonal sprouting after stroke. *Exp. Neurol.* 287, 384–394. doi: 10.1016/j.expneurol.2016.02.007

Cassidy, J. M., and Cramer, S. C. (2017). Spontaneous and therapeutic-induced mechanisms of functional recovery after stroke. *Transl. Stroke Res.* 8, 33–46. doi: 10.1007/s12975-016-0467-5

Chang, J., Yao, X., Zou, H., Wang, L., Lu, Y., Zhang, Q., et al. (2016). BDNF/PI3K/Akt and Nogo-A/RhoA/ROCK signaling pathways contribute to neurorestorative effect of Houshiheisan against cerebral ischemia injury in rats. *J. Ethnopharmacol.* 194, 1032–1042. doi: 10.1016/j.jep.2016.11.005

Chavez, L. M., Huang, S. S., MacDonald, I., Lin, J. G., Lee, Y. C., Chen, Y. H., et al. (2017). Mechanisms of acupuncture therapy in ischemic stroke rehabilitation: a literature review of basic studies. *Int. J. Mol. Sci.* 194:18. doi: 10.3390/ijms18112270

Chen, B., Tao, J., Lin, Y., Lin, R., Liu, W., Chen, L., et al. (2015). Electro-acupuncture exerts beneficial effects against cerebral ischemia and promotes the proliferation of neural progenitor cells in the cortical peri-infarct area through the Wnt/β-catenin signaling pathway. *Int. J. Mol. Med.* 36, 1215–1222doi: 10.3892/ijmm.2015.2334

Chen, J., Huang, Y., Lai, X., Tang, C., Yang, J., Chen, H., et al. (2013). Acupuncture at Waiguan (TE5) influences activation/deactivation of functional brain areas in ischemic stroke patients and healthy people: a functional MRI study. *Neural Regen. Res.* 8, 226–232. doi: 10.3969/j.issn.1673-5374.2013.03.004

Chen, J., Wang, J., Huang, Y., Lai, X., Tang, C., Yang, J., et al. (2014). Modulatory effect of acupuncture at Waiguan (TE5) on the functional connectivity of the central nervous system of patients with ischemic stroke in the left basal ganglia. *PloS One* 9:e96777. doi: 10.1371/journal.pone.0096777

Chen, L., Fang, J., Ma, R., Froym, R., Gu, X., Li, J., et al. (2014). Acupuncture for acute stroke: study protocol for a multicenter, randomized, controlled trial. *Trials* 15:214. doi: 10.1186/1745-6215-15-214

Chen, S. Q., Cai, D. C., Chen, J. X., Yang, H., and Liu, L. S. (2020). Altered brain regional homogeneity following contralateral acupuncture at quchi (LI 11) and zusanli (ST 36) in ischemic stroke patients with left hemiplegia: an fMRI study. *Chin. J. Integr. Med.* 26, 20–25. doi: 10.1007/s11655-019-3079-6

Chen, S., Wang, H., Xu, H., Zhang, Y., and Sun, H. (2020). Electroacupuncture promotes axonal regrowth by attenuating the myelin-associated inhibitors-induced RhoA/ROCK pathway in cerebral ischemia/reperfusion rats. *Brain Res.* 1748:147075. doi: 10.1016/j.brainres.2020.147075

Cheng, C. Y., Lin, J. G., Tang, N. Y., Kao, S. T., and Hsieh, C. L. (2014). Electroacupuncture-like stimulation at the Baihui (GV20) and Dazhui (GV14) acupoints protects rats against subacute-phase cerebral ischemia-reperfusion injuries by reducing S100B-mediated neurotoxicity. *PLoS One* 9:e91426. doi: 10.1371/journal.pone.0091426

Cramer, S. C. (2008). Repairing the human brain after stroke. II. Restorative therapies. *Ann. Neurol.* 63, 549–560. doi: 10.1002/ana.21412

Dąbrowski, J., Czajka, A., Zielińska-Turek, J., Jaroszyński, J., Furtak-Niczyporuk, M., Mela, A., et al. (2019). Brain functional reserve in the context of neuroplasticity after stroke. *Neural Plast.* 63:9708905. doi: 10.1155/2019/9708905

Darian-Smith, C. (2009). Synaptic plasticity, neurogenesis and functional recovery after spinal cord injury. *Neuroscientist* 15, 149–165. doi: 10.1177/1073858408331372

Deng, B., Bai, F., Zhou, H., Zhou, D., Ma, Z., Xiong, L., et al. (2016). Electroacupuncture enhances rehabilitation through miR-181b targeting PirB after ischemic stroke. *Sci. Rep.* 6:38997. doi: 10.1038/srep38997

Ekdahl, C. T., Kokaia, Z., and Lindvall, O. (2009). Brain inflammation and adult neurogenesis: the dual role of microglia. *Neuroscience* 158, 1021–1029. doi: 10.1016/j.neuroscience.2008.06.052

Fang, Z., Ning, J., Xiong, C., and Shulin, Y. (2012). Effects of electroacupuncture at head points on the function of cerebral motor areas in stroke patients: a pet study. *Evid. Based Complement. Alternat. Med.* 2012:902413. doi: 10.1155/2012/902413

Felling, R. J., and Song, H. (2015). Epigenetic mechanisms of neuroplasticity and the implications for stroke recovery. *Exp. Neurol.* 268, 37–45. doi: 10.1016/j.expneurol.2014.09.017

Fouda, A. Y., Alhusban, A., Ishrat, T., Pillai, B., Eldahshan, W., Waller, J. L., et al. (2017). Brain-derived neurotrophic factor knockdown blocks the angiogenic and protective effects of angiotensin modulation after experimental stroke. *Mol. Neurobiol.* 54, 661–670. doi: 10.1007/s12035-015-9675-3

Gibon, J., and Barker, P. A. (2017). Neurotrophins and proneurotrophins: focus on synaptic activity and plasticity in the brain. *Neuroscientist* 23, 587–604. doi: 10.1177/1073858417697037

Go, A. S., Mozaffarian, D., Roger, V. L., Benjamin, E. J., Berry, J. D., Blaha, M. J., et al. (2014). Heart disease and stroke statistics–2014 update: a report from the american heart association. *Circulation* 129, e28–e292. doi: 10.1161/01.cir.0000441139.02102.80

He, X. K., Sun, Q. Q., Liu, H. H., Guo, X. Y., Chen, C., Chen, L. D., et al. (2019). Timing of acupuncture during LTP-like plasticity induced by paired-associative stimulation. *Behav. Neurol.* 2019:9278270. doi: 10.1155/2019/9278270

Hickmott, P. W., and Ethell, I. M. (2006). Dendritic plasticity in the adult neocortex. *Neuroscientist* 12, 16–28. doi: 10.1177/1073858405282417

Hinman, J. D. (2014). The back and forth of axonal injury and repair after stroke. *Curr. Opin. Neurol.* 27, 615–623. doi: 10.1097/WCO.0000000000000149

Hong, J., Wu, G., Zou, Y., Tao, J., and Chen, L. (2013). Electroacupuncture promotes neurological functional recovery via the retinoic acid signaling pathway in rats following cerebral ischemia-reperfusion injury. *Int. J. Mol. Med.* 31, 225–231. doi: 10.3892/ijmm.2012.1166

Huang, J., You, X., Liu, W., Song, C., Lin, X., Zhang, X., et al. (2017). Electroacupuncture ameliorating post-stroke cognitive impairments via inhibition of peri-infarct astroglial and microglial/macrophage P2 purinoceptors-mediated neuroinflammation and hyperplasia. *BMC Complement. Altern. Med.* 17:480. doi: 10.1186/s12906-017-1974-y

Huang, Y., Chen, J. Q., Lai, X. S., Tang, C. Z., Yang, J. J., Chen, H., et al. (2013). Lateralisation of cerebral response to active acupuncture in patients with unilateral ischaemic stroke: an fMRI study. *Acupunct. Med.* 31, 290–296. doi: 10.1136/acupmed-2012-010299

Huang, Y., Tang, C., Wang, S., Lu, Y., Shen, W., Yang, J., et al. (2012). Acupuncture regulates the glucose metabolism in cerebral functional regions in chronic stage ischemic stroke patients–a PET-CT cerebral functional imaging study. *BMC Neurosci.* 13:75. doi: 10.1186/1471-2202-13-75

Hung, C. Y., Wu, X. Y., Chung, V. C., Tang, E. C., Wu, J. C., Lau, A. Y., et al. (2019). Overview of systematic reviews with meta-analyses on acupuncture in post-stroke cognitive impairment and depression management. *Integr. Med. Res.* 8, 145–159. doi: 10.1016/j.imr.2019.05.001

Jiang, S., Chen, W., Zhang, Y., Chen, A., Dai, Q., Lin, S., et al. (2016). Acupuncture induces the proliferation and differentiation of endogenous neural stem cells in rats with traumatic brain injury. *Evid. Based Complement. Alternat. Med.* 2016:2047412. doi: 10.1155/2016/2047412

Jiang, Y., Wei, N., Zhu, J., Lu, T., Chen, Z., Xu, G., et al. (2010). Effects of brain-derived neurotrophic factor on local inflammation in experimental stroke of rat. *Mediators Inflamm.* 2016:372423. doi: 10.1155/2010/372423

Kalaria, R. N., Akinyemi, R., and Ihara, M. (2016). Stroke injury, cognitive impairment and vascular dementia. *Biochim. Biophys. Acta* 1862, 915–925. doi: 10.1016/j.bbadis.2016.01.015

Keefe, K. M., Sheikh, I. S., and Smith, G. M. (2017). Targeting neurotrophins to specific populations of neurons: NGF, BDNF and NT-3 and their relevance for treatment of spinal cord injury. *Int. J. Mol. Sci.* 18:915. doi: 10.3390/ijms18030548

Kim, E., Owen, B., Holmes, W. R., and Grover, L. M. (2012). Decreased afferent excitability contributes to synaptic depression during high-frequency stimulation in hippocampal area CA1. *J. Neurophysiol.* 108, 1965–1976. doi: 10.1152/jn.00276.2011

Kim, J. H., Choi, K. H., Jang, Y. J., Kim, H. N., Bae, S. S., Choi, B. T., et al. (2013). Electroacupuncture preconditioning reduces cerebral ischemic injury via BDNF and SDF-1α in mice. *BMC Complement. Altern. Med.* 13:22. doi: 10.1186/1472-6882-13-22

Kim, M. W., Chung, Y. C., Jung, H. C., Park, M.-S., Han, Y.-M., Chung, Y.-A., et al. (2012). Electroacupuncture enhances motor recovery performance with brain-derived neurotrophic factor expression in rats with cerebral infarction. *Acupunct. Med.* 30, 222–226. doi: 10.1136/acupmed-2011-010126

Kim, Y. R., Ahn, S. M., Pak, M. E., Lee, H. J., Jung, D. H., Shin, Y. I., et al. (2018). Potential benefits of mesenchymal stem cells and electroacupuncture on the trophic factors associated with neurogenesis in mice with ischemic stroke. *Sci. Rep.* 8:2044. doi: 10.1038/s41598-018-20481-3

Kim, Y. R., Kim, H. N., Ahn, S. M., Choi, Y. H., Shin, H. K., Choi, B. T., et al. (2014). Electroacupuncture promotes post-stroke functional recovery via enhancing endogenous neurogenesis in mouse focal cerebral ischemia. *PloS One* 9:e90000. doi: 10.1371/journal.pone.0090000

Kwon, S. E., and Chapman, E. R. (2011). Synaptophysin regulates the kinetics of synaptic vesicle endocytosis in central neurons. *Neuron* 70, 847–854. doi: 10.1016/j.neuron.2011.04.001

Li, A. H., Zhang, J. M., and Xie, Y. K. (2004). Human acupuncture points mapped in rats are associated with excitable muscle/skin-nerve complexes with enriched nerve endings. *Brain Res.* 1012, 154–159. doi: 10.1016/j.brainres.2004.04.009

Li, X., and Wang, Q. (2013). Acupuncture therapy for stroke patients. *Int. Rev. Neurobiol.* 111, 159–179. doi: 10.1016/B978-0-12-411545-3.00008-0

Li, Y., Wang, Y., Zhang, H., Wu, P., and Huang, W. (2015). The effect of acupuncture on the motor function and white matter microstructure in ischemic stroke patients. *Evid. Based Complement. Alternat. Med.* 2015:164792. doi: 10.1155/2015/164792

Li, Z., Yang, M., Lin, Y., Liang, S., Liu, W., Chen, B., et al. (2021). Electroacupuncture promotes motor function and functional connectivity in rats with ischemic stroke: an animal resting-state functional magnetic resonance imaging study. *Acupunct. Med.* 39, 146–155. doi: 10.1177/0964528420920297

Liang, S., Lin, Y., Lin, B., Li, J., Liu, W., Chen, L., et al. (2017). Resting-state functional magnetic resonance imaging analysis of brain functional activity in rats with ischemic stroke treated by electro-acupuncture. *J. Stroke Cerebrovasc. Dis.* 26, 1953–1959. doi: 10.1016/j.jstrokecerebrovasdis.2017.06.018

Liao, S. L., Lin, Y. W., and Hsieh, C. L. (2017). Neuronal regeneration after electroacupuncture treatment in ischemia-reperfusion-injured cerebral infarction rats. *Biomed Res. Int.* 2017:3178014. doi: 10.1155/2017/3178014

Lillard, A. S., and Erisir, A. (2011). Old dogs learning new tricks: neuroplasticity beyond the juvenile period. *Dev. Rev.* 31, 207–239. doi: 10.1016/j.dr.2011.07.008

Lin, R., Wu, Y., Tao, J., Chen, B., Chen, J., Zhao, C., et al. (2016). Electroacupuncture improves cognitive function through Rho GTPases and enhances dendritic spine plasticity in rats with cerebral ischemia-reperfusion. *Mol. Med. Rep.* 13, 2655–2660. doi: 10.3892/mmr.2016.4870

Lin, Y. W., and Hsieh, C. L. (2010). Electroacupuncture at Baihui acupoint (GV20) reverses behavior deficit and long-term potentiation through N-methyl-d-aspartate and transient receptor potential vanilloid subtype 1 receptors in middle cerebral artery occlusion rats. *J. Integr. Neurosci.* 9, 269–282. doi: 10.1142/s0219635210002433

Liu, A. J., Li, J. H., Li, H. Q., Fu, D.-L., Lu, L., Bian, Z.-X., et al. (2015). Electroacupuncture for acute ischemic stroke: a meta-analysis of randomized controlled trials. *Am. J. Chin. Med.* 43, 1541–1566. doi: 10.1142/S0192415X15500883

Liu, F., Li, Z. M., Jiang, Y. J., and Chen, L. D. (2014). A meta-analysis of acupuncture use in the treatment of cognitive impairment after stroke. *J. Altern. Complement. Med.* 20, 535–544. doi: 10.1089/acm.2013.0364

Liu, H., Chen, L., Zhang, G., Jiang, Y., Qu, S., Liu, S., et al. (2020). Scalp Acupuncture enhances the functional connectivity of visual and cognitive-motor function network of patients with acute ischemic stroke. *Evid. Based Complement. Alternat. Med.* 2020:8836794. doi: 10.1155/2020/8836794

Liu, S. J., Zheng, S. S., Dan, Q. Q., Liu, J., and Wang, T. H. (2014). Effects of Governor Vessel electroacupuncture on the systematic expressions of NTFs in spinal cord transected rats. *Neuropeptides* 48, 239–247. doi: 10.1016/j.npep.2014.04.004

Liu, W., Wu, J., Huang, J., Zhuo, P., Lin, Y., Wang, L., et al. (2017). Electroacupuncture regulates hippocampal synaptic plasticity via miR-134-Mediated LIMK1 function in rats with ischemic stroke. *Neural Plast.* 2017:9545646. doi: 10.1155/2017/9545646

Luo, D., Fan, X., Ma, C., Fan, T., Wang, X., Chang, N., et al. (2014). A study on the effect of neurogenesis and regulation of GSK3β/PP2A expression in acupuncture treatment of neural functional damage caused by focal ischemia in MCAO rats. *Evid. Based Complement. Alternat. Med.* 2014:962343. doi: 10.1155/2014/962343

Magnusson, J. P., Göritz, C., Tatarishvili, J., Dias, D. O., Smith, E. M., Lindvall, O., et al. (2014). A latent neurogenic program in astrocytes regulated by Notch signaling in the mouse. *Science (New York, NY)* 346, 237–241. doi: 10.1126/science.346.6206.237

Mang, C. S., Campbell, K. L., Ross, C. J., and Boyd, L. A. (2013). Promoting neuroplasticity for motor rehabilitation after stroke: considering the effects of aerobic exercise and genetic variation on brain-derived neurotrophic factor. *Phys. Ther.* 93, 1707–1716. doi: 10.2522/ptj.20130053

Manni, L., Albanesi, M., Guaragna, M., Barbaro Paparo, S., and Aloe, L. (2010). Neurotrophins and acupuncture. *Auton. Neurosci.* 157, 9–17. doi: 10.1016/j.autneu.2010.03.020

Manni, L., Florenzano, F., and Aloe, L. (2011). Electroacupuncture counteracts the development of thermal hyperalgesia and the alteration of nerve growth factor and sensory neuromodulators induced by streptozotocin in adult rats. *Diabetologia* 54, 1900–1908. doi: 10.1007/s00125-011-2117-5

Martino, G., Pluchino, S., Bonfanti, L., and Schwartz, M. (2011). Brain regeneration in physiology and pathology: the immune signature driving therapeutic plasticity of neural stem cells. *Physiol. Rev.* 91, 1281–1304. doi: 10.1152/physrev.00032.2010

Matsuzaki, M., Honkura, N., Ellis-Davies, G. C., and Kasai, H. (2004). Structural basis of long-term potentiation in single dendritic spines. *Nature* 429, 761–766. doi: 10.1038/nature02617

Merson, T. D., and Bourne, J. A. (2014). Endogenous neurogenesis following ischaemic brain injury: insights for therapeutic strategies. *Int. J. Biochem. Cell Biol.* 56, 4–19. doi: 10.1016/j.biocel.2014.08.003

Mishra, S., Kelly, K. K., Rumian, N. L., and Siegenthaler, J. A. (2018). Retinoic acid is required for neural stem and progenitor cell proliferation in the adult hippocampus. *Stem Cell Rep.* 10, 1705–1720. doi: 10.1016/j.stemcr.2018.04.024

Morrison, H. W., and Filosa, J. A. (2013). A quantitative spatiotemporal analysis of microglia morphology during ischemic stroke and reperfusion. *J. Neuroinflammation* 10:4. doi: 10.1186/1742-2094-10-4

Mundy, W. R., Robinette, B., Radio, N. M., and Freudenrich, T. M. (2008). Protein biomarkers associated with growth and synaptogenesis in a cell culture

model of neuronal development. *Toxicology* 249, 220–229. doi: 10.1016/j.tox.2008.05.012

Murphy, T. H. (2015). Two-photon imaging of neuronal structural plasticity in mice during and after ischemia. *Cold Spring Harb. Protoc.* 2015, 548–557. doi: 10.1101/pdb.prot087486

Murphy, T. H., and Corbett, D. (2009). Plasticity during stroke recovery: from synapse to behaviour. *Nat. Rev. Neurosci.* 10, 861–872. doi: 10.1038/nrn2735

Nakajima, K., Yamamoto, S., Kohsaka, S., and Kurihara, T. (2008). Neuronal stimulation leading to upregulation of glutamate transporter-1 (GLT-1) in rat microglia in vitro. *Neurosci. Lett.* 436, 331–334. doi: 10.1016/j.neulet.2008.03.058

Neumann, J., Gunzer, M., Gutzeit, H. O., Ullrich, O., Reymann, K. G., Dinkel, K., et al. (2006). Microglia provide neuroprotection after ischemia. *FASEB J.* 20, 714–716. doi: 10.1096/fj.05-4882fje

Neves, G., Cooke, S. F., and Bliss, T. V. (2008). Synaptic plasticity, memory and the hippocampus: a neural network approach to causality. *Nat. Rev. Neurosci.* 9, 65–75. doi: 10.1038/nrn2303

Park, K., Heo, H., Han, M. E., Choi, K., Yi, J. H., Kang, S. J., et al. (2015). Learning-induced synaptic potentiation in implanted neural precursor cell-derived neurons. *Sci. Rep.* 5:17796. doi: 10.1038/srep17796

Pekna, M., Pekny, M., and Nilsson, M. (2012). Modulation of neural plasticity as a basis for stroke rehabilitation. *Stroke* 43, 2819–2828. doi: 10.1161/STROKEAHA.112.654228

Pocock, J. M., and Kettenmann, H. (2007). Neurotransmitter receptors on microglia. *Trends Neurosci.* 30, 527–535. doi: 10.1016/j.tins.2007.07.007

Qing, P., Chai, T. Q., Ding, H. M., Zhao, C. H., and Hu, J. (2016). Effect of electroacupuncture combined with rehabilitation training on neurological function and expression of neuronal growth associated protein 43 and synaptophysin in rats with focal cerebral ischemia/reperfusion injury. *Zhen Ci Yan Jiu* 41, 314–320. doi: 10.13702/j.1000-0607.2016.04.006

Rathore, S. S., Hinn, A. R., Cooper, L. S., Tyroler, H. A., and Rosamond, W. D. (2002). Characterization of incident stroke signs and symptoms: findings from the atherosclerosis risk in communities study. *Stroke* 33, 2718–2721. doi: 10.1161/01.str.0000035286.87503.31

Sandvig, I., Augestad, I. L., Håberg, A. K., and Sandvig, A. (2018). Neuroplasticity in stroke recovery. The role of microglia in engaging and modifying synapses and networks. *Eur. J. Neurosci.* 47, 1414–1428. doi: 10.1111/ejn.13959

Schacher, S., and Hu, J. Y. (2014). The less things change, the more they are different: contributions of long-term synaptic plasticity and homeostasis to memory. *Learn Mem.* 21, 128–134. doi: 10.1101/lm.027326.112

Sha, R., Han, X., Zheng, C., Peng, J., Wang, L., Chen, L., et al. (2019). The effects of electroacupuncture in a rat model of cerebral ischemia-reperfusion injury following middle cerebral artery occlusion involves MicroRNA-223 and the PTEN signaling pathway. *Med. Sci. Monit.* 25, 10077–10088. doi: 10.12659/MSM.919611

Shao, T. Y., Ding, M. R., Ye, Z. X., Qian, M. X., Zhou, X., Jin, Z. Q., et al. (2021). Governor vessel acupuncture for acute ischemic stroke: a systematic review and meta-analysis. *Ann. Palliat. Med.* 10, 7236–7246. doi: 10.21037/apm-21-691

Shih, C. C., Liao, C. C., Sun, M. F., Su, Y.-C., Wen, C.-P., Morisky, D. E., et al. (2015). A retrospective cohort study comparing stroke recurrence rate in ischemic stroke patients with and without acupuncture treatment. *Medicine (Baltimore)* 94:e1572. doi: 10.1097/MD.0000000000001572

Silver, J., and Miller, J. H. (2004). Regeneration beyond the glial scar. *Nat. Rev. Neurosci.* 5, 146–156. doi: 10.1038/nrn1326

Sims, N. R., and Yew, W. P. (2017). Reactive astrogliosis in stroke: contributions of astrocytes to recovery of neurological function. *Neurochem. Int.* 107, 88–103. doi: 10.1016/j.neuint.2016.12.016

Song, M., Martinowich, K., and Lee, F. S. (2017). BDNF at the synapse: why location matters. *Mol. Psychiatry* 22, 1370–1375. doi: 10.1038/mp.2017.144

Stewart, M. R., and Dringenberg, H. C. (2016). Potential role of synaptic activity to inhibit LTD induction in rat visual cortex. *Neural Plast.* 2016:1401935. doi: 10.1155/2016/1401935

Stogsdill, J. A., and Eroglu, C. (2017). The interplay between neurons and glia in synapse development and plasticity. *Curr. Opin. Neurobiol.* 42, 1–8. doi: 10.1016/j.conb.2016.09.016

Sun, Y., Xue, S. A., and Zuo, Z. (2012). Acupuncture therapy on apoplectic aphasia rehabilitation. *J. Tradit. Chin. Med.* 32, 314–321. doi: 10.1016/s0254-6272(13)60031-x

Tan, F., Wang, J., Liu, J. X., Wang, C., Li, M., Gu, Y., et al. (2018). Electroacupuncture stimulates the proliferation and differentiation of endogenous neural stem cells in a rat model of ischemic stroke. *Exp. Ther. Med.* 16, 4943–4950. doi: 10.3892/etm.2018.6848

Tao, J., Xue, X. H., Chen, L. D., Yang, S. L., Jiang, M., Gao, Y. L., et al. (2010). Electroacupuncture improves neurological deficits and enhances proliferation and differentiation of endogenous nerve stem cells in rats with focal cerebral ischemia. *Neurol. Res.* 32, 198–204. doi: 10.1179/174313209X414506

Tao, J., Zheng, Y., Liu, W., Yang, S., Huang, J., Xue, X., et al. (2016). Electroacupuncture at LI11 and ST36 acupoints exerts neuroprotective effects via reactive astrocyte proliferation after ischemia and reperfusion injury in rats. *Brain Res. Bull.* 120, 14–24. doi: 10.1016/j.brainresbull.2015.10.011

Tejeda, G. S., Esteban-Ortega, G. M., San Antonio, E., Vidaurre, Ó. G., and Díaz-Guerra, M. (2019). Prevention of excitotoxicity-induced processing of BDNF receptor TrkB-FL leads to stroke neuroprotection. *EMBO Mol. Med.* 11:e9950. doi: 10.15252/emmm.201809950

Wake, H., Moorhouse, A. J., Jinno, S., Kohsaka, S., and Nabekura, J. (2009). Resting microglia directly monitor the functional state of synapses *in vivo* and determine the fate of ischemic terminals. *J. Neurosci.* 29, 3974–3980. doi: 10.1523/JNEUROSCI.4363-08.2009

Wang, J., Pei, J., Khiati, D., Fu, Q., Cui, X., Song, Y., et al. (2017). Acupuncture treatment on the motor area of the scalp for motor dysfunction in patients with ischemic stroke: study protocol for a randomized controlled trial. *Trials* 18:287. doi: 10.1186/s13063-017-2000-x

Wang, K., Zhang, R., He, F., Lin, L.-B., Xiang, X.-H., Ping, X.-J., et al. (2012). Electroacupuncture frequency-related transcriptional response in rat arcuate nucleus revealed region-distinctive changes in response to low- and high-frequency electroacupuncture. *J. Neurosci. Res.* 90, 1464–1473. doi: 10.1002/jnr.23028

Wen, T., Zhang, X., Liang, S., Li, Z., Xing, X., Liu, W., et al. (2018). Electroacupuncture ameliorates cognitive impairment and spontaneous low-frequency brain activity in rats with ischemic stroke. *J. Stroke Cerebrovasc. Dis.* 27, 2596–2605. doi: 10.1016/j.jstrokecerebrovasdis.2018.05.021

World Health Organization (2002). *Acupuncture: Review and Analysis of Reports on Controlled Clinical Trials*. Geneva: World Health Organization.

Wu, J., Lin, B., Liu, W., Huang, J., Shang, G., Lin, Y., et al. (2017). Roles of electro-acupuncture in glucose metabolism as assessed by 18F-FDG/PET imaging and AMPKα phosphorylation in rats with ischemic stroke. *Int. J. Mol. Med.* 40, 875–882. doi: 10.3892/ijmm.2017.3057

Wu, P., Zeng, F., Yin, C., Xiong, Y., Bai, Y., Wang, D., et al. (2017). Effect of acupuncture plus conventional treatment on brain activity in ischemic stroke patients: a regional homogeneity analysis. *J. Tradit. Chin. Med.* 37, 650–658.

Wu, P., Zhou, Y. M., Liao, C. X., Tang, Y. Z., Li, Y. X., Qiu, L. H., et al. (2018). Structural changes induced by acupuncture in the recovering brain after ischemic stroke. *Evid. Based Complement. Alternat. Med.* 2018:5179689. doi: 10.1155/2018/5179689

Xia, W. G., Zheng, C. J., Zhang, X., and Wang, J. (2017). Effects of nourishing liver and kidney acupuncture therapy on expression of brain derived neurotrophic factor and synaptophysin after cerebral ischemia reperfusion in rats. *J. Huazhong Univ. Sci. Technol. Med. Sci.* 37, 271–278. doi: 10.1007/s11596-017-1727-7

Xiao, L. Y., Wang, X. R., Yang, Y., Yang, J.-W., Cao, Y., Ma, S.-M., et al. (2018). Applications of acupuncture therapy in modulating plasticity of central nervous system. *Neuromodulation* 21, 762–776. doi: 10.1111/ner.12724

Xiao, X., Lin, Q., Lo, W. L., Mao, Y.-R., Shi, X.-C., Cates, R. S., et al. (2017). Cerebral reorganization in subacute stroke survivors after virtual reality-based training: a preliminary study. *Behav. Neurol.* 2017:6261479. doi: 10.1155/2017/6261479

Xie, G., Song, C., Lin, X., Yang, M., Fan, X., Liu, W., et al. (2019). Electroacupuncture regulates hippocampal synaptic plasticity via inhibiting janus-activated kinase 2/signal transducer and activator of transcription 3 signaling in cerebral ischemic rats. *J. Stroke Cerebrovasc. Dis.* 28, 792–799. doi: 10.1016/j.jstrokecerebrovasdis.2018.11.025

Xu, L., Yan, X. Z., Li, Z. Y., Cao, X. F., and Wang, M. (2017). Effect of xingnao kaiqiao zhenfa (acupuncture technique for restoring consciousness) combined with rehabilitation training on nerve repair and expression of growth-associated protein-43 of peri-ischemic cortex in ischemic stroke rats. *Zhen Ci Yan Jiu* 42, 223–228. doi: 10.13702/j.1000-0607.2017.03.006

Yamashita, T., Ninomiya, M., Hernández Acosta, P., García-Verdugo, J. M., Sunabori, T., Sakaguchi, M., et al (2006). Subventricular zone-derived neuroblasts migrate and differentiate into mature neurons in the post-stroke adult striatum. *J. Neurosci.* 26, 6627–6636. doi: 10.1523/JNEUROSCI.0149-06.2006

Yang, A., Wu, H. M., Tang, J. L., Xu, L., Yang, M., Liu, G. J., et al. (2016). Acupuncture for stroke rehabilitation. *Cochrane Database Syst. Rev.* 8:CD004131. doi: 10.1002/14651858.CD004131.pub3

Yang, Y., Eisner, I., Chen, S., Wang, S., Zhang, F., Wang, L., et al. (2017). Neuroplasticity changes on human motor cortex induced by acupuncture therapy: a preliminary study. *Neural Plast.* 2017:4716792. doi: 10.1155/2017/4716792

Ye, Y., Li, H., Yang, J. W., Wang, X. R., Shi, G. X., Yan, C. Q., et al. (2017). Acupuncture attenuated vascular dementia-induced hippocampal long-term potentiation impairments via activation of d1/d5 receptors. *Stroke* 48, 1044–1051. doi: 10.1161/STROKEAHA.116.014696

Yi, W., Xu, N. G., and Wang, G. B. (2006). Experimental study on effects of electro-acupuncture in improving synaptic plasticity in focal cerebral ischemia rats. *Zhongguo Zhong Xi Yi Jie He Za Zhi* 26, 710–714.

Zhang, J., Malik, A., Choi, H. B., Ko, R. W., Dissing-Olesen, L., MacVicar, B. A., et al. (2014). Microglial CR3 activation triggers long-term synaptic depression in the hippocampus via NADPH oxidase. *Neuron* 82, 195–207. doi: 10.1016/j.neuron.2014.01.043

Zhang, Q., Li, J., Huang, S., Yang, M., Liang, S., Liu, W., et al. (2021). Functional connectivity of the retrosplenial cortex in rats with ischemic stroke is improved by electroacupuncture. *Acupunct. Med.* 39, 200–207. doi: 10.1177/0964528420921190

Zhang, S., Jin, T., Wang, L., Liu, W., Zhang, Y., Zheng, Y., et al. (2020). Electroacupuncture promotes the differentiation of endogenous neural stem cells via exosomal microRNA 146b after ischemic stroke. *Front. Cell. Neurosci.* 14:223. doi: 10.3389/fncel.2020.00223

Zhang, Y., Zhang, Z. L., Wang, X., and Xinjv, L. I. (2018). Exploration on the characteristics of meridian points in the treatment of Spasticity paralysis after stroke with acupuncture and moxibustion based on the data mining technology. *Nei Mongol J. Tradit. Chin. Med.* 33:940. doi: 10.16040/j.cnki.cn15-1101.2018.02.044

Zhao, J., Sui, M., Lü, X., Jin, D., Zhuang, Z., and Yan, T. (2015). Electroacupuncture promotes neural stem cell proliferation and neurogenesis in the dentate gyrus of rats following stroke via upregulation of Notch1 expression. *Mol. Med. Rep.* 12, 6911–6917. doi: 10.3892/mmr.2015.4279

Zhao, J., Xu, H., Tian, Y., Hu, M., and Xiao, H. (2013). Effect of electroacupuncture on brain-derived neurotrophic factor mRNA expression in mouse hippocampus following cerebral ischemia-reperfusion injury. *J. Tradit. Chin. Med.* 33, 253–257. doi: 10.1016/s0254-6272(13)60135-1

Zhao, X., Bai, F., Zhang, E., Zhou, D., Jiang, T., Zhou, H., et al. (2018). Electroacupuncture improves neurobehavioral function through targeting of SOX2-mediated axonal regeneration by MicroRNA-132 after ischemic stroke. *Front. Mol. Neurosci.* 11:471. doi: 10.3389/fnmol.2018.00471

Zhao, Z. Q. (2008). Neural mechanism underlying acupuncture analgesia. *Prog. Neurobiol.* 85, 355–375. doi: 10.1016/j.pneurobio.2008.05.004

Zhou, F., Guo, J., Cheng, J., Wu, G., and Xia, Y. (2013). Effect of electroacupuncture on rat ischemic brain injury: importance of stimulation duration. *Evid. Based Complement. Alternat. Med.* 2013:878521. doi: 10.1155/2013/878521

Zhou, Y. C., Wu, X. G., and Xiao, Y. C. (2011). Effects of electroacupuncture at Zusanli (ST 36) and Neiguan (PC 6) on expression of GAP-43 in cerebral infarction rats. *Zhongguo Zhen Jiu* 31, 55–59. doi: 10.13703/j.0255-2930.2011.01.016

Zhuo, Y., Xu, M., Deng, S., Zhang, Y., Lu, X., Wu, B., et al. (2021). Efficacy and safety of dissimilar acupuncture intervention time-points in treating stroke: a systematic review and network meta-analysis. *Ann. Palliat. Med.* 10, 10196–10212. doi: 10.21037/apm-21-1127

10.3389/fncel.2022.817732

Glossary

2VO	2-vessel occlusion model
Akt	protein-serine-threonine kinase
BDNF	brain-derived neurotrophic factor
BI	Barthel Index
BrdU	5-bromo-2'-dexoyuridine
CNS	central nervous system
CREB	cyclic adenylate monophosphate response element-binding protein
CST	corticospinal tract
CXCR4	C-X-C chemokine receptor 4
EA	electroacupuncture
ERK	extracellular signal-regulated kinase
F-actin	Filamentous actin
FMI	Fugl-Meyer Assessment scale
FOXG1	forkhead box protein G1
GAP-43	growth associated protein-43
GDNF	glia cell line-derived neurotrophic factor
GFAP	glial fibrillary acidic protein
GSK3	glycogen synthase kinase 3
IFN-γ	interferon-gamma
IGF	insulin-like growth factor
IL-10	interleukin-10
IL-1β	interleukin-1beta
JAK2	Janus-activated kinase 2
LIMK1	LIM domain kinase 1
LPs	superior parietal lobule
LTD	long-term depression
LTP	long-term potentiation
M1	primary motor area
MAPK	mitogen-activated protein kinase
MCAO	middle cerebral artery occlusion
miRNAs	miRs, microRNAs
MSCs	mesenchymal stem cells
NGF	nerve growth factor
NogoA	Neurite outgrowth inhibitor A
Notch1	Neurogenic locus notch homolog protein 1
NPCs	neural precursor cells
NR1	N-methyl-d-aspartate receptor subtype 1
NR4R3	nuclear receptor subfamily 4, group A, member 3
NSCs	neural stem cells
NT-4	neurotrophin-4
NTFs	neurotrophic factors
PI3K	phosphatidylinositol-3-kinase
PirB	paired immunoglobulin-like receptor B
PRG5	plasticity-related gene 5
PSD	postsynaptic density
PTEN	Phosphatase and tensin homolog deleted on chromosome 10
RA	Retinoic Acid
Rac1	RAS-related C3 botulinus toxin substrate 1
RCTs	randomized controlled trials
RhoA	Ras homolog family member A
ROCK	Rho-associated coiled-coil-containing protein kinase
SCI	spinal cord injury
SGZ	subgranular zone
SOX2	SRY-box transcription factor 2
STAT3	signal transducer and activator of transcription 3
SVZ	subventricular zone
SYN	synaptophysin
TNF-α	tumor necrosis factor alpha
TrkA	tropomyosin-related kinase A
TrkC	tropomyosin receptor kinase C
TRPV1	transient receptor potential vanilloid subtype 1
VEGF	vascular endothelial growth factor
ZNF423	zinc finger protein 423

Advantages of publishing in Frontiers

OPEN ACCESS
Articles are free to read for greatest visibility and readership

FAST PUBLICATION
Around 90 days from submission to decision

HIGH QUALITY PEER-REVIEW
Rigorous, collaborative, and constructive peer-review

TRANSPARENT PEER-REVIEW
Editors and reviewers acknowledged by name on published articles

Frontiers
Avenue du Tribunal-Fédéral 34
1005 Lausanne | Switzerland

Visit us: www.frontiersin.org
Contact us: frontiersin.org/about/contact

REPRODUCIBILITY OF RESEARCH
Support open data and methods to enhance research reproducibility

DIGITAL PUBLISHING
Articles designed for optimal readership across devices

FOLLOW US
@frontiersin

IMPACT METRICS
Advanced article metrics track visibility across digital media

EXTENSIVE PROMOTION
Marketing and promotion of impactful research

LOOP RESEARCH NETWORK
Our network increases your article's readership